AN ABSTRACT OF THE THESIS OF

Mark S. McCutcheon for the degree of Master of Science in Geology
Presented on September 19, 2003.
Title: Stratigraphy and Sedimentology of the Middle Eocene Cowlitz Formation and Adjacent Sedimentary and Volcanic Units in the Longview-Kelso Area, Southwest Washington.

Abstract approved: _____
Alan R. Niem

Geologic mapping of the Longview-Kelso area and the measurement and description of a composite 650-meter thick stratigraphic section of the Cowlitz Formation (Tc) in Coal Creek using bio-, magneto-, litho-, and sequence stratigraphy reveals a complex interplay of Cowlitz micaceous, lithic arkosic shelf to tidal/estuarine to delta plain facies associations, and Grays River basalt lava flows and interbedded basalt volcaniclastics from nearby Grays River eruptive centers (e.g., Mt. Solo and Rocky Point). The lower 100 meters of the Coal Creek section (informal unit 1, Chron 18r) consists of micaceous, lithic arkosic sandstone and siltstone and minor coals, was deposited as part of a highstand system tract (HST) at the base of 3rd order cycle number 3. This unit consists of four dominantly tidal shoaling-upward arkosic sandstone parasequences reflecting upper shoreface to delta plain depositional environments. The overlying unit 2 (Chron 18n) is defined by abundant Grays River basalt volcaniclastic interbeds that intertongue with Cowlitz lithic arkoses. This unit represents the latter part of 3rd order cycle 3, and consists of mostly fining- and thinning-upward parasequences of middle shoreface to delta plain successions of an aggradational to transgressive parasequence set. Near the top of unit 2 is a maximum marine flooding surface depositing lower shoreface lithic arkosic sandstone to shelf siltstones over upper shoreface micaceous lithic arkose. Unit 3 comprises 3rd order cycle 4 (Chron 17r), a lowstand system tract, and consists of 6 mostly fining- and thinning-upward parasequences of lower shoreface to delta plain facies associations. A parasequence or erosional boundary at the base of unit 5 (Chron 17r) consists of submarine channel-fill scoured into underlying micaceous siltstones, produced during a lowstand system tract (LST) of 3rd order cycle 5. This deep marine channel-fill sequence is overlain by thinly-

bedded to laminated overbank distal turbidites and hemipelagic siltstones that define the top of the Coal Creek section. These 5 informal units in Coal Creek lithologically and chronologically correlate to 5 similar informal units defined by Payne (1998) in the type section of Cowlitz Formation in Olequa Creek near Vader ~30 km to the north.

Middle Eocene Grays River Volcanics of the study area are mapped as two separate units: a lower unit over 150 meters thick in places, consisting of subaerial basaltic flows and invasive flows (Tgv1), intrusions (Tgvis and Tgvid), and volcaniclastics (Tgvs1); and an upper unit consisting of commonly mollusk-bearing, shallow marine basaltic sedimentary interbeds that intertongue with the Cowlitz Formation (Tgvs2), particularly Cowlitz unit 2 of the Coal Creek section. These volcaniclastic deposits are intrabasinal, derived from volcanic highlands to the west and northwest, and local phreatomagmatic tuff cones. The lower Grays River volcaniclastic unit typically overlies Grays River flows in the study area and is divided into 5 informal facies. Geochemically, Grays River flows in the study area fall within normal parameters (3 to 4% TiO_2 and high iron tholeiitic basalts). However, basalt flows and bedded scoriaceous breccias near Rocky Point are anomalously low in TiO_2 and are considered in this study to be a separate volcanic subunit (Rocky Point Basalts), time equivalent to and interfingering with Grays River lavas, but may represent mixing with shallower western Cascade calc-alkaline magma. Over 60 younger Grays River dikes intrude the Cowlitz Formation in Coal Creek. A dike low in the Coal Creek section is dated at 40 ± 0.36 Ma, and an invasive flow at Mt. Solo is dated at $36.98 \pm .78$ Ma. Volcanics capping the hills east of the Cowlitz River are chemically distinct as slightly younger western Cascade basaltic andesite flows, and two dikes east of the river are chemically distinct as western Cascade andesite

Overlying Grays River Volcanics and Cowlitz Formation in much of the study area, are clayey and commonly tuffaceous siltstones and silty sandstones, possibly of the late Eocene-early Oligocene Toutle Formation, a new unit to this area. The Toutle Formation is a mixture of wave and stream reworked micaceous and arkosic Cowlitz Formation and fresh silicic pyroclastic ash and pumice from the active western Cascade arc.

An angular unconformity separates the Paleogene Grays River Volcanics, Cowlitz Formation, and Toutle Formation from the early to middle Miocene Columbia River Basalt Group. Based on lithology, geochemistry, stratigraphic relationships, and magnetic polarity, 6 individual Columbia River Basalt flows have been mapped in this study. The three lower Grande Ronde flows are of normal polarity and Ortley low MgO chemical composition. The lowermost flow (N_2 Ortley #1) is absent in the Columbia Heights area, low MgO, about 10 meters thick and consists of pillow-palagonite sequences in the upper quarry on Mt. Solo. Aphyric N_2 Ortley flow #2 is over 35 meters thick with well-developed upper and lower colonnade, and of intermediate MgO. N_2 Ortley flow #3 is pillow-palagonite in the Storedahl Quarry and low MgO. A ~4-meter thick tuffaceous overbank siltstone and basalt conglomeratic channel interbed separates the three low MgO Ortley flows from the overlying high MgO N_2 Grande Ronde Sentinel Bluffs flow. A single exposure of well-developed large colonnade with sparse 1 cm labradorite laths, and reddish oxidized soil, defines the N Sand Hollow flow of the Frenchman Springs Member of the Wanapum Formation. The overlying Pomona Member is mapped based on previous work by other authors.

Pliocene gravels and arkosic sand of the Troutdale Formation form upland terrace deposits up to 100 meters thick in southern parts of the study area, and represent the uplifted paleo-thalweg and overbank flood deposits of the downcutting, antecedent ancestral Columbia River. Well-rounded clasts are a mixture of extrabasinal granitic and metamorphic quartzite, and intrabasinal porphyritic basaltic andesite, dacite, and basalt from the western Cascades and Columbia River Basalts. Troutdale terrace gravels grade northward into contemporaneous volcanic pebble and cobble gravel terrace deposits produced along the ancestral Cowlitz River that are dominantly composed of porphyritic andesite gravel and volcanic sand from the western Cascades. Lower terraces along the Cowlitz River were deposited by the late Pleistocene Missoula Floods. All of these unconsolidated to semiconsolidated gravels and sands are prone to landslides, and the Aldercrest-Banyon landslide, the second worst landslide disaster in American history, occurred in the Troutdale Formation gravels.

After eruption of the Grays River Volcanics and deposition of the Cowlitz Formation, the forearc underwent a period of transtension in the late-middle Eocene

related to magmatic upwelling and reorganization of the subducting Farallon Plate. This event produced a northwest-trending set of oblique slip normal faults, along which Grays River dikes intruded. Starting in the early Miocene the region underwent a transpressional event, reactivating many of the northwest-trending faults, and producing the Columbia Heights Anticline, Hazel Dell Syncline, the Coal Creek Fault, and the Kelso Fault Zone. The paleotopography resulting from this event was stream eroded to a nearly flat plain before emplacement of the Columbia River Basalts, which are nearly horizontal today. Continued offset along the northwest-trending fault set has also offset the Columbia River Basalts. Continued oblique slip post-Miocene broad arching of the Coast Range and downcutting by the Columbia and Cowlitz Rivers has resulted in Pliocene and Pleistocene terraces, and produced an east-west fault set that offsets all earlier structural features.

© by Mark S. McCutcheon
September 19, 2003
All Rights Reserved

Stratigraphy and Sedimentology of the Middle Eocene Cowlitz Formation and Adjacent Sedimentary and Volcanic Units in the Longview-Kelso Area, Southwest Washington

By
Mark S. McCutcheon

A THESIS

Submitted to

Oregon State University

In partial fulfillment of
the requirements for the
degree of

Master of Science

Presented September 19, 2003
Commencement June, 2004

Master of Science thesis of Mark S. McCutcheon presented on September 19, 2003.

APPROVED

Alan R. Niem

Major Professor, representing Geology

Chair of the Department of Geosciences

Sally Francis

Dean of the Graduate School

I understand that my thesis will become part of the permanent collection of Oregon State University libraries. My signature below authorizes release of my thesis to any reader upon request.

Mark S. McCutcheon

Mark S. McCutcheon, Author

ACKNOWLEDGEMENTS

I am grateful for the financial support offered for this study by Dave Pauli and George Sharp of Weyerhaeuser Corporation that made this study possible. I am also thankful for the financial and geologic assistance for obtaining thin sections, geochemistry, well logs, and landslide locations, that was provided by Karl Wegmann and Dr. Tim Walsh of the Washington Department of Natural Resources. Thanks also go to Wendy Niem for computer advice and assistance above and beyond the call of duty, and reading the second draft of this thesis. And of course, without the wisdom and experience of my thesis advisor Dr. Alan Niem (professor emeritus) in the field and the classroom, this project would not be nearly as comprehensive. I am also thankful to Dr. Niem for not giving up on me through some challenging times.

Appreciation also goes to several other people who contributed valuable and vital data to this study. Molluscan assemblage identification and interpretation provided by Dr. Elizabeth Nesbitt of the University of Washington Burke Museum proved to be invaluable. I would also like to thank Dr. Reed Glasmann for x-ray diffraction data of clay and other minerals and review of the thesis, Dr. Bob Lillie of Oregon State University for his review of the thesis and enlightenment in the classroom, Dr. Charles Langford, professor of Sociology and Oregon State University for taking on the (likely larger than expected) role of being my fourth committee member and reviewing the thesis, Dr. Robert Duncan, professor of the College of Oceanic and Atmospheric Sciences at Oregon State University for Ar^{40}/Ar^{39} radiometric dating of a basalt sample, Dr. Estella Leopold of the University of Washington for running palynology samples, Dr. Jeff Meyers of Western Oregon

University for important information regarding fossil leaves, Russ Evarts of the USGS for an enlightening day in the field, and Dr. Robert Bentley, professor emeritus of Central Washington University for opening my eyes to new ideas regarding emplacement of the Columbia River Basalts.

I would like also to state my appreciation to Dr. Kenneth Hamblin and Dr. Keith Rigby of Brigham Young University, and Dr. Richard Moyle, Dr. Adolf Yonkee, and Dr. Sidney Ashe of Weber State University for taking me under their wings. Moral support from former fellow students Derik Kleibacker and Drew Eriksson and many others was much appreciated. I would also like to express my appreciation to the many public school teachers (who chose me to be a part of their classroom as a substitute teacher), staff, and students who gave me reason to hold my head high, and kept my bills paid. Most importantly, I would like to thank my family. The moral and financial support from my mother Maurine, and my brother Alan is appreciated beyond words. I would also like to thank my brother for the many trips to the observatory, mountains, and coast that sparked and maintained my interest in science. I also need to mention my outrageous German Shepherd, Lucy. I doubt a dog has ever played a more important role in a person's life.

TABLE OF CONTENTS

Page

INTRODUCTION

OBJECTIVES 1

LOCATION AND ACCESS.....2

REGIONAL GEOLOGIC SETTING AND STRATIGRAPHY.....2

PREVIOUS WORK.....11

METHODS OF INVESTIGATION.....15

STRATIGAPHY AND LITHOFACIES OF THE COAL CREEK SECTION OF THE COWLITZ FORMATION

INTRODUCTION.....19

LITHOFACIES AND DESCRIPTIONS.....20

UNIT 1.....23
UNIT 2.....37
UNIT 3.....58
UNIT 4.....65
UNIT 5.....68

DEPOSITIONAL ENVIRONMENTS.....72

PETROGRAPHY.....97

LITHIC ARKOSES AND CARBONACEOUS STRATA.....99
UPPER GRAYS RIVER VOLCANICLASTIC INTERBEDS.....111

X- RAY DIFFRACTION.....114

SEQUENCE STRATIGRAPHY AND CORRELATION TO THE COWLITZ TYPE SECTION.....120

TABLE OF CONTENTS (continued)

Page

TOUTLE FORMATION ?

INTRODUCTION.....129

LOCAL STRATIGRAPHY AND THICKNESS.....131

LITHOLOGY AND OUTCROP CHARACTERISTICS.....135

PETROGRAPHY.....142

X-RAY DIFFRACTION.....144

DEPOSITIONAL ENVIRONMENTS.....149

VOLCANICS

GRAYS RIVER VOLCANICS.....151

AGE.....154
DISTRIBUTION AND STRATIGRAPHY.....156
PETROLOGY.....164
GRAYS RIVER FLOWS.....164
DIKES.....169
LOWER VOLCANICLASTICS.....172
GEOCHEMISTRY.....186
DEPOSITIONAL ENVIRONMENTS AND PALEOGEOGRAPHIC RECONSTRUCTION.....190

WESTERN CASCADE BASALTIC ANDESITE.....196

GEOCHEMISTRY.....197
LITHOLOGY AND PETROGRAPHY.....197

WESTERN CASCADE ANDESITE DIKES.....199

GEOCHEMISTRY AND FIELD CHARACTERISTICS.....199
PETROGRAPHY.....200

COLUMBIA RIVER BASALT GROUP.....203

INTRODUCTION.....203
LOCAL DISTRIBUTION.....204
GRANDE RONDE STRATIGRAPHY.....206

TABLE OF CONTENTS (continued)

Page

FLOW UNITS CORRELATION AND GEOCHEMISTRY.....208
LITHOLOGY AND PETROGRAPHY.....214
INTERBEDS AND CONTACT RELATIONS.....222

TROUTDALE FORMATION AND PLIOCENE ANDESITIC TERRACE GRAVELS

INTRODUCTION.....229

LOCAL DISTRIBUTION AND LITHOLOGY.....230

QUATERNARY UNITS

PLEISTOCENE-HOLOCENE TERRACES.....234

LANDSLIDES.....235

MT. ST. HELENS LAHAR, MAY 18th, 1980.....238

HOLOCENE AND LATE PLEISTOCENE ALLUVIUM.....239

STRUCTURAL GEOLOGY

INTRODUCTION.....241

LOCAL STRUCTURE.....243

COLUMBIA HEIGHTS ANTICLINE AND HAZED DELL SYNCLINE.....245
N 50-70 W-TRENDING FAULTS.....249
COAL CREEK FAULT.....256
EAST-WEST-TRENDING FAULTS.....259
NORTH-SOUTH-TRENDING FAULTS.....260
KELSO FAULT ZONE.....264
KALAMA STRUCTURE ZONE.....268

HYDROCARBON POTENTIAL.....274

POTENTIAL LOCAL HYDROCARBON GENERATION.....276

TABLE OF CONTENTS (continued)

Page

POTENTIAL LOCAL HYDROCARBON RESERVOIRS.....278

POTENTIAL STRATIGRAPHIC AND STRUCTURAL TRAPS.....280

GEOLOGIC HAZARDS.....284

GEOLOGIC HISTORY.....290

CONCLUSIONS.....297

REFERENCES 306

APPENDICES.....315

APPENDIX I: MACROFOSSIL IDENTIFICATION.....316

APPENDIX II: MAGNETIC POLARITY OF BASALT SAMPLES.....319

APPENDIX III: VOLCANIC GEOCHEMISTRY.....320

APPENDIX IV: POINT COUNTS.....324

APPENDIX V: CHEMISTRY OF METHANE SAMPLE 325

APPENDIX VI: MT. SOLO $^{40}AR/^{39}AR$ RADIOMETRIC DATE.....326

LIST OF FIGURES

Figure Page

1. Boundary and location of the study area, southwest Washington.....3

2. Location of the study area, in the forarc basin of the Cascadia subduction zone....4

3. Regional geologic map of Eocene and Oligocene sedimentary and volcanic units of southwest Washington and northwest Oregon (Modified from Payne, 1998; Walsh et at., 1987; and Robertson, 1997).....6

4. Southwest Washington to northwest Oregon stratigraphic correlation chart (Modified from Payne, 1998 and Kleibacker, 2001).....9

5. Profile of onshore-offshore depositional environments and lithofacies water depths (modified from Payne, 1998).....22

6. Descriptions and interpretations of parasequences 1 through 4 of the Coal Creek section.....26

7. Photographs of lithologies of Coal Creek parasequences 1 through 4.....29

8. More photographs of lithologies of Coal Creek parasequences 1 through 4.....35

9. Descriptions and interpretations of parasequences 5 through 7 of the Coal Creek section.....40

10. Photographs of lithofacies c2 from the northern part of the Coal Creek section, graded beds of basaltic sandstone to siltstone.....41

11. Photographs of lithologies of parasequences 5 through 8.....42

12. Descriptions and interpretations of parasequences 8 through 11 of the Coal Creek section.....50

13. Photographs of lithologies of parasequences 9 through 12.....55

14. Descriptions and interpretations of parasequences 12 and 13 of the Coal Creek section.....57

15. Descriptions and interpretations of parasequences 14 through 17 of the Coal Creek section.....59

16. Photographs of lithologies of parasequences 14 through 17.....60

LIST OF FIGURES (continued)

Figure Page

17. Descriptions and interpretations of the top part of the Coal Creek section.....66

18. Photographs of distal turbidites from near the top of the Coal Creek section...67

19. Unique characteristics of clastic tidal deposits recording tide fluctuation cycles in tidal megaripple and tidal rhythmite facies.....75

20. Estuarine sediment grain size in present day Willapa Bay, southwest Washington.....86

21. Sandstone classification ternary diagrams plotting several Coal Creek samples of varying lithology.....98

22. Photomicrographs of Coal Creek section lithofacies g, massive, well-sorted micaceous, arkosic sandstones with <5% Grays River basalt clasts.....100

23. Photomicrographs of basalt-lithic samples of lithofacies g or j.....102

24. Photomicrographs of sandstones of lithofacies f, flaser-draped sigmoidal mega-ripples of a tidal channel or tidal bar.....105

25. Photomicrographs of sandstones of lithofacies e (tidal rhythmites).....108

26. Photomicrographs of lithofacies k and h of the Coal Creek section.....110

27. Photomicrographs of Grays River shallow marine volcaniclastic interbeds (Tgvs2) within the Coal Creek section.....112

28. X-ray diffraction pattern of the <15μm fraction of Coal Creek section sample CC-22d.....116

29. X-ray diffraction pattern of the <2μm fraction of Coal Creek section sample CC-22d.....116

30. X-ray diffraction pattern of the <2μm fraction of Coal Creek section sample CC-48.....117

31. X-ray diffraction pattern of the <15μm fraction of Coal Creek section sample CC-80.....117

32. X-ray diffraction pattern of the <2μm fraction of Coal Creek section sample CC-80.....118

LIST OF FIGURES (continued)

Figure Page

33. X-ray diffraction pattern of the <2μm fraction of Coal Creek section sample CC-79.....119

34. Coal Creek – Germany Creek – Olequa Creek correlation diagram.....124

35. Paleogeographic reconstruction of the Toutle Formation showing depositional environments and unconformable stratigraphic relationship with underlying Cowlitz Formation (modified from Payne, 1998).....132

36. Thin-bedded to laminated, clay-rich siltstones and fine-grained sandstones of the Toutle Formation facies 2, at Site 49 atop Columbia Heights.....137

37. Unusual trace fossils of uncertain origin in tuffaceous, clayey siltstones of the Toutle Formation at Site 49.....138

38. Sandstones and siltstones of the Toutle Formation exposed in the headscarp of a landslide at Site 59.....140

39. Cross-bedded tuffaceous arkosic sandstones of Toutle Formation lithofacies 3.....141

40. Photomicrographs of Toutle Formation sandstones and siltstones.....143

41. X-ray diffraction pattern of the <2μm fraction of Toutle Formation sample from Site 60.....145

42. X-ray diffraction pattern of the <15μm fraction of Toutle Formation sample from Site 60.....146

43. X-ray diffraction pattern of the <2μm fraction of Toutle Formation sample from Site 49.....147

44. X-ray diffraction pattern of the <15μm fraction of Toutle Formation sample from Site 49.....148

45. Residual wavelength-filtered gravity anomaly map and volcanic geology map superimposed to show relationship of shallow crustal features and surface geology. The large anomaly centered on Grays River Volcanics may be the eruptive center.....153

46. Magnetic polarity stages and Ar^{40}/Ar^{39} age-diagram of Grays River Volcanics, showing age progression toward the present day northeast.....155

LIST OF FIGURES (continued)

Figure Page

47. Time stratigraphic chart of geologic units within the study area.....158

48. Grays River flows in the Terra Firma Quarry on the south side of Mt. Solo...159

49. Quarry at Site 7, on the south side of Mt. Solo, illustrating the intermingling of Grays River lava (Tvgl) and associated lower Grays River autoclastic breccia (Tgvsl).....161

50. Grays River basalt intrusions into the Cowlitz Formation.....163

51. Photomicrographs of Grays River flows from the south side of Mt. Solo.....167

52. Photomicrographs of Grays River flows from near the Cowlitz River (Rocky Point Volcanics).....168

53. Photomicrographs of a Grays River dike from Coal Creek (CC-44).....171

54. Photomicrographs of Lower Grays River Volcaniclastic from Mt. Solo.....177

55. Lower Grays River Volcaniclastics from Site 9 (Carrolls I-5 exit).....181

56. Photomicrographs of two Lower Grays River Volcaniclastics from Site 14 and Site 5.....184

57. $Na_2O + K_2O$ and FeO/MgO vs. SiO_2 plots of Irvine and Barager (1971) and Miyashiro (1974) for Grays River Volcanics, western Cascade Basaltic Andesite, and western Cascade Andesite.....187

58. TiO_2 and FeO vs. SiO_2 plots for Grays River Volcanics, western Cascade Basaltic Andesite, and western Cascade Andesite.....188

59. Paleogeographic reconstruction of Grays River Volcanics and Cowlitz Formation tidal and supratidal facies associations.....191

60. Photomicrographs of western Cascade Basaltic Andesite flows.....198

61. Photomicrographs of western Cascade Andesite from east of the Cowlitz River.....201

LIST OF FIGURES (continued)

Figure Page

62: Grande Ronde basalt flows in the Storedahl and Sons Quarry, near Eufaula.....207

63. Composite section of Columbia River Basalts and interbeds in the map area.....209

64. TiO_2 and P_2O_5 vs. MgO for Grande Ronde Basalt flows 1-4. Columbia River Basalt rectangular fields of Beeson and others (1989) and Reidel And others (1989) are shown for TiO_2 vs. MgO.....211

65. TiO_2 vs. P_2O_5 plot for Grande Ronde Basalts. Rectangular fields of Beeson and others (1989) and Reidel and others (1989) are shown.....212

66. Ortley flow #1 photograph from a quarry on Mt. Solo, and Ortley flow #1 photomicrograph from the Storedahl and Sons Quarry (BC-3).....216

67. Ortley flow #2 photograph from the West Side Quarry and contact with underlying Toutle Formation, and photomicrograph of flow #2 from the lower colonnade in the Storedahl and Sons Quarry.....218

68. Photomicrographs of Ortley flow #3, and Sentinel Bluffs flow #4.....221

69. Interbed between Ortley flow #2 and #3 in the Storedahl and Sons Quarry...224

70. Contorted interbed between Ortley flow #2 and #3 in the West Side Quarry showing possible invasive relationship, and interbed between Ortley flow #3 and Sentinel Bluffs Flow #4 in the Storedahl and Sons Quarry.....225

71. Two facies of the interbed between Ortley flow #3 and Sentinel Bluffs flow #4 in the Storedahl and Sons Quarry.....227

72. Headscarp of the Aldercrest-Banyon landslide exposing gravels and sands of the Troutdale Formation, and close up photograph of andesite terrace gravels (Ttr).....232

73. Portion of southwest Washington State Geologic Map by Walsh and Phillips (1987), showing system of northwest-trending oblique slip faults and folds.....250

LIST OF FIGURES (continued)

Figure Page

74. DEM (digital elevation model) image of the Longview-Kelso area (courtesy Phil Dinterman of the USGS).....251

75. East-west trending faults from Site 49 in Toutle Formation clayey siltstones.....261

76. More east-west trending faults from Site 49 in Toutle Formation clayey siltstones.....262

77. N 20 W faults exposed at Site "IS" in Coal Creek interval 22 along Coal Creek Road.....263

78. Exposures of the Kelso Fault Zone at Site 9 (Carrolls I-5 exit).....265

79. N 30 W normal fault in the Kelso Fault Zone juxtaposing the western Cascade Basaltic Andesite unit and Lower Grays River Volcaniclastic at Site 9.....267

80. Structure of northwest and central part of the Newport-Inglewood fault zone and southwestern shelf of the Los Angeles basin (Modified from Harding (1971)..... 272

81. Property damage and headscarp of the Aldercrest-Banyon landslide.....288

STRATIGRAPHY AND SEDIMENTOLOGY OF THE MIDDLE EOCENE COWLITZ FORMATION AND ADJACENT SEDIMENTARY AND VOLCANIC UNITS IN THE LONGVIEW-KELSO AREA, SOUTHWEST WASHINGTON

INTRODUCTION

Objectives

Among the objectives of this study was to interpret the sequence stratigraphy, depositional environments, ages, paleocurrent dispersal patterns, and provenances of the Cowlitz Formation. In addition, sedimentary facies within the Cowlitz Formation (e.g., separate volcaniclastic units, delta plain arkosic and micaceous sandstones, siltstones, and coals, tidal flat, estuarine, and delta front sandstones) were to be identified and correlated. Another objective was to interpret the local and regional stratigraphic relationship between the Cowlitz Formation strata and adjacent Eocene and Miocene volcanic units. The Cowlitz Formation in the Longview-Kelso area was to be correlated to the five units and several facies described in the type section by Payne (1998) to the north, and the two Cowlitz units defined by Robertson (1997) in the producing Mist Gas Field to the south in northwest Oregon. Another objective, using petrography and x-ray diffraction analysis, was to determine the diagenetic history of the Cowlitz sandstones in order to evaluate the reservoir potential (porosity and permeability) of the unit and define potential source rocks and their thermal maturation. With the above data, the hydrocarbon potential of the area was to be assessed.

Another objective was to reconstruct the sequential structural history of the area and interpret this history in a regional structural and tectonic framework. Individual Columbia River Basalt flows in the area were to be resolved, separated, and mapped

using magnetic polarity, geochemistry, lithology, petrography, and stratigraphic relationships. Also, a geologic map (~80 mi^2) of the Longview-Kelso area at 1:24,000 scale was to be produced and drafted on computer, as well as a composite stratigraphic column of the Cowlitz Formation in Coal Creek. Finally, the natural hazard potential of the area was assessed, especially given the devastating Aldercrest/Banyon landslide that occurred within the map area in 1998.

Location and Access

The thesis area includes the cities of Longview and Kelso and the low-lying stream dissected hills to the north and northwest in southwest Washington, a total area of approximately 195 km^2 (~80 mi^2) (Figure 1, Plate 1). Other communities within the area are Eufaula, Coal Creek, Lexington, Ostrander, Pleasant Hill, and Tucker. Major topographic features include the Cowlitz and Columbia Rivers, the Coal Creek, Clark Creek, and Hazel Dell Creek drainages, Eufaula Heights (west of Coal Creek), Columbia Heights (east of Coal Creek and west of the Cowlitz River), and the isolated hill Mt. Solo. Access to this lushly vegetated and hilly area is provided by Interstate 5, numerous paved highways and county roads, Willamette Industries logging roads, private driveways, and streams. Good exposures of the Cowlitz Formation and associated volcanic units occur in Coal Creek during low summer discharge, and along a 16-kilometer (~10 mile) stretch of Interstate 5.

Regional Geologic Setting and Stratigraphy

The thesis area lies between the Cascade calc-alkaline volcanic arc and forearc (Figure 2) and, as part of an active subduction zone complex, contains structures and

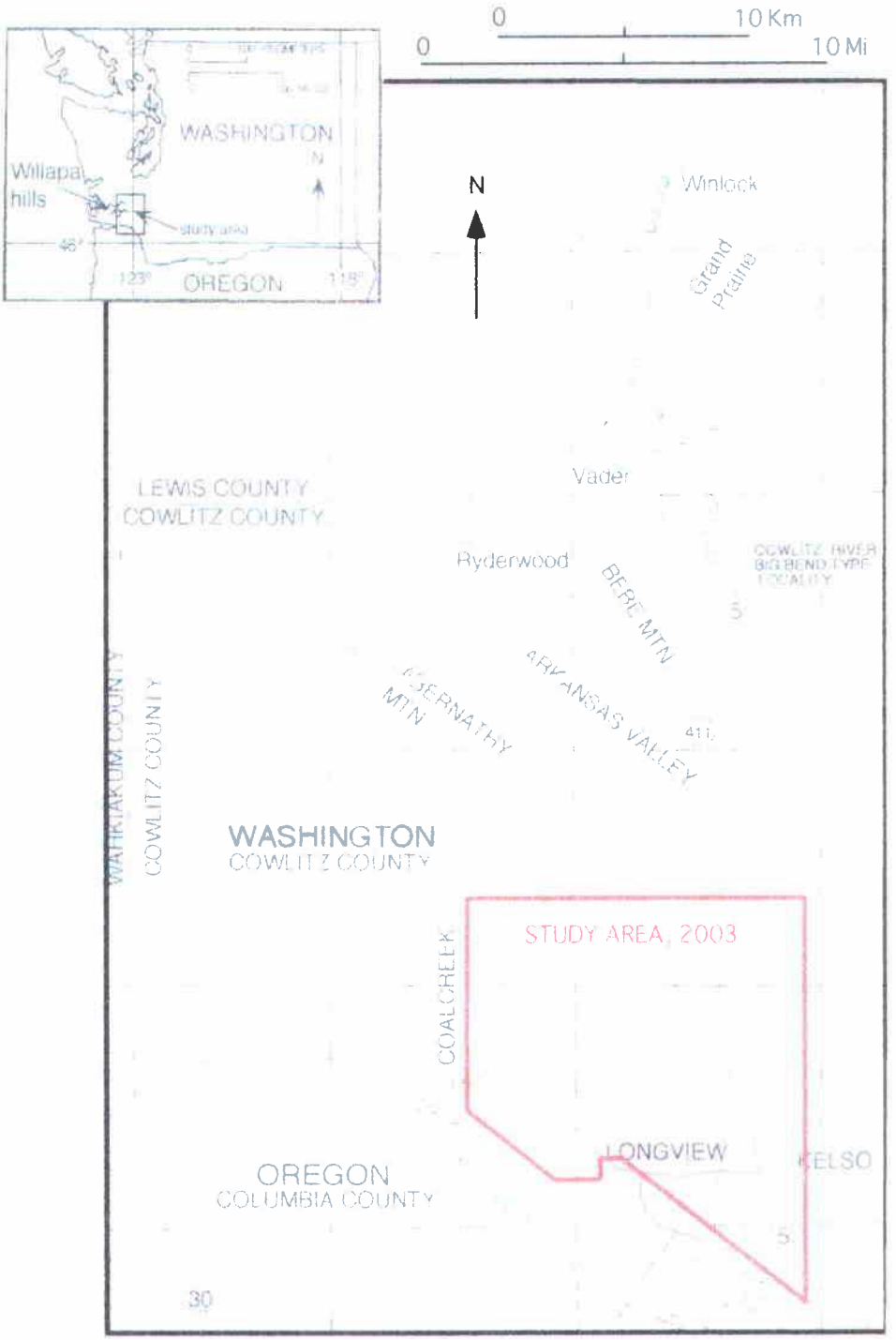

Figure 1: Boundary and location of the study area (Red), and study areas of Payne (1998) and Kleibacker (2001) Modified from Payne, 1998.

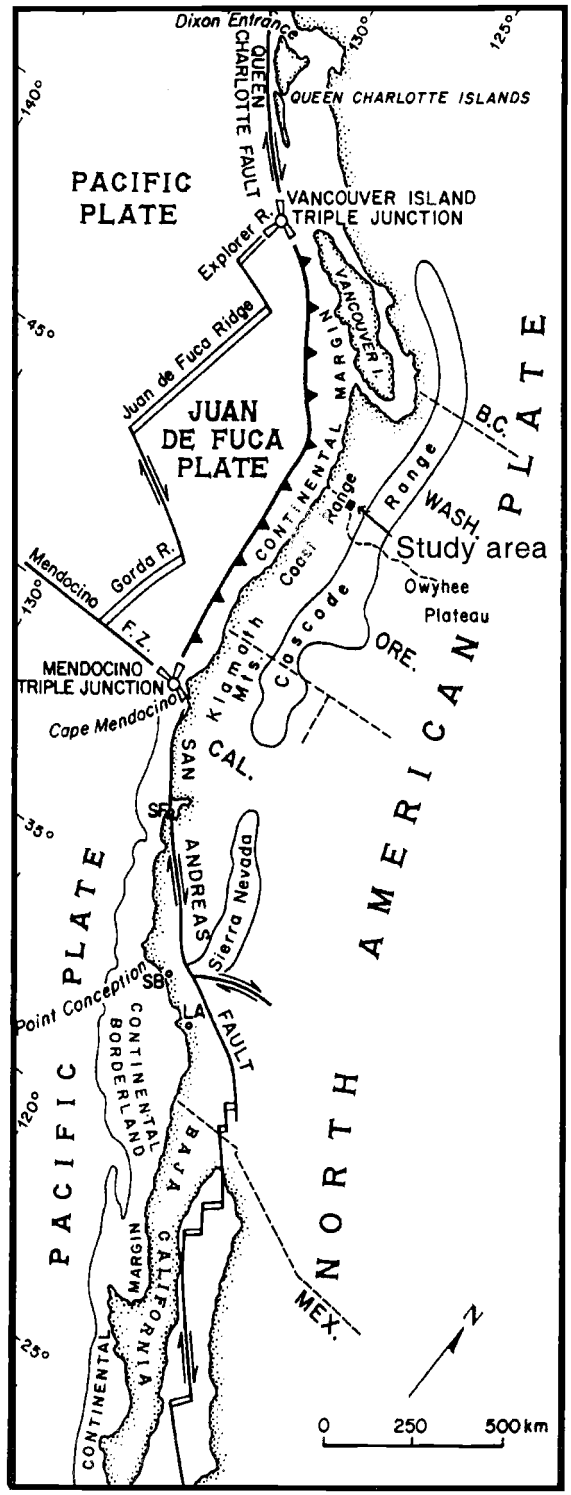

Figure 2: Location of the study area, in the forearc basin/ Coast Range of the Cascadia subduction zone.

Tertiary and Quaternary units that reflect a complex geologic history. Previous regional or reconnaissance geologic maps of the Longview-Kelso area (e.g., Livingston, 1966; Walsh and Phillips, 1987) include volcanic and sedimentary rocks ranging in age from early-late Eocene to middle Miocene (Figure 3). The oldest rocks of the Oregon and Washington Coast Ranges are the early to middle Eocene Siletz River Volcanics of northwest Oregon and the equivalent Crescent Formation of southwest Washington (Wells, 1981), with an average K-Ar age of ~49 Ma (Duncan, 1982), but range up to 59 Ma (Niem personal communication, 2003). These lower to middle Eocene units are collectively termed the Siletzia Terrain and form the 10- to 20-kilometer thick volcanic basement of the region. This terrain is composed of tholeiitic to alkalic breccias and pillow basalts to local subaerial flows with minor interbeds of deep-marine basaltic sandstone and siltstone. These thick volcanic piles may be the accreted remnants of an oceanic seamount province on the subducting Farallon oceanic plate, produced by eruption along an oceanic ridge possibly associated with the very early stages of Yellowstone hot spot volcanism (Duncan, 1982). In this view, the plate was accreted to the North American margin by middle Eocene. Alternatively, these oceanic basalt volcanics may have formed by *in situ* mafic volcanism associated with rifting of a pullapart marginal basin, due to the oblique subduction between the Farallon and North American Plates, possibly along a leaky transform fault (Wells et al., 1984; Snavely, 1987; Ryu and Niem, 1992). After emplacement of the oceanic crust, and clogging of the early-middle Eocene subduction zone by this buoyant oceanic seamount province in the middle-late Eocene, a new subduction zone formed farther to the west,

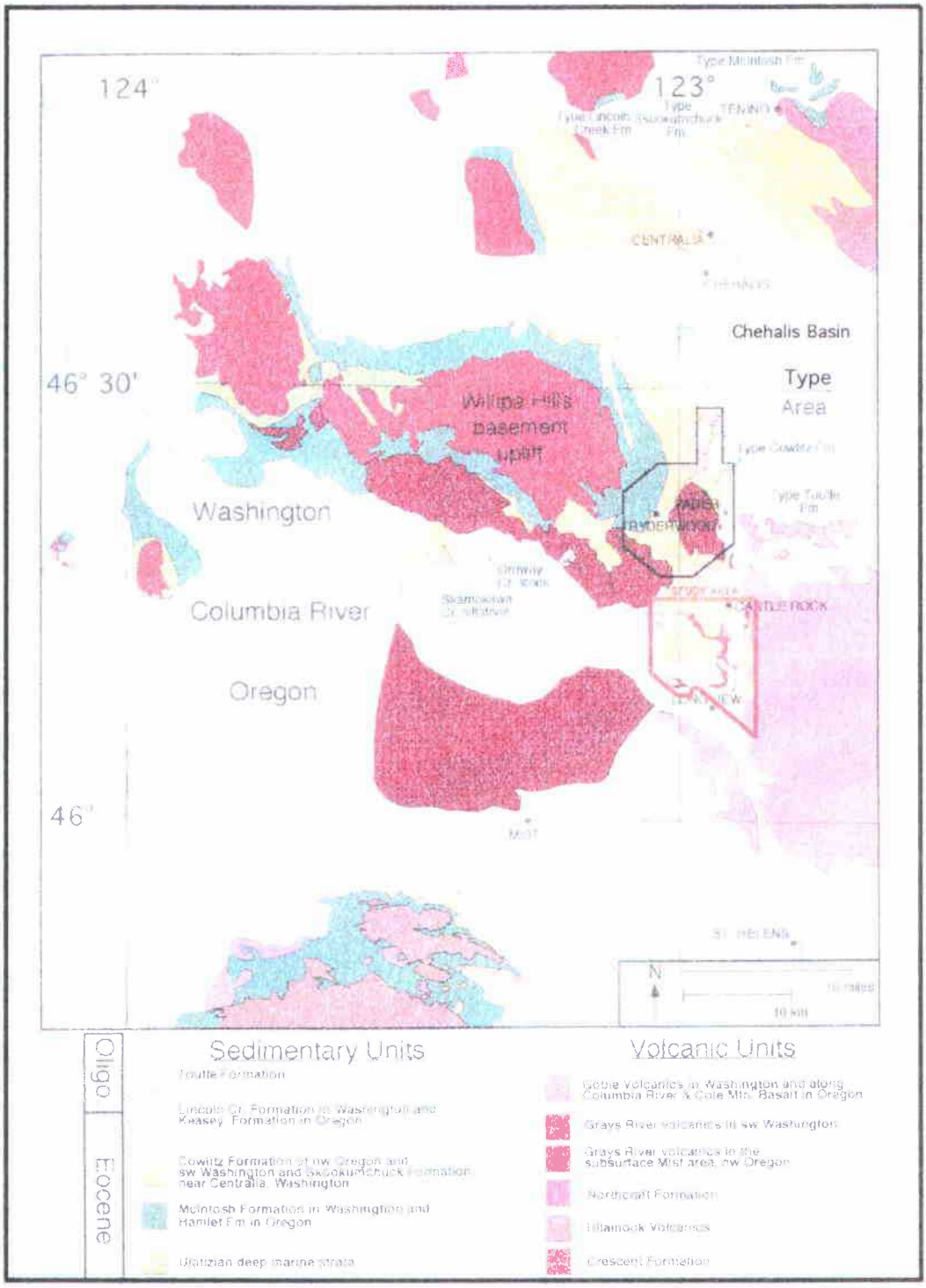

FIGURE 3: Regional geologic map of Eocene and Oligocene sedimentary and volcanic units of southwest Washington and northwest Oregon. Modified from Payne, 1998; Walsh et al., 1987; and Robertson, 1997. Study area outlined in red.

near the position of the present outer continental shelf (Wells et al., 1984; Wells and Coe, 1985; Snavely, 1987; Armentrout, 1987).

As a result of continued oblique subduction in the late Eocene, this soft collision plate tectonic boundary in southwest Washington became a zone of north-south transcurrent faulting and subsequent Reidel shear, resulting in clockwise rotation of small discrete crustal blocks and development of northwest-trending conjugate faults (Wells and Coe, 1985; Armentrout, 1987). Paleomagnetic evidence from Eocene to Miocene sedimentary and volcanic rocks of the Oregon and Washington Coast Ranges indicates that more than 30 to 75 degrees of clockwise tectonic rotation has occurred by this process with a possible pivot point in southwest Washington (Simpson and Cox, 1977; Wells and Coe, 1985; Wells et al., 1998; Prothero and others, 2002). Early to middle Eocene uplift associated with this accretion and shear rotation produced a structural high, with Crescent Formation in its core, due to basement uplift in the Willapa Hills area, producing the first major unconformity (sequence boundary) in southwest Washington (Armentrout, 1987).

A deep forearc basin about 640 km long, extending from northwest Washington to southwest Oregon, formed east of the subduction zone in late-middle Eocene time due to crustal extension and subsidence (Niem and Niem, 1984). More than 2,100 m of shallow- and deep-marine sediments and local mafic volcanics accumulated within this forearc basin during the middle to late Eocene. The southern part of the basin in Oregon began to fill with deltaic and submarine fan facies of the Tyee Formation (Ryu and others, 1992). Concurrently, in southwest Washington, deep-marine slope mudstones and minor

turbidite-deltaic sandstones of the McIntosh Formation were deposited. Those sediments appear to onlap the older Crescent Volcanics in the Willapa Hills area, suggesting that there the basement rocks formed either a paleo-bathymetric or subaerial high (Niem and Niem, 1984; Moothart, 1992; Payne, 1998; Stanley et al., 1994).

Approximately 3,500 m of high TiO_2 and Fe_2O_3 Tillamook Volcanics in northwest Oregon and slightly younger Grays River Volcanics in southwest Washington were erupted in the forearc during late-middle and late Eocene time from ~36.8 to ~45 Ma (Niem and Niem, 1985). These flows are interpreted to have been erupted by coalescing submarine mafic shield volcanoes that built up above wave base to become subaerial oceanic islands. The lower flows of these volcanic piles are locally tholeiitic submarine breccias and pillow basalts, but in some areas differentiate upward into subaerial plagioclase- and augite-phyric, platy, basaltic andesites, andesites, and some dacites and associated dikes (Rarey, 1985; Mumford, 1988). These volcanic edifices and oceanic islands subsequently subdivided the late-middle Eocene forearc basin into smaller basins in which 1,000 m of deep marine mudstone and minor micaceous, arkosic sandstones of the Yamhill and Hamlet Formations (in northwest Oregon) and the McIntosh Formation (in southwest Washington) were deposited (Niem and Niem, 1984) (Figure 4).

Prograding over these largely deeper marine sediments and volcanics in the late-middle Eocene (late Narizian), are the 1,300 to 1,500 m (~4,300 to 5,000 ft) of deltaic, micaceous, sandstones, siltstones, mudstones, and coals of the Cowlitz Formation. These sediments were deposited as the southern extension of a much wider late Eocene

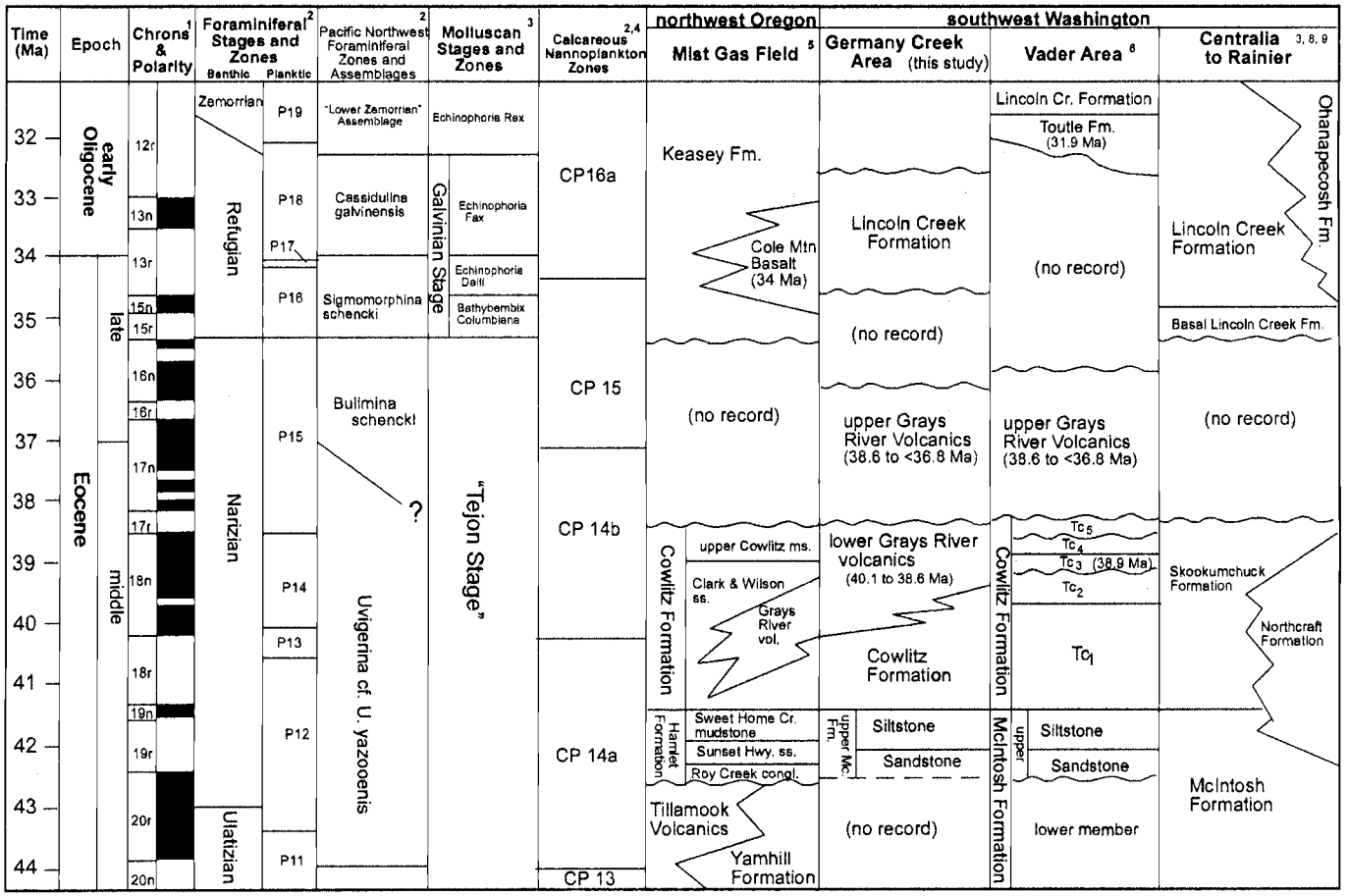

Figure 4: Southwest Washington to northwest Oregon stratigraphic correlation chart (modified from Payne, 1998; and Kleibacker, 2001).

deltaic system, the Puget Group, that filled the northeastern part of the 640 km long forearc basin (Buckovic, 1979). The Skookumchuck Formation of the Chehalis Basin 25 km (~15 mi, Figure 3) to the north and northeast of the Longview-Kelso area is the largely non-marine equivalent of the Cowlitz Formation (Buckovic, 1979; Johnson and others, 1997). Petrologic and heavy mineral studies of the Cowlitz sandstones indicate a granitic and metamorphic provenance, including the Idaho Batholith (Olbinski, 1983; Nelson, 1985; Farr, 1989; Robertson, 1997; Payne, 1998). Concurrent with progradation of the Cowlitz delta/estuary were continued mafic eruptions of overlapping shield volcanoes in the forearc, forming the largely subaerial Grays River Volcanic lavas and intrusions in the Washington forearc, and the slightly later (late Eocene) eruptions of more andesitic Goble Volcanics from the emerging western Cascade calc-alkaline arc to the east. In the study area, the bulk of Grays River Volcanics underlies the Cowlitz Formation, with interfingering Grays River volcaniclastics and local dikes. However, Payne (1998) and Kleibacker (2001) identified younger Grays River Volcanic subaerial lavas overlying the Cowlitz Formation north of the study area.

The tuffaceous marine and marginal marine Keasey, Pittsburg Bluff, Scappoose, and Smuggler Cove Formations of northwest Oregon and the Lincoln Creek Formation and Toutle Formations of southwest Washington unconformably overlie the Cowlitz Formation. These tuffaceous forearc deep and shallow marine sedimentary units were derived from wave- and current-reworked silicic explosive volcanic ash falls and flows erupted in the developing calc-alkaline western Cascade arc during late Eocene to

Oligocene time (Niem and Niem, 1984). Thick subaerial basalt flows of the middle Miocene Columbia River Basalt Group (Grande Ronde, Frenchman Springs, and Pomona) overlie with angular unconformity many of the sedimentary and volcanic Paleogene units in the area, suggesting renewed backarc mafic volcanic tectonism in early to middle Miocene time. The Oregon and Washington Coast Ranges were gently folded, tilted and rotated from late-middle Miocene to the present due to ongoing subduction of the Juan de Fuca oceanic plate beneath the North America continental plate, and the northward translation of western Oregon and southern Washington Coast Ranges against the Vancouver Island buttress (Wells et al., 1998).

Previous Work

The first paleontological and stratigraphic investigation in southwest Washington was undertaken by C.E. Weaver (1912). In that report, Weaver named the Cowlitz Formation for a 60-meter section of Eocene siltstone and sandstone at the "Big Bend" locality along the Cowlitz River. In 1937, Weaver published a comprehensive report on the Tertiary stratigraphy of the area, and expanded his 1912 definition of the Cowlitz to include 1,300 m (~4,000 ft) of upper Eocene predominantly shallow- marine fossiliferous sandstone, siltstone and coals along Olequa Creek near Vader, Washington. This comprehensive report also included several reconnaissance maps, measured sections, and a list of molluscan fossil localities, including a more than 59-meter (~1870 ft.) section of Coal Creek (Weaver, 1937; Nesbitt, 1995).

Warren and Norbisrath (1946) formalized the Tertiary stratigraphy of the upper Nehalem River basin in northwest Oregon. Their report and the preceding

reconnaissance geologic map (Warren and others, 1945) differentiated three distinct groups of rocks: the Eocene Tillamook and Goble Volcanics, several late Eocene to middle Miocene marine units, and the middle Miocene Columbia River Basalts. They also divided the Cowlitz Formation in northwest Oregon into four informal members: 1) a basal conglomerate, 2) a lower shale member, 3) a sandstone member, and 4) an upper shale member.

Henriksen (1956) modified Weaver's (1912, 1937) original definition of the Cowlitz Formation by including 1,600 m (5,250 ft) of bathyal mudstone and minor arkosic sandstone at the base of the type Cowlitz Formation in southwest Washington. He called this mudstone the Stillwater Creek Member, and named the overlying sandstone the Olequa Creek Member. In 1981, Wells on his regional geologic map of Willapa Hills restricted the type Cowlitz Formation in the Willapa Hills to a sequence of upper Narizian sandstones and coals corresponding to the Olequa Creek section as originally defined by Weaver (1912). Wells renamed the underlying deep-marine mudstone of Henriksen's Stillwater Creek Member the McIntosh Formation (Figure 4). In this study the Cowlitz Formation is a predominantly sandstone unit, as defined by Weaver in 1937, and the formation is a mappable, lithologically distinct unit.

Payne (1998) in a detailed study of the Cowlitz and McIntosh Formations in the type section along Olequa and Stillwater Creeks retained Wells's nomenclature, but subdivided the Cowlitz Formation into five informal mappable lithostratigraphic units. The basal unit 1 consists of multiple prograding parasequences of shoreface, wave dominated, lithic-arkosic sandstones (unit 1A), and coal bearing deltaic plain facies (unit

1B). Unit 2 is composed of thickening- and coarsening-upward storm-dominated, hummocky shelf to delta front arkosic sandstone parasequences, and outer shelf deep marine siltstones and mudstones. This unit also contains several Grays River basaltic, volcaniclastic interbeds and thick basaltic, fossiliferous sandstones. Unit 3 is in a slightly unconformable contact (i.e., sequence boundary) with the lower shallow marine portion of unit two, and consists of thinning- and fining-upward subtidal, intertidal, and delta plain facies, with minor basaltic volcaniclastic interbeds associated with the coals. Unit 4 consists of wave dominated shoreface arkosic sandstone and bioturbated mudstone. These first four units comprise 10 coarsening-upward parasequences of a retrogradational set. Unconformably overlying unit 4, unit 5 consists of deep marine, well-laminated micaceous siltstone, thin-bedded arkosic turbidites, and thick submarine channel arkosic sandstone with mudstone rip-up clasts, and slump-folded and soft-sediment deformed intervals.

The nomenclature of igneous rock units in southwest Washington has also had a long history. The Goble Volcanics mapped by Henriksen (1956) and Wells (1981) in the Longview and Kelso area were subsequently renamed Grays River Volcanics by Phillips (1987) based on geochemical and age differences of these forearc mafic volcanics with the more calc-alkaline andesitic Goble Volcanics of the nearby western Cascades.

Many graduate students (Timmons, 1981; Jackson, 1983; Shaw, 1986; Kenitz, 1997) at Portland State University working under Dr. R.O. Van Atta, Dr. Paul Hammond, and Dr. R.E. Thoms have done detailed stratigraphic and paleontological investigations of the Cowlitz Formation in Washington and Columbia counties of northwest Oregon.

Other graduate students under the guidance of Dr. A.R. Niem at Oregon State University (Olbinski, 1983; Nelson, 1985; Rarey, 1986; Mumford, 1988; Robertson, 1997; Payne, 1998; Kleibacker, 2001; Eriksson, 2002) have mapped and described the Cowlitz Formation and adjacent volcanic and sedimentary Eocene units in northwest Oregon and southwest Washington.

Livingston (1966), in a detailed report of the ferruginous bauxite potential of the Longview-Kelso area, produced a detailed geologic map of part of the thesis area at 1:40,000 scale. Areas west and northwest of the cities of Longview and Kelso, including Coal Creek, were mapped at a more generalized scale of 1:62,500. No distinction was made between the Columbia River Basalt flow units on the map. Wells (1981), in a reconnaissance map of the Willapa Hills that included the western part of the map area, subdivided the Columbia River Basalts into Grande Ronde, Frenchman Springs, and Pomona. In addition, some Grays River Volcanic units were mapped as part of the Cowlitz Formation by Livingston (1966), and a distinction was not made between Grays River flow units and volcaniclastic units. Walsh and Phillips (1987) on a regional map of 1:250,000 scale, later modified Livingston's (1966) maps to include these Cowlitz volcanic units within the Grays River Volcanics. Livingston (1966) described and mapped several large regional faults and folds as part of an analysis of the structural features of the area. He explained the various orientations of beds in Coal Creek as the result of several east-west trending anticlines and synclines, as Weaver had done in 1937.

Methods of Investigation

Most of the fieldwork conducted for this study was accomplished during the summer months of 1997 and 1998. During that time, a preliminary geologic map of the Longview-Kelso area was created using United States Geological Survey 7.5-minute quadrangle topographic maps, Willamette Industries logging road maps, a 1997 road map of Longview, Kelso, and surrounding communities, 1993 aerial photographs at 1:12,000 scale provided by GeoResources Inc., and SLAR and DEM digital imagery (provided by the USGS). Older geologic maps produced by Livingston (1966), and Walsh and Phillips (1987) were used as a guide to the geology of the area. A detailed 1:24,000 scale computerized geologic map (with cross sections) has since been produced using the program Canvas version 6 (Deneba Software) with USGS 7.5 minute topographic maps serving as the base, including all of the Kelso quadrangle, the eastern half of the Coal Creek quadrangle, and a portion of the northeast corner of the Rainier, Oregon quadrangle (Plate 1). Additional subsurface data from Cowlitz County water well logs provided by Karl Wegmann of the Washington Department of Natural Resources was useful in creating this geologic map and cross sections. Field mapping also included sampling volcanic and sedimentary units for petrographic, geochemical, paleontological, and paleomagnetic studies to be conducted later in the laboratory.

Much of the summer of 1997 was also spent traversing the bed of Coal Creek in order to produce detailed field descriptions of the 650-meter thick Coal Creek stratigraphic section of the Cowlitz Formation. Unusually low flow conditions in the summer of 2000 exposed much of the creek bed that had been previously inaccessible. The section was measured using a Jacob staff and Abney level along approximately 7 km

(~4.5 miles) of the creek, beginning at the SW ¼ of the SE ¼ of Sec. 10, T 8 N, R 3 W, and ending at the SW ¼ of the SW ¼ of Sec. 27, T 9 N, R 3 W (Plates 1 and 2). During this measured traverse, detailed descriptions of lithologies, sedimentary structures, macrofaunal assemblages, and structural features were made. Over 150 samples of Cowlitz Formation arkosic sandstone, siltstone, and coal units, and Grays River volcaniclastic interbeds and intrusions were collected. Over 30 macrofaunal assemblages were collected from this stratigraphic section, and 21 were sent to Elizabeth Nesbitt of the Burke Museum of the University of Washington for identification and paleoenvironmental analysis (see Appendix I). Coal Creek sedimentary samples were brought back to the laboratory, and using lithologic and grain-size charts, the color, grain-size, sorting, rounding, bedding, and ichnofabric were described. Macrofossils (mollusk and plant fossils) and trace (ichno) fossils proved to be important in interpreting depositional environments of the Coal Creek section beds.

Nineteen volcanic samples of Grays River Volcanics and Columbia River Basalts were spatially oriented in the field and collected for magnetic polarity measurements using a portable fluxgate magnetometer (see Appendix II). Twenty nine volcanic samples were analyzed by XRF (X-ray fluorescence) for major and trace element geochemistry (Appendix III) by Dr. Peter Hooper at Washington State University's GeoAnalytical Laboratory, Pullman, through financial assistance from the Washington Department of Natural Resources (Tim Walsh and Karl Wegmann). Twelve are Grays River Volcanics, 3 are western Cascade basaltic andesite, 2 are western Cascade andesite, and 12 are Columbia River Basalts (see Appendix III, Figures 57, 58, 64, 65, and Plate 1). Thirty thin sections were prepared from volcanic samples in the study area by San

Diego Petrographic (5 Grays River flows or intrusions, 14 Grays River volcaniclastics, 3 western Cascade basaltic andesite flows, 2 western Cascade andesite intrusions and possibly one flow, and 6 Columbia River Basalts). One Grays River volcaniclastic interbed from Coal Creek was impregnated with blue dye to assist in estimating porosity, since it is such a common lithology in the Coal Creek section. One Grays River flow sample was submitted to Dr. Robert Duncan of the College of Oceanic and Atmospheric Science, Oregon State University, Corvallis for Ar^{40}/Ar^{39} incremental-heating age using a laser-fusion mass spectrometer (Appendix VI).

Laboratory work on Paleogene sedimentary rocks in the study area (Cowlitz and Toutle Formations) included preparation of 21 thin sections by San Diego Petrographic for determination of composition, rounding, sorting, porosity, diagenetic history, and provenance using a Nikon petrographic binocular microscope. Nineteen are of Cowlitz Formation arkosic and mixed arkosic-volcanic sandstones and siltstones from the Coal Creek section, and 2 of Toutle Formation clayey siltstones (see locations on Plate 1). Four hundred points were counted in 4 Cowlitz Formation thin sections and categorized into 16 variables (Appendix IV). Two thin sections were impregnated with blue dye to facilitate visual porosity and permeability estimates. Identification of clay and silt-size mineral grains forming the matrix of 6 sandstones and siltstones (including Grays River volcaniclastic interbeds) was accomplished using a Phillips Automated X-ray Diffractometer (XRD) by Dr. Reed Glasmann of the Geosciences Department, Oregon State University, Corvallis. Additionally, one gas sample from a well along Coal Creek was collected for determination of the origin (biogenic or thermogenic) of the natural gas (see Appendix V), and fossil leaves were studied by Dr. Jeff Myers or Western Oregon

University to help determine age and depositional environment of Toutle Formation strata.

STRATIGRAPHY AND LITHOFACIES OF THE COAL CREEK SECTION OF THE COWLITZ FORMATION

Introduction

Weaver (1937) in a molluscan fossil study, measured and described nearly 590 meters of thick sandstones, siltstones, carbonaceous shales, and coals of the middle to late Eocene Cowlitz Formation, along the approximately 7 km length of the lower part of Coal Creek. The entire thickness of this section was traversed by Weaver (moving down-section and upstream in the creek) between SW ¼ of the SE ¼ of Sec. 10, T 8 N, R 3 W and NE ¼ of the SW ¼ of Sec. 2, T 8 N, R 3 W, a horizontal distance of 2.5 km. Strata in this part of the section dip between 8 and 25 degrees to the southwest and strike northwest-southeast. Northward, over the next 2 km of creek, bed orientation changes to gently dip to the north and northwest (<10 degrees unless near a fault). Weaver interpreted this ~135 degree change in dip orientation to be due to a large northeast-trending anticline, with beds dipping more steeply near the axis. He also incorporated about 1000 feet (~308 meters) of additional strata in the measured section along this 2 km traverse of the northern limb of the anticline (now moving upsection) within his stratigraphic column based on stratigraphic position, rather than lithologic correlation. Smaller-scale changes in dip orientation along the northern 4 km of creek were also interpreted by Weaver as resulting exclusively from minor anticlinal and synclinal folds.

A different interpretation is being proposed in this study. Rather than an anticlinal axis, the increase in dip, varying orientation of beds, and large fracture sets near the base of the section are explained by a major northwest-trending transpressional fault (Coal Creek Fault, Plates 1 and 2, see structure section), up to the north, with

approximately 100 m of vertical and right lateral offset. Concurrent with the change in strike and dip of bedding across this structure, Cowlitz Formation subunits change to include lithologies (e.g., thick mudstones) not encountered while moving down-section in the southern part of the creek. In addition to anticlinal and synclinal folds, small faults with local drag have been discovered in the creek that account for many of the small-scale changes in strike and dip, and that produce several repeated sections within the creek (see Plate 2). Accounting for these faults and folds, the total thickness of section north of the Coal Creek fault is approximately 150 meters, with an additional 60 meters added to the base of Weaver's section for a total thickness of ~650 meters (Plate 2).

The Coal Creek section was measured and described for this study during portions of the summer months of 1997 and 1998. Unusually low flow conditions during July of 2000 exposed most of the creek bed, allowing study of several intervals that were previously inaccessible. Intervals described in this section were numbered as they were encountered while walking the creek from south to north (Plate 2). Intervals 0 to 57 were described while traversing down-section and up-stream south of the Coal Creek Fault, intervals 58 to 93 represent the shallow-dipping, folded, and faulted section north of the Coal Creek Fault (Plate 1, cross section C-C'). The complex structure of this northern section, and the meandering nature of the creek, resulted in some horizons being encountered several times (e.g., coal A in intervals 66, 82, and 88, correlated in Plate 2) while moving up and down through a relatively small part of the total section.

Lithofacies and Descriptions

Coal Creek and its tributaries have eroded through overlying Oligocene (?) and Miocene sedimentary and volcanic units, exposing a nearly continuous ~650-meter

section of the middle to upper Eocene Cowlitz Formation. This section is intruded by numerous northwest-southeast trending late Eocene Grays River dikes (Plates 1and 2). Eleven lithofacies (a through k) occur within this stratigraphic section, many repeatedly, representing a variety of lower-shoreface to delta plain depositional environments within a tide-dominated deltaic system (Figure 5):

(a) heterolithic, micro-cross laminated, light gray, arkosic siltstone lenses or thin beds alternating with wavy-laminated, dark gray, silty mudstone; a combination of shelfal mudstone and lower shoreface siltstone (shelf to shoreface transition, *Cruziana* ichnofacies), (b) hummocky to swaley lenticular beds of well-sorted, fine- to medium-grained arkosic, micaceous sandstone with low-angle (<15 degrees) cross-laminations (middle shoreface, *Cruziana* ichnofacies), (c1) thick-bedded to massive, poorly-sorted, basaltic pebble conglomerate, breccia, and coarse basaltic sandstone of Grays River Volcanic composition, commonly containing shallow-marine molluscan fossil assemblages (storm-lag, wave reworked volcaniclastic debris flows, or minor transgressions) and (c2) thin-bedded to laminated, graded Gray River basalt volcaniclastics with substantial basaltic siltstone interbeds (representing volcanic debris flow deposits into bay or estuary), (d) massive, planar-laminated, or mottled and heavily bioturbated mudstone, silty mudstone, or siltstone with abundant carbonaceous debris (quiet-water bay), (e) heterolithic, thin-bedded to laminated, cyclically alternating grayish orange arkosic micaceous sandstone, and drapes of gray carbonaceous and micaceous siltstone to mudstone (tidal rhythmites), (f) tangential to sigmoidal, high-angle (>15 degrees) cross-beds in medium- to coarse-grained grayish orange arkosic micaceous sandstone with gray, flaser-bedded foresets rich in mica and carbonaceous debris

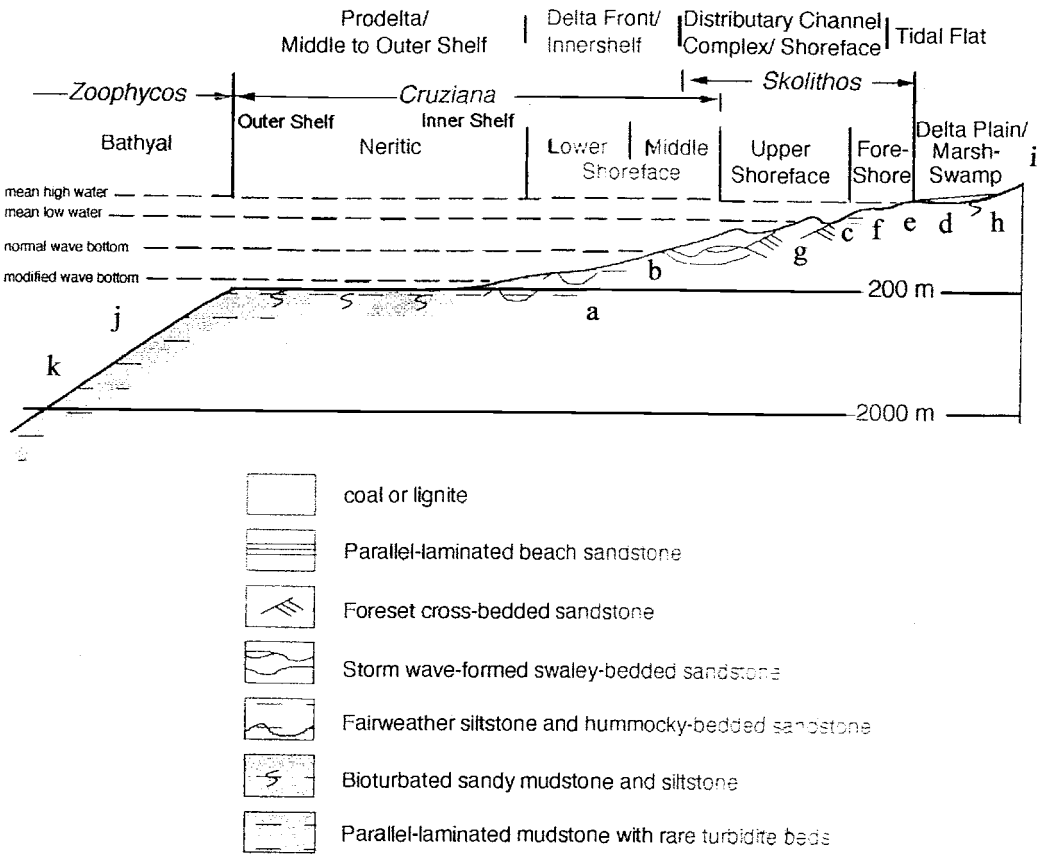

Figure 5: Profile of onshore-offshore depositional environments and lithofacies water depths (modified from Payne, 1998). See also Figure 59 for details of tidal and supratidal depositional environments.

(prograding tidal bar or channel), (g) massive- to parallel-bedded, well- sorted, medium- to coarse-grained arkosic sandstone (delta front sand, shoal, or beach), (h) carbon-rich mudstone to siltstone, carbonaceous shale, and coal (delta plain, supratidal swamp), (i) high-angle cross-beds in moderately well-sorted medium to coarse arkosic sandstone, lacking flaser drapes (distributary or tidal channel), (j) massive deep marine channel sandstones, and (k) thinly-laminated shelf to lower shoreface overbank distal turbidites.

Detailed Stratigraphy and Descriptions

Based upon southwest dip and structure, the stratigraphically lowest interval of the Cowlitz Formation exposed in Coal Creek, interval 58 (NE ¼ of the SW ¼ of Sec. 2, T 8 N, R 3 W, Figure 6, Plate 2), occurs upstream of approximately 15 meters of cover, immediately north of the Coal Creek Fault, forming a very low gradient stream bed along several meters of creek. This interval (lithofacies d) is the lowest unit in a coarsening and thickening-upward parasequence, and consists of hackly fractured, medium gray, silty, micaceous mudstone with poorly defined bedding planes, that weathers into a series of 1.5-2 cm wide fragments. Whole carbonized leaves and twig fragments are common, with minor possible fossil insect fragments. Ovoid calcareous concretions 1-2 cm wide and vertical burrows are common. The hackly mudstone of interval 58 is in sharp contact with the lowest sandstone bed of interval 59, a nearly horizontal cliff-former along ~800 meters of creek (Figures 6, 7b and c). This heterolithic interval, unique in the Coal Creek section, consists of ~20 meters of 0.3-1.2 meter thick, brownish, laminated sandstone (lithofacies e) alternating cyclically with 0.4-1.5 meter thick dark gray mudstone and siltstone (lithofacies d). Micaceous, arkosic sandstone interbeds are fine- to medium-

grained, moderately well-sorted, and wavy- to planar-laminated. Individual laminae are 1 mm to 2 cm thick, commonly graded, and defined by carbonaceous and micaceous drapes less than 1-mm thick. Sedimentary structures within the sandstone beds include abundant micro-cross laminations, clastic dikes, 1-2 cm wide ovoid mudstone and siltstone rip-up clasts, and 3-4 cm diameter calcareous concretions. The sandstone unit 2 meters above the base of this interval is highly concretionary, averaging 5-10 per square-meter of outcrop. Vertical *Skolithos* burrows to ichnofabric 1 (Droser and Bottjer, 1986), averaging 0.5-2 cm in diameter and several centimeters long are common, and are commonly infilled with the darker gray mudstone and siltstone of the adjacent interbeds, producing a wavy and indistinct contact.

Siltstone to mudstone interbeds range from dark to medium gray with abundant carbonaceous organic material. Burrows are common in most beds, ranging from ichnofabric 3-5, giving the beds a mottled appearance (petrology sample cc-59). Within the upper 10 meters of interval 59, sandstone interbeds become coarser-grained, thicker, and more common, with abundant mudstone, siltstone, and carbonaceous mudstone rip-up clasts. Large, angular pieces of carbonaceous plant debris several centimeters in diameter are more common, and the wavy and micro-cross laminations grade into low-angle trough cross-beds with flaser-drapes (lithofacies f). These drapes are carbonaceous and micaceous and form mud couplets between sandstone beds, and reactivation surfaces on the foresets. The uppermost sandstone bed in interval 59 is trough to sigmoidally cross-bedded with 0.5-meter thick mud-draped foresets. Large (2-cm wide) *Skolithos* burrows and coalified woody material become more common upward in this interval.

Interval 60 (Figure 6) is in sharp contact with the trough cross-bedded uppermost sandstone unit of interval 59. This dark to medium gray hackly mudstone to silty mudstone (lithofacies d) is 7.1 meters thick. Bioturbation to ichnofabric 4 and fracturing have destroyed all primary sedimentary structures, resulting in a massive, mottled appearance. This interval grades imperceptibly upward into interval 61 (Figure 6), 1 meter of highly fractured, medium-grained, micaceous, arkosic, organic-rich siltstone. Color ranges from medium brown to medium gray, with abundant carbonized leaf and twig fragments. Burrows to ichnofabric 5 have destroyed original laminations.

Interval 61 grades upward to the heterolithic lowermost unit of interval 62, a three-meter thick series of cyclically alternating beds of planar to micro-cross laminated fine-grained sandstone and siltstone, and highly carbonaceous laminated mudstone (lithofacies e, Figure 8c). Toward the base, laminations and beds are wavy and range in thickness from 1 mm to 5 cm. Sandstone interbeds are moderately well-sorted, fine to coarse-grained, grayish orange, micaceous arkoses, and many are lenticular. Micro-cross laminations are common with flaser bedding defined by extremely organic-rich 1-mm thick dark gray or brown mudstone drapes. These ripple-laminated sandstone beds are separated by 1-cm thick, organic-rich mudstone drapes. Sandstone and siltstone beds are intensely bioturbated (ichnofabric 5) in places by burrows. The contact between these beds is bioturbated and gradational. Toward the top, micro-cross laminated sandstone interbeds are thicker and coarser with steeper foresets. Planar sandstone interbeds of the lower portion grade upward to become nested sandstone lenses a few centimeters thick and less than 1-meter across.

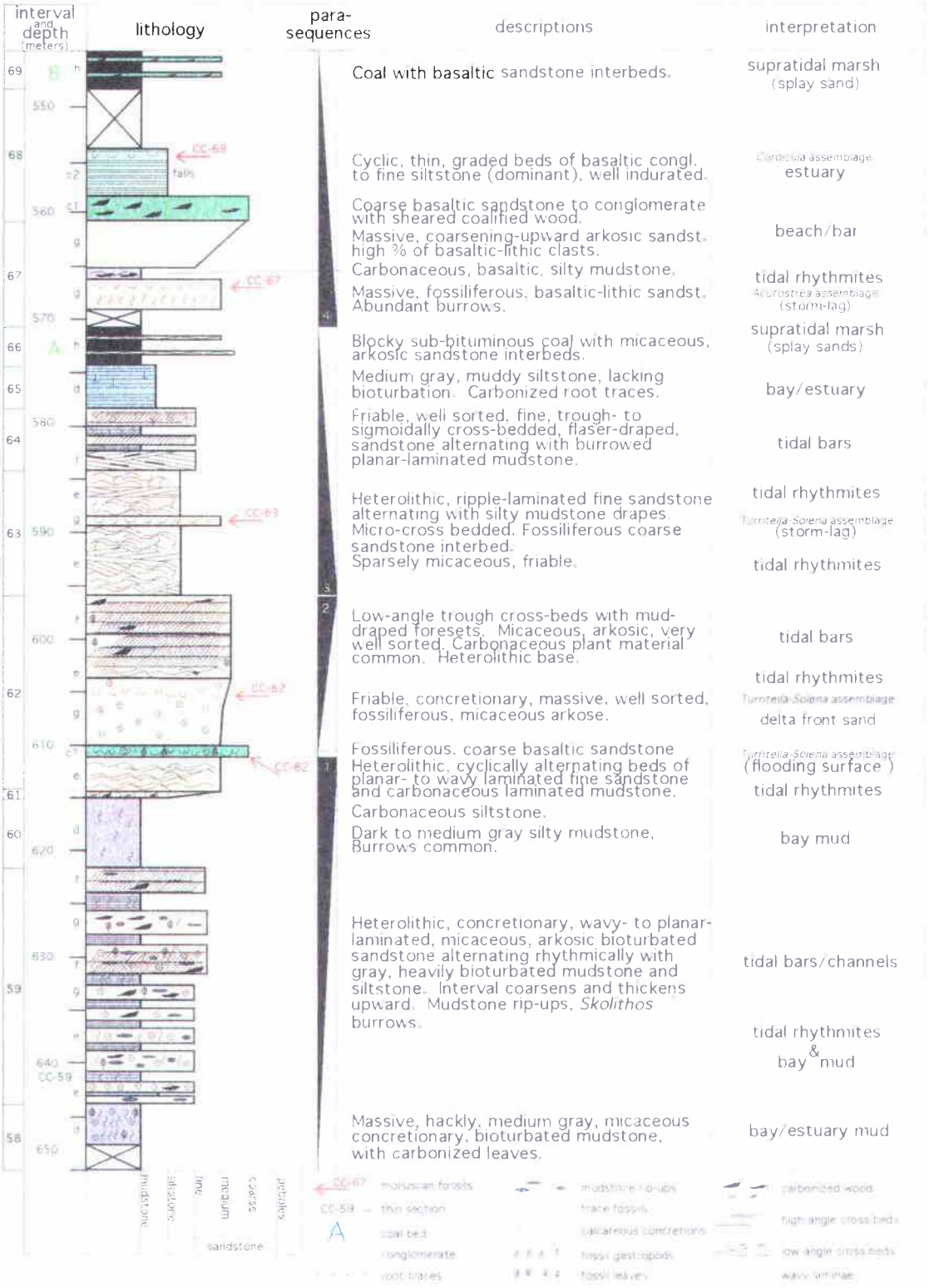

Figure 6: Descriptions and lithofacies of parasequences 1 through 4 of the Coal Creek section.

Scoured into the upper surface of lithofacies e (interval 62) is a 1-meter thick concretionary, highly indurated and calcite cemented, fossiliferous, coarse-grained basaltic sandstone of lithofacies c1 that marks the base of parasequence 2 (Figure 6). The sandstone is massive, poorly-sorted, coarse- to medium-grained, with sub-angular basaltic clasts and a minor (< 10%) micaceous, arkosic component. Molluscan fossils (nearly a coquina in places) of the *Turritella-Solena* assemblage (macrofaunal sample cc-62), including the thick-shelled species *Venericardia clarki* (some to 10 cm), *Turritella uvasana stewarti, Pitar californiana,* and *Polinices nuciformis* (Nesbitt, personal communication, 1999), are disarticulated, fragmented, and worn. Vertical *Skolithos* or *Thalassinoides* burrows 2-cm wide and 10-cm long, filled with dark brown sandstone, are rare.

Abruptly overlying this coarse-grained volcanic sandstone is 7 meters of concretionary, friable, medium-grained, well-sorted, massive, micaceous, arkosic sandstone. Bedding is evident in the form of a few horizons of carbonaceous plant fragments. Calcareous spherical concretions range from 2 to 5 cm in diameter, with as many as 10 per square-meter of outcrop. From 5 to 7 meters above the base, this unit becomes coarser-grained and more fossiliferous with abundant *Acutostrea idriaensis* oysters (*Acutostrea* assemblage) mixed with several species of the *Turritella-Solena* assemblage.

In sharp contact with the coarse-grained sandstone beneath, is a 1.5-meter thick heterolithic unit of alternating thin beds of micro-cross laminated fine to medium-grained micaceous, arkosic sandstone and ripple-laminated carbonaceous mudstone and siltstone

(lithofacies e). Carbonized leaf fragments and coalified plant debris are rare. Carbonaceous, finer-grained interbeds consist of ripple-laminated, dark gray, monolithic mudstone and siltstone. The top of this unit grades upward to a 7-meter thick sequence of relatively low-angle tangential cross-beds with mud-draped foresets (Figure 7a). This uppermost portion of parasequence 2 is light to medium brown, very well-sorted, medium sandstone devoid of any noticeable trace fossils, mollusks, concretions, or mudstone rip-ups. Cross-bed sets are lenticular and range from 0.3-0.7 meter thick. Mud-drapes are 1-3 mm thick, dark gray to black, and are most concentrated on the lower foresets, becoming progressively thinner and less distinct upward within each cross-bedded lense. A carbonaceous shale interbed exists half way through this cross-bedded unit.

Several lithofacies (including c1, d, e, and f) from the two underlying parasequences are repeated in parasequence 3; however, this parasequence terminates with coals in its uppermost beds (lithofacies h, Figure 6), and is therefore a fining- and thinning-upward succession. This succession also differs from parasequences 1 and 2 in that lateral changes in lithofacies across several kilometers can be correlated (Plate 2). The upper coal A of parasequence 3 (intervals 66, 82a, and 88) is a marker bed along nearly the entire northern half of Coal Creek, allowing for confident placement of units within the stratigraphic column.

Interval 63, and its correlative intervals 82b (section #3) and 86 (section #4), form the base of parasequence 3. Interval 63 consists of 12 meters of heterolithic (lithofacies e), ripple-laminated sandstone (70%) alternating with silty mudstone (30%), with a 1-meter thick-bedded, basaltic, coarse-grained, fossiliferous sandstone (lithofacies c1) 7

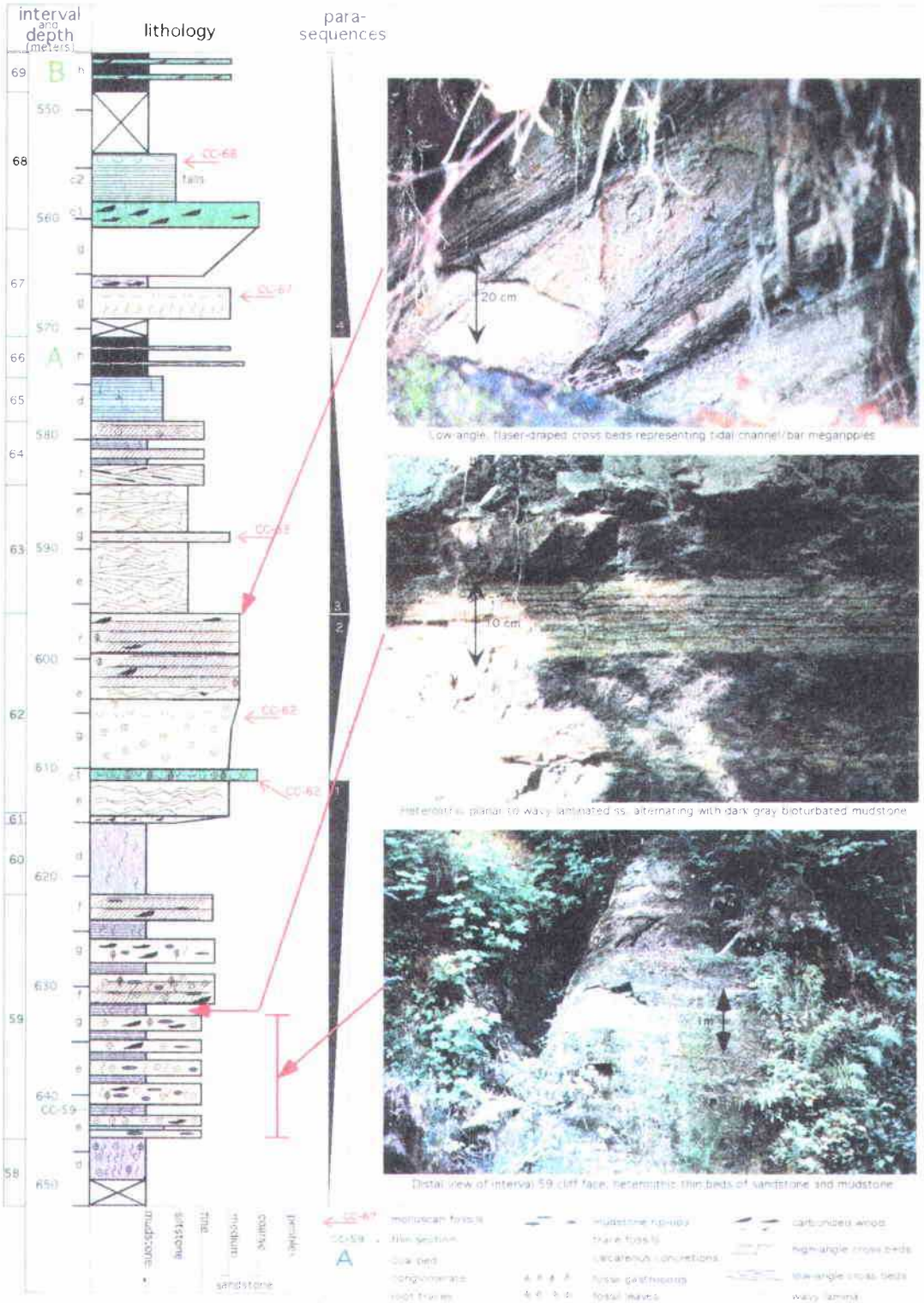

Figure 7: Photographs of lithologies of Coal Creek parasequences 1-4.

meters from the base (Figure 6, Plate 2). Contact with the underlying tangentially cross-bedded, mud-draped upper sandstone unit of interval 62 is abrupt. The sandstone component of this heterolithic facies is fine-grained, arkosic, sparsely micaceous, friable, well-sorted, pale yellowish brown, and ripple laminated and micro-cross bedded throughout. Individual sandstone beds range in thickness from 2 mm to 20 cm, and are lenticular over several meters. The mudstone component of this interval forms thin, discontinuous, ripple- to wavy-laminated drapes between cross-bed sets, and as armor on the foresets. Muddy laminae are less than 5-mm thick, dark yellowish brown, and nearly devoid of the carbonized leaves and twigs of similar lithofacies lower in the stratigraphic section. The 1-meter thick fossiliferous, dark brown, basalt volcaniclastic interbed is poorly-sorted, with subangular to rounded clasts ranging in size from fine- to coarse-grained sand. Color is dark brown, weathering to light brown. Molluscan fossils of the *Turritella-Solena* assemblage (two species of *Pitar* and *Pachydesma_aragoensis*) are abundant and relatively unbroken or worn (macrofaunal sample CC-63).

Interval 63 correlates to interval 82b, 2 km to the northwest (section #3, Plate 2), which consists of heterolithic, ripple- to wavy- to planar-laminated, fine-grained arkosic sandstone, siltstone, and mudstone beds (lithofacies e). Siltstone laminae are micaceous and arkosic, pale yellowish brown, and mottled due to intense bioturbation to ichnofabric 5, particularly in the upper 3 meters, contrasting with the lithologically similar, but less bioturbated siltstone interbeds of interval 63. The correlative interval 86 (section #4, Plate 2), approximately 0.7 km northwest of outcrops of interval 82b, consists of ten meters of heterolithic wavy- to low-angle trough cross-bedded medium sandstone,

alternating with beds of highly carbonaceous mudstone and siltstone (lithofacies e). Interval 86 also contains sparse molluscan fossil shells of the *Turritella-Solena* assemblage (macrofaunal sample CC-86) including *Venericardia clarki, Siphonalia sopenahensis,* and *Polinices nuciformis,* and abundant burrows.

In gradational contact with the uppermost heterolithic beds of interval 63 is the lowermost of three sandstone beds of interval 64. This 2-meter thick interval consists of relatively low-angle trough cross-bedded, friable, well-sorted, fine-grained arkosic sandstone beds alternating with medium gray planar-laminated mudstone interbeds. One to two mm thick, wavy laminae of silt, carbonaceous shale, or mudstone occur as drapes on individual foresets or interbeds between sandstone lenses. Near the top, intermittent laminae of lignitic coal or carbonaceous shale, with 0.25-0.3-meter thick, fine-grained trough cross-bedded micaceous, arkosic sandstone alternating with carbonaceous sandstone or siltstone. Color on weathered surfaces ranges from grayish orange to very pale grayish orange. Overlying this sandstone, separating it from the overlying sandstone unit, is a 0.5-meter thick bed of massive medium gray silty mudstone, mottled by intensive bioturbation to ichnofabric 4-5 (lithofacies d).

The overlying arkosic sandstone is scoured into the mudstone interbed and consists of tangential to sigmoidal cross-beds lacking mud-draped foresets (lithofacies f or i). Beds are lenticular and several meters in length, with foreset laminae 1-2 cm thick defined by concentrations of mica. The sandstone is micaceous and arkosic, medium orange gray, well-sorted, medium-grained, and moderately friable. Another mottled, gray silty mudstone interbed (lithofacies d) separates this sandstone from the uppermost

unit of interval 64, a 2-meter thick, sigmoidally cross-bedded, well-sorted, micaceous arkose (lithofacies f). Most of this sandstone unit is relatively clean, medium-grained, and grayish orange, consisting of 3 or 4 nested megaripple sets separated by 2-cm thick sandstone interbeds. The uppermost portion is coarser-grained, and has abundant 1-cm thick dark brown, carbonaceous mudstone interbeds. Well preserved flame structures, load casts, clastic dikes, and convoluted bedding are common. Discoid calcareous concretions up to 2-meters in diameter occur near the top of this interval, forming convenient stepping stones across the creek.

The uppermost cross-bedded and concretionary unit of interval 64 is in sharp contact with interval 65, 4.5 meters of medium gray, muddy siltstone with little or no bioturbation (lithofacies d). The upper meter of this interval forms an underclay for interval 66 (with root traces), 3.5 meters of coal and carbonaceous shale (coal A) with micaceous, arkosic sandstone interbeds (lithofacies h) that form the cap of fining- and thinning-upward parasequence 3. This interval (lithofacies h) consists of three nearly 1-meter thick resistant, blocky-weathered sub-bituminous coals. Separating the coal beds are coarse-grained, thin beds of wavy-laminated and micro-cross bedded, poorly-sorted, micaceous, arkosic sandstones, dark colored due to a high percentage of disseminated carbonaceous plant debris.

The correlative stratigraphic intervals of these coal beds with underlying carbonaceous siltstone (intervals 66 and 65 respectively, section #1, Plate 2) are intervals 82a (section #3) with underlying siltstone unit possibly covered) 1.75 km to the northwest, and intervals 88 and 87 (section #4), 2.5 km to the northwest (Plate 2). These

marker beds are repeated in the creek due to extensive faulting and folding in the northern part of the creek. Coal interval 82a differs from interval 66 in that it consists of about 3-meters total thickness of lignitic to sub-bituminous coal, separated into several coaly, wavy-bedded units by carbonaceous mudstone, siltstone, and tuffaceous siltstone interbeds (lithofacies h). These interbeds are intensely bioturbated, mottled light gray and light brown due to bioturbation to ichnofabric 4, and rich in carbonized leaf fragments, twigs, and roots. Correlative sub-bituminous coal interval 88 in the northwest part of Coal Creek (0.75 km from interval 82a) is 2.5 meters thick, without interbeds, and weathers to a blocky, resistant cliff in the northwest part of Coal Creek. The underlying siltstone (interval 87) is a 2-meter thick, medium gray, intensely bioturbated siltstone, coarser-grained than the equivalent intervals in the southeast part of Coal Creek. Overlying the interval 88 coal A, in this most northwest exposure of parasequence 3, are 3 meters of low-angle trough cross-bedded, well-sorted, medium-grained sandstone with flaser bedded foresets (lithofacies f).

Parasequence 4 (Figure 6, Plate 2) drastically changes in lithology from dominantly basaltic sandstone to the south, to dominantly micaceous and arkosic sandstone to the north. Local depositional conditions over a 4-km distance have resulted in a fining-upward subtidal to marsh succession to the south, and a coarsening- and thickening-upward succession to the north (all lithofacies associations, however, are indicative of shoaling-upward, or delta progradation). Correlation of these intervals with such disparate lithologies is possible due to their position stratigraphically above the

upper coal of parasequence 3 (coal A), and beneath the very thick and distinctive cliff forming volcaniclastic interval above (parasequence 5, Figures 9, 10, and 11, Plate 2).

Parasequence 4, in the southernmost exposure (section #1), begins with a fossiliferous, medium- grained basaltic (60%) and micaceous, arkosic (40%) sandstone above a 2-meter covered interval (lithofacies c1 or g). This lowermost unit of interval 67 is medium gray, poorly-sorted, fine- to coarse-grained with <10% altered basaltic clasts, heavily bioturbated to ichnofabric 4 toward the base and ichnofabric 1 toward the top, disturbing most of the original laminations and bedding. The upper 1.5 meters contains a molluscan fossil assemblage consisting of *Acutostrea idriaensis* and *Pitar eocenica* (macrofaunal sample CC-67, Nesbitt written communication 1999, Appendix I). Discontinuous laminae of carbonized twig and leaf fragments occur in recognizable bands, hinting at original bedding. Above this unit is a basaltic, muddy siltstone bed 1-meter thick (lithofacies d or c2), with wavy laminations and abundant chunks of carbonaceous plant material. This is in sharp upper contact with 3 meters of massive, coarsening-upward lithic arkosic sandstone (lithofacies g) that is both basaltic (50%) and feldspar and quartz rich (50%). Clast size at the base is fine-grained sandstone, but grades upward to a poorly-sorted, mostly basaltic coarse-grained sandstone. This upper portion of interval 67 correlates to interval 76, 0.6 km to the northwest (Plate 2).

After approximately 2 meters of cover, the basal unit of resistant interval 68 forms a 4-meter high waterfall in Coal Creek (Figure 8a). This coarse basaltic sandstone to fine pebble conglomerate (Figure 8b) is very poorly-sorted, medium to dark gray fresh but weathers to grayish orange and dark brown, and well indurated by calcite cement

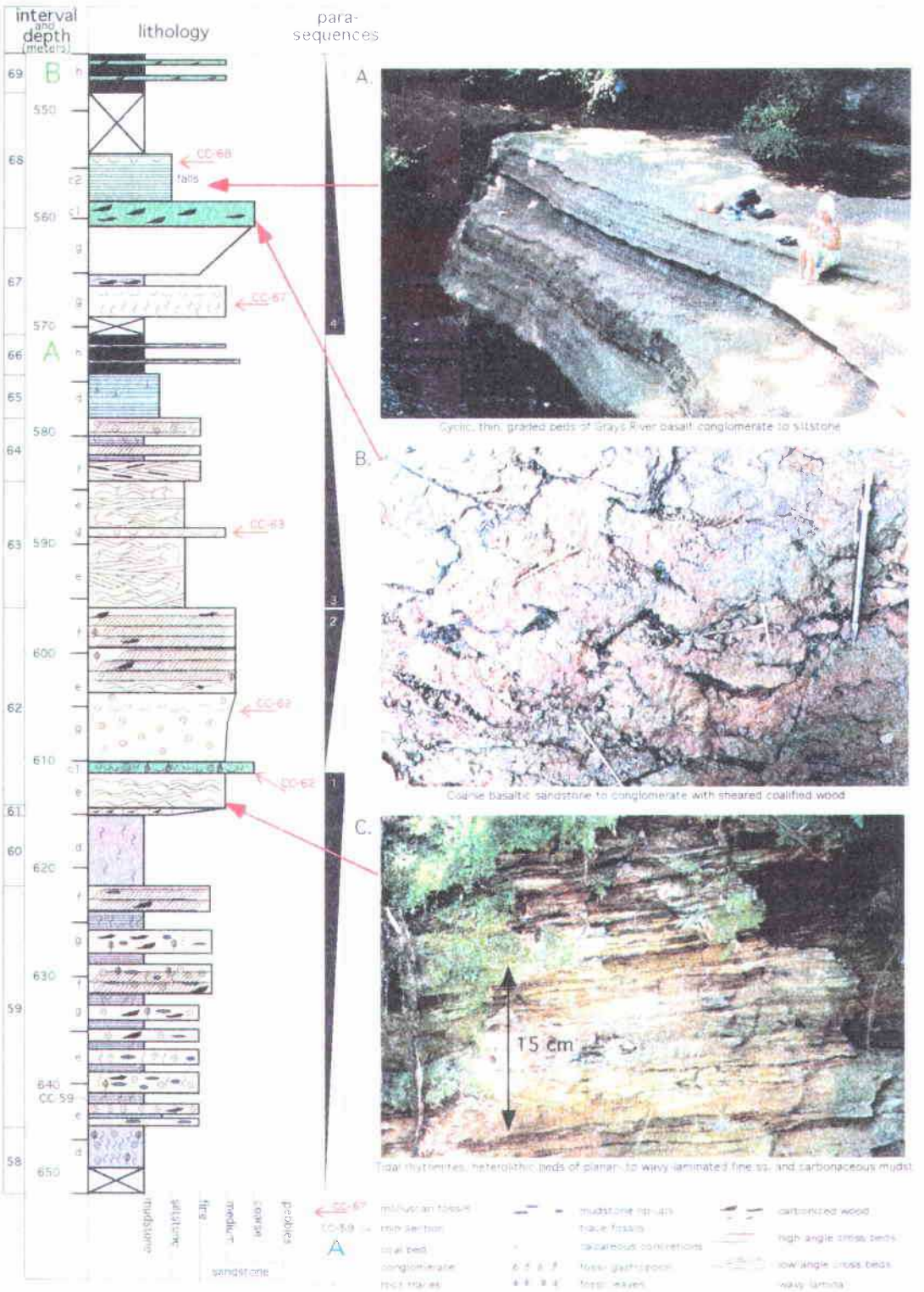

Figure 8. Photographs of lithologies of Coal Creek parasequences 1-4.

(lithofacies c1). A unique feature of this unit is the randomly oriented and apparently sheared pieces of bituminous-grade carbonaceous plant material. Individual pieces have a central body of thicker (5-15 cm) carbonized plant material, with 1 to 3 branches a few centimeters long in random orientations. These appear to be preserved primary structures, perhaps carbonaceous flame structures with associated load casts (Figure 8b). The bulk of interval 68, well exposed in the face of the waterfall, consists of cyclic, graded basalt volcaniclastic beds ranging in thickness from a few mm to 30 cm in the thickest bed (lithofacies c2, Figure 8a). Thicker beds are fine pebble conglomerate or coarse-grained sandstone at the scoured bases, grading upward to a fine-grained basaltic sandstone or siltstone. Thinner laminae, in turn, grade upward from fine-grained sandstone at the base to fine basaltic siltstone at the top. Color ranges from dark to light gray when fresh, and weathers to light brown. Approximately 1 meter from the top of this interval is a 0.3-meter thick basaltic siltstone bed with abundant brackish water articulated *Corbicula cowlitzensis* bivalves (macrofaunal sample CC-68, Nesbitt written communication 1999, Appendix I).

Farther upstream, after about 4 meters of cover, interval 69, a 3-meter thick unit, consists of resistant, sub-bituminous, blocky coal (coal B, Plate 2) with carbonaceous sandstone and silty sandstone interbeds (lithofacies h) that cap parasequence 4. Brownish resistant sandstone interbeds are basalt-volcaniclastic, well-indurated by calcite cement, and poorly-sorted, with subrounded clasts ranging from fine to coarse sand-size (largest clast is 3 mm), and are the stratigraphically lowest units containing euhedral greenish

black augite crystals (1-mm long). Carbonaceous plant material (some leaves nearly whole) is common, with <1% mica.

The correlative intervals 76 (section #2, lithofacies g, petrology sample CC-76) and lower 77 (lithofacies h), 0.5 km to the north, consist of a basal basaltic sandstone correlative to the upper portion of interval 67 (Plate 2). This mostly massive, medium gray, medium-grained lithic sandstone is moderately well-sorted, with rounded clasts and a few carbonaceous laminae. Five meters from the base, this sandstone is highly (calcareous) concretionary, and the uppermost 2.5 meters is wavy-laminated with carbonaceous, basaltic, siltstone interbeds. The cyclic, graded beds forming the waterfall and resistant ledge in interval 68 (Figure 8a) pinch out to the north (Plate 2), so that in this part of the section, coal B with sandy interbeds (lowermost interval 77) sits directly above interval 76. The lower coal of interval 77 is approximately 2-meters thick and has abundant fine- to medium-grained, poorly-sorted basalt lithic sandstone interbeds, containing 1-mm long euhedral augite crystals.

Lithofacies of fining- and thinning-upward parasequence 4 change drastically 1.2 km to the northwest of exposures of intervals 76 and lower interval 77. Here, micaceous, arkosic lithofacies dominate and the uppermost coal unit (coal B of lowermost interval 77b), which occurs as an interbed within the volcaniclastic unit, has pinched out. Interval 80 (section #3), and 90 and 91 (section #4) are separated by approximately 1.1 km, but exposures in Coal Creek occur nearly along strike (see Coal Creek inset, Plate 2). Interval 80 consists of 2 meters of silty mudstone (lithofacies h) in sharp contact with the upper coal (coal A) of parasequence 3, and with similar lithology to the interbeds within

the coal. The mudstone is dark to medium gray, hackly, sparsely bioturbated, and contains minor fragments of carbonized leaves and twigs.

Ten meters of cover separate the lower mudstone of interval 80 from the 4-meter thick upper sandstone (lithofacies f). The base is massive, coarse-grained, micaceous, and arkosic with a high percentage (~30%) of basalt and rounded siltstone clasts. The lower half of this unit is very poorly-sorted, light olive gray when fresh to dark yellowish orange when weathered, and contains discontinuous laminae of carbonaceous plant material and abundant unidentifiable calcareous molluscan shell fragments. The upper two meters is low-angle trough-cross bedded, with abundant mica and carbonaceous debris defining individual foresets, and contains abundant calcareous concretions,

Together, intervals 90 and 91 are 15 meters thick (section #4, Plate 2), consisting of a lower coarse-grained fossiliferous sandstone bed (interval 90, lithofacies c1, *Acutostrea idriaensis* macrofaunal sample CC-90, Nesbitt written communication 1999, Appendix I) and a thick overlying muddy siltstone (interval 91, lithofacies d). The lower sandstone is coarse-grained, massive, poorly-sorted, micaceous, and arkosic with 20-30% rounded basalt-lithic clasts. Abundant *Acutostrea idriaensis* oyster shells exclusively occur in this bed (Nesbitt, written communication 1999, Appendix I). The overlying interval 91 is nearly 13 meters thick and grades imperceptibly upward from a micaceous, arkosic, mostly massive silty mudstone to a siltstone. Color ranges from light to dark gray, with abundant carbonaceous plant material and no noticeable trace fossils.

Parasequence 5 (Figure 9, Plate 2) perhaps should not be considered a true parasequence, but rather an interfingering Grays River volcaniclastic basaltic debris or

hyperconcentrated flow deposit within the deltaic Cowlitz Coal Creek section. It consists of up to 35 meters of multiple basaltic, matrix supported breccias, conglomerates, and coarse-grained sandstones (lithofacies c1) and interbedded basaltic siltstones (lithofacies c2, Figure 10, geologic map unit Tvgs2, Plate 1), with minor micaceous, arkosic sandstone interbeds up to a few meters thick. This distinctive unit is used to correlate the southern (upper) part of the Coal Creek section with the northern (lower) part of the section, across the Coal Creek Fault (Plate 2, Coal Creek inset map and cross section C-C').

Intervals 53 (lower) and 54 (section #1, Figures 9 and 11c) are the stratigraphically lowest units in the southern Coal Creek section (included in section #1 with the correlative intervals 70, 71, 72, and 73 for the purpose of simplifying the Coal Creek section diagram, plate 2), and consist of about 25 meters of basaltic sandstone (petrology sample CC-53b), and graded beds of basaltic conglomerate to siltstone (petrology sample CC-54) with numerous thin interbedded basalt lithic, micaceous, arkosic sandstones. Portions of the pebbly debris flow deposit beds are breccias with angular to subrounded basaltic clasts in matrix support, with euhedral augite crystals ranging in diameter from 0.5 to 5 mm. Coarse sandstone to conglomerate intervals have large (1-3 cm) wide flattened carbonaceous mudstone rip-ups. Color ranges from dark gray to brownish gray when fresh, but weathers to light brownish gray. Interval 53 contains a molluscan fossil assemblage 0.6-meters thick of abundant (coquina in places) *Acutostrea idriaensis* oysters, with one *Pitar eocenica* specimen obtained (macrofaunal sample CC-53, Nesbitt written communication 1999, Appendix I). Numerous units

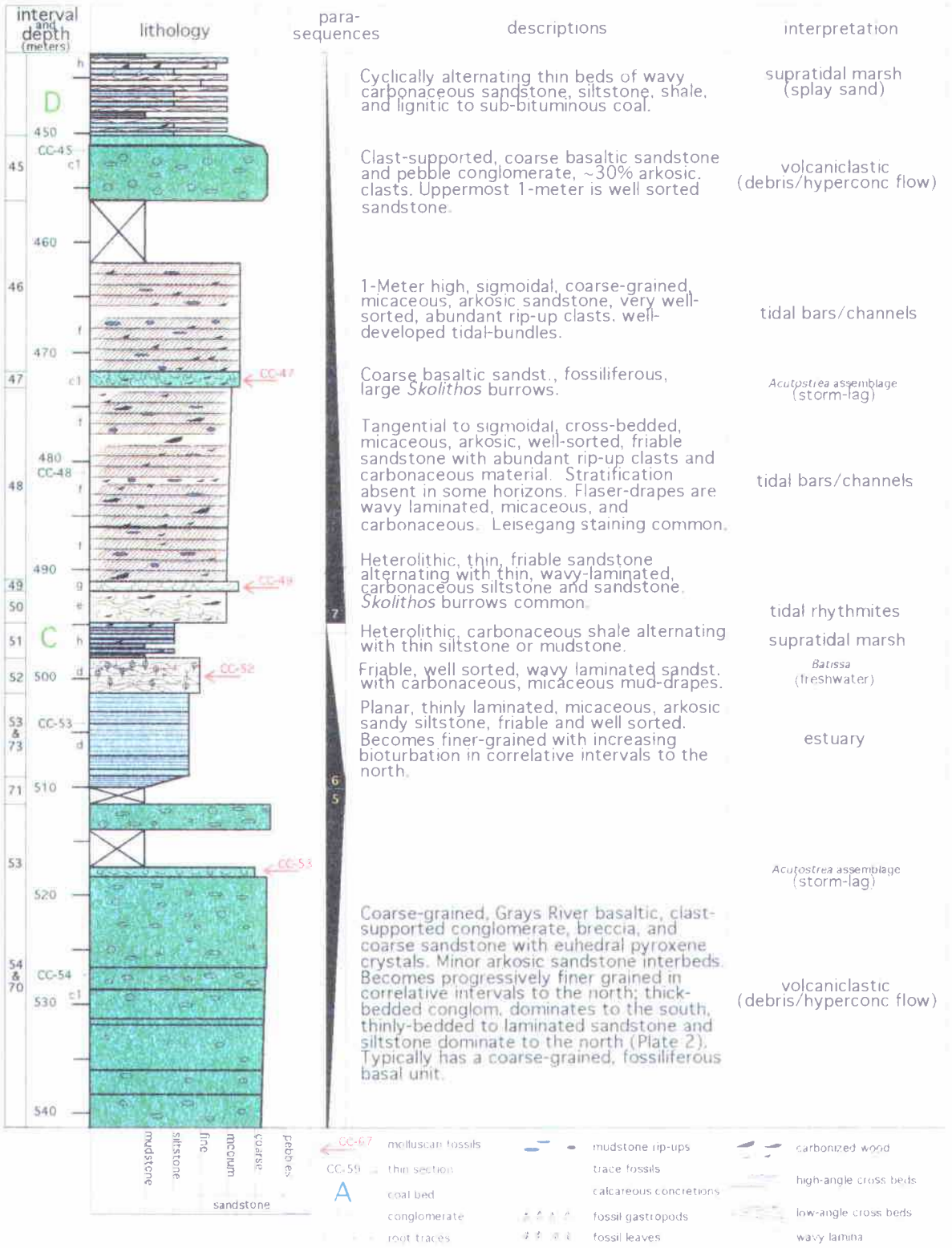

Figure 9: Descriptions and interpretations of parasequences 5 through 7 of the Coal Creek section.

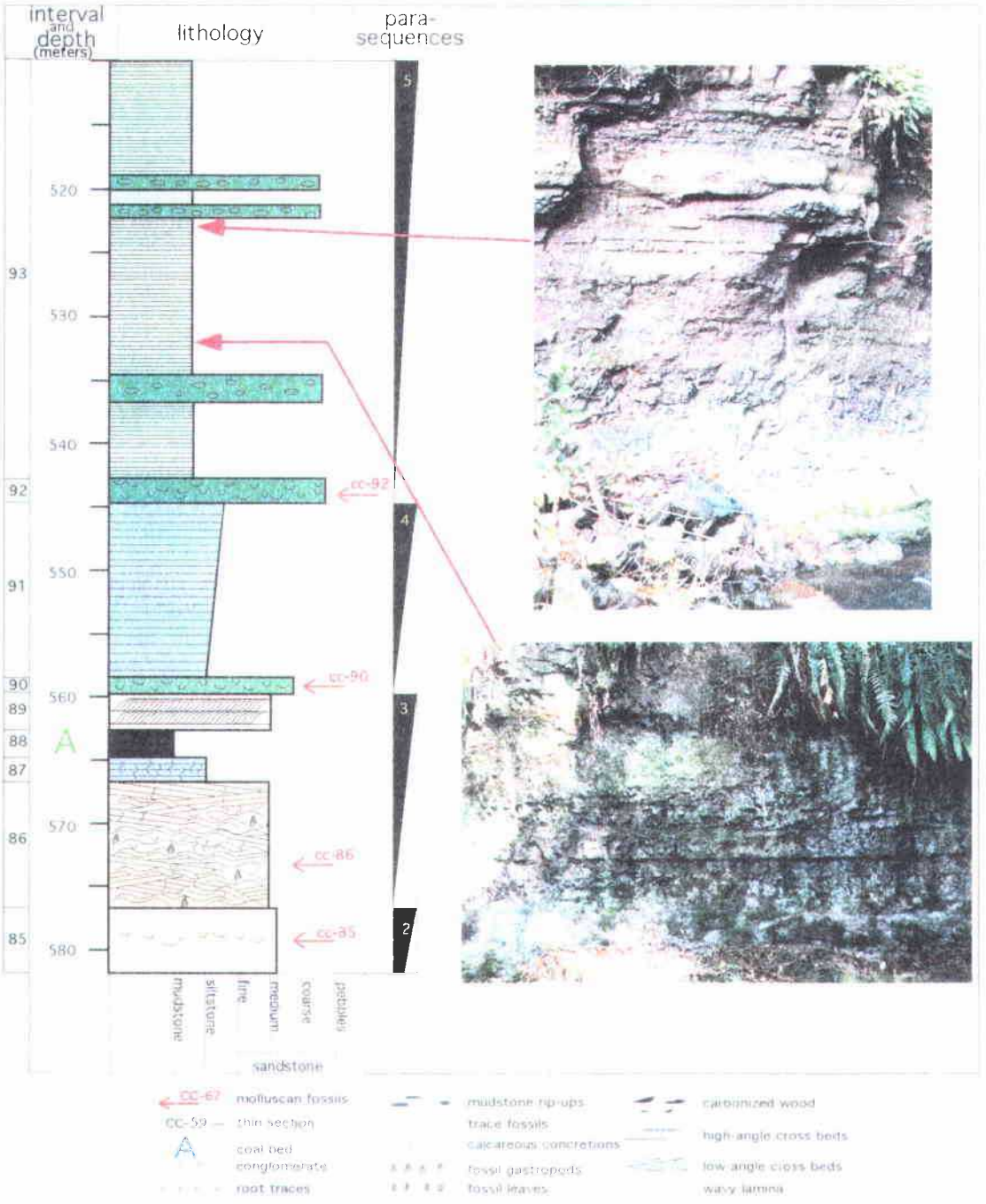

Figure 10: Photographs of lithofacies c2 from the northern part of Coal Creek, graded thin beds of basaltic sandstone to siltstones.

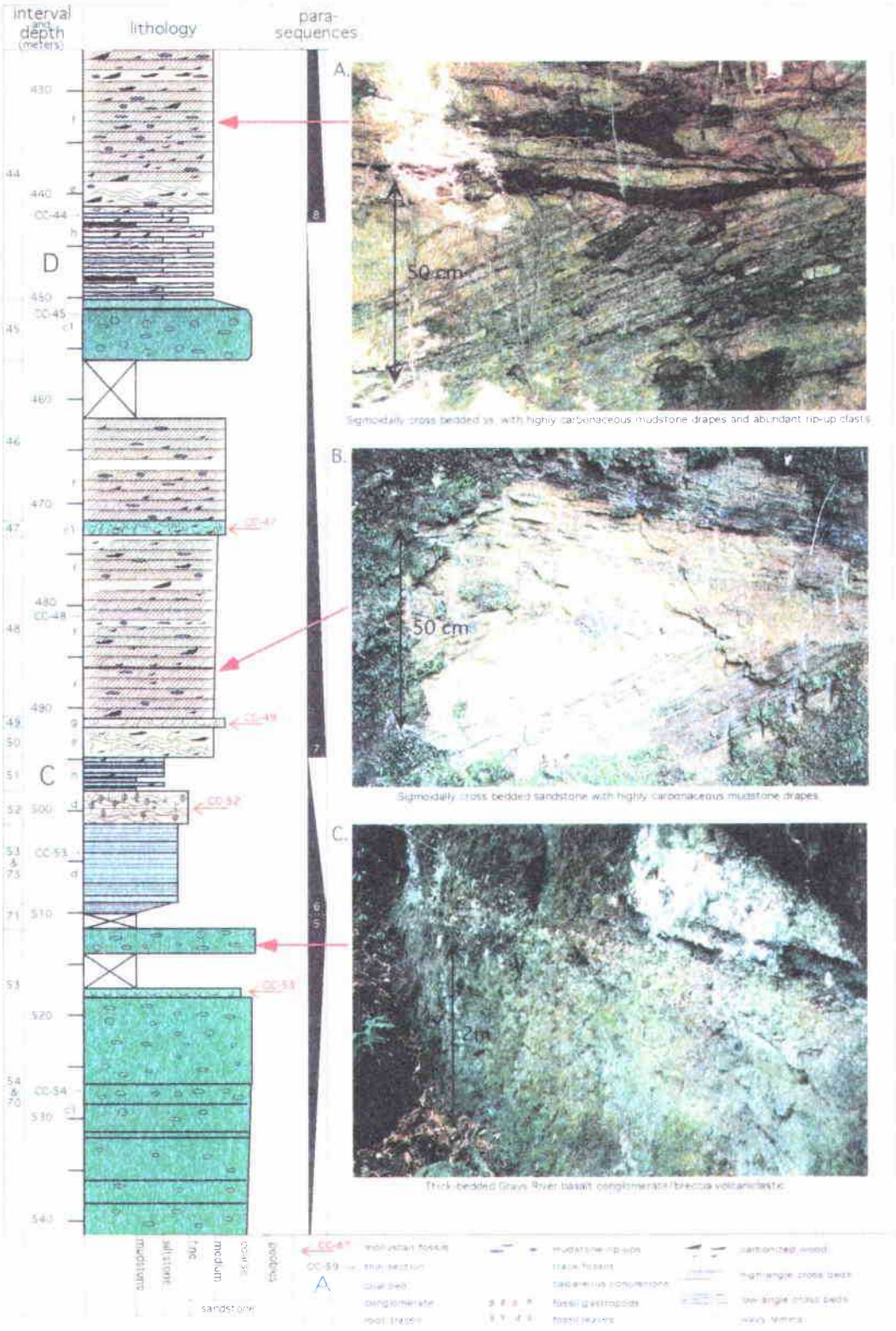

Figure 11: Photographs of lithologies of parasequences 5-8.

within interval 54 are similar in lithology to that described for interval 68 (lithofacies c2), cyclic, graded bedding of basaltic conglomerate to siltstone with minor wavy-laminated siltstone beds up to 3 meters thick.

Micaceous, arkosic interbeds, particularly common in intervals 53 and 54, are typically heterolithic, with thin sandstones alternating with thin mudstones and siltstone interbeds (lithofacies e). Sandstone interbeds up to 1-meter thick are lenticular, well-sorted, medium-grained, commonly ripple micro-cross bedded, contain <10% basalt lithic fragments and mudstone rip-ups, and range in color from light gray to medium orange gray. Mudstone and siltstone interbeds are medium brownish gray, wavy- to ripple-laminated, and rich in carbonized leaf and twig fragments. Flame structures of dark mudstone intruding into overlying sandstone interbeds are common and suggest rapid loading of sand on hydroplastic mud.

Interval 70, exposed nearly 2.1 km north of intervals 53 and 54, consists of approximately 30 meters of extremely poorly-sorted, clast supported, basaltic pebble to cobble conglomerate, with interbedded poorly-sorted basaltic breccias (similar to interval 53, Figure 11c). Largest basaltic clasts are cobble-sized (5-6 cm). This interval is well indurated with white sparry calcite cement; fractures are filled with white coarsely crystalline calcite. Bedding is on the order of one to several meters, defined by fine-grained sandstone or siltstone interbeds a few centimeters thick. Color is dark to medium gray when fresh, weathering to medium or dark brown. Euhedral augite crystals up to 0.5-cm long are common throughout, especially concentrated in the basalt breccia interbeds. Interval 77 (0.5 km north if interval 70, section #2, Plate 2) is similar but with

finer basaltic conglomerate or sandstone near the base. Basaltic siltstone interbeds (lithofacies c2, petrology sample CC-77) occur near the base, with very fine-grained silt in some beds. The base of interval 77 is a 1-meter thick bed of coarse-grained sand with disarticulated and fragmented *Acutostrea idriaensis* oyster valves (macrofaunal sample CC-77, Nesbitt written communication 1999, Appendix I). The base of the correlative thick basalt volcaniclastic unit 1.3 km to the northwest has a similar basaltic fossil rich horizon (interval 81, macrofaunal sample CC-81, section #3, Plate 2), scoured into the tangentially cross-bedded upper sandstone of parasequence 4 (interval 80). It is fine- to medium-grained basaltic sandstone with disarticulated and broken shells of the shallow marine *Turritella-Solena* molluscan fossil assemblage of Nesbitt (written communication, 1999). Overlying this bed is nearly 30 meters of cyclically alternating coarse-grained basalt volcaniclastic conglomerates interbedded with fine-grained sandstone and siltstone (lithofacies c1 and c2, interval 79, similar to interval 93, Figure 10a and b). Coarse-grained beds are 0.5 to 2-meters thick with finer- grained interbeds averaging 0.3-meters thick. Interval 79 is dominated by laminated micaceous siltstones near the base and pebble conglomerates toward the top.

The correlative section farthest to the northwest (section #4), interval 93 (Figure 10a and b), also has a basal fossiliferous unit (interval 92, macrofaunal sample CC-92) of very coarse-grained basaltic sandstone to pebble conglomerate, 2-meters thick, scoured into the underlying siltstones of parasequence 4 (interval 91). Molluscan fossils consist exclusively of the shallow-marine bivalve *Glycymeris sagittata* (Nesbitt written communication 1999, Appendix I). Overlying this bed is interval 93, the northernmost

interval exposed in Coal Creek, where this Eocene unit is in unconformable contact with an overlying Grays River flow. This sequence consists of 35 meters of planar- to wavy-laminated fine basaltic siltstone (lithofacies c2) with interbedded conglomerates (petrology sample CC-93) up to 2-meters thick containing euhedral augite crystals.

Overlying the thick basalt volcaniclastic intervals (parasequence 5) throughout the section are the relatively fine-grained, micaceous, arkosic sandstones in the lower interval of parasequence 6 (Plate 2). The southernmost exposure in Coal Creek is upper interval 53 and its nearly lithologically identical correlative interval 73 (combined in Figure 11 and Plate 2). These intervals consist of 3 mm to 1 cm planar-laminated, micaceous, arkosic, well-sorted, fine-grained, friable, and grayish orange sandstone (foreshore lithofacies g). Concentrations of mica and carbonaceous debris define internal stratification. The correlative interval 75 (and the uppermost 2 meters of interval 77, section #2), exposed 0.5 km to the north of interval 73, is a light gray, mottled, muddy, micaceous, arkosic siltstone (lithofacies d), with ~10% basaltic clasts, bioturbated to ichnofabric 5. Another 0.4 km to the northwest, correlative interval 78 is also an intensely bioturbated light gray siltstone containing 5 cm diameter spherical calcareous concretions.

In gradational contact with interval 53 (in the southernmost interval of parasequence 6, Figures 9 and 11) is interval 52, a 3-meter thick, well-sorted, friable, wavy-laminated and micro-cross-bedded, fine- to medium-grained, light orange brown, micaceous, and arkosic sandstone. Foresets within the micro-cross laminations are defined by highly micaceous and carbonaceous laminae. Well-preserved whole

carbonized leaves are common in the interbeds, as are articulated freshwater *Batissa newberri* bivalves (macrofaunal sample CC-52, Nesbitt written communication, 1999). Capping parasequence 6 is interval 51, 3 meters of black, extremely carbonaceous shale and coal (coal C) and siltstone (lithofacies h) in gradational contact with interval 52.

Parasequence 7 is a ~54-meter thick progradational shoreface succession (Figures 9 and 11). The lowermost interval 50 is heterolithic (lithofacies e), 3-meters thick, and consists of 2-5 cm thick micaceous, arkosic sandstone beds alternating with 1-10 mm thick, wavy-laminated carbonaceous siltstone and fine-grained sandstone. Sandstone interbeds are medium- to coarse-grained, well-sorted, friable, and range from light gray to moderate yellowish brown with pervasive liesegang limonite staining. Bioturbation by vertical *Skolithos* burrows 2-cm in diameter and several cm long to ichnofabric 1, sparse unidentifiable molluscan shell fragments, and large chunks of coalified wood are common. The wavy-laminated, fine-grained sandstone to siltstone interbeds are dark yellowish brown and have large pieces of carbonized leaves and twigs, and abundant, larger that average (2-3 mm) biotite and lesser muscovite flakes.

Interval 49 is in abrupt scoured contact with interval 50 and consists of medium to coarse- grained, poorly-sorted, micaceous, yellowish brown, arkosic sandstone with approximately 10% basalt lithic fragments, and 10% flattened clasts of carbonaceous plant debris. Fossiliferous shell hash is common, but fragmental beyond identification (macrofaunal sample CC-49, Nesbitt personal communication, 1999). Interval 48 is an 18-meter thick sandstone dominated by flaser-draped, 0.3-1 meter high tangential to sigmoidal cross-beds (lithofacies f, Figures 9 and 11), but massive in places (lithofacies

g). Sandstone foresets are micaceous, arkosic, medium-grained, well-sorted, friable, and contain abundant mudstone rip-up clasts and carbonized plant material. Color is light brownish gray weathering to grayish orange, with dark yellowish orange liesegang staining common in some intervals, forming evenly spaced bands resembling bedding. Foresets are typically 0.5-1 cm thick, mudstone flaser-bedded, with wavy carbonaceous and highly micaceous mudstone and siltstone laminae (petrology sample CC-48). Beds with steeper sigmoidal foresets are relatively clean, with little dark carbonaceous plant material on the foresets. This interval coarsens slightly in the upper 5 meters, with some contorted foresets due to slumping.

A 1.5-meter thick coarse basalt volcaniclastic sandstone (interval 47, lithofacies c1) with broken *Acutostrea idriaensis* oyster valves separates the lower cross-bedded interval and the overlying coarser-grained sigmoidally cross-bedded interval 46. This micaceous, arkosic sandstone interval, with cross-beds to 1-meter high is well-sorted and friable, ranging from medium- to coarse- grained. Color is light grayish orange weathering to dark yellowish orange. Flaser-bedding is defined by extremely micaceous and dark gray carbonaceous mudstone and siltstone drapes on individual arkosic sandstone foresets and also between cross-bed sets.

After approximately 6 meters of cover is a 5-meter thick basalt volcaniclastic (interval 45, Figures 9 and 11, Plate 2), poorly-sorted coarse-grained sandstone and conglomerate (lithofacies c1, petrology sample CC-45) with ~30% arkosic grains. The lower 3 meters is a dark olive gray, well-indurated, calcite-cemented, extremely poorly-sorted, framework-supported, ledge-forming conglomerate. Basalt clasts are well-

rounded and up to 0.5 cm in diameter. The uppermost meter is fairly well-sorted, massive, basaltic sandstone.

In sharp contact with interval 45 is the lower 9 meters of interval 44, a coal-bearing sequence that caps parasequence 7, composed of cyclically alternating 0.3-meter thick beds of carbonaceous sandstone (petrology sample CC-44), carbonaceous siltstone, carbonaceous shale, and coal seams (coal D, lithofacies h). Sandstones and siltstones are micaceous, arkosic, well-sorted, wavy- to micro-cross laminated, and typically grayish orange. Small (<1 cm) rounded mudstone and carbonaceous shale rip-up clasts and carbonized wood debris are common throughout. Individual coal seams are lignitic to sub-bituminous, and 6-7 cm thick.

Parasequence 8 is another set of thinning- and fining-upward lithofacies terminating in a coal (coal E, Figure 12, Plate 2). The lowermost 2 meters, near the middle of interval 44, are heterolithic with brownish sandstone alternating with grayish muddy siltstone (lithofacies e). The lithology is similar to that described for the base of parasequence 7 (interval 50). Abundant carbonized leaf and twig fragments with mica are common in finer sandstone interbeds. Wavy bedding, micro-cross laminations, and mudstone rip-up clasts, are common throughout. Silty, organic-rich (carbonaceous) interbeds are bioturbated to ichnofabric 4. This lithology grades upward into approximately 13 meters of sigmoidally cross-bedded medium to coarse-grained micaceous, arkosic sandstone with highly carbonaceous and micaceous mudstone-draped foresets up to 1.3-meters high. Mudstone couplets define the tidal bundles (lithofacies f, Figure 11a). Carbonaceous mudstone rip-up clasts range from a few millimeters to a

maximum of 10-cm long, and tend to concentrate along mud-draped foresets. The sandstone component is medium- to coarse-grained, moderately well-sorted, and friable to well-indurated, cemented by calcite or limonite. Less than 10% of clasts are basaltic in composition. Dark brown to black mudstone drapes are highly carbon-rich (i.e., carbonaceous shale), and can be up to 10-cm thick. Individual cross-bedded lenses have scoured bases eroded into the underlying cross-beds, creating nested sets. Contorted bedding and clastic sandstone dikes occur infrequently. Individual beds up to 1-meter thick can be massive with randomly oriented carbonaceous plant material (lithofacies g?).

Overlying interval 44 in sharp contact is interval 43 (Figure 12, Plate 2), a 3-meter thick coarse-grained basaltic sandstone (lithofacies c1). The lower 1.5 meters is moderately well-sorted, dark gray, massive, and coarsens-upward from medium- to coarse-grained sandstone. The upper 1.5 meters is coarse-grained and poorly-sorted, with disarticulated and fragmented *Acutostrea idriaensis* fossil oyster valves (Nesbitt written communication 1999, Appendix I). In sharp contact with interval 43 is interval 42, a 4-meter thick, coarse-grained micaceous and arkosic sandstone with discontinuous, wavy carbonaceous laminae (lithofacies g). Sandstone is well-sorted, grayish orange, and parallel-laminated in places. Vertical *Skolithos* burrows to ichnofabric 1 are sparse and widely scattered. This is overlain in sharp, scoured contact with interval 41, a 2-meter thick, dark olive gray, basaltic pebble conglomerate to coarse-grained sandstone containing disarticulated mollusks of the *Turritella-Solena* fossil assemblage (Nesbitt written communication 1999, Appendix I). Lenticular, brownish, basaltic siltstone interbeds 1-5 cm thick and a few centimeters long occur throughout. Bedding is 0.3-0.5

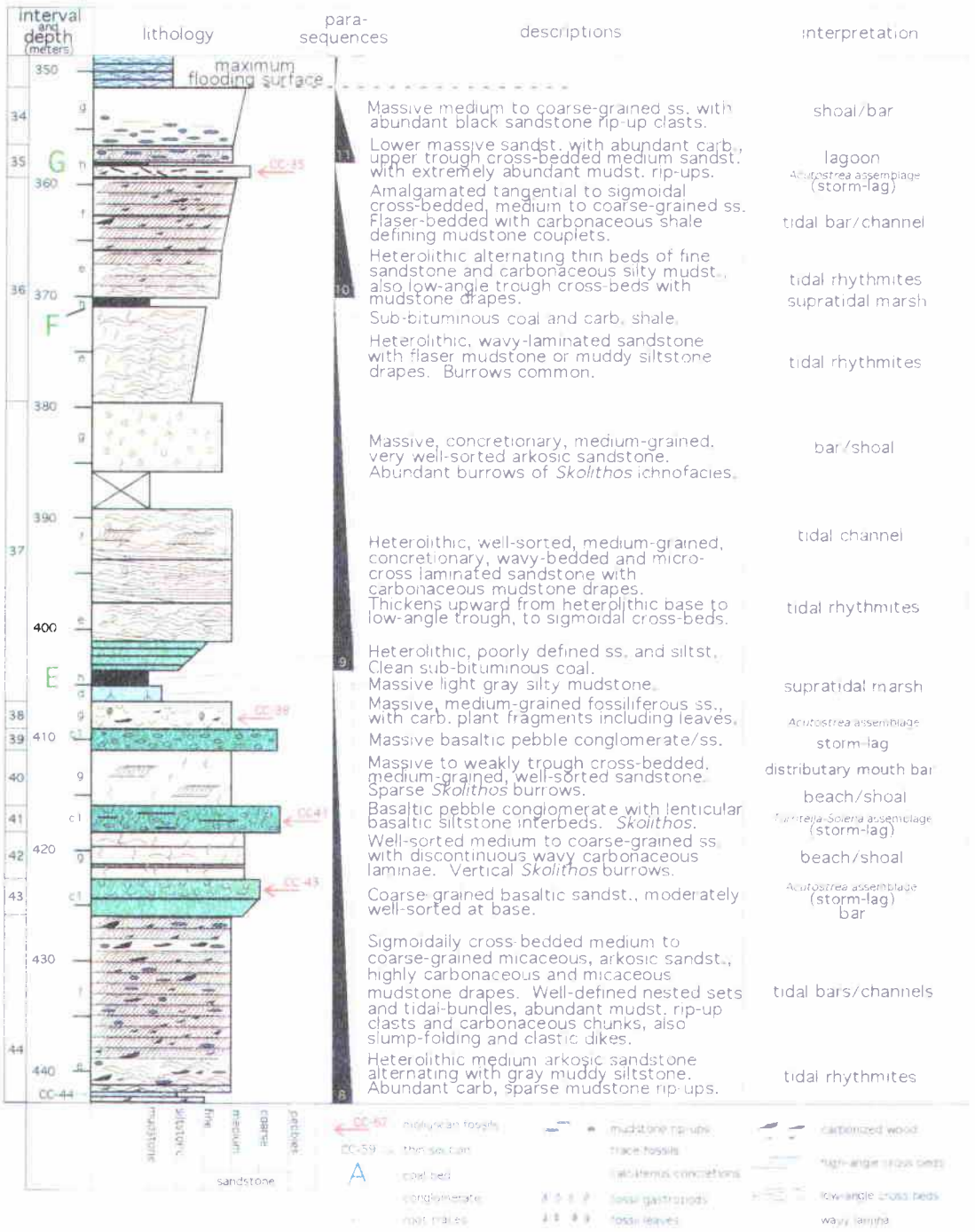

Figure 12: Descriptions and interpretations of parasequences 8 through 11 of the Coal Creek section.

meters thick with poorly developed low-angle trough cross-bedding in places (Lithofacies f to g).

Interval 40 is in sharp contact with interval 41. This interval is 5-meters thick, and consists of massive to faintly trough cross-bedded, medium-grained, well-sorted, micaceous, and arkosic sandstone. Discontinuous carbonaceous laminae and sparse *Skolithos*-type burrows occur throughout. Overlying this unit in sharp scoured contact is another basaltic pebble conglomerate, medium-grained, and 2-meters thick. This unit is unique in having a bimodal grain-size distribution of 0.5 mm medium-grained sand and pebble-sized (0.3 cm diameter) conglomerate clasts. The unit is also unfossiliferous, and has no trace fossils, bedding, laminations, or grading. The overlying interval 38 is a 2-meter thick, medium-grained, micaceous and arkosic, light grayish orange sandstone. The oyster fossil *Acutostrea idriaensis* is common, with rare *Pitar eocenica* bivalves, (macrofaunal sample CC-38, Nesbitt written communication 1999, Appendix I). Coalified wood and carbonized leaves and twigs are found throughout. This unit is overlain by a massive light gray silty mudstone and a 0.6-meter thick clean sub-bituminous coal (coal E) with very few clastic particles (lithofacies h).

Parasequence 9 (Figure 12) fines- and thins-upward and includes interval 37 and the lower portion of interval 36. The lowermost three meters are heterolithic, consisting of alternating, poorly defined beds of sandstone and siltstone (lithofacies e). Throughout this interval, sandstone beds dominate and are invariably wavy-bedded and micro-cross laminated with carbonaceous mudstone-draped foresets. Sandstone beds are 1-10 cm thick, micaceous and arkosic, pale yellowish orange to dark yellowish orange and well-

sorted, with beds ranging from fine- to medium-grained. Spherical calcareous concretions up to 5-cm in diameter are common throughout. Micro-cross laminated sandstone beds with very little mudstone component grade upward into sandstone beds with a high percentage of mudstone and micaceous drapes. Laminae range from 0.5 mm on the foresets to 1-cm thick between sandstone lenses. This lithology gradually changes upward over the next 9 meters into thicker sandstone beds with low-angle (<10 degrees) trough cross-beds, and thicker mudstone-drapes. Near the top of this heterolithic sequence, higher-angle trough cross-beds and thick (1-5 cm) wavy-laminated mudstone drapes dominate (lithofacies f). This grades upward into a 9-meter thick, massive sandstone (lithofacies g) that appears to be in gradational contact with the underlying flaser-draped cross-beds. This unit is highly concretionary, medium- to coarse-grained, friable, and well-sorted with abundant large burrows of the *Skolithos* ichnofacies. The lowermost lithologic unit of interval 36 is an 8-meter thick wavy-laminated, heterolithic facies that consists of wavy-bedded, micro-cross laminated, fine- to medium-grained sandstone with abundant 1-mm thick flaser mud-drapes on 1-2 cm high foresets (lithofacies e). Sandstone beds range in thickness from 5 cm to 1 meter, are light gray weathering to grayish orange, moderately well-sorted, and defined by 1-cm thick wavy-bedded micro-cross laminated mudstone or muddy siltstone drapes which are dark gray, micaceous, and rich in carbonized leaf fragments. This lithology gradually becomes coarser-grained upward and passes into a medium-grained sandstone, with thicker sandstone interbeds and higher amplitude and higher angle cross-bedding, with thicker silty mudstone drapes. The upper meter is cyclically bedded 0.3-meter thick medium-

grained sandstone alternating with wavy-bedded, carbonaceous, silty mudstone interbeds. This lower portion of interval 36 is bioturbated throughout to ichnofabric 1-3. A nearly 1-meter thick coal (coal F) with carbonaceous shale separates the lower and upper portions of interval 36, and caps parasequence 9.

Parasequences 10 and 11are relatively thin, with a cumulative thickness of about 20 meters. This shoaling-upward lithofacies sequence could be interpreted as one shoaling-upward parasequence with carbonaceous shale interbeds. The lowermost 2-3 meters of parasequence 10 is a combination of the typical alternating bands of sandstone and carbonaceous silty mudstone (lithofacies e), and low-angle trough-cross beds with mudstone drapes (lithofacies f). Overlying these lithofacies is approximately 9 meters of amalgamated, flaser-bedded, tangentially to sigmoidally cross-bedded, medium- to coarse-grained sandstone. Cross-bedded sand units are either lenticular or wedge-shaped in cross section and up to 2- meters thick, with foresets up to 1-meter high. Typical foresets are 2-3 cm thick with carbonaceous, micaceous drapes consisting of wavy-laminated, 1-mm thick black siltstone and 1-mm thick light grayish orange fine-grained sandstone. Between cross-bedded lenses are black carbonaceous shale interbeds several centimeters thick, producing well-defined tidal mud-couplets.

Interval 35 overlies interval 36 in sharp contact, and consists of two discrete, nearly 1-meter thick sandstone units separated by a 0.3-meter thick coal (G) than caps parasequence 10 (Figure 12). The lowermost bed is coarse-grained sandstone containing rare *Acutostrea idriaensis* fossil oyster valves and abundant large pieces of coalified wood (lithofacies g, macrofaunal sample CC-35b). Overlying the coal in sharp contact is

the upper sandstone unit of interval 35, which constitutes the lowermost interval of parasequence 11. This example of lithofacies f, unique to the Coal Creek section, consists of relatively low-angle trough cross-beds with highly carbonaceous, dark gray to black, wavy-bedded sandstone laminae defining the foresets. This lithology grades upward into a trough cross-bedded to massive, medium to coarse-grained sandstone consisting almost exclusively of 1-5 cm diameter, organic rich, dark gray to black, medium- to coarse-grained sandstone rip-up clasts. Some horizons are clast-supported, rip-up clast conglomerates (Figure 13c) with a pale yellowish orange medium sandstone matrix, grading upward to a thick bedded to massive, coarse-grained, well-sorted, grayish orange sandstone. Dark gray to black rounded sandstone rip-ups become less common toward the top.

Parasequence 12 is a thickening- and coarsening-upward lower to middle shoreface succession, nearly 40-meters thick, that comprises the lower half of interval 33 (33d, 33c, and 33b, Figure 13 and 14, Plate 2). The relatively deep-water interval 33d was deposited in sharp contact over the wave-reworked, coarse-grained upper sandstone of parasequence 12 (interval 34). This lithofacies a (Figure 13b) is not expressed in the underlying Coal Creek section, and represents the beginning of a new system tract deposited on a transgressive marine flooding surface.

Interval 33d is approximately 14 meters of heterolithic fine-grained siltstone and dark gray mudstone (Lithofacies a, Figure 13a and b and Figure 14). It consists of discontinuous, ripple-laminated, micro-cross bedded, light gray siltstone lenses or discontinuous beds alternating with wavy laminated, dark gray, silty mudstone. Laminae

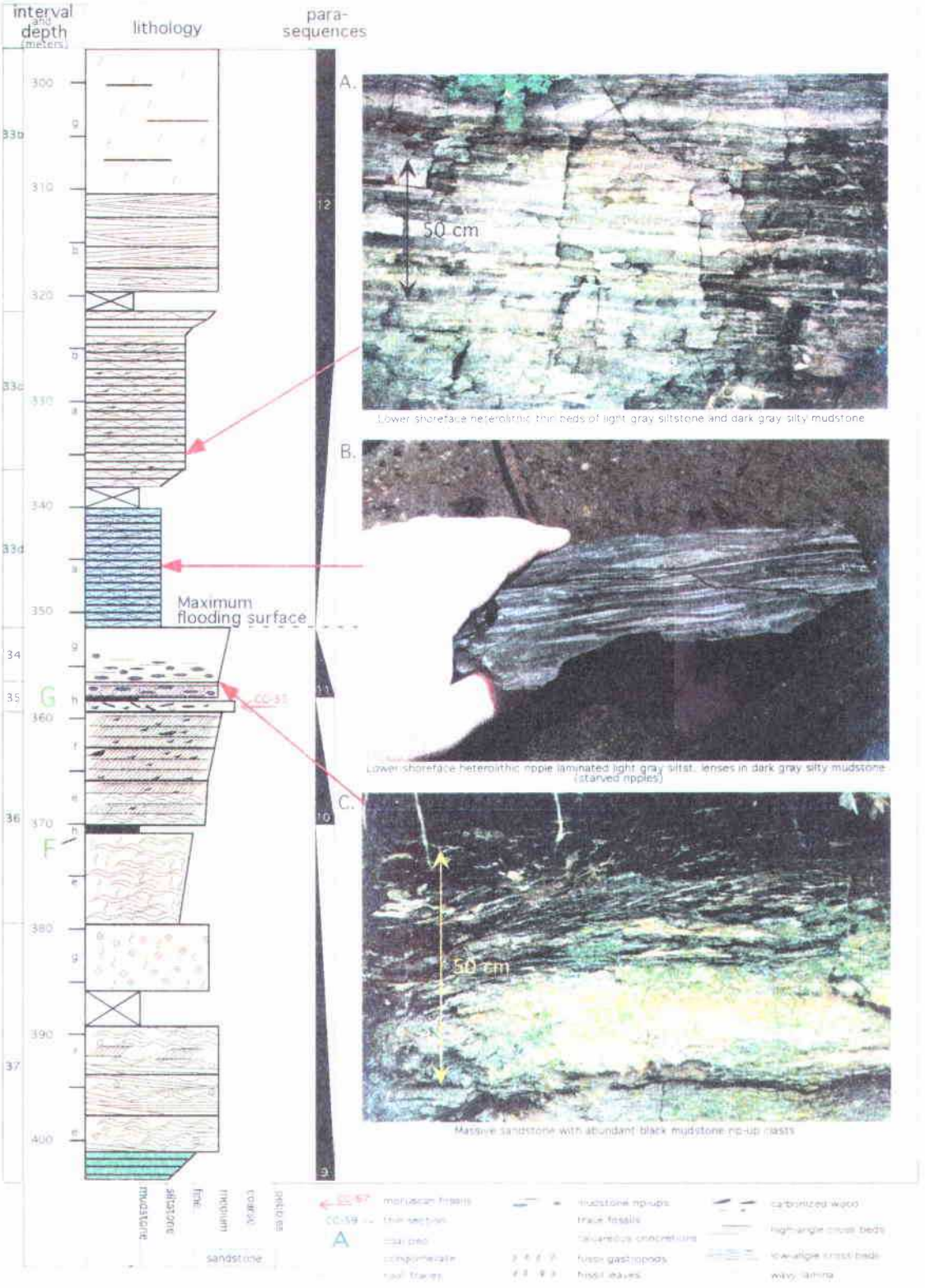

Figure 13: Photographs of lithologies of parasequences 9-12.

vary in thickness from 0.5 mm to nearly 1 cm. Horizontal bioturbation of the *Cruziana* ichnofacies is negligible, locally to ichnofabric 1. Light gray siltstone lenses have dark gray silty mudstone-draped foresets. Lenses tend to be symmetrical, with ripple foresets showing multiple current directions. Siltstone laminae are highly micaceous. Darker silty mudstone interlaminations are sparsely and finely micaceous, and are more laterally continuous than the fine-grained siltstone lenses, traceable over several meters.

Interval 33d grades upward into interval 33c, a heterolithic facies consisting of alternating continuous thin beds of light gray siltstone and very fine-grained sandstone, and dark gray silty mudstone (lithofacies a, Figure 13a and 14). Siltstone and fine-grained sandstone beds are wavy and range from 1-7 cm in thickness, coarser-grained beds are commonly highly micaceous and carbonaceous. Thicker and more continuous siltstone or very fine-grained sandstone beds have mud-draped hummocky and swaley internal cross-stratification. Mudstone drapes and laminations contain more silt, larger mica flakes, and larger pieces of carbonized plant material than interval 33d. This lithology grades upward into interval 33b, a low angle cross-bedded, hummocky and swaley fine-grained sandstone sequence nearly 15-meters thick (lithofacies b). Beds range from 0.3-0.5 meters in thickness. Sandstone laminae are 1-2 cm thick, parallel- to wavy-laminated, and defined by concentrations of mica and carbonaceous mudstone drapes. This sandstone is pale yellowish brown and weathers to dark yellowish orange, and is well-sorted and friable, with abundant *Thalassinoides* burrows. This hummocky- and swaley-bedded sandstone is in sharp, scoured contact with 14 meters of thick-bedded

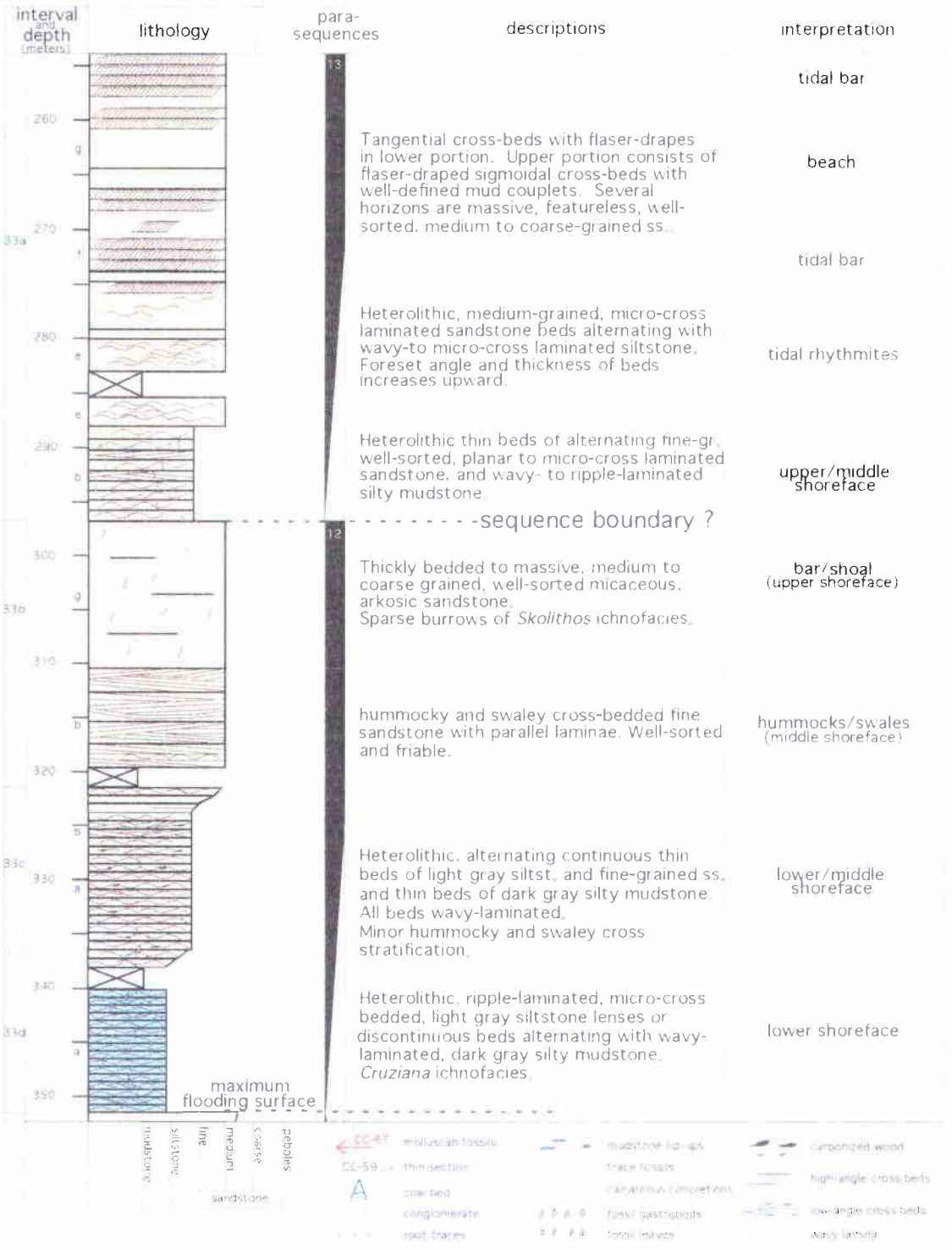

Figure 14: Descriptions and interpretations of parasequences 12 and 13 of the Coal Creek section.

(2 meters thick) to massive medium-grained sandstone with scattered *Skolithos* burrows (lithofacies g).

Parasequence 13 (interval 33a, Figure 14) is a nearly 50-meter thick coarsening- and thickening-upward mid- to upper-shoreface succession. The lowermost 9 meters consists of heterolithic, 10-cm thick beds of alternating fine-grained sandstone and wavy- to ripple-laminated silty mudstone (lithofacies e). Sandstone interbeds are light gray to grayish orange, well-sorted, planar- to micro-cross laminated with 1-mm thick mudstone drapes. Burrows are present but rare within the 1-2 cm thick mudstone interbeds. In some beds, the silty mudstone laminae consist of thicker mud drapes on 1-2 cm thick ripple-laminated fine-grained sandstone. Mudstone drapes are dark brown to moderate reddish brown, and contain very fine carbonaceous plant debris. This lithofacies grades into about 12 meters of alternating 20-cm thick medium-grained sandstone, and 2-3 cm thick wavy- to micro-cross laminated siltstone. Foresets in sandstone beds increase in amplitude upward to nearly 10 cm and are defined by 0.5- cm thick silty mudstone drapes. Mudstone interbeds are dark gray and contain some sandy laminae. This lithofacies grades upward into 25-cm thick tangential cross-beds with flaser drapes, and ultimately into sigmoidal, flaser-bedded, medium- to coarse-grained, well-sorted sandstone toward the top (lithofacies f). Parasequence 14 (Figure 15) begins with interval 32, an 8-meter thick, coarse-grained basaltic sandstone and pebble conglomerate (lithofacies c1) with basaltic siltstone interbeds, and up to 40% micaceous and arkosic sandstone clasts. *Acutostrea* oyster fossil-rich basaltic beds occur at 3 and 7 meters.

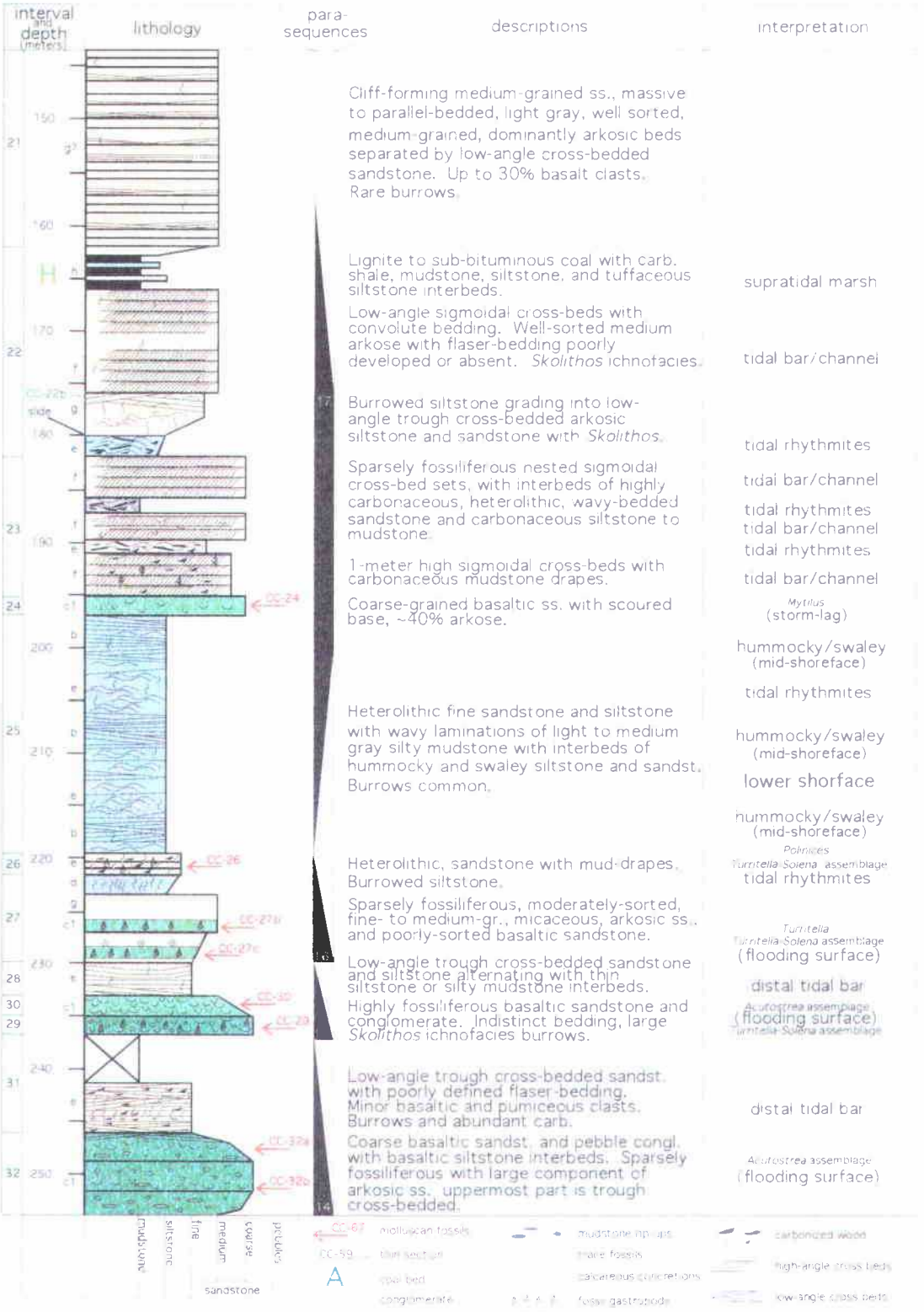

Figure 15: Descriptions and interpretations of parasequences 14 through 17 of the Coal Creek section.

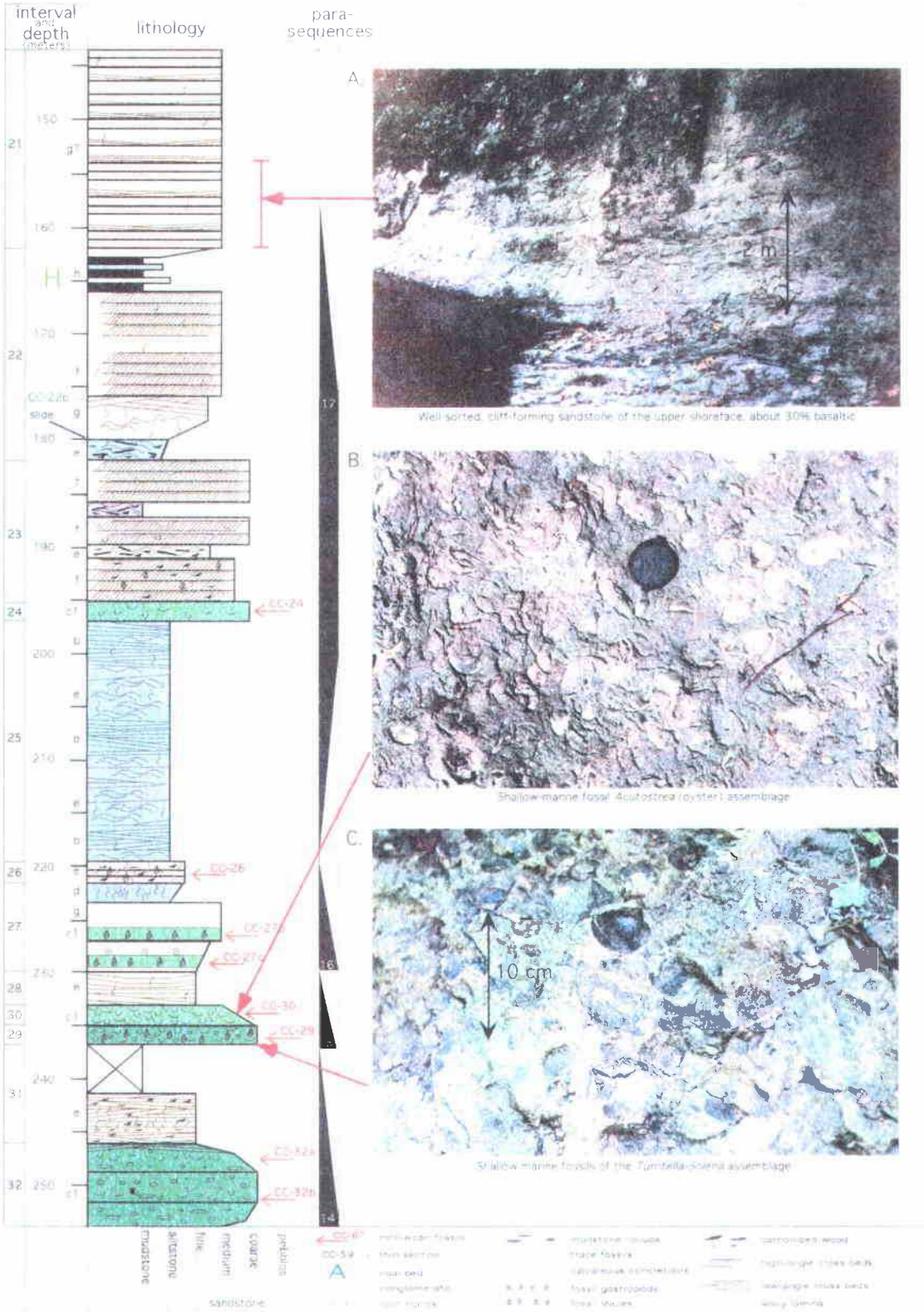

Figure 16: Photographs of lithologies of parasequences 14-17.

The upper interval 31 is in sharp contact with the underlying basalt pebble conglomerate and coarse-grained basaltic sandstone of interval 32, and is 5 meters of low-angle (5-10 degrees) trough cross-bedded sandstone with poorly defined flaser-bedding. Individual cross-bedded lenses are up to 0.3-meters thick, poorly-sorted and dominantly fine-grained, with <10% brown or gray basalt-lithic clasts and <1% lighter colored pumice clasts. Siltstone drapes on bottomsets and foresets are light gray, fine-grained, typically 1mm to 5cm thick, and contain abundant carbonized plant material. Some finer-grained sandstone interbeds are bioturbated to ichnofabric 4. Coarser-grained sandstone lenses have vertical *Skolithos* burrows from 0.5-2 cm wide and up to 0.3 meter long. Some individual siltstone laminae are highly carbonaceous, with incidence increasing upward.

After 5 meters of cover is parasequence 15, the lowermost beds consisting of intervals 29 and 30 (Figures 15, 16b and c, Plate 2), two highly fossiliferous basalt volcaniclastic conglomerates and sandstones that total 4-meters in thickness. Interval 29 is a richly fossiliferous fine pebble conglomerate to coarse-grained gray basaltic sandstone with over 20 species (collected for this study) of the normal marine (subtidal) *Turritella-Solena* assemblage (macrofaunal sample CC-29, Figure 16b). Bivalves are disarticulated but not broken or worn to any great extent. Bedding is indistinct but averages nearly 0.3 meters in thickness as indicated by fossil concentrations. This interval is medium to dark gray, poorly-sorted, and up to 40% arkosic sandstone. *Skolithos* burrows 2.5-cm wide and over 20 cm long are common. Interval 30 overlies 29 in gradational contact and is distinguished by very abundant *Acutostrea idriaensis* fossil

oyster valves, with a minor component of the mussel shell *Mytilus sp.* (macrofaunal sample CC-30, Figure 16b). The upper 3 meters of Parasequence 15 consists of low-angle (<10 degree) cross-bedded sandstone and siltstone, alternating with darker thin siltstone or silty mudstone interbeds and drapes. The Sandstone component is dark yellowish orange to moderate yellowish brown, well-sorted, with the 1-mm thick foresets or wavy laminae commonly bioturbated to ichnofabric 4. Silty mudstone drapes are light gray to medium dark gray with highly abundant carbonaceous material and mica.

The lower 7 meters of parasequence 16 consists of interbeds of generally coarsening-upward sparsely fossiliferous, moderately well-sorted, fine- to medium-grained, micaceous, arkosic sandstone, and poorly-sorted basalt volcaniclastic coarse-grained sandstones and conglomerates. Interval 27 has two beds containing *Turritella uvasana* (macrofaunal samples CC-27b, CC-27c, Nesbitt written communication 1999, Appendix I), and several beds with unidentifiable shell material (one bed contains a well-preserved shark tooth). Near the top of parasequence 16 is a 2-meter thick bed of intensely bioturbated siltstone (lithofacies d), mottled to ichnofabric 5, that coarsens-upward to fine-grained gray sandstone. Capping parasequence 16 is interval 26, 2 meters of heterolithic, 0.5-5 cm thick micro-cross bedded to massive, medium- to coarse-grained, micaceous, arkosic sandstone alternating with 0.5 cm thick wavy-laminated light gray siltstone to silty mudstone (lithofacies e). Sandstone interbeds contain <20% basalt clasts, and broken bivalve fossil shells of *Polinices nuciformis* (Nesbitt written communication 1999, Appendix I)

Parasequence 17 is approximately 45 meters of generally coarsening- and thickening-upward lithofacies (Figure 15). The lower 23 meters (interval 25), is a combination of fine-grained heterolithic siltstone and fine arkosic sandstone of lithofacies e, and hummocky and swaley siltstones and sandstones of lower shoreface lithofacies b. The sandstone component of lithofacies e is fine-grained, micro-cross laminated, and grayish orange, with sparse burrows (ichnofabric 1). These fine-grained sandstone to siltstone intervals are interrupted by wavy laminations of light to medium gray silty mudstone with a minor component of carbonaceous plant debris and mica. Units of Lithofacies b within this interval are very low-angle hummocky and swaley cross-bedded fine-grained sandstone. Stratification is defined by very thin (<1mm) laminae of carbonaceous and micaceous detritus.

The uppermost heterolithic 5 meters of interval 25 is abruptly overlain (and scoured into) by 2 meters of massive, friable, coarse-grained basaltic sandstone of interval 24. Sandstone composition is dominantly basaltic, but contains up to 40% micaceous and arkosic (i.e., quartz and feldspar) components, producing a uniform light to medium gray color. Broken and worn valves of the mussel *Mytilus* are common (macrofaunal sample CC-24, Figure 15).

Interval 24 forms the base of a nearly 10-meter high cliff, exposing the bulk of interval 23, illustrating the relationship between lithofacies e and f. The beds 3 or 4 meters above the contact with interval 24 are medium- to coarse-grained arkosic sandstone with trough to sigmoidal cross-beds. Foresets can be over 1-meter high, and draped with extremely carbonaceous shaley laminae, in which entire carbonized leaves

can be distinguished. Alternating with this lithofacies (f) is heterolithic lithofacies e. Sandstone interbeds are massive to wavy-bedded, grayish orange, and a few centimeters to 0.3-meters thick. This facies alternates with very carbonaceous, medium to dark gray, wavy-laminated siltstone to carbonaceous shale. The middle portion of this interval has 4 nested sigmoidal cross-bed sets, each 1-meter high. Shelly fossil debris is more prevalent toward the bottom, carbonaceous drapes and beds become thicker and more prevalent toward the top, and overall grain-size increases slightly upward.

Interval 22, exposed upstream in Coal Creek from a significant slide, is composed of four lithofacies. The lowermost 0.5 meter consists of mottled light and medium gray siltstone, bioturbated (including spreiten), and has abundant 3-4 cm nearly spherical calcareous concretions (Lithofacies d). The next 2.5 meters consists of low-angle trough cross-bedded, micaceous, arkosic fine-grained sandstone (lithofacies e, petrology sample CC-22b). Lenses are up to 10-cm high, and consist of uniform 1-mm thick, gray, parallel-laminated foresets. Grayish brown vertical *Skolithos* burrows are common. This grades upward into relatively low-angle sigmoidal cross-beds up to 1-meter high (that mark the base of parasequence 18) with some convolute bedding, in grayish brown, well-sorted, medium-grained sandstone, in which flaser bedding is not well defined (lithofacies i?). Overlying the sandstone is nearly 3 meters of lignitic to sub-bituminous coal and carbonaceous shale (coal H) interbedded with light gray silty and tuffaceous mudstone (Figure 15). This interval is poorly exposed in Coal Creek, but is well exposed along a 40-meter long road cut on Coal Creek Road, about 0.3 km to the northwest of the creek exposure (SE ¼ of the NW ¼ of Sec. 11, T 8 N, R 3 W).

Overlying the upper coal of parasequence 18 is a 21-meter thick cliff-forming sandstone (interval 21, Figures 15 and 16a) that differs in lithology from all lower intervals. This interval consists of parallel bedded, light gray, well-sorted, medium-grained, dominantly micaceous and arkosic sandstone beds 10-80 cm thick, separated by several centimeters of wavy-bedded, light gray, fine-grained sandstone. The sandstone is basalt-lithic, with up to 30% volcanic clasts (basalt and pumice) giving the interval its gray color. Beds are massive, with only a few flakes of carbonaceous plant debris; some beds containing <30% rounded and flattened, medium gray mudstone rip-up clasts, which in turn contain up to 50% sand-size basalt or arkosic fragments.

Interval 21 is overlain by interval 20 (Figures 17 and 18). It is heterolithic, consisting of thin alternating laminae, 1-10 mm thick, of fine-grained sandstone, and muddy siltstone (lithofacies k). Sandstone interlaminations are micaceous and arkosic, fine-grained, dark yellowish orange, and parallel- to wavy-laminated. Siltstone interlaminations are fine-grained, medium to dark gray, 1-3 mm thick, and rich in carbonaceous plant debris and fine mica, commonly producing flame structures into overlying sandstone laminae.

This lithofacies is overlain by about 3 meters of micaceous, arkosic siltstone (lithofacies a), that is intensely bioturbated to a mottled medium gray and grayish brown (ichnofabric 5). This interval is abruptly overlain by heterolithic wavy-laminated siltstone and fine-grained sandstone that grades-upward into planar-laminations remarkably uniform in thickness (1-3 mm) and continuous over several meters (lithofacies k, Figure 18b). Sandstone laminae are grayish orange, fine-grained, and well-

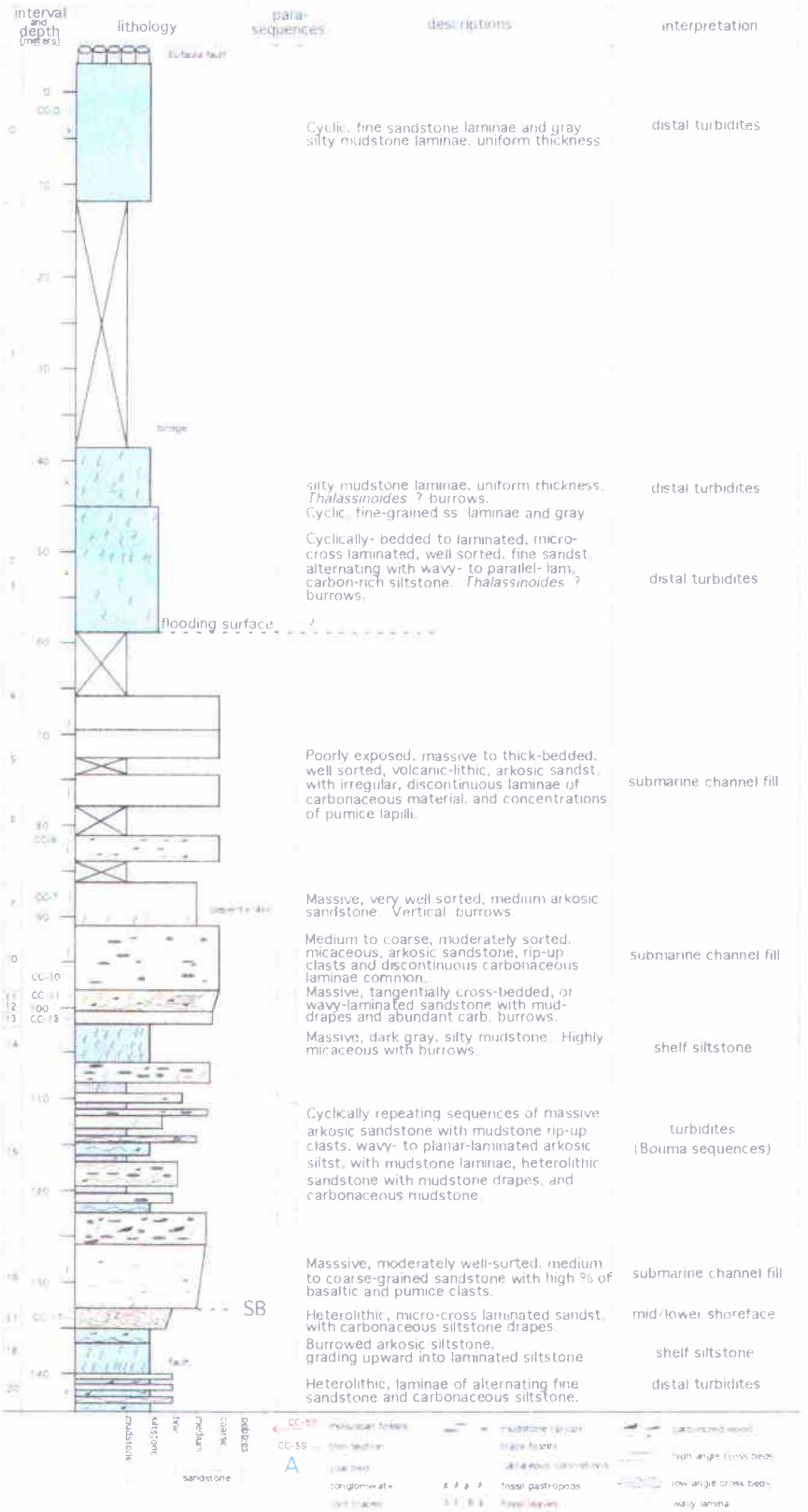

Figure 17: Descriptions and interpretations of the top of the Coal Creek section.

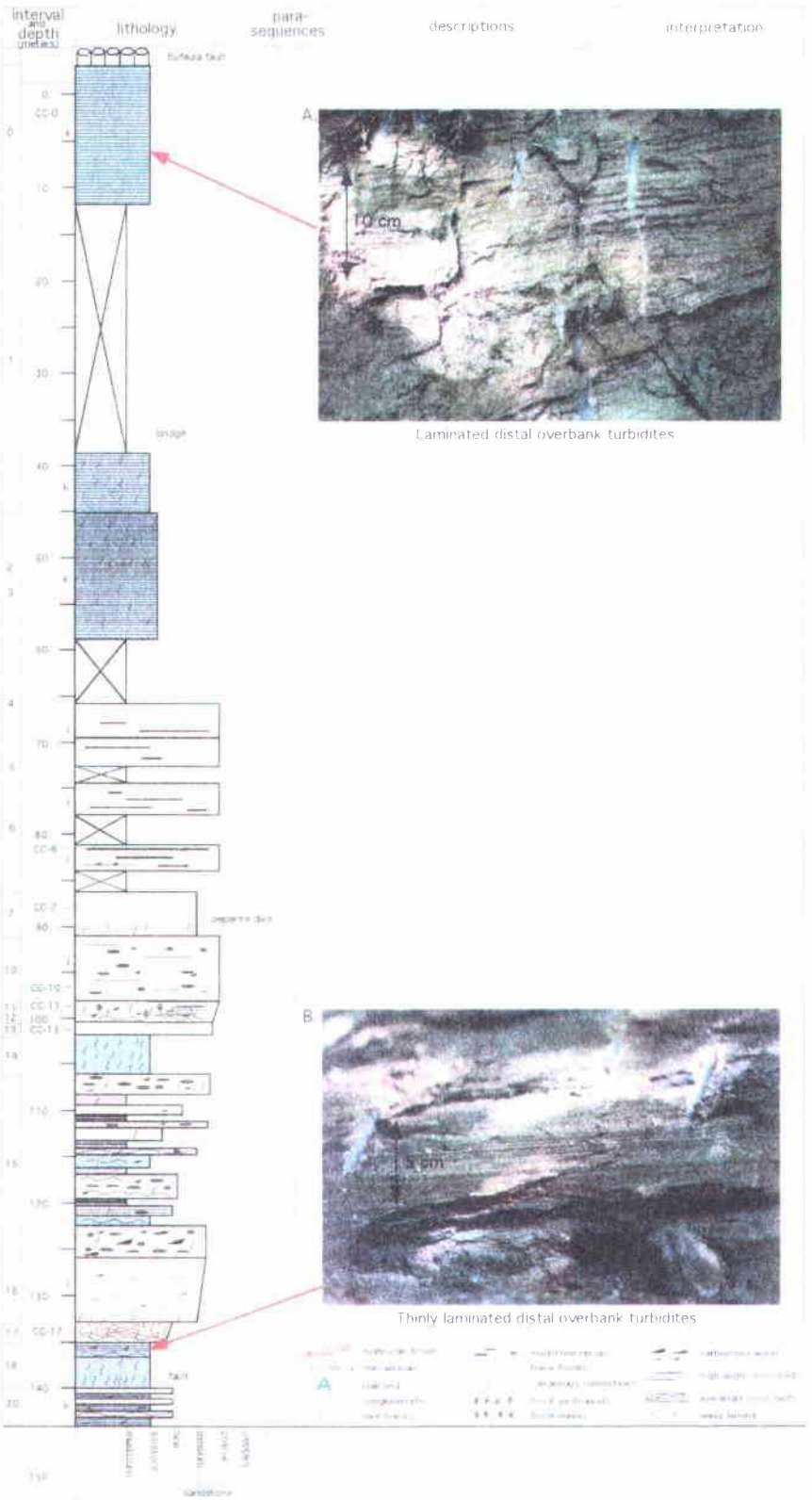

Figure 18: Photographs of distal turbidites from near the top of the Coal Creek section

sorted. Medium gray siltstone laminae are consistently 1-mm thick, well-sorted, and contain finely disseminated carbonaceous material. These lithologies grade upward into interval 17 (petrology sample CC-17), where sandstone laminations thicken to 2 cm, grain size coarsens to medium sand with micro-cross laminations, and individual dark gray carbonaceous siltstone drapes thicken to 4 mm. The top 20 cm have mudstone-draped foresets in lenticular sandstone beds (up to 5-cm thick), which in places are invaded by 1-2 cm wide sub-horizontal burrows filled with medium to coarse-grained sandstone from the overlying interval 16. Lithology of interval 16 is similar to interval 21, but not as well-sorted. This lithic arkosic sandstone is scoured into the underlying interval 17, and is light gray, micaceous, and feldspathic with ~40% basalt clasts and ~5% rounded pumice clasts. Dark gray mudstone to siltstone rip-up clasts, carbonaceous wood chunks, and bivalve fossil shell fragments are common. The entire 8-meter interval (lithofacies j) is massive with thin, discontinuous carbonaceous laminae.

Interval 15 overlies interval 16 in sharp contact, and consists of repeating sequences of sandstone, siltstone, and mudstone. The lowermost 4 meters is a massive, medium- to coarse-grained, arkosic, micaceous, and dark yellowish orange sandstone. Discontinuous bands of rounded carbonaceous mudstone clasts, and dark gray mudstone rip-ups occur throughout, as well as infrequent burrows. This bed is sharply overlain by 1 meter of grayish orange siltstone (dominantly) with alternating beds of siltstone and wavy carbonaceous mudstone laminae. This grades upward into heterolithic, alternating 5-10 cm beds of grayish orange, medium-grained sandstone, and medium to dark gray,

carbon-rich siltstone to fine-grained sandstone. Overlying this facies is 1 meter of carbonaceous mudstone. The next nine meters repeats these sequences several times.

From 100 to 65-meters depth (cover in the stream and small faults make exact thickness determination impossible) massive coarse-grained sandstones of lithofacies j dominate. Interval 14 is 4-meters thick, overlying the uppermost sandstone of interval 15 in sharp contact, and is a massive, light to medium gray, highly micaceous, extensively bioturbated, arkosic, shelfal siltstone (mottled to ichnofabric 4-5). This is abruptly overlain by interval 13, a 1.8-meter thick medium- to coarse-grained, massive, arkosic sandstone (lithofacies j, petrology sample CC-13), which grades upward into combined intervals 12 and 11. The lower meter consists of a heterolithic sequence of alternating, wavy laminations of 1-mm to 1-cm thick medium-grained sandstone, and 1-3 mm thick wavy-laminated carbonaceous mudstone (petrology sample CC-11). This grades upward into a medium- to coarse-grained, moderately well-sorted micaceous and arkosic sandstone, mostly massive with discontinuous laminations of carbonaceous material. Carbonaceous mudstone rip-ups and large pieces of carbonized leaves are common.

Intervals 12 and 11 grade upward into interval 10, very coarse-grained sandstone to fine-grained pebble conglomerate (petrology sample CC-10). This 8-meter thick interval is light gray, ~50% micaceous lithic arkose, ~40% rounded to subangular pumice lapilli, ~5% basalt lithic fragments, and ~5% greenish, angular clay rip-up clasts. Beds average nearly 1-meter thick, as indicated by very discontinuous dark carbonaceous laminae. Intervals 8 and 9 together are a 6-meter wide amygdaloidal peperite dike of Grays River composition (not shown in the stratigraphic column) that intruded between

exposures of intervals 10 and 7. Interval 7 is a massive, very well-sorted, medium-grained, sparsely micaceous, arkosic sandstone (petrology sample CC-7). No evidence of bedding, molluscan assemblages, or trace fossils are apparent in the upper 4 meters. Vertical burrows to ichnofabric 1 are found in the lower meter.

The overlying intervals 6, 5, and 4 (Figure 17) are exposed in largely inaccessible and lushly vegetated cliffs several meters to the side of the lower part of Coal Creek, where it widens to a flood plain. Bedrock exposures in the creek itself are unavailable due to 100% cover by rounded Columbia River Basalt boulders originating from a landslide upstream. As a result, these poorly exposed, dominantly micaceous and arkosic sandstone intervals are incompletely described and unsatisfactorily understood. Toward the base, informal interval 6 (petrology sample CC-6) is moderately well-sorted coarse-grained sandstone with a low percentage of basalt- and pumiceous- lithic clasts. Irregular, wavy, discontinuous laminae of carbonaceous plant debris, and concentrations of pumice lapilli are common throughout. Toward the top of these intervals, moderately well-sorted, medium- to coarse-grained sandstone with pebbly pumice lapilli dominate. Pervasive yellowish brown liesegang limonite staining gives the upper portion the appearance of parallel bedding.

The upper 50 to 60 meters consists of thin, cyclically-bedded to cyclically-laminated, massive to micro-cross laminated fine-grained sandstone alternating with wavy- to planar-laminated carbonaceous siltstone. The lithology is very similar in the lower portion (intervals 3 and 2) to the cyclically-bedded lithofacies e of several previously described intervals, and much like the sandstone and siltstone of the sandy interbeds of interval 59, and the upper 2 meters of interval 18. Heterolithic interval 3 is

fine-grained, grayish orange, well-sorted sandstone, micro-cross laminated, with light gray siltstone drapes. Sandstone interbeds are moderately bioturbated to ichnofabric 3, average about 10-cm thick, and can be lenticular with low-angle trough cross-beds. Grading upward into interval 2, sandstone beds thin to <2 cm, and the angle of the foresets decreases. Gray silty mudstone interlaminae become uniformly 2-3 mm thick. In outcrop, interval 2 has a thinly-striped appearance due to the uniformity of lamina thickness.

Interval 2 grades into interval 1(Figures 17 and 18), where coarser laminae become fine silty sandstone. Scattered trough cross-beds up to 7-cm thick with siltstone drapes occur in this interval. Minor vertical *Thalassinoides*? burrows to ichnofabric 1 occur in intervals 3, 2, and 1. Approximately 25 meters of cover downstream from the Eufaula Rd. Bridge separate interval 1 and the similar but more indurated interval 0 (petrology sample CC-0, Figure 18a), which is highly fractured and terminates in a high angle fault against down-dropped Miocene Columbia River Basalt. This is the stratigraphically highest part of the Cowlitz Formation exposed in Coal Creek.

Depositional Environments

Together, intervals 58, 59, 60, and the lower 4 meters of 62 at the base of the Coal Creek section constitute parasequence 1, a coarsening- and thickening-upward, upper-shoreface succession approximately 45-meters thick (Figure 6, Plate 2). The base of the sequence is an intensely bioturbated silty mudstone (interval 58, lithofacies d), with abundant carbonaceous plant material in the form of whole carbonized leaves, and twig and insect fragments, indicating deposition in a marginal marine setting (bay or estuary), rather than deep marine mud (outer shelf/upper slope). This is overlain by interval 59, a heterolithic, micro-cross and wavy-laminated, well-sorted, medium-grained, micaceous, arkosic sandstone with mudstone rip-up clasts, chunks of carbonized wood, and tidally formed carbonaceous mudstone-drapes, alternating cyclically with heavily bioturbated, carbonaceous mudstones.

This coarsening- and thickening-upward parasequence is consistent with progressively higher-energy tidal currents affecting a slightly shallower quiet-water protected bay/estuary setting. Thinly-laminated sandstone interbeds (tidal rhythmites) may represent the higher energy currents of spring tides; the thinner bioturbated mudstone interbeds may represent lower-energy deposition during neap tides. Planar- and wavy-laminated sandstone interbeds of lithofacies e coarsen- and thicken-upward in this interval, grading into lithofacies f. From ~632 to 622 meters, coarser and thicker sandstone beds dominate with 0.5-meter high trough cross-beds, more abundant and larger rip-up clasts, and flaser mud-drapes defining tidal bundles. Similar lithofacies associations in the recent Mont Saint-Michel Bay, France are interpreted by Nio and

Yang (1991) to form by tidal sandbars prograding into a distributary bay or estuary, along the delta front of a tide-dominated delta. These lithofacies associations could alternatively have been formed by recurring minor deltaic fans breaking through a distributary levee (distributary splays) into a quiet bay environment. The presence of mudstone rip-up clasts in the sandstone beds of this parasequence is support for this hypothesis.

The uppermost 10 meters consists of mostly micaceous, arkosic, flaser-bedded, upper shoreface to marginal marine lithofacies. The lower massive, intensely bioturbated silty mudstone (interval 60, lithofacies d), immediately above the uppermost tidal-bar sand of interval 59, is also interpreted to have formed in a quiet-water bay/estuary setting. Burrows of the *Skolithos* ichnofacies, and the abundant carbonaceous plant fragments, are consistent with this interpretation. This massive silty mudstone grades upward into interval 61, an arkosic siltstone, indicating transition to a slightly higher current energy environment.

Interval 61 siltstone then grades upward into the lower heterolithic beds of interval 62, consisting of alternating planar- to wavy-bedded, fine- to medium-grained sandstone, and ripple-laminated carbonaceous siltstone and massive mudstone (lithofacies e). This lithology is common in the type Cowlitz Formation (Payne, 1998) and in exposures north and west of Coal Creek described by Kleibacker (2001), and is consistent with a tidal rhythmite sequence as described by Nio and Yang (1991) in Mont Saint-Michel Bay, France. These characteristic vertically stacked, thinly ripple-laminated beds are interpreted to have formed in intertidal to subtidal mud-flats, and record tidal

fluctuation cycles. Micro-cross bedded ripple-laminated sandstone interbeds are produced during the relative high energy of tidal ebb and flood current reversals, and the mud drapes below and above (a mud-couplet) represent the two slack-water stages during a flood-ebb cycle (Figure 19, and 8c).

Scoured into the underlying micaceous and arkosic heterolithic facies is a 1-meter thick, coarse-grained, highly fossiliferous, basalt volcaniclastic sandstone (lithofacies c1) that marks the base of parasequence 2. The fossils are dominantly of the normal-marine (shallow subtidal) *Turritella-Solena* molluscan fossil assemblage, but there is a minor component of the *Acutostrea* (oyster) assemblage of shallow water embayments or estuaries, and *Mytilus* (mussels washed off intertidal rocks). These shells are thick and robust, and are found in this coarse-grained basaltic sandstone disarticulated, fragmented, and partly rounded. Nesbitt (written communication, 1999) interprets such deposits as storm wave-generated shell-lag deposits. Large storm wave events, or possibly even tsunamis, could periodically wash in coarse-grained volcanic sediment and associated shallow marine shelly organisms from the nearby, eroding Grays River volcanic headlands and possible seastacks to the southwest, into the mouths of the Cowlitz deltaic tidal estuaries. This high-energy pulse would overwhelm normal deltaic sedimentation, and deposit a coarse-grained basaltic sand or pebble or gravel conglomerate, with robust-shelled, rocky intertidal mollusks, and normal-marine mollusks, broken and jumbled together. Another possibility is that catastrophic volcanic events occurring in the nearby Grays River volcanic edifice(s) produced debris flows and large waves that washed both volcanic sediment and robust shells into the arkosic Cowlitz delta/estuary. Nesbitt

A.

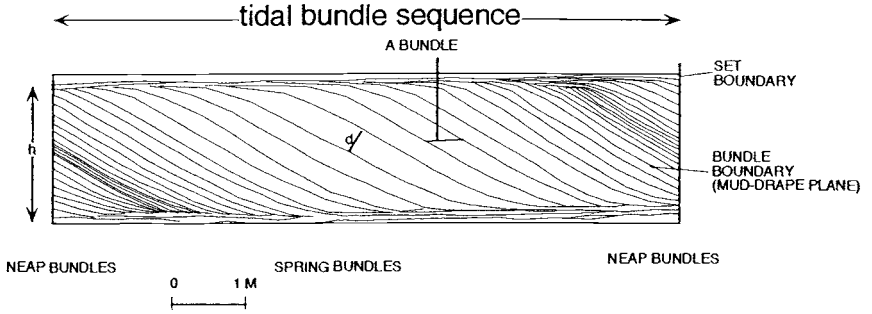

B.

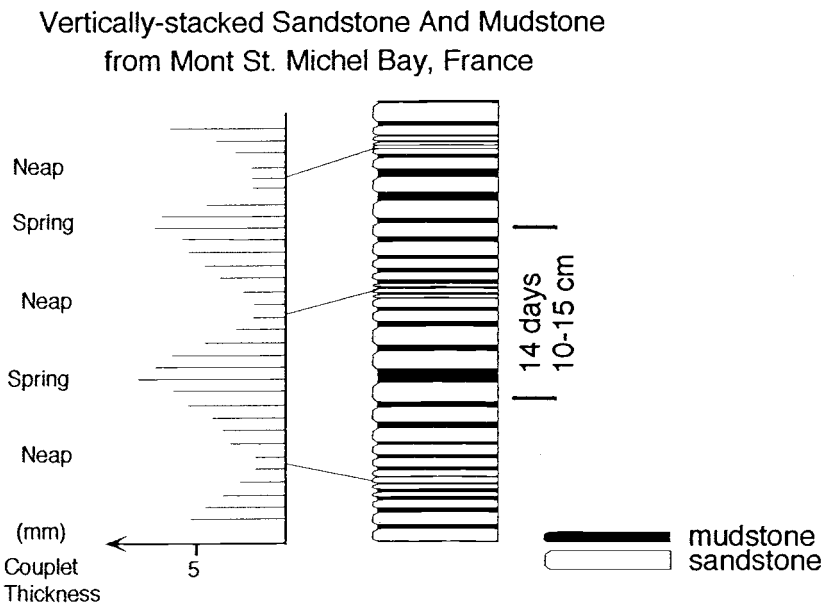

Figure 19. Unique characteristics of clastic tidal deposits recording tide fluctuation cycles: (A) tidal bundle sequences (schematic) and (B) vertically stacked, thinly laminated tidal rhythmites (from the recent Mont Saint-Michel Bay, France) (after Yang and Nio, 1985). The bundle boundaries have thin mud drapes and/or erosional reactivation surfaces. Mudstone drapes in tidal-bundle sequences and vertically-stacked tidal rhythmites were deposited during dominant and subordinate current reversals (slack-water). Variation in mudstone drape and sandstone foreset thickness record neap-spring tidal cycles (14 day cycles).

(written communication, 1999) has also suggested that such molluscan fossil rich beds overlying tidal or delta plain facies may represent minor onlaps (marine flooding surfaces). The presence of these same beds in the study areas of Payne (1998) and Kleibacker (2001) to the north indicates that they form in response to basin wide changes in sea level.

Overlying the coarse-grained basaltic sandstone in interval 62 is a massive, friable, well-sorted, micaceous and arkosic sandstone unit 7-meters thick. This interval has few discernable primary sedimentary structures other than a few carbonaceous laminae, and a sparse *Turritella-Solena* assemblage near the top. A well-sorted, massive sandstone suggests extensive reworking by waves, and may result from wave-reworked distributary mouth- or tidal-bars such as those present in the Cowlitz age-equivalent Eocene Coaledo strata in southwest Oregon (Chan and Dott, 1986). Such delta-front sands are deposited seaward of active distributary mouth bars (or tidal bars) and sometimes reworked by waves and longshore current into a shoal. A similar (and possibly correlative) delta-front sand/beach occurs in the same stratigraphic position within parasequence 2, nearly 3 km to the northwest in Coal Creek (interval 85, section #4, Plate 2). If this unit and the overlying coal are correlative to intervals 85 and 88, it is evidence for a north-northwest trending delta front at the time, a hypothesis consistent with the general west-southwest trending average paleocurrent vector of cross-beds in Coal Creek.

The overlying 8 meters of dominantly tangentially cross-bedded, flaser-draped sandstone caps parasequence 2. The lower 1-meter of this bedset consists of cyclically alternating thin beds of sandstone and carbonaceous mudstone (lithofacies e), interpreted as tidal rhythmites. This facies grades upward into higher-energy 0.3-0.7 meter thick cross-bedded sandstone with mud-drapes of lithofacies f. These are interpreted as prograding megaripples in a tidal channel or tidal sandbar with mud-draped reactivation surfaces, and upper and lower mud-couplets, producing tidal bundles. This association of tidal rhythmites underlying, or grading into, sub-tidal channel or bar prograding megaripples is common within the Coal Creek section.

Parasequence 3 repeats many of the lithofacies described in underlying intervals. However, rather than being capped by cross-bedded, and flaser-bedded sandstone, this upper shoreface to delta-plain succession terminates in a coal (coastal supratidal swamp) at (or very near) the top, and lateral changes in lithofacies across several kilometers of delta front can be studied in this shoaling-upward parasequence. The upper coal (coal A) is a marker bed along nearly the entire northern half of Coal Creek, allowing for confident correlation and placement of units within the stratigraphic column.

Parasequence 3 is a fining- and thinning-upward progradational parasequence, including thin-bedded heterolithic lithofacies e toward the base, grading upward into thicker trough cross-bedded sandstone of lithofacies f. Unlike the lower parasequences, this sequence is overlain by fining- and thinning-upward mudstone and siltstone of lithofacies h and capped in a coal (Plate 2). This represents a supratidal delta plain marsh, and the coarse sandstone interbeds are likely thin levee splay deposits. Lithofacies within

parasequence 3 can be correlated over 3 km, and show lateral changes in depositional environments from south to north (Plate 2, see Coal Creek stratigraphic section of text).

Interval 63 at the base of parasequence 3 is a heterolithic facies consisting of very fine-grained, micro-cross bedded sandstone with discontinuous wavy-laminated mud drapes (lithofacies e). These interbedded mudstone laminae, while containing enough finely disseminated organic component to make it dark gray in color, do not contain larger carbonized fragments of leaves or twigs. This interval may be a lower energy, deeper, quieter water equivalent of the tidal rhythmites described in the underlying interval 62. It is finer-grained, and the mud-drapes lack fragmental organic debris, possibly because it had settled out of suspension in shallower water (likely tidal flats) closer to the source. The lower percentage of mud could likewise result from suspended mud particles settling out in tidal flats. The basalt-volcaniclastic interbed of lithofacies c1 is finer-grained than the similar unit in interval 62, and contains thinner-shelled bivalves (including two species of Pitar and *Pachydesma aragoensis)* that are less fragmented and rounded (e.g., below wave base). Lithofacies above this fossiliferous bed remain unchanged from those below, indicating that this may represent storm wave lag, not a minor marine flooding surface.

The correlative interval 82b, 2.1 km to the northwest (section #3) is slightly coarser-grained than interval 63, thicker-bedded, and the basalt volcaniclastic pinches out to the north (Plate 2). Correlative interval 86 (section #4), 0.6 km north of 82b is coarser still, with broken and disarticulated, wave transported molluscan fossils of the shallow subtidal *Turritella-solena* assemblage. These features could indicate decreasing water

depth and higher energy conditions to the north at this time. The upper coal (coal A) maintains a constant relative thickness over this distance, but sandstone splay interbeds in interval 66 (section #1), and mudstone interbeds in interval 82a (section #3) are not present in interval 88 farthest to the north (section #4).

Overlying interval 63 (in the southernmost exposure of parasequence 3, section #1) is interval 64, three tangentially to sigmoidally cross-bedded sandstone units with flaser-bedded foresets, separated by thin mudstones of lithofacies d. These are inferred to be separate progradations of increasingly higher-energy megaripples of a tidal sandbar or subtidal channel (indicated by thickness and higher angle of foresets). Parasequence 3 terminates in a delta plain succession consisting of an underlying siltstone (lithofacies d or h), and a coal with fine- to coarse-grained interbeds representing marsh/swamp muds and sand deposited from progradation of interdistributary crevasse splays or large storm events that breach the larger distributary channel levees.

Parasequence 4 is a shoaling-upward, upper-shoreface to delta-plain succession, with varying lithologies resulting from the complex interplay of dominantly basaltic sand and pebbly gravel influx to the south, derived from local eroding Grays River shield volcanoes, and normal deltaic deposition of micaceous and arkosic sediment to the north. The southernmost exposures (intervals 67, 68, and 69, section #1) are a mostly fining-upward sequence, with offshore shallow-marine bioturbated sandstone at the base grading upward into subaerial coaly delta-plain facies. The lowermost medium-grained, largely basalt-lithic, poorly-sorted, fossiliferous sandstone is interpreted to be another storm-wave generated shell-lag deposit. The association of the oyster *Acutostrea idriaensis* and

Pitar eocenica suggests this unit was deposited in a shallow water open embayment (Nesbitt written communication, 1999) or estuary, a conclusion also supported by the fine-grained tidal rhythmite sequence immediately above. The overlying coarsening-upward sandstone culminating in a well-sorted, coarse-grained arkosic sandstone with abundant large pieces of coalified wood suggests a prograding distributary mouth channel or tidal sandbar reworked by wave action.

The overlying basaltic, cyclically-bedded sandstone and siltstone, with interbeds containing articulated and unworn *Corbicula cowlitzensis*, a brackish water bivalve (Nesbitt written communication 1999, Appendix I), indicates that this upper portion of parasequence 4 was deposited in a protected bay/estuarine environment. Individual graded lithic sandstone beds could have been produced by pulses of volcaniclastic sediments entering the bay, estuary, or lagoon, possibly from storm events associated with flooding from a basaltic source, with the finer basaltic siltstone at the top of each bed resulting from suspended particles settling out with time. Alternatively, these could be basaltic tidal rhythmites, the siltstones settling out of suspension during slack-water stages between ebb and flood tide. This fining-upward parasequence terminates in sub-bituminous coal B (supratidal freshwater marsh) with coarse-grained basaltic overbank levee splay or storm wave-generated sandstone interbeds. The individual cyclic beds of interval 68 with *in-situ*, thin-shelled, articulated brackish water *Corbicula* clams, as well as the overlying interbedded coal, indicates that these multiple basaltic beds were deposited over a substantial period of time, as opposed to a single volcanic debris-flow flood event. The correlative basaltic interval 76 to the north lacks the cyclic sandstones

and siltstones, suggesting the protected, quiet-water tidal flat/bay/estuary environment of interval 68 was limited to the south. Here, well-sorted medium-grained basaltic sandstone with planar bedding suggests reworking of the sand by waves into a barrier bar, or distributary mouth bar.

The northernmost exposure of this correlated parasequence 4 (section #4) begins with a storm-generated (or marine transgressive), coarse-grained, fossiliferous basaltic unit (interval 90) with broken valves of *Acutostrea idriaensis,* that is possibly correlative to the similar lithofacies of the lower part of interval 67 in the southernmost exposure (section #1). Above this, interval 91 (section #4), and lower interval 80 (section #3), are protected bay deposits of well-laminated mudstone and micaceous, arkosic siltstone. The upper 4 meters of interval 80, with large-scale flaser-bedded trough cross-beds and unidentifiable shell hash shows that, in this part of the delta sequence, a tidal channel and/or sandbar prograded into the bay or estuary.

Parasequence 5 (Plate 2) consists of interbedded thick basaltic breccias, conglomerates, sandstones, and siltstones that mark the lowermost beds of a ~140 meter section that contains abundant basaltic interbeds, likely correlative to informal unit 2 of the type Cowlitz Formation section as described by Payne (1998). At the base of this sequence in each Coal Creek section (#1-4, Plate 2) is a fossiliferous bed of basaltic sandstone or pebble conglomerate (except for interval 70 where it is likely covered). This represents a high-energy pulse of coarse volcanic sediment entering the length of the delta front or estuary, perhaps the result of large waves produced during the initial intrabasinal phase of the explosive basaltic Grays River volcanic activity, that would deposit up to 35

meters of volcanic sediment (parasequence 5, Figures 9 and 10) over the mostly micaceous and arkosic extrabasinal deltaic facies of underlying intervals (parasequences 1-4, Plate 2, Figures 6, 7, and 8). These locally derived basaltic sediments, including some conglomerates with angular to subrounded cobble-sized clasts in matrix support, are interpreted as catastrophic, hyperconcentrated flood/debris flow deposits entering the estuary from a nearby explosive volcanic high (Figure 59). The angular, matrix supported breccia interbeds of Grays River basalt composition, with euhedral pyroxenes, suggests that the eruptive center may have been near the southern Coal Creek exposures. Such interbeds could have originated from near Mt. Solo (Plate 1), where quarry and roadcut exposures of thick Grays River breccias of identical lithology commonly occur intermingled with columnar autoclastic basalt dikes, sills, and subaerial flows.

Changes in lithofacies of this parasequence (5) to the north are expressed as a decrease in grain size and thickness of the conglomerates, breccias, and coarse-grained sandstones (lithofacies c1, correlative sections #2, #3, and #4, Plate 2), and an increase in fine-grained basaltic sandstones and siltstones (lithofacies c2). Beds with conglomerate at the base grading upward to siltstone resemble divisions a and d of the Bouma turbidite sequence. A similar sequence in the type Cowlitz section at Vader 10 km to the north (at the base of informal unit 2, lithofacies 2f of Payne, 1998) was interpreted as debris flow deposits produced in an inner neritic setting. He concluded that such units might be records of a series of explosive air fall and base-surge eruptive events that abruptly entered the shallow-marine arkosic sandstone to mudstone environments. Such volcanic surges upon entering water of an appropriate depth, would rapidly deposit the coarser-

grained gravel component, and the finer-grained component would settle out over a period of time (similar to the process described for interval 68). Over a period of time, several eruptive pulses would produce cyclic, graded basaltic beds with coarse-grained scoured bases and an overlying drape of fine-grained particles that slowly settled out of suspension. The preponderance of very fine-grained basaltic siltstone in the northernmost exposures of this volcanic interval, with fewer conglomeratic interbeds, could be explained as deposits produced farther away from the southern Mt. Solo Grays River eruptive source, in deeper (subtidal) or calmer water. The *Glycymeris saggitata* pelecypod found in the basaltic conglomerate of interval 92, according to Nesbitt (written communication, 1999), indicates a shallow subtidal marine environment.

Parasequence 6 is a micaceous, arkosic shoaling- and fining-upward succession (Figure 9), the lower part of which can be correlated across 3 km due to its position immediately above the thick volcaniclastic intervals of parasequence 5 (section #1-4, Plate 2). This parasequence in its southernmost exposures (section #1) is well-sorted and medium-grained, with parallel laminations of both heavy minerals, and micaceous carbonaceous material, characteristics of beach or bar deposits where wave-reworking and wave action in the swash zone produces the characteristic sorting and planar-laminae. This deposit is likely a wave-reworked distributary mouth bar or subtidal bar, deposited seaward of an active distributary channel.

Correlative intervals to the north and west (sections #2 and #3, Plate 2) are finer-grained and extensively bioturbated, suggesting deposition in a protected bay/estuary. Alternatively these could be offshore middle- to lower-shoreface bioturbated siltstones

formed below wave base. In gradational contact with the southernmost interval 53 is a wavy-laminated, micro-cross bedded fine-grained arkosic sandstone containing well preserved carbonized leaves and the fresh-water bivalve *Batissa newberri* (Nesbitt written communication 1999, Appendix I) grading upward into an extremely carbonaceous interval of shale, carbonaceous siltstone, and thin coal (coal C). These features indicate a fresh water delta-plain depositional environment, such as a supratidal marsh, where periodic overbank flooding events would produce the wavy- and micro-cross laminated ripple interbeds.

Parasequence 7 is a generally shoaling-upward succession produced largely by prograding tidal sandbars or subtidal channel sequences along the front of a tide-dominated delta lobe or estuary. The parasequence begins with interval 50 (Figure 9), a carbon-rich heterolithic facies abruptly overlying the uppermost supratidal marsh and crevasse splay succession of parasequence 6. This wavy-laminated bioturbated bedset of alternating sandstone and carbonaceous fine-grained sandstone and siltstone is a sequence of tidal rhythmites (lithofacies e). The thickness and coarse grain-size of the sandstone interbeds, and the large *Skolithos* ichnofacies burrows, suggest a high-energy, shallow-marine tidal environment. A likely scenario is deposition immediately bayward of a prograding tidal bar or tidal delta at an estuary mouth, where tidal current energy is sufficient to carry coarse sand, but not strong enough to produce the characteristic large megaripples of lithofacies f. This is overlain by interval 49, another poorly-sorted storm wave-generated broken and disarticulated, unidentifiable shell-lag deposit.

Tangential and sigmoidal, flaser-bedded, tidal channel or tidal bar sandstones typically overlie tidal rhythmites throughout the Coal Creek section. Parasequence 7 is an excellent

example of a tidal bar or subtidal channel progradation into a tidal flat or estuary (similar to modern Willapa Bay, Washington (Figure 20). Fine-grained intertidal rhythmites (interval 50) grade upward into the higher-energy facies of tangentially cross-bedded medium-grained sandstone of interval 48 (large tidal megaripples), further grading into higher-angle sigmoidally cross-bedded coarser sandstone, with soft-sediment slump deformation, larger and more abundant mudstone rip-up clasts, and coalified wood debris (interval 46). A 1.5-meter thick basaltic, coarse-grained, bed occurs at the base of the coarse-grained interval 46 (interval 47) that is rich in fossil shells of the *Acutostrea* assemblage. This may represent the shell lag at the base of the subtidal channel that produced interval 46, a relationship observed in the recent deposits of Willapa Bay (Clifton et al, 1989).

Overlying these arkosic and micaceous tidal lithofacies is another poorly-sorted basalt volcaniclastic coarse-grained sandstone and matrix-supported conglomerate (interval 45), likely produced by channelized hyperconcentrated flow from a nearby volcanic edifice. The lack of molluscan assemblages associated with this unit, or any sign of bioturbation or grading suggests that this surge may have been initially subaerial, with little reworking by wave or tidal processes. The top of parasequence 7 is a heterolithic facies (lower interval 44) consisting of thin interbeds of coal, siltstone, and mudstone (coal D) that can be interpreted in two ways. These beds could be a series of thin, fine-grained interdistributary crevasse levee splays periodically flowing into a supratidal marsh in the estuary or bay, depositing micro-cross laminated overbank arkosic sandstone or siltstone depending on the severity of the flood event. Rounded pieces of carbonaceous plant debris and mudstone rip-up clasts, and thin coal seams, support this model.

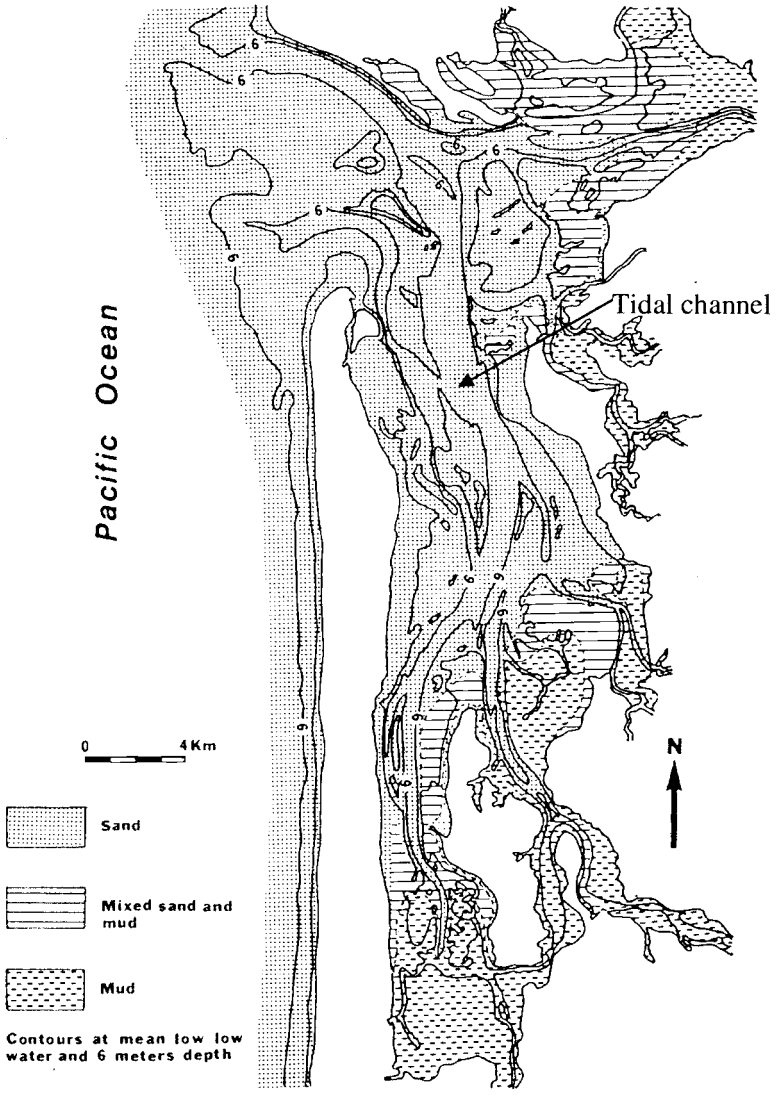

Figure 20: Estuarine sediment grain size in present day Willapa Bay, southwest Washington. Sand dominates the central and northern parts of the bay as well as the tidal channel floors (flaser-draped megaripples). Tidal channel sand grades into mixed sand and mud (tidal rhythmites), and ultimately into mud in the upper portion of the estuary. (Modified from Clifton and others, 1989). This is a useful model to explain facies relationships in the tide-dominated Coal Creek section.

Alternatively, this cyclically bedded interval could be interpreted as unusually carbonaceous intertidal rhythmites, with mud-drapes composed largely of carbonized plant debris. Their position beneath the tangentially cross-bedded and flaser-bedded sandstones of the upper portion of interval 44 (Figure 11) supports this tidal flat model. No molluscan fossils were found to allow discrimination between fresh, brackish, or shallow marine water depositional environments.

Parasequence 8 (Figure 12, Plate 2) is another fining- and thinning-upward sequence representing another progradation of tidal sandbars or subtidal channels, and ultimately a supratidal marsh, into an estuarine environment (Figure 59). Such shoaling-upward sequences culminating in a tidal channel or bar sand, beach, or marsh, and then overlain by shallow marine facies of the next parasequence could represent minor transgressions caused by third-order eustatic sea level change. It may also represent fourth-order apparent sea level change produced by distributary channel switching, allowing for a few meters of subsidence by compaction of the underlying intertidal to supratidal fine-grained sediment before deposition of coarse sand is again concentrated in that area.

The lower beds of parasequence 8 constitute a two-meter thick, heterolithic, cyclic, relatively coarse-grained and carbon-rich intertidal rhythmite sequence (the carbonaceous beds of lower interval 44 could also be part of this parasequence). This protected intertidal facies grades upward into relatively low-angle, flaser-bedded trough

cross-beds, and ultimately into nested, high-amplitude sigmoidal cross-beds. A similar lithologic parasequence was described by Payne (1998) in the uppermost part of his informal unit 3 (location 11e) of the type Cowlitz Formation. The uppermost portion of interval 44 consists of an amalgamated subtidal channel-fill sequence with flaser-draped foresets and wavy mud- or carbonaceous shale-draped reactivation surfaces. Payne interpreted the dominant paleocurrent direction (southwest in the case of Coal Creek sediments) to reflect the dominant ebb tides, whereas the few cross-beds trending northeast resulted from weaker flood-tides. The part of this Coal Creek sequence that lacks cross-bedding is a massive, well-sorted arkosic sandstone with chunks of carbonaceous wood, that was likely produced by local reworking of tidal bar sand by wave action into offshore bars or shoals.

This interval is overlain by alternating thick beds of poorly-sorted and commonly fossiliferous, coarse-grained, basaltic sand or basaltic pebble conglomerate (intervals 43, 41, and 39), and well-sorted, planar-laminated to massive micaceous, medium-grained arkosic sandstones (intervals 42, 40, and 38). The massive to planar-bedded arkosic sandstone intervals represent distributary mouth bars or tidal bars in a tide-dominated delta, reworked by wave-action and longshore current into shoals or barrier bars fronting the tidal flat/estuary. Large *Skolithos* burrows, prevalent in high-energy shoreface environments, support this interpretation. The thick, massive to wavy-bedded basaltic pebble conglomerates or coarse-grained sandstones represent a temporary influx of coarser-grained sediment via storm-waves (or possibly minor marine transgressions) into this shallow marine environment. Parasequence 8 is capped by a carbon-rich, silty,

basaltic-lithic mudstone to siltstone underclay with minor root-traces and twigs, and an overlying 1-2 meter thick clean, sub-bituminous coal (coal E, lithofacies h, Figures 12 and 13), reflecting progradation of a coastal marsh over the barrier bar facies.

Parasequence 9 (Figures 12 and 13) is an upper-shoreface succession consisting in large part of lithofacies e and g. The lower tidal rhythmite sequence coarsens- and thickens-upward with more abundant and steeper cross-beds. The middle well-sorted sandstone is another example of a wave-reworked delta-front sand with *Skolithos* burrows. The upper part of parasequence 9 consists of a lower coarsening- and thickening-upward heterolithic and cyclically-bedded sandstone with carbonaceous mudstone interbeds. This is a progressively higher energy (shoaling-upward) sequence of tidal rhythmites produced by a prograding tidal bar or tidal channel, capped by a supratidal marsh (coal F).

Parasequences 10 and 11 (Figures 12 and 13) together constitute two shoaling-upward parasequences, or could alternatively be considered one thinning- and fining-upward parasequence with coal and carbonaceous shale interbeds. The tidal bar sequence immediately overlying parasequence 9 consists of coarsening- and thickening-upward, flaser-bedded, megaripples (parasequence 10) with flaser-bedding composed of disseminated carbonaceous plant debris rather than mudstone or siltstone. Carbonaceous shale interbeds suggest proximity to a source of abundant plant material. This parasequence is capped by a storm wave-generated coarse-grained arkosic sandstone containing broken and disarticulated lag of *Acutostrea idriaensis,* and large pieces of carbonized wood and capped by a thin upper coal (coal G). These carbonaceous layers

may alternatively be thick concentrations of plant debris deposited during flood events, and do not represent the subaerial supratidal swamp cap of a parasequence. Parasequence 11 overlying the thin coal consists of extremely carbonaceous flaser-bedded megaripples, with a high percentage of nearly black sandstone rip-up clasts, with a large amount of disseminated carbonaceous matter, and black sandstone foresets. This grades upward into a coarser, more massive sandstone unit with the percentage of rip-up clasts decreasing upward, representing another distributary or barrier bar reworked by wave action and/or extensive bioturbation.

Parasequence 12 is a nearly 40-meter thick coarsening- and thickening-upward shelf to middle shoreface succession, the first deposits above a maximum marine flooding surface (Figure 13 and 14, Plate 2). The lithofacies of underlying parasequences are representative of shallower water upper-shoreface to delta-plain depositional environments, predominantly upper-shoreface (lithofacies c-g). Overlying these lithofacies in sharp contact with beach or barrier bar interval 34 (parasequence 11), are heterolithic, ripple-laminated fine-grained siltstones and mudstones with burrows of the *Cruziana*-ichnofacies (lithofacies a, interval 33d, Figure 13b). This grades upward into thicker, coarser-grained, and more continuous sandstone beds with steeper foresets, alternating with thinner ripple-laminated mudstones (lithofacies a, interval 33c, Figure 13a) and ultimately into arkosic hummocky and swaley bedded sandstone of interval 33b. These thickening- and coarsening-upward lithofacies associations are similar to those parasequences described by Kleibacker (2001) from the Cowlitz Formation northwest of Coal Creek, and also in the Cretaceous Price River Formation of the Book Cliffs in Utah

(Van Wagoner et al., 1992), where these fine-grained, storm ripple-generated lithofacies were interpreted as forming in relatively deep water during a sea level rise over a lower system tract (HST, parasequences 1 - 12). The dominantly symmetrical ripples result from the oscillatory motion produced by wave currents of the lowermost reaches of storm-wave base. This lithofacies grades upward into amalgamated hummocky and swaley cross-bedded fine-grained sandstone with carbonaceous fairweather mudstone and siltstone drapes (lithofacies b, lower interval 33b) of the middle shoreface. These also form by strong oscillatory motion of storm-wave base, as storm waves impinge on the ocean floor at depths greater that those reached by fairweather wave base (Chan and Dott, 1986). A similar shoaling-upward parasequence in the Eocene lower Coaledo Formation of southwest Oregon was described by Chan and Dott (1986). Overlying these lower- to middle-shoreface, wave-dominated facies is a massive to thick-bedded, well-sorted sandstone with *Skolithos* burrows, consistent with an upper shoreface, wave-reworked and burrowed delta front sand or a shoal/sandbar. This immediate juxtaposition of upper shoreface over middle shoreface may indicate the presence of a sequence boundary at this horizon, in a similar stratigraphic position to one described by Payne (1998)(see sequence stratigraphy section of text), or may simply result from shoreface progradation.

Parasequence 13 (interval 33a, Figure 14) is an excellent example of finer-grained micro-cross laminated sandstone interbeds of tidal rhythmites (lithofacies e) gradually coarsening- and thickening-upward, with steeper foresets, as tidal wave energy (due to tidal bar progradation) increases from bottom to top. This succession ultimately grades

upward into tidally formed flaser-bedded, sigmoidal cross-beds (megaripples or sand waves) of a subtidal sand bar or tidal channel. Massive sandstone bar or shoal intervals, particularly near the top, are due to reworking by wave-action or bioturbation. The uppermost sigmoidal cross-beds lack flaser-drapes. This could be due to deposition near the relatively high-energy axis of the main channel, where strong tidal currents prevent deposition of slack-water mud-drapes.

The overlying poorly-sorted basalt-volcaniclastic pebble to cobble conglomerate of parasequence 14 contains two shell hash horizons with *Acutostrea idriaensis* oysters, and likely represent subtidal-channel fill as observed in Willapa Bay (supporting the above subtidal channel hypothesis), produced during a minor marine transgression. Alternatively, this could be a wave-reworked supratidal distributary or river channel of the upper delta plain filled with basaltic debris from a volcanic hyperconcentrated flood event. Overlying this thick basalt volcaniclastic is a lower arkosic, trough-cross bedded, mud-draped unit (interval 31). The lower trough cross-bedded interval has the typical features of lithofacies f, but the sandstone component is fine-grained, and the foresets are very low-angle (< 10 degrees), indicating deposition some distance from the active tidal-channel.

Highly fossiliferous coarse-grained basaltic sandstone and fine pebble conglomerate of parasequence 15 overlies the tidal facies of interval 31, and represents yet another minor marine transgression. Contact between these lithofacies is unknown due to approximately 5 meters of cover. Interval 29 (Figures 15 and 16c) is an extremely fossil-rich, basaltic, coarse sandstone and pebble conglomerate containing over 20 species

(collected for this study alone) of the molluscan *Turritella-Solena* assemblage (Appendix I). Lithic clasts are subangular to subrounded, indicating some degree of transport before final deposition, possibly in a tidal channel, explaining the concentration of a variety of mollusks. The bivalves are disarticulated, but not excessively broken or worn, indicating that the sediment was transported a greater distance than the molluscan fossils. Very thin-shelled and fragile bivalves such as razor clams (*Solena columbiana)* are disarticulated but not broken. Overlying interval 29 in gradational contact is interval 30 (Figure 15 and 16b), a 2-meter thick coarse basaltic sandstone with abundant, disarticulated and worn valves of *Acutostrea idriaensis* oyster shells with minor *Mytilus sp.* mussel shells, apparently a transported soft-sediment embayment oyster assemblage, with a lesser component of tough-shelled, rocky shore intertidal bivalves mixed in. Parasequence 16 repeats these lithofacies (and may be a repeat section produced by a hidden fault).

Parasequence 17 is a coarsening- and thickening-upward mid-shoreface to delta-plain succession, culminating in tidal channel/rhythmite facies (Figures 15 and 16). The lower ~23 meters of this 45-meter thick parasequence consists of a fine-grained heterolithic facies, where siltstones and very fine arkosic sandstones are interbedded with drapes of dark, silty mudstone. This lithofacies is interbedded with fine-grained hummocky and swaley cross-bedded sandstone of the middle-shoreface, allowing for two interpretations of the heterolithic interbeds. They could be mid- to upper-shoreface extensions of the tidal rhythmite facies, seaward of the main prograding barrier sand-bar, an interpretation supported by the shallow water *Mytilus*-rich bed (likely a storm wave

deposit) and tidal-megaripples (flaser-draped, lithofacies f) immediately above. Alternatively, they could represent the transition from lower- to middle-shoreface, and be the shoreward, higher energy version of lithofacies a. Lack of carbonaceous debris in the fair-weather mudstone interbeds supports this hypothesis.

Interval 23 and lower interval 22 consist of 20 meters of alternating sigmoidally cross-bedded sandstones with highly carbonaceous mudstone to carbonaceous shale drapes (lithofacies f), and heterolithic wavy-bedded sandstone alternating with silty mudstone to carbonaceous shale. These facies are exposed in a nearly 10-meter cliff section (interval 23), and illustrate the close relationship between these two alternating lithofacies. Tidal rhythmites are the lower-energy version of the same depositional system as the tidal sandbars or tidal channel, possibly produced by tidal currents strong enough to move sand size particles, but insufficient energy for the production of megaripples or sand waves (more distal from the tidal channel). It is possible that megaripples are produced when sediment influx into the delta or estuary is high (flood events), and heterolithic facies are produced when influx is lower. The most likely possibility is that this interval shows the relationship between tidal flats (tidal rhythmites, lithofacies e) and the tidal channel meandering through the tidal flat (flaser-draped megaripples of lithofacies d, see Figure 20).

Parasequence 18 is fining- and thinning-upward and consists of 10 meters of sigmoidally cross-bedded, medium-grained sandstone with little or no flaser bedding, that could represent either the main axis of the subtidal channel (lithofacies f), or a supratidal distributary channel in the upper part of the delta plain (lithofacies i). Evidence for the

latter interpretation is the association of this facies with the thick upper coal and carbonaceous shale (coal H), becoming an interbed of the coal 0.5 km to the north in a roadcut along Coal Creek Rd. (SE ¼ of the NW ¼ of Sec. 11, T 8 N, R 3 W).

Interval 21 is a unique lithological unit in the Coal Creek section, and the depositional environment is uncertain. Individual beds are parallel and well-sorted, many with a high percentage of mudstone rip-up clasts. These features have throughout the section consistently been associated with delta front sands reworked by wave-action into a shoal, seaward of the active tidal channel or prograding tidal sandbars. Finer-grained, wavy-laminated interbeds could be the result of wave action during high tide on a beach with heavy tidal influence.

Intervals 20, 18, and 17 are relatively deep water facies overlying another marine flooding surface at the top of interval 21, consisting of distal turbidites (lithofacies k) and extensively bioturbated shelf to lower shoreface siltstones. Interval 20 and the upper two meters of interval 17 contain remarkably uniform parallel laminations of fine sandstone and siltstone representing distal turbidites (similar facies occur in intervals 3 through 0). Intervals 16 through 4 consist of massive to thick-bedded medium- to coarse-grained dominantly arkosic sandstone containing abundant and large mudstone rip-up clasts and rounded chunks of carbonaceous material. Similar massive sandstones with large and abundant mudstone rip-up clasts at a similar stratigraphic horizon were described by Payne (1998) from the type Cowlitz Formation stratigraphic section as submarine channel sandstones carved into underlying strata at the base of a lowstand system tract. Interval 15 consists of these massive sandstones with rip-up clasts, but also includes fine-grained

sandstone, siltstone, and carbonaceous mudstone interbeds that are interpreted as deep-water Bouma sequences.

Intervals 3-0 (Figures 17 and 18) exhibit lithofacies that are uncommon in the lower intervals of the Coal Creek section, and reflect either a rapid transgressive flooding surface, or a return to fine-grained turbidite sedimentation when the underlying submarine channel was abandoned. Interval 3 is similar to laminated beds of lithofacies e, where it occurs beneath thicker-bedded lithofacies e, and low-angle cross-beds of lithofacies f. This uppermost portion of the section is heterolithic and unusual in that the sandstone component is massive to low-angle, and low amplitude, trough cross-beds that become thinner, finer, and more uniform upward, to resemble the lithology of interval 18 and the laminated sandstone interbeds of interval 59 (associated with tide dominated upper shoreface successions). These uppermost intervals are unusual in thickness and uniformity for lithofacies e, and may therefore represent deep-water distal turbidites.

Petrography

Seventeen thin sections were prepared from Cowlitz Formation samples collected from the Coal Creek section (Plate 2), and an additional two were collected from the "IS" roadcut in interval 22 along Coal Creek Road (location on Plate 1). These samples were chosen for petrographic study, in part, because they represent the widest variety of lithologic types constituting the Coal Creek section. The samples were also chosen for the purpose of studying the provenance and diagenetic history of the arkosic Cowlitz Formation micaceous sandstones and siltstones, and interbedded basaltic conglomerates, lithic sandstones, and siltstones of the upper Grays River sedimentary unit (Tgvs2, Plates 1 and 2). Thin section study helps to also evaluate the reservoir potential (e.g., porosity and pore types) of clean, well-sorted, friable arkosic sandstones. To this goal, three thin section samples, representing the three most common Cowlitz Formation sandstone lithologies in the study area, were impregnated with blue dye to aid in the estimation of both porosity and relative permeability of the sandstone beds in the Coal Creek section. Four lithic arkoses and arkoses were point counted (thin sections CC-7, CC-17, CC-48, and CC-53b, Appendix IV) in order to more precisely determine the composition of Cowlitz Formation arkoses within the study area.

Sediment compositions in the Coal Creek section are the result of a complex interplay of mostly extrabasinal micaceous, arkosic deltaic sandstones and micaceous siltstones of the Cowlitz Formation, and less abundant basaltic (lithic) sandstones and pebble conglomerates derived from nearby forearc Grays River volcanic highlands and (possible) seamounts. Arkosic sandstone beds in the study area are rarely without some

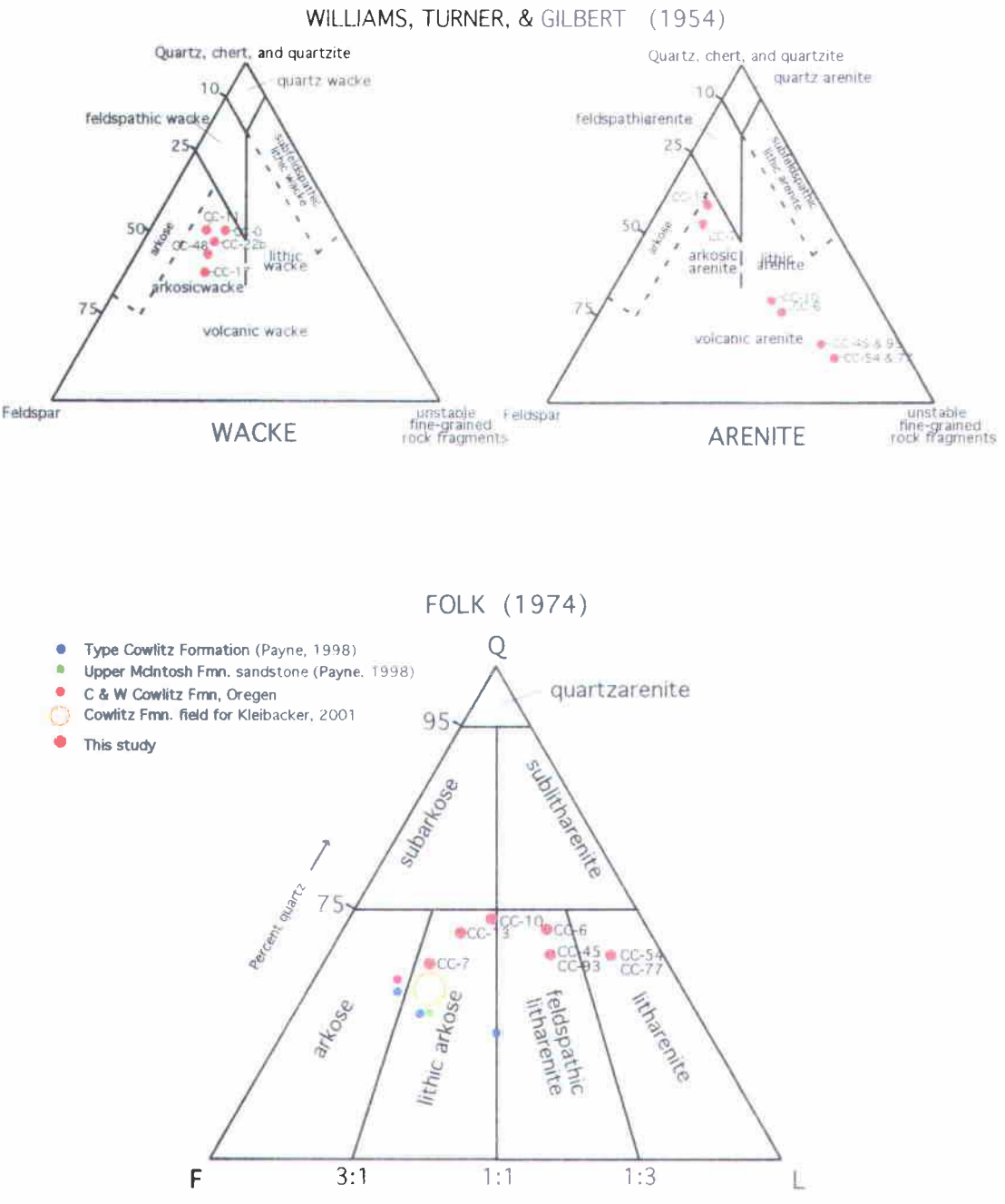

Figure 21: Sandstone classification ternary diagrams plotting several samples from the Coal Creek stratigraphic section.

rounded basaltic clasts, and most Grays River volcaniclastic beds throughout the study area have at least a minor micaceous, arkosic component. Grays River volcaniclastic interbeds, in the Coal Creek section (Tgvs2) in particular, contain a high arkosic mineral component (10-50%). Rare pure arkosic or pure basaltic volcaniclastic beds in the Coal Creek section are considered here to be end members of a compositional series, in which nearly every combination of the two sediment compositional types occurs. Sandstones and siltstones with less than 50% basaltic component (but more than 25% basaltic fragments) are considered lithic arkoses of the Cowlitz Formation (map unit Tc, Plates 1 and 2). Those with more than 50% basalt lithics are included in the Upper Grays River Volcaniclastic unit (map unit Tgvs2, Plates 1 and 2). Arkosic lithics are more than 75% feldspar, quartz, and mica. Several lithic arkosic arenites, wackes, and Grays River volcaniclastic beds are plotted on ternary diagrams based on the classification schemes of Williams and others (1954) and Folk (1974)(Figure 21).

Lithic arkoses and carbonaceous strata

Massive to poorly bedded sandstones possibly representing lowstand submarine channels (lithofacies j), or wave-reworked delta front sands (lithofacies g) are common in the upper 300 meters of the Coal Creek section. Five thin sections from these lithofacies were prepared, and one sample (CC-7) was impregnated with blue dye and point counted (Figure 22b, Appendix IV). Thin section sample CC-13 (Figure 22a), illustrating composition typical for these lithofacies when a relatively small percentage (<10%) of basaltic clasts are present, is well-sorted, and classifies as an arkosic arenite in the classification of Williams and others (1954) and lithic arkose in Folk's (1974) classification

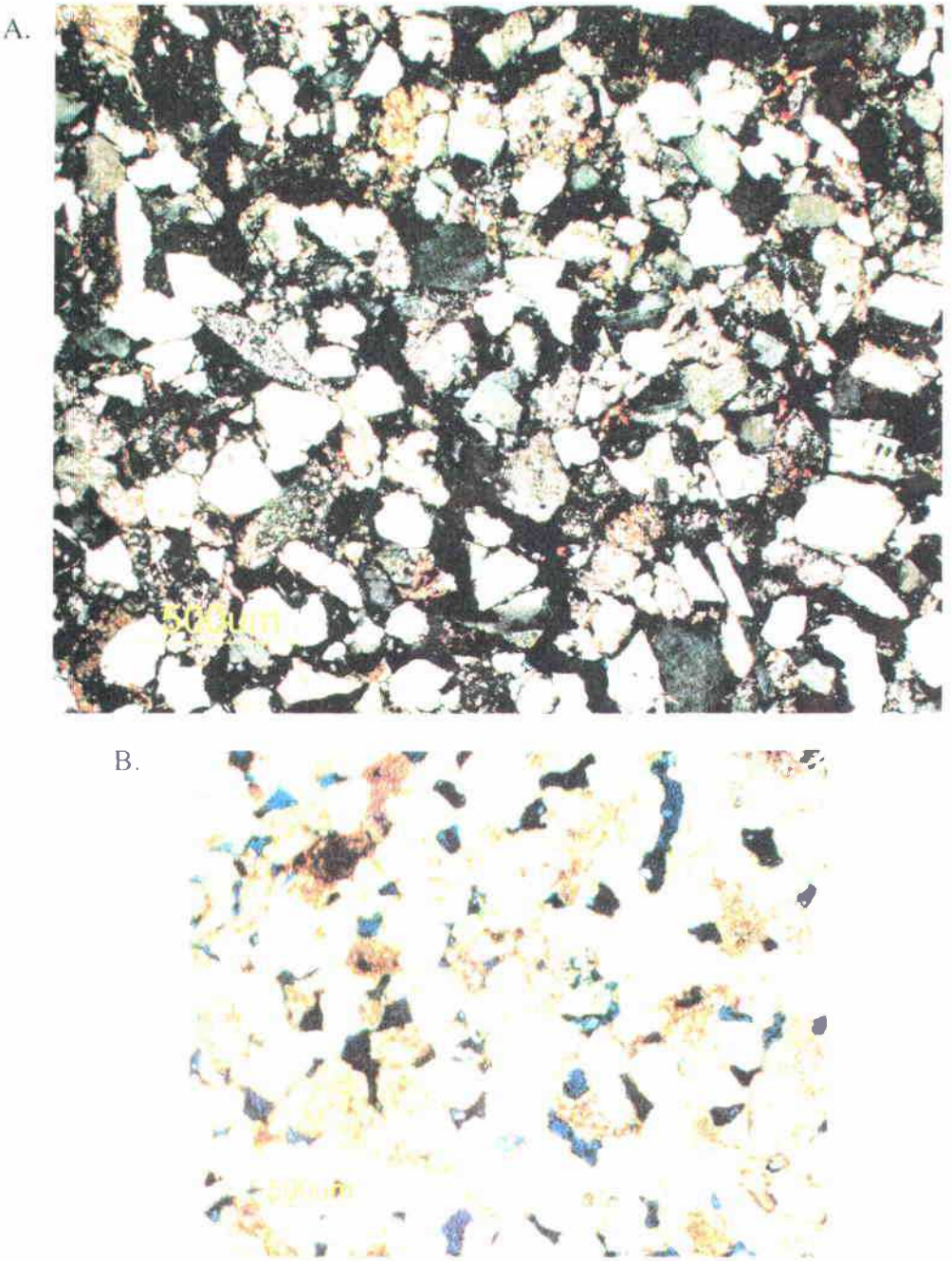

Figure 22: Photomicrographs of Coal Creek section lithofacies g, massive, well-sorted micaceous, arkosic sandstones with <5% Grays River basalt clasts.

A. Sample CC-13, moderately well-sorted lithic arkosic sandstone typical of Coal Creek interval 13 (crossed-nicols).

B. Sample CC-7, lithic arkosic sandstone from interval 7 impregnated with blue-dye filling the pore spaces (plane-polarized).

(Figure 21). This sample consists of about 35% quartz, 15% potassium feldspar, 5% calcium plagioclase, 5-10% opaque to translucent brown carbonaceous plant debris, and about 5% basalt, metamorphic clasts (quartzite, schist, and gneiss), mica, and chert. The remainder consists of metamorphic and plutonic minerals (e.g., epidote, hornblende, and augite). Quartz and feldspar are the dominant framework minerals and tend to be angular to subrounded, whereas basalt and chert fragments are subrounded to well-rounded.

Arkosic sandstone thin section CC-7 was impregnated with blue dye (Figure 22b), and while being similar in composition to sample CC-13 (also plotting as an arkosic arenite), is significantly more porous, with approximately 15% porosity. This sample is also moderately well-sorted, friable, and both compositionally and texturally mature to submature. Four hundred points were counted (the results are listed in appendix IV). The sample consists of 26% subangular monocrystalline quartz, 15% polycrystalline quartz, 15% potassium feldspar, 8% albite twinned calcic plagioclase, and about 10% basalt (nearly half of which is amygdaloidal, amygdules commonly filled with celadonite and chlorophaeite). Sandstone thin section CC-7 differs from CC-13 in having nearly 5% biotite and <1% opaque carbonaceous plant material.

Basaltic lithic arenites in the upper 130 meters of the Coal Creek section (Plate 2, thin sections CC-10 and CC-6) are poorly-sorted, with arkosic framework grains (i.e., quartz and feldspar) that are angular to subrounded, and basaltic rock fragments that are subangular to subrounded. Medium-grained sandstone (thin section CC-6, Figure 23a) contains basaltic clasts that are significantly larger (coarse sand) than the quartz and feldspar grains, with the largest being nearly 3mm in diameter. This sandstone consists of

A.

B.

Figure 23: Photomicrographs of basalt-lithic samples, lithofacies g or j.

A. Basalt-lithic arkosic sandstone, relatively well-sorted, with basalt clasts larger and relatively well-rounded compared to arkosic component (sample CC-6), celadonite-clay cemented (crossed-nicols).

B. Basalt-lithic, poorly-sorted coarse-grained arkosic sandstone, with sparry calcite cement (sample CC-10)(crossed-nicols).

approximately 25% quartz (both mono- and polycrystalline), 5% potassium feldspar (1:1 ratio of orthoclase and microcline), 5% albite twinned calcic plagioclase, and about 5% quartzite. Just less than 50% of the sample consists of volcanic lithic clasts, 35% of which are highly altered aphyric basalt or contain randomly oriented plagioclase microlites, 20% is pilotaxitic basalt, and 5% consists of pumice lapilli. The remainder of the sample consists of carbonaceous mudstone clasts and chert. Sandstone CC-10 (Figure 23b) is a poorly-sorted, coarse-grained sandstone to fine pebble conglomerate and classifies as a (borderline) lithic arkose in Folk's (1974) classification and a volcanic arenite in Williams and others (1954) classification. Framework grains include approximately 30% monocrystalline quartz, 5% polycrystalline quartz, 10% potassium feldspar, 5% calcic plagioclase, and minor mica (<1%), schist, and gneiss. About 25% of the sample consists of basalt clasts with randomly oriented plagioclase microlites in an aphyric matrix, and 25% basalt with pilotaxitic flow texture of plagioclase microlites, about 10% of which is amygdaloidal. The remainder of the framework grains are mostly metamorphic quartzite and white chert, and the sample is well-cemented with sparry calcite.

All thin section samples of lithofacies g and j show some degree of alteration of volcanic and feldspar clasts, compaction of ductile minerals, and a cement rind that can be either smectite clay or sparry calcite. Porosity varies greatly. Sample CC-13 (Figure 22a) shows a relatively high degree of compaction, whereas sample CC-7 (Figure 22b) shows little compaction, with a high degree of tangential contacts between brittle subangular quartz and feldspar grains. Due to compaction and smectite clay cement rimming the grains, little primary intergranular porosity or pore throat spaces remain in most samples of

this lithofacies (e.g., sample CC-13), and they therefore have low permeability (low interconnectivity due to clay filled pore throats). Some secondary porosity has resulted from the high degree of clay alteration and partial dissolution of potassium feldspar grains. The relatively high secondary porosity in samples such as CC-7 (~15%) seems largely to have resulted from such dissolution of potassium feldspars, and likely some glassy basalt lava clasts as well. Interconnectedness of interparticle pores and pore throats in this thin section, despite being weakly cemented by thin smectite clay rims and a minor amount of sparry calcite, implies that this Coal Creek interval has some degree of permeability. Sandstone samples of lithofacies g and j (Plate 2) with a higher percentage (20-50%) of basalt clasts are better cemented with authigenic smectite clay. This clay forms a thin rim around the grains in all samples, and is the dominant cement in sandstone CC-6, virtually eliminating all primary porosity. Thin section CC-10 has mostly tangential grain contacts, showing that little compaction has occurred. This sandstone originally had about 15% primary intergranular porosity that has been filled by sparry calcite cement (Figure 23b).

Large flaser-draped megaripples representing sand filled tidal channels or prograding tidal bars (lithofacies f, thin sections CC-22b and CC-48, Figure 24) are a common lithology in the Coal Creek section. Since these beds result from ebb and flood tidal influences, including the slack water stage, there is a significantly higher percentage of detrital mud, mica, and finely disseminated carbonaceous plant debris (draping the foresets) than in samples of lithofacies g. As with samples of lithofacies g, monocrystalline quartz and feldspar grains are angular to subrounded, and basalt and chert grains are subrounded to well-rounded. Thin section 22b (Figure 24a) is from an

A.

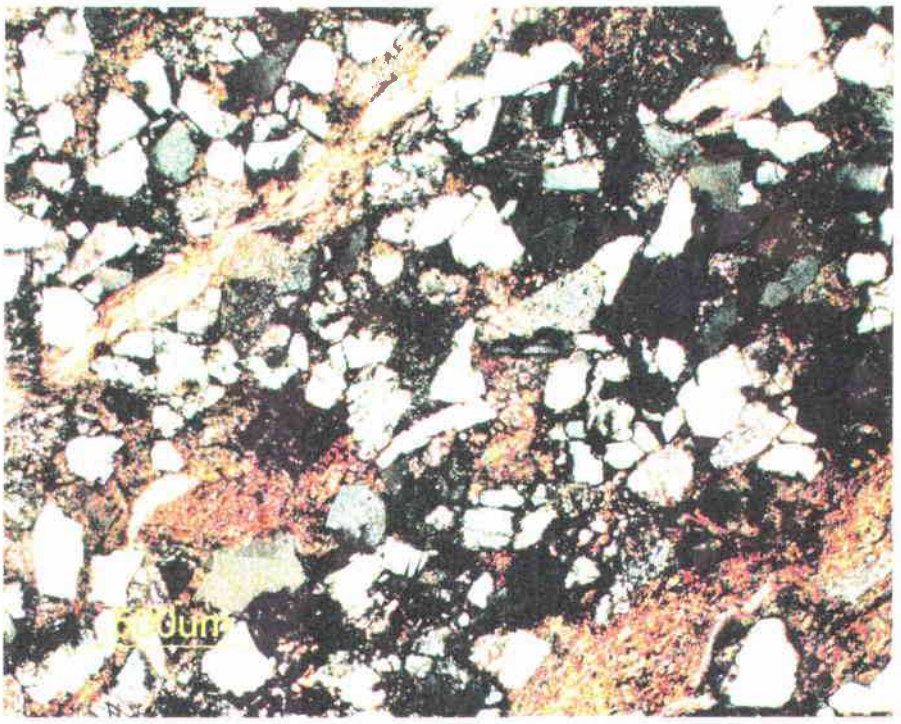

B.

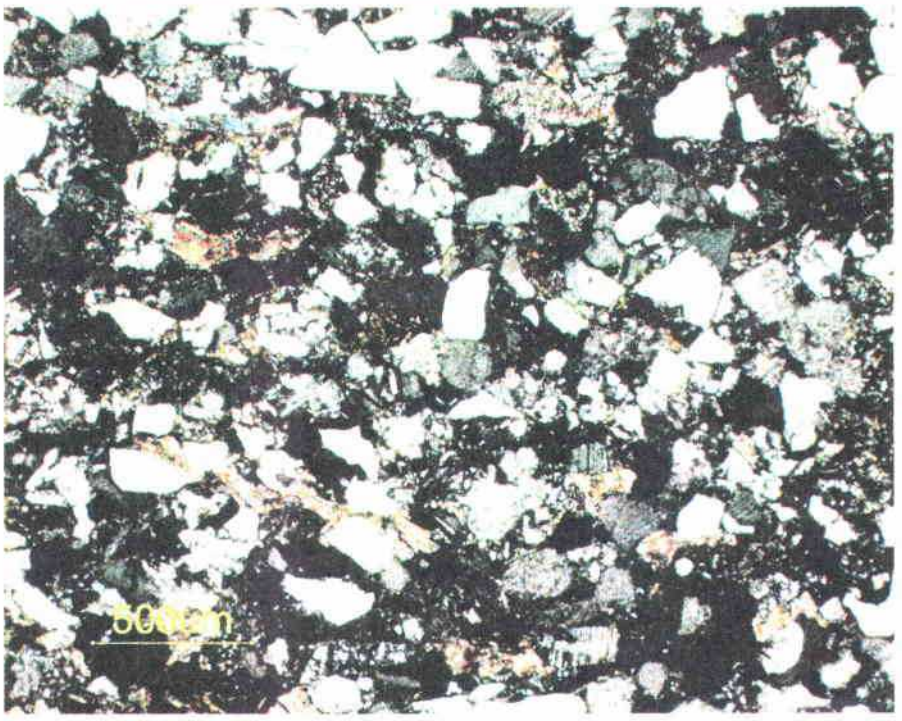

Figure 24: Photomicrographs of sandstones of lithofacies f, flaser-draped sigmoidal megaripples of a tidal channel or tidal bar (crossed-nicols).

A. Mud and carbon-rich foreset of a 1-meter thick flaser drape (CC-22b).

B. Foreset from a megaripple of interval 48 (CC-48). Note compacted muscovite flake and high percentage of dark carbonaceous plant debris.

approximately 20-cm thick sigmoidal sandstone bed in Coal Creek (not from the IS outcrop on Coal Creek Road where this same interval is better exposed), that has ~1-cm thick flaser-draped foresets. This sample is moderately well-sorted and consists of about 35% quartz (30% monocrystalline and 5% polycrystalline), 5% mica, 15% clay and chlorite flakes combined, 10% carbonaceous plant debris, 10% potassium feldspar, 5% albite twinned calcic plagioclase, 10% basalt lava fragments, and ~7% chert, classifying as a micaceous arkosic wacke (Figure 21). Thin section CC-48 (Figure 24b) is from a 1-meter high, flaser-draped, sigmoidally cross-bedded, medium-grained sandstone. Four hundred points were counted, and the results are listed in appendix IV. About 40% of the sample consists of (mainly) monocrystalline quartz, 10% carbonaceous plant material, and 14% altered basalt clasts. This composition is similar to samples of lithofacies g and j, but with a higher percentage of mica and carbonaceous plant material constituting up to 50% of the flaser-drapes, classifying as a carbonaceous arkosic/volcanic wacke (Figure 21). In both these samples, feldspars and volcanic fragments are clay altered, and chlorite and clay have formed pseudomatrix in flaser-draped laminae. Ductile contorted micas and chlorite show a substantial amount of compaction between the quartz and feldspar grains. Thin section CC-22b is weakly cemented with smectite clay, and porosity and permeability are near zero. Thin section CC-48 is compacted to a lesser degree, and is well indurated by both greenish brown smectite clay and sparry calcite cement.

Lithofacies e (represented by thin sections CC-17 and CC-11) is a heterolithic tidal rhythmite facies produced in a bay or estuarine setting, characterized by alternating thin beds or laminae of wavy- or micro-cross laminated, fine- to medium-grained

sandstone, and drapes of carbonaceous and micaceous laminae or thin beds of darker gray claystone. This lithofacies represents a lower energy depositional environment than lithofacies f and g, and as such, has a higher percentage of mudstone, mica, and carbonaceous plant debris. Lithofacies e also has a lower percentage (typically < 5%) of larger basalt clasts.

Both samples are micro-cross laminated, with thin sandstone beds averaging about 2cm in thickness, and framework quartz and feldspar grains that are subangular to subrounded. Dark foreset laminae are silty mudstone, containing arkosic silt-sized clasts in an abundant clay matrix. Four hundred points were counted in thin section CC-17 (Figure 25a, Appendix IV). The composition is similar to CC-11, and consists of about 40% quartz (35% monocrystalline), 11% biotite, 5% muscovite, 13% potassium feldspar (nearly all orthoclase), 6% albite twinned calcic plagioclase, 15% contorted carbonaceous plant debris along laminae, and about 10% clay matrix, classifying as an arkosic wacke (Figure 21). This sample was also impregnated with blue dye, and has less than 5% porosity. Thin section CC-11 (Figure 25b) has a higher percentage of biotite (~15%), and only about 5% brownish clay matrix. Flaser-draped laminae are up to 70% carbonaceous plant debris, and nearly pure coal (fusane) laminae occur intermittently. Potassium feldspars (mainly orthoclase) in this lithofacies are highly altered, some completely to clay, and all feldspar grains have at least a thin rim of clays. Compaction is relatively high in these samples, warping and contorting the biotite, and most biotites are partly to completely altered to greenish chlorite. Carbonaceous laminae have been squeezed between grains in place to become a pseudomatrix.

A.

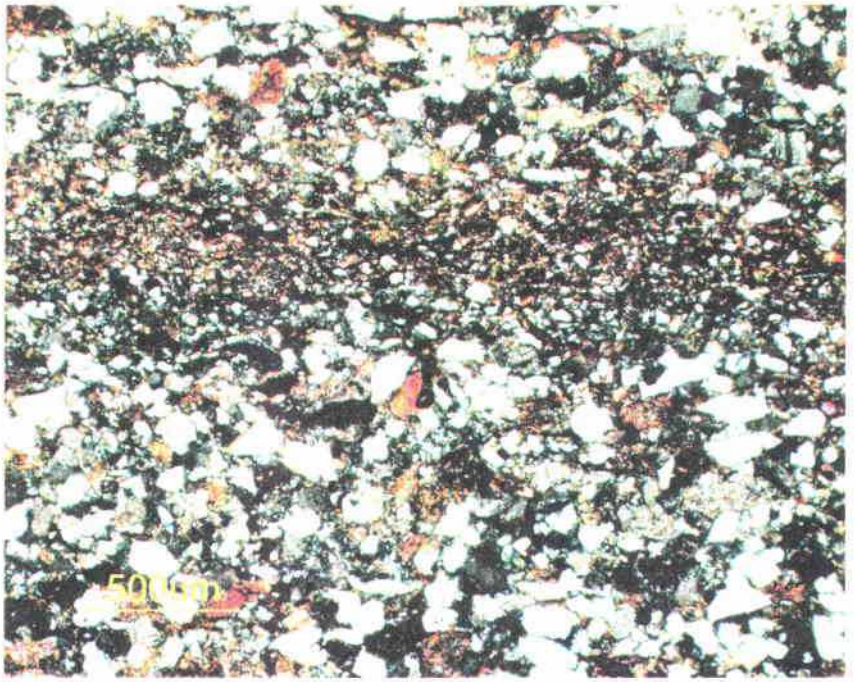

B.

Figure 25: Photomicrographs of sandstones of lithofacies e (tidal rhythmites). Note that samples are rich in carbonaceous debris/biotite (crossed-nicols).

A. Sample CC-17, illustrating moderately well-sorted, medium- to fine-grained arkosic sandstone, with a siltstone lamina rich in carbonaceous plant debris and biotite.

B. Sample CC-11. Note upper lamina contains abundant carbonaceous plant debris and biotite.

Intervals 0 through 2 of the Coal Creek section (constituting the upper ~45 meters, Plate 2) have a unique lithology. The depositional environment is uncertain, but could represent distal (deeper water) tidal rhythmites (lithofacies e), or more likely shelfal turbidites (lithofacies k). This lithology consists of 0.5-2-mm thick, fine-grained sandstone laminae alternating with dark colored carbonaceous and micaceous 0.5-2-mm thick clayey siltstone laminae (thin section CC-0, Figure 26a). Sandstone laminae consist of about 40% quartz (~35% monocrystalline and 5% polycrystalline), 15% biotite, 5% muscovite, 10% potassium feldspar (mostly orthoclase), 5% plagioclase, 10% nearly opaque carbonaceous plant debris, 5% basalt lava (mostly randomly oriented plagioclase microlites) and about 10% clay matrix. Carbonaceous siltstone laminae consist of about 40% monocrystalline quartz, 20% biotite, 10% muscovite, 10% potassium feldspar, 5% plagioclase, and 15% carbonaceous material. Some dark laminae are more than 70% biotite and carbonaceous plant material. This sample classifies overall as a micaceous, carbonaceous arkosic wacke (Figure 21). An unusual feature of interval 0 of the Coal Creek section is that the grain size is commonly larger in the muddy, carbonaceous drapes. Thin section CC-0 is calcite cemented, but clay mineral alteration products and carbonaceous plant material, due to compaction, have formed pseudomatrix. Ductile micas are bent and contorted due to compaction during burial.

One thin section was prepared of a coal/carbonaceous shale bed exposed in the roadcut on Coal Creek Road, with lithology typical for lithofacies h of the Coal Creek section (IS coal, Figure 26b). This coal consists of wavy laminae of opaque black charcoal (plant fusane or inertinite) and some wavy laminae of translucent reddish vitrinite.

A.

B.

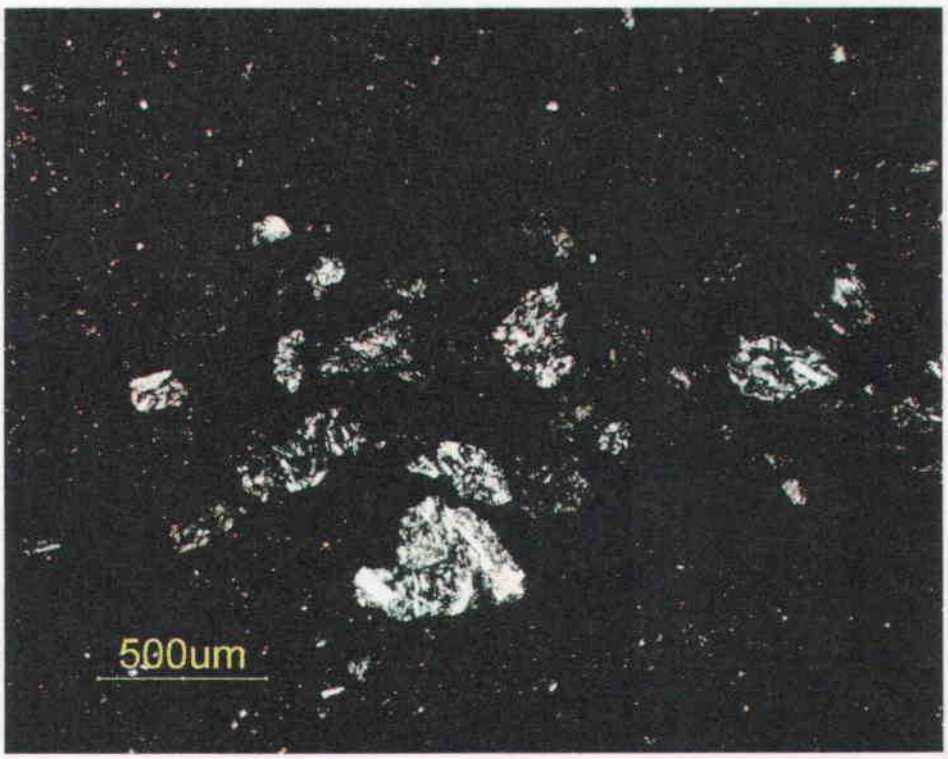

Figure 26: A. Photomicrograph of interval 0 (CC-0) (crossed-nicols). Carbonaceous siltstone alternates with sandy biotite-rich and carbonaceous drapes.
B. Thin section of a coal (lithofacies h) from Coal Creek interval 22 (IS coal)(crossed-nicols). Note highly porphyritic sand-sized clasts.

There is also a component (~10%) of arkosic siltstone, and one thin lamina containing medium- to coarse-grained, subangular to subrounded clasts of highly plagioclase porphyritic volcanic lithic sand. In the roadcut, this coal bed is associated with several silicic, tuffaceous interbeds, so the porphyritic clasts may also be derived from a western Cascade source. The lithology of these clasts is similar to that found in Cascade-derived basaltic andesite and andesite within the study area.

Upper Grays River Volcaniclastic Interbeds (Tgvs2)

Over fifteen beds of Grays River volcaniclastics of 1-meter thickness or greater occur as interbeds of the arkosic Cowlitz Formation within the Coal Creek stratigraphic section (Plate 2), particularly in informal unit 2. The thickest volcaniclastic at the base of unit 2 has a maximum thickness of nearly 35 meters. These units range from siltstone to cobble-bearing, grain-supported, gravel conglomerates, and commonly contain shallow-marine to freshwater fossil molluscan assemblages. In fact, about 90% of fossil assemblages collected for this study were found in Coal Creek intervals that are greater than 60% basalt clasts. Grays River basalt clasts with a pilotaxitic flow texture of plagioclase microlites are also present to some degree in nearly all dominantly arkosic or carbonaceous beds of the Cowlitz Formation in the study area. Likewise, interbeds of arkosic Cowlitz Formation sandstone and siltstone occur throughout the area in the Lower Grays River Volcaniclastic unit (Tgvs1) that underlies most of the dominantly arkosic Cowlitz Formation in the area, and also occur in the thick Upper Grays River Volcaniclastic interbeds in the Coal Creek section (Tgvs2).

A.

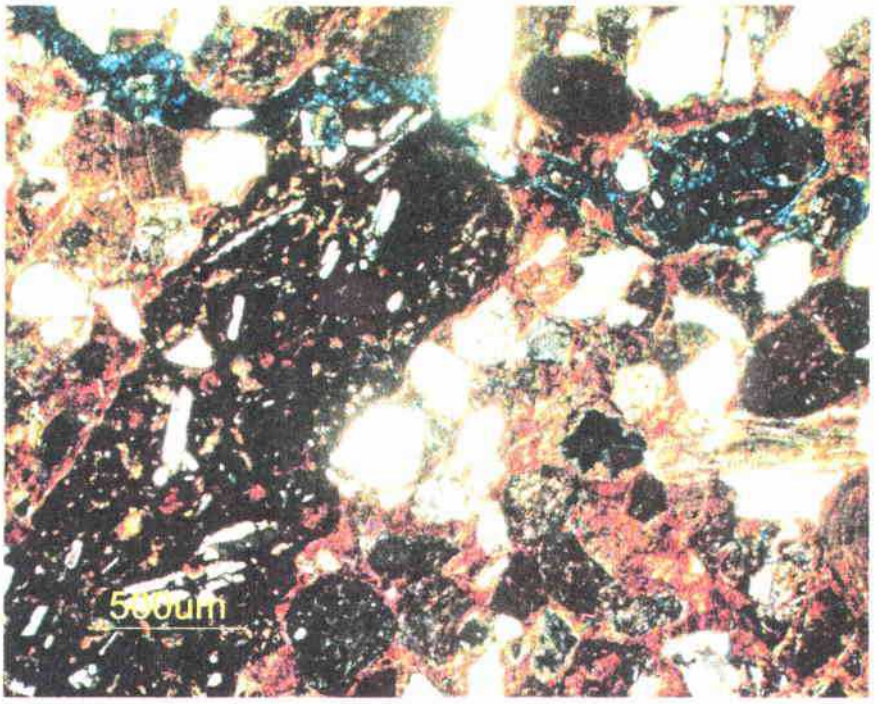

B.

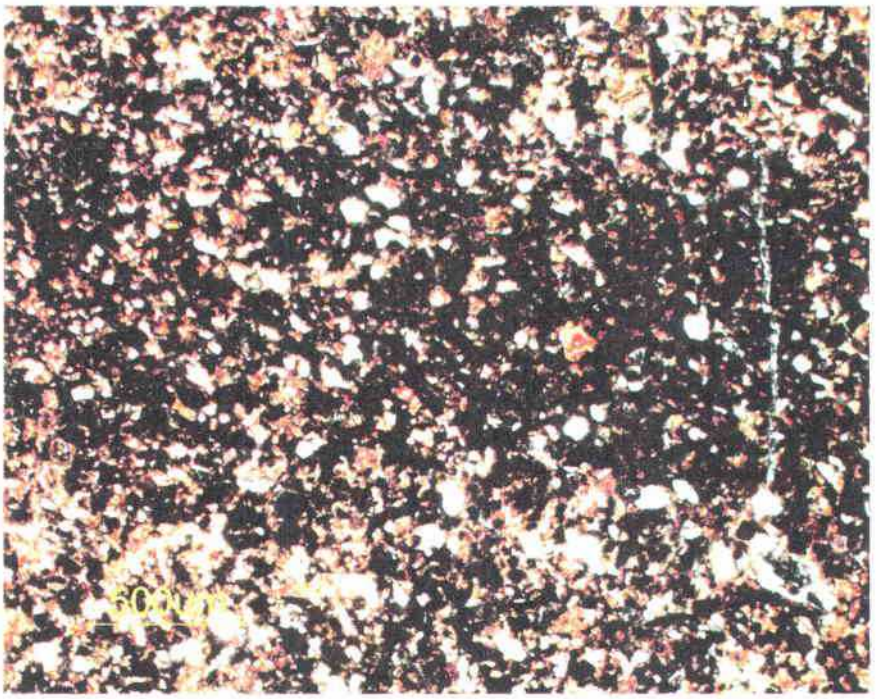

Figure 27: Photomicrographs of Grays River shallow marine volcaniclastic interbeds (Tgvs2) within the Coal Creek stratigraphic section (crossed-nicols).
A. Basalt pebble conglomerate of lithofacies c1 from interval 45 (CC-45). Clasts are a combination of well-rounded pilotaxitic and intersertal basalt, and Cowlitz Formation arkosic clasts. Celadonite cement dominates.
B. Basaltic siltstone of lithofacies c2 from interval 54 (CC-54). Cement is both smectite clay and sparry calcite.

Basalt conglomerate samples (CC-45 and CC-93, lithofacies c1) are poorly-sorted and consist of well-rounded to subangular framework clasts that are a mixture of pilotaxitic, massive, and scoriaceous basalt up to 0.5 cm in diameter. These samples also contain up to 30% micaceous, arkosic minerals (quartz, feldspar, and mica), and classify as feldspathic litharenites in Folk's (1974) classification, and volcanic arenite in Williams and others (1954) classification (Figure 21). They consist of about 10% quartz (dominantly monocrystalline, but some clasts are polycrystalline), <1% mica (biotites are altered to pleochroic green chlorite), 10% potassium feldspar, 5% plagioclase, and about 60% basalt lava clasts (50% with intersertal texture and scoriaceous, and 10% pilotaxitic). A high degree of clay alteration has occurred in these samples. Thin section CC-45 (Figure 27a) is tightly cemented with smectite clay, and most basaltic clasts have at least a thin rim of clay alteration. Augite phenocrysts within basaltic clasts are altered to brownish clay. This sample was also impregnated with blue dye, showing that most of the porosity is due to small fractures, but some is due to secondary dissolution and alteration of augite. Thin section CC-93 is highly clay altered, with approximately 20% of the clasts nearly dissolved away. Many of the resulting pore spaces are filled with clay. Vesicle space in the scoriaceous clasts and much of the altered clay matrix is filled with or replaced by sparry calcite cement.

Basaltic sandy siltstone samples (CC-54 and CC-77c, lithofacies c2) are well indurated and thinly-laminated. Lighter laminae consist of a higher percentage of calcite cement, and darker laminae have less calcite cement and more silt-sized basaltic clasts. This facies consists of 60-70% basalt clasts with intersertal texture, and about 10%

monocrystalline quartz derived from the extrabasinal Cowlitz Formation arkosic source. These sandstones classify as litharenite in Folk's (1974) classification and as volcanic arenite in the classification of Williams and others (1954)(Figure 21). The extent of clay alteration can be high (CC-54, Figure 27b) or low (CC-77c), and sparry calcite cement varies from about 15% (CC-54) to approximately 30% (CC-77c), explaining why this lithofacies is resistant and cliff-forming within the creek (particularly interval 68 where it forms a four-meter high waterfall, see Figure 8a). Thin section CC-77c contains <1% calcareous broken shell fragments.

X-ray Diffraction

Three micaceous arkosic sandstones of the Cowlitz Formation and one Grays River basalt volcaniclastic interbed from the Coal Creek stratigraphic section were analyzed by Dr. Reed Glasmann at Oregon State University by x-ray diffraction to further illustrate the mineralogy and diagenetic history of the Paleogene sedimentary rocks in the study area. Among these samples were flaser-draped tidal megaripples from interval 22 (sample CC-22d, lithofacies f), and flaser-draped tidal rhythmites from interval 48 (sample CC-48, lithofacies e). The <15 μm fraction shows strong peaks (intensity) for quartz, muscovite, and anorthite (feldspar of volcanic origin) as expected for the Cowlitz Formation (Figure 28), illustrating the Rocky Mountain provenance of these sediments. A peak for calcite also indicates that sample C-22d is somewhat calcite cemented, as seen in several thin sections of this lithofacies. A fairly strong peak (2,000 to 3,000 counts) for chamosite (iron-rich chlorite) in sample 22d shows that some of the larger size fraction consists of altered biotite, as would be expected from the flaser-draped foresets of the

megaripples. For the clay fraction (<2μm), sample 22d (Figure 29), and CC-48 (Figure 32) show strong peaks for smectite, as expected from the degree of clay-rim cementation observed in thin section. CC-22d shows a fairly strong peak (~5,000 counts) for chlorite, whereas sample CC-48 shows a much stronger peak (~7,000 count). This is a result of the higher percentage of flaser-draped micaceous mudstone in lithofacies e, often representing 50% or more of the sample. Biotite in the drapes has altered to chlorite. The iron-rich smectite (nontronite) is a low temperature smectite, suggesting that the Cowlitz Formation sediments in Coal Creek have not undergone much geothermal heating, or flash point heating by Grays River intrusions. This also suggests that thermal maturation of source rocks in the area may be low. Sample CC-80 is from a relatively clean sandstone (low percentage of flaser-draped carbonaceous mud and mica). The <15μm fraction for this sample (Figure 30) shows strong peaks for quartz, muscovite, montmorillonite and chamosite (chlorite). The clay fraction is relatively high in montmorillonite (Figure 31).

The Grays River basalt volcaniclastic sample from interval 79 (CC-79), for the <15μm fraction, shows a comparatively weak peak for quartz, and a comparatively high peak for anorthite, suggesting that this interbed has a very small Cowlitz Formation micaceous, arkosic extrabasinal component. The <2μm clay fraction (Figure 33) shows a high peak for iron-rich smectite, and essentially no chlorite. The lack of chlorite (altered biotite) also illustrates the low component of micaceous arkose, and the lack of tidal slack water influence.

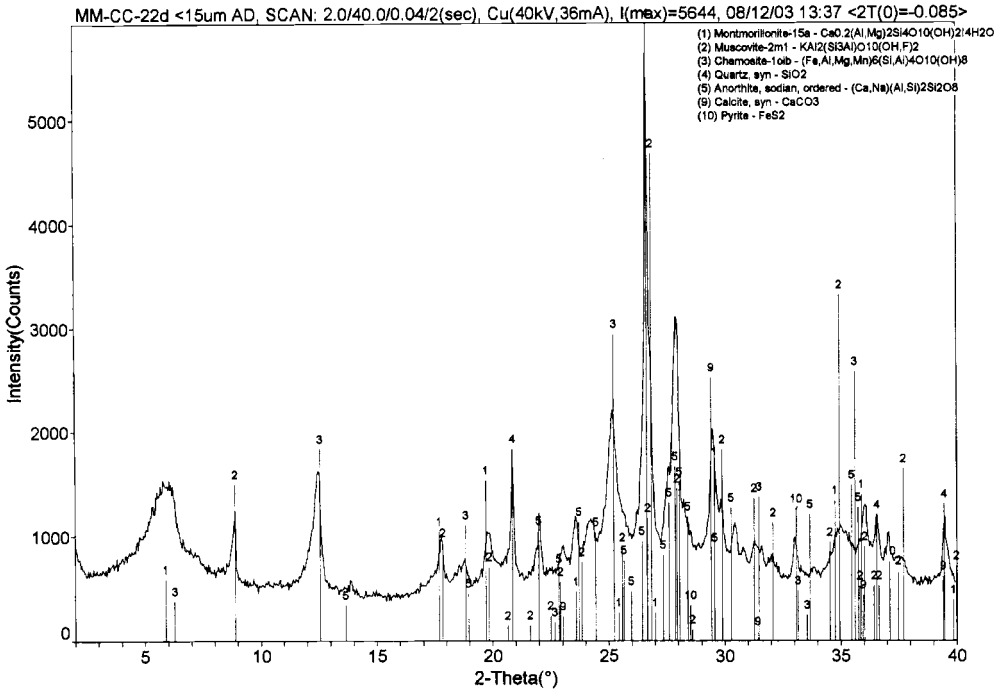

WGS Figure 28: <15 micrometer fraction of Coal Creek sample 22d

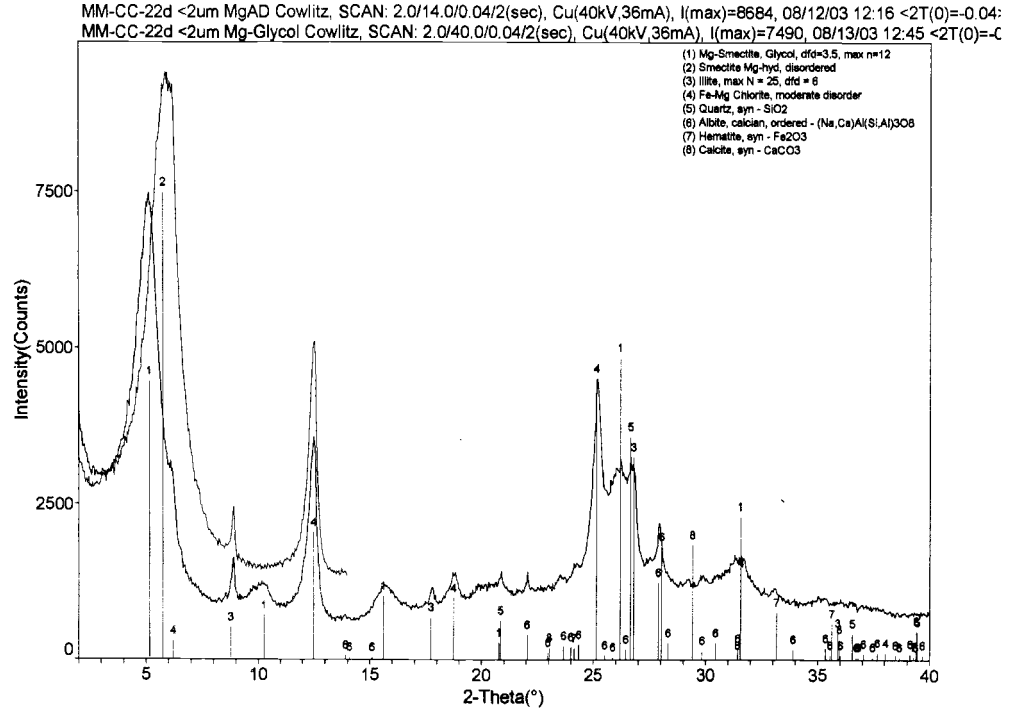

WGS Figure 29: <2 micrometer fraction of Coal Creek sample cc-22d

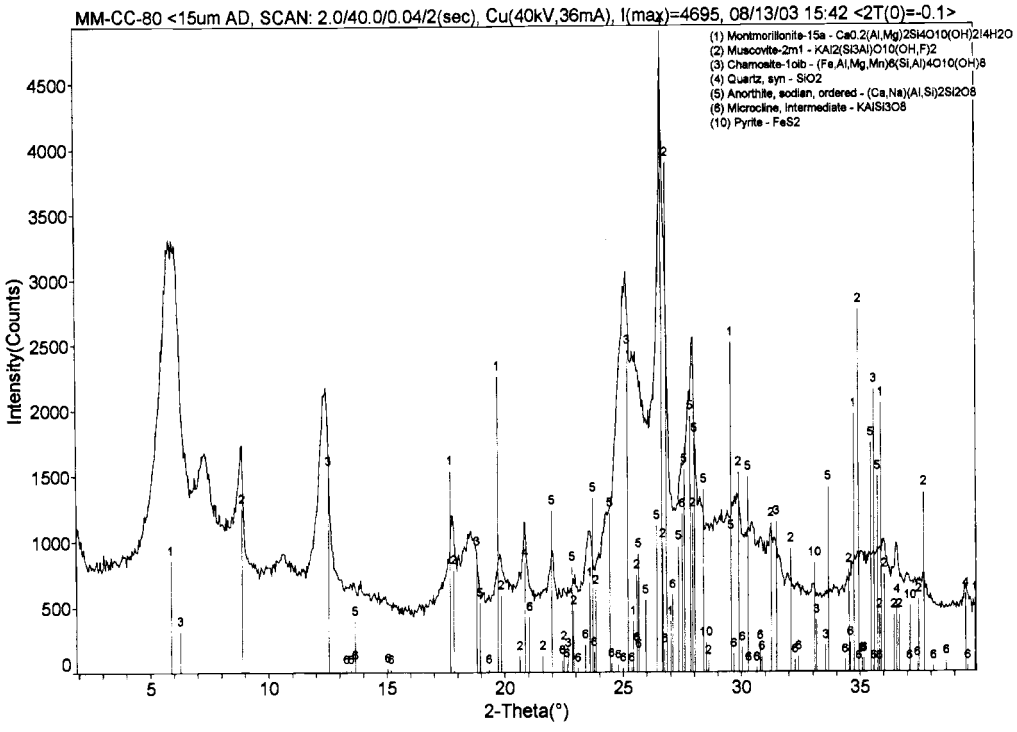

WGS Figure 30: <15 micrometer fraction of Coal Creek sample cc-80

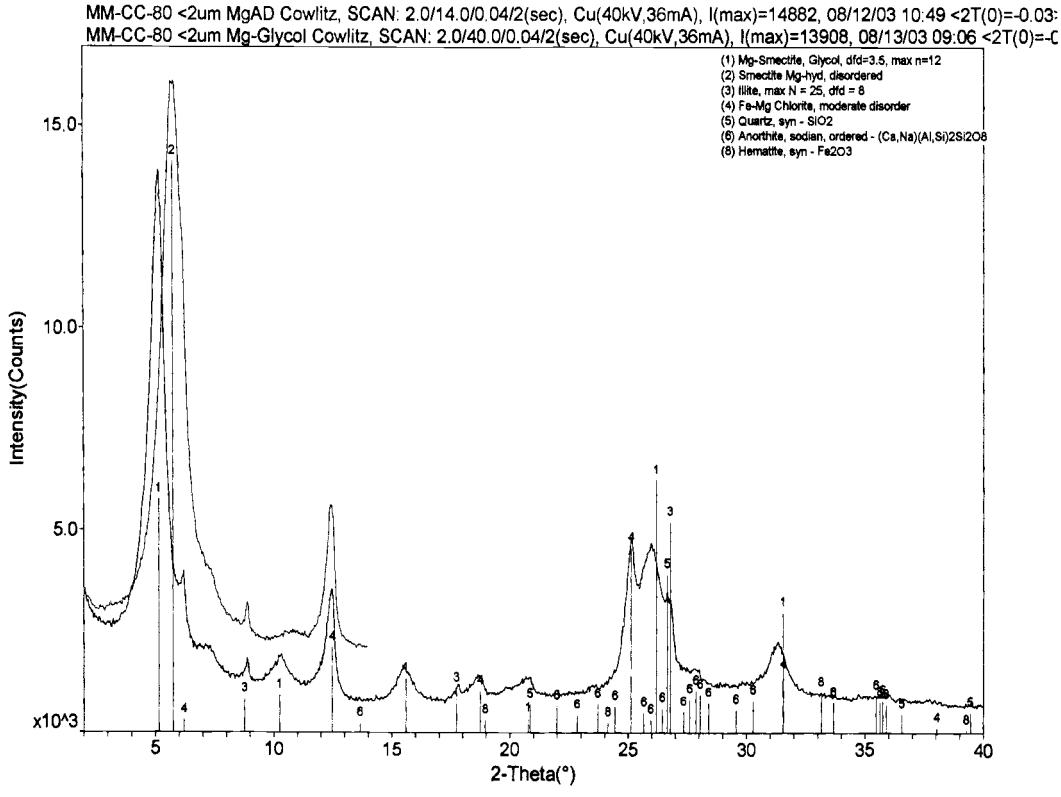

VGS Figure 31: <2 micrometer fraction of Coal Creek sample cc-80

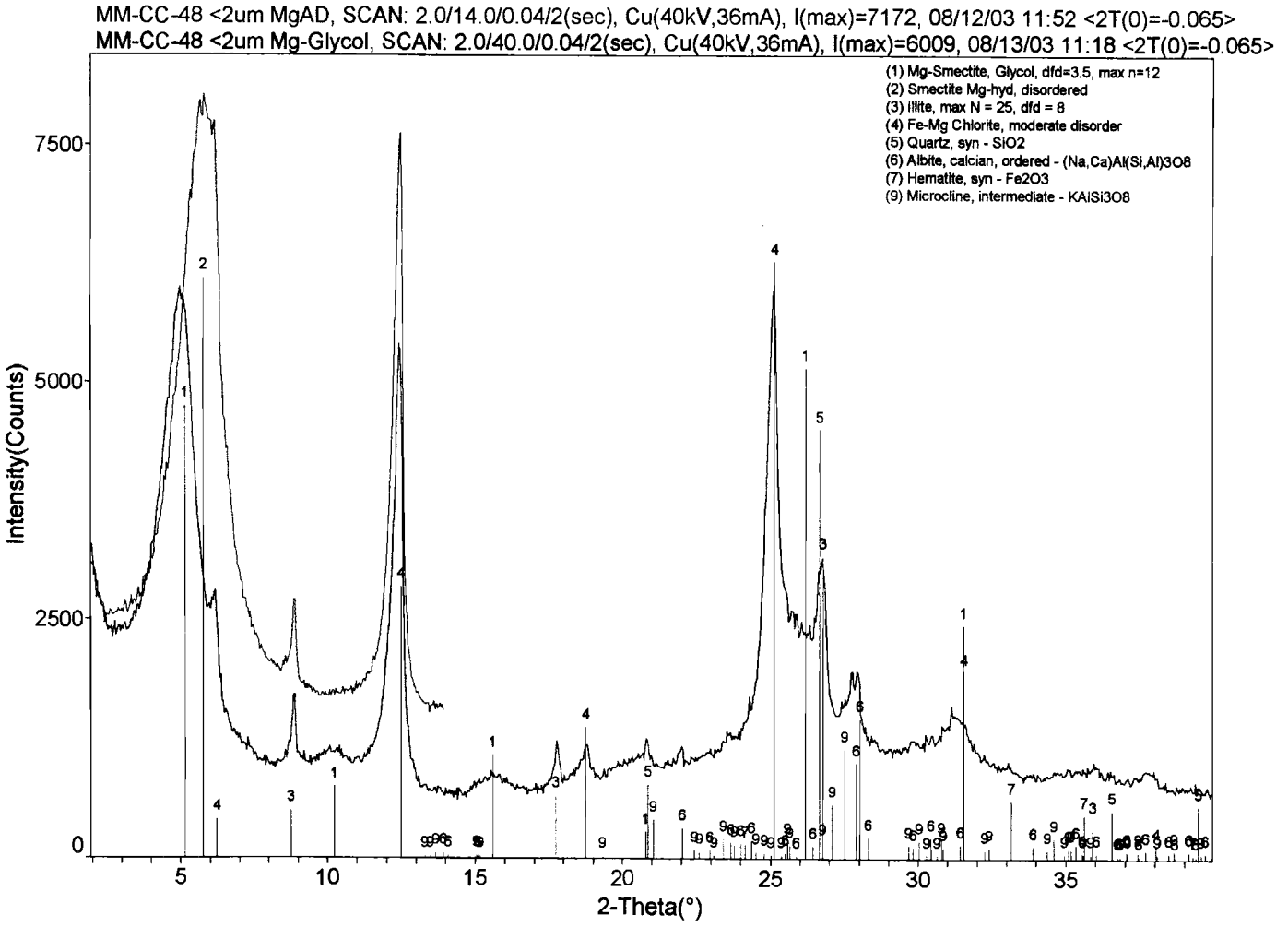

Figure 32: <2 micrometer fraction of Coal Creek sample cc-48

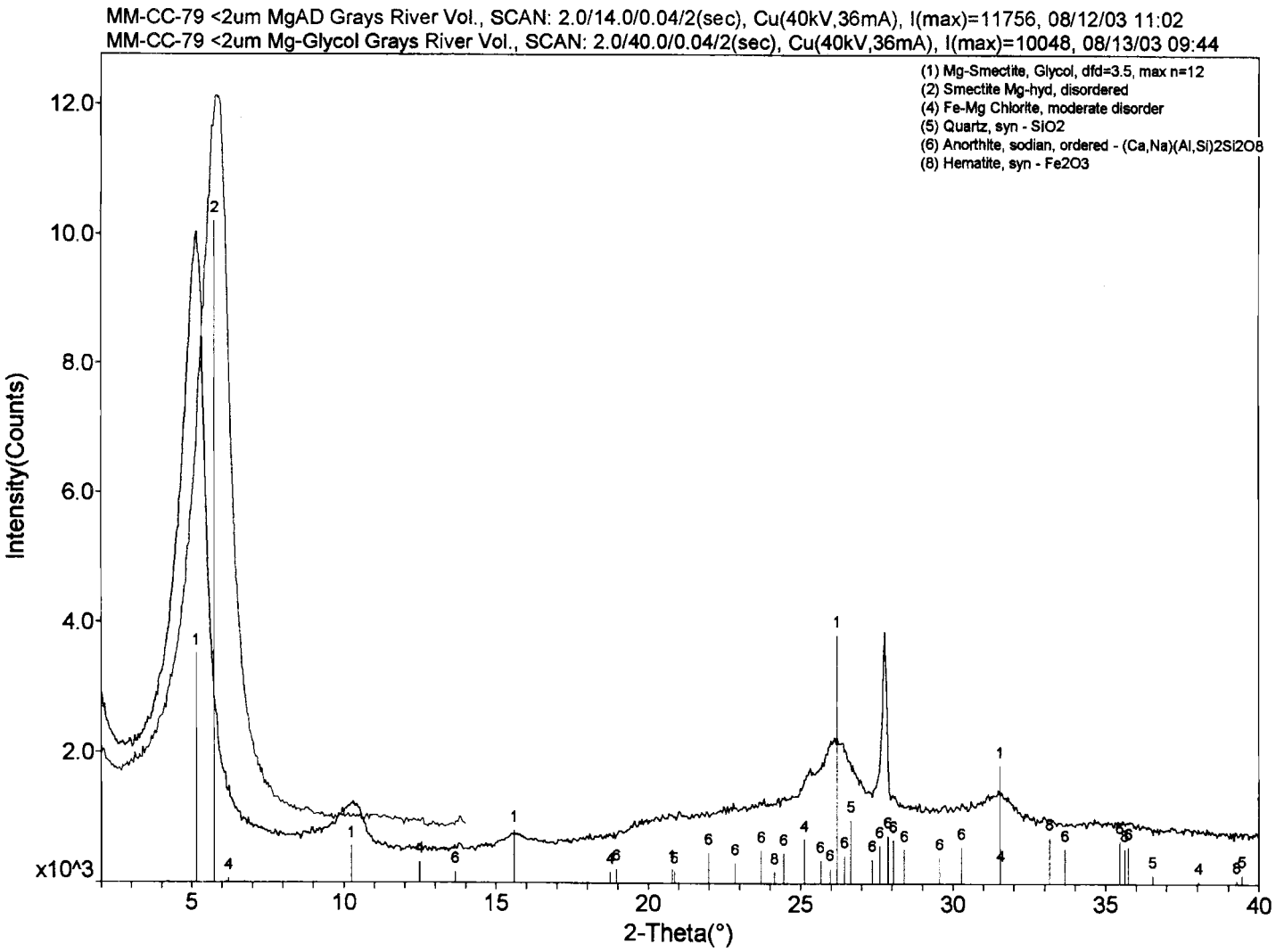

Figure 33: <2 micrometer fraction of Coal Creek sample cc-79

Sequence Stratigraphy and Correlation to the Cowlitz Type Section

Sequence stratigraphy is the study of genetically related facies within a framework of chronostratigraphically significant surfaces (Van Wagoner et al., 1992). Before sequence stratigraphy was understood, most studies were based on lithostratigraphic rather than time stratigraphic correlation. This relatively new (within the last ~20 years) approach to studying sedimentary rock successions, places sedimentary units into a hierarchical classification of progressively thicker chronostratigraphic units (representing increasing duration of deposition) that includes, laminae, lamina sets, beds, bedsets, parasequences, parasequence sets, and sequences (Van Wagoner et al., 1992). Such units are cyclic and result from relative changes or fluctuations in sea level, and are classified according to the magnitude (scale and duration) of the cycles (i.e., 3rd, 2nd, and 1st order cycles). A sequence as defined by Mitchum (1977) is a relatively conformable succession of strata that are genetically related, and bounded by unconformities or their correlative conformities. Boundaries between sequences occur during periods of relative falls in sea level, and the unconformity produced (the sequence boundary) separates facies that are unrelated to each other both physically and temporally. However, seaward in the deeper parts of the basin a conformity may exist between sequences. Such sequences can be subdivided based on transgressive surfaces and maximum flooding surfaces, and are composed of multiple parasequences forming parasequence sets.

A parasequence (typically tens of meters thick) is defined as a set of beds that are genetically related and relatively conformable, and bounded by marine flooding surfaces (Van Wagoner et al., 1992). Parasequences have been defined in a variety of marine and

nonmarine depositional settings including shelf, estuarine, tidal, beach, and coastal plain (Van Wagoner, 1985). Vertical facies associations within parasequences, either coarsening- and thickening- or fining- and thinning-upward, are interpreted by Van Wagoner et al. (1992) to represent progradational bedsets deposited in shoaling-upward depositional environments, which are abruptly overlain by the basal marine flooding surface of the next parasequence. A parasequence set is a succession of genetically related parasequences that form a characteristic stacking pattern, and are typically bounded by major marine flooding surfaces. The stacking pattern can be: 1) progradational, where each parasequence in the set can becomes thicker and coarser upward, or thinner and finer upward, 2) retrogradational, where parasequences become thinner and finer upward, or 3) aggradational, where subsidence keeps pace with sedimentation rate and relatively little change in bed thickness and coarseness occurs upward. Both parasequences and parasequence sets form in response to relatively rapid increases in water depth related either to eustatic and/or local tectonic basinal changes. Each depositional sequence between sequence boundaries can also be divided into stratigraphic units known as systems tracts which consist of a parasequence set, and are defined as a linkage of contemporaneous depositional systems. Such systems tracts can be lowstand (LST), transgressive (TST), highstand (HST), or shelf margin (SMST), depending on whether they form during relatively low water, increasing water depth, or high water respectively during a depositional cycle.

Sequence stratigraphic analyses have been applied to the study of sedimentary units within the Tertiary Cascadia forearc basin of southwest Washington and northwest Oregon by Armentrout (1987), Ryu and Niem (1992), as well as graduate students from

Oregon State University (Payne, 1998; Kleibacker, 2001). Armentrout (1987) defined four unconformity-bounded sequences in the Tertiary formations of southwest Washington. These sequences are second order megacycles (~5 to 50 m.y. in duration) separated by three tectonically controlled regional sequence boundaries (unconformities representing relative sea level fall resulting from regional forearc tectonics). The McIntosh and Cowlitz Formations, as well as the Grays River Volcanics, were included by Armentrout (1987) in his 2nd order sequence II, between regional unconformities 4 and 3, which is estimated to be 6 m.y. in duration. Payne (1998) in his study of the type Cowlitz Formation section in Olequa Creek, further divided the ~1000-meter thick middle Eocene McIntosh Formation and ~1,240-meter thick late-middle Eocene Cowlitz Formation collectively into five 3rd order cycles that ranged from 1 to 5 m.y. in duration with some radiometric dating and microfossil control. He was able to determine these durations by calculating the average sedimentation rate of a ~1400 meter section spanning the base of the upper McIntosh Formation to near the middle of the Cowlitz Formation (in his informal unit 3). The sequence boundary between the upper and lower McIntosh Formation was correlated to the eustatic sequence boundary of Haq et al. (1987) at 42.5 Ma, and the upper boundary was determined by dating a tuff bed in unit 3 at 38.9 Ma. This produced an average sedimentation rate of 39 cm/1000 yrs. Similarly, Kleibacker (2001) determined an average sedimentation rate of 22 cm/1000 yrs in the Cowlitz Formation of his Germany Creek section by using the 42.5 Ma eustatic sequence boundary at the base, and a Grays River lava flow dated at 39.36 Ma at the top. Using the average of these two findings of ~30 cm/1000 yrs (and the known durations of magnetic chrons, Figure 46) the Coal Creek section likely took ~2 m.y. to be deposited.

In this study, short-term thinning- and fining-upward, and coarsening-and thickening-upward (shoaling-upward) cycles define 4th order parasequences (of ~100,000 year duration) that stack to form 3rd order regional sequences (Cowlitz Formation cycles 3, 4, and 5 of Payne, 1998) of 1 to 5 m.y. duration. Lithologically, the Coal Creek stratigraphic section of this study correlates well to the type section of the Cowlitz Formation as described by Payne (1998) in Olequa Creek near Vader (Figure 34). Informal unit 1 of the Cowlitz type section contains multiple coal beds in its upper 100 meters, which are immediately overlain by ~30 meters of Grays River basalt volcaniclastic representing the base of Payne's unit 2. Unit 2 also contains multiple interbeds of basalt volcaniclastic throughout. The same general stratigraphy and lithology occurs deep in the Coal Creek section, where at least 2 thick coals (coals A and B) immediately underlie a ~35-meter thick Grays River Basalt volcaniclastic interbed (Tgvs2). Overlying this thick volcaniclastic are multiple basalt pebble conglomerate and coarse-grained sandstone interbeds, as well as thick shallow marine arkosic sandstone sequences, similar to Payne's informal unit 2. This similarity in lithology suggests that the lower ~340 meter portion of the Coal Creek section is lithologically correlative to informal units 1 and 2 of the type section as described by Payne (1998). Overlying units 1 and 2 of the type section is Payne's unit 3, characterized by abundant tidal sandstone facies and coals. The same general lithology occurs in the Coal Creek section from ~310 to 145 meters depth.

In the type Cowlitz Formation section, the shallow marine to coastal plain facies of unit 3 is overlain by about 160 meters of the comparatively deep-water facies of unit 4. Except for the nearly 10 meters of lower shoreface to shelf beds of intervals 20, 18, and

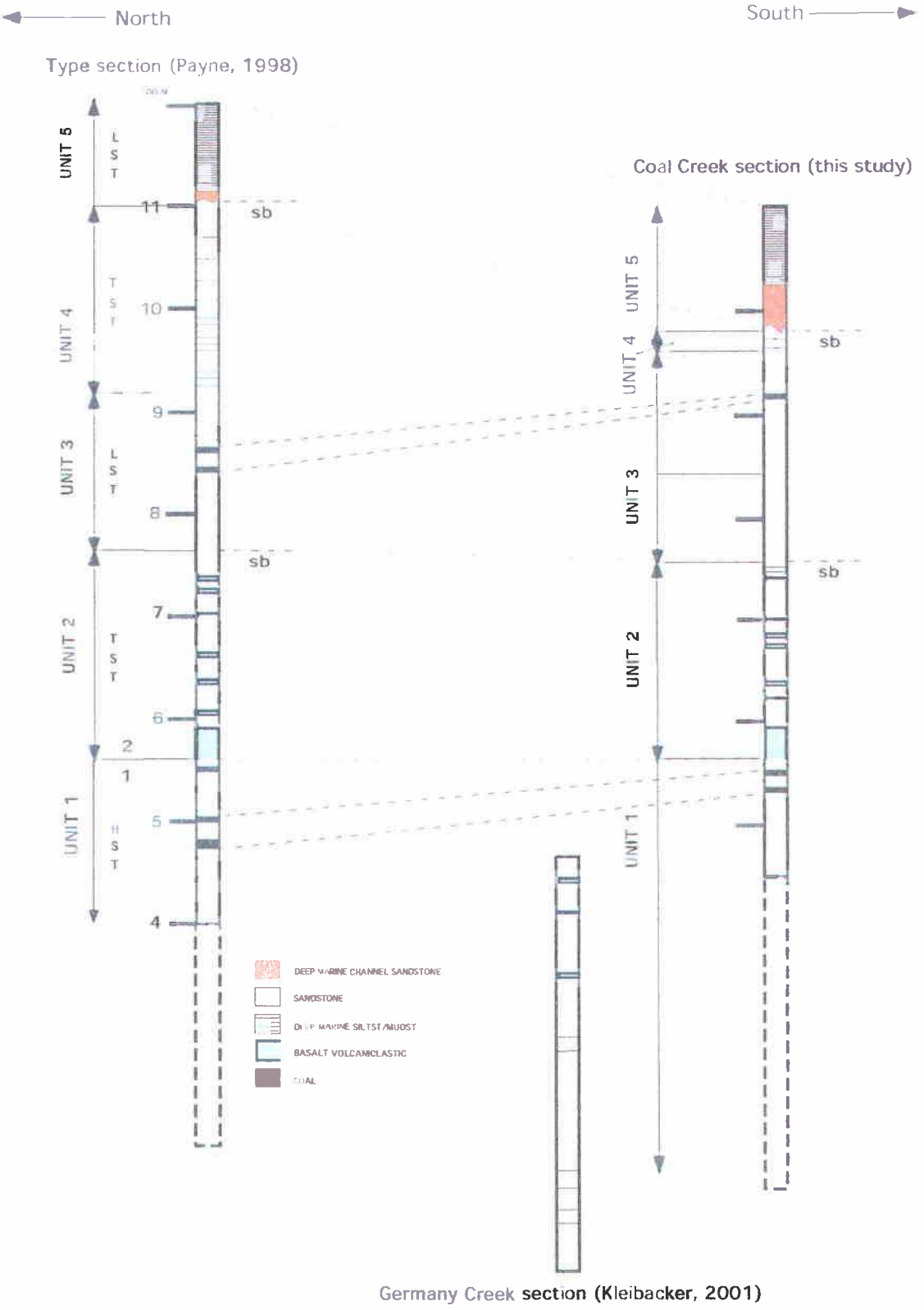

Figure 34: Olequa Creek–Germany Creek-Coal Creek Cowlitz Formation correlation diagram.

17, this thick deeper marine facies overlying Payne's unit 3 does not occur in the Coal Creek section, indicating that unit 4 is only poorly represented in Coal Creek. However, overlying these deep marine facies of unit 4 in the type section is unit 5, consisting of about 30 meters of submarine channel sandstone facies consisting of massive to thickly-bedded sandstones with abundant mudstone rip-up clasts. Payne interpreted these as grain-flow and high concentration turbidites. This is abruptly overlain by fine-grained, even, thin-bedded prodelta overbank turbidites. The same lithologic sequence occurs in the Coal Creek section. Massive to very thickly bedded sandstones of intervals 16 through 4 are overlain by thin-bedded, well-laminated turbidites of intervals 3 through 0.

As stated previously, based on lithologic similarities and stratigraphic position, it is inferred that the lower ~110 meters of the Coal Creek section is correlative to the upper portion of Payne's informal unit 1 (unit 1B) of the type Cowlitz Formation stratigraphic section. This 3rd order sequence of cycle III is progradational, consisting of four shoaling-upward parasequences occurring near the top of a high stand systems tract. This parasequence set consists of shoaling shallow marine and lower delta plain to tidal flat facies successions, with parasequences 1 and 2 consisting of coarsening- and thickening-upward bedsets, and parasequences 2 and 3 consisting of fining-upward tidal successions terminating in Coals A and B respectively (refer to the Coal Creek stratigraphic section, Plate 2, and depositional environments section for more detailed descriptions). Parasequences 1 and 2 represent only minor sea level fluctuations from estuary/bay to tidal rhythmites and tidal channels to delta front shallow marine sands. However, shallow marine oysters immediately overlying coals at the top of parasequence 4 indicates a marine flooding surface occurs there.

The uppermost coal of unit 1(coal B or its shallow marine estuarine time equivalent units to the north, Plate 2) throughout the Coal Creek section is abruptly overlain by highly fossiliferous basalt sandstone and pebble conglomerate containing the shallow marine *Turritella-Solena* assemblage, which is then overlain by a thick Grays River basalt volcaniclastic. This same relationship occurs in the type section of the Cowlitz Formation, with the basalt volcaniclastic containing shallow marine molluscan shell-lag of the *Turritella-Tivelina* assemblage, representing a marine flooding surface that defines the base of unit 2. This 3rd order sequence is the uppermost part of Payne's (1998) cycle III, and in Coal Creek consists of at least 9 shoaling upward parasequences representing an aggradational to retrogradational parasequence set. Five parasequences (6 through 10) fine upward and terminate in coals (C through G). Lower portions of these parasequences are coarsening-upward tidal channel/tidal flat to delta front sand successions. Each Grays River basalt volcaniclastic bed containing marine fossils likely represents minor flooding surfaces (short lived transpressional events) if overlying beds represent deeper water facies, and storm wave or tsunami lag if lithofacies above and below are the same. Near the top of unit 2 (at nearly 350-meters depth) is a maximum flooding surface placing lower shoreface heterolithic ripple-laminated siltstone and mudstone stratigraphically above probable distributary channel or distributary mouth bar sandstones. This is the stratigraphically lowest major flooding surface in the Coal Creek section. Over the next 40 meters of section parasequence 12 coarsens- and thickens-upward, and ultimately grades-upward into middle shoreface storm wave-produced swaley and hummocky sandstones.

A sequence boundary likely occurs at approximately 296-meters depth, where massive to thickly-bedded delta front bioturbated sandstones immediately underlie the middle shoreface sandstone of parasequence 13 (see Figure 14). This is the same stratigraphic position of a sequence boundary described by Payne (1998) in the Cowlitz Formation type section. Above this sequence boundary, lithofacies again become dominantly shallow subtidal to tidal, and correlate to Payne's 3rd order, low stand cycle 4, (tide-dominated unit 3). This unit consists of multiple shoaling-upward parasequences. From ~295 to ~255 meters parasequence 13 thickens- and coarsens-upward, transitioning from mid shoreface to tidal channels or tidal bars to beach. From ~255 to ~220 meters, small onlaps (minor flooding surfaces) result in basaltic deposits with abundant shallow marine fossil assemblages overlain by tidal rhythmite facies. This shallow subtidal to distal tidal bar or channel succession (parasequences 14, 15, and 16) is abruptly overlain by another major marine flooding surface, depositing low- to mid-shoreface storm wave hummocky bedded fine-grained sandstones and fair-weather siltstones over tidal rhythmites. Over the next ~40 meters, this parasequence (number 17) shoals to tidal rhythmite and tidal channel facies. The overlying parasequence 18 is capped by supratidal marsh coal H, with interbedded tuffs that correlates well in lithology and stratigraphic position to Payne's (1998) unit 3 coal seam C. A marine flooding surface immediately overlies this upper coal, which is in turn abruptly overlain by deeper marine turbidites and fine-grained sandstones and siltstones of intervals 20, 18, and 17, which may correlate to the upper beds of Payne's (1998) unit 4 (a transgressive systems tract of cycle 4).

Scoured into the upper surface of interval 17 is the beginning of about 135 meters of massive to thickly-bedded sandstone with abundant large mudstone rip-up clasts and rounded chunks of carbonaceous plant debris (e.g., logs). Intermittent siltstone and mudstone interbeds are common in the lower portion but uncommon in the upper portion of this interval. This massive sandstone sequence is in turn abruptly overlain by thinly-laminated, deep-water, distal turbidites of intervals 3, 2, 1, and 0. This succession is similar to the top of the type Cowlitz Formation section described by Payne (1998). Intervals 18 and 20 again are deep marine facies that may be the lithologic equivalents of Payne's unit 4, that immediately underlie a sequence boundary defined by the overlying channel sandstone facies and prodelta turbidites of lowstand unit 5 (3^{rd} order cycle 5).

Toutle Formation ?

Introduction

The Oligocene Toutle Formation, exposed at several localities in southwest Washington, is variable in thickness, lithology, and environment of deposition throughout its outcrop distribution. Toutle Formation in the type area, 18 km east of Olequa in the Washington Cascades, consists of a lower 60-meter thick marine member, and an upper 100-meter thick non-marine fluvial member (May, 1980). The lower member is in unconformable contact with the underlying Hatchet Mountain Volcanics (basaltic andesite that unconformably overlies the Cowlitz Formation). This member, based on microfossils and molluscan fossil assemblages, was deposited in nearshore subtropical marine conditions (May, 1980). A Galvinian (upper Eocene to lower Oligocene) molluscan assemblage characterizes the lower member, and is within the *Echinophoria dalli* and *Echinophoria fax* zones of Armentrout (1973) within the Refugian foraminiferal stage (May, 1980). The upper member was formed in fluvial, lacustrine, or swampy depositional environments (May, 1980), and might be within the *Echinophoria fax* zone to the *Echinophoria rex* zone of the Galvinian, within the Zemorrian foraminiferal stage (34 to 31 Ma)(May, 1980).

Payne (1998) in a masters thesis study, ~25 km (~16 mi) north of this study area near Vader, Washington, split the Toutle Formation into three informal units based on his measured section in Olequa Creek: 1) a fluvial valley-fill sequence ~105 meters thick (unit A), 2) a marginal marine sequence ~85 meters thick (unit B), and 3) an upper fluvial sequence ~75 meters thick (unit C), for a total of approximately 265 meters. Payne's (1998) unit A is possibly correlative to the upper fluvial member of the type Toutle

Formation of Roberts (1958) to the east in the western Cascades based on lithologic similarities, stratigraphic position, and radiometric age of a dated tuff bed (approximately 32 Ma). Payne's unit A consists of numerous shallow channels filled with cross-bedded, tuffaceous, moderately-sorted, feldspathic volcanic-litharenites. These cross-beds are lined with black carbonaceous plant debris including roots and carbonized logs. Imprints of leaves are also common. These channels are interbedded with friable, faintly cross-bedded, clay-rich arkosic sandstone containing little mica. Unit A also contains abundant sandy, clayey, carbonaceous siltstone with clay interbeds. Also common are blue-gray tuffaceous siltstones and pumice lapilli tuff beds. The possibly correlative type Toutle Formation section ~18 km (~11 mi) to the east consists mostly of volcanic sandstones and tuffs with interbedded massive siltstones and lesser coal beds toward the top. Payne's (1998) unit B consists of clay-rich sandy siltstone, clay-rich silty sandstone, tuffaceous mudstone, and volcanic arkosic sandstone. Toutle Formation unit C is dominantly tuffaceous sandstone and siltstone with a high percentage of carbonized woody material. Coarse-grained volcanic sandstone to pebble conglomerate lenses are also abundant.

The Toutle Formation in the study area of Payne (1998) immediately overlies a basin-wide unconformity that marks the top of the Cowlitz Formation, produced by a relative sea-level fall (i.e., a sequence boundary). The Toutle Formation was subsequently produced as part of a lowstand systems tract, with non-marine fluvial sandstones incised into the deep marine siltstones of the Cowlitz Formation (Payne, 1998). Therefore, much of the lower portion of the Toutle Formation consists of incised valley-fill, with clasts consisting of a mixture of stream- and wave-reworked deltaic

Cowlitz Formation derived from tectonically uplifted and eroding Cowlitz micaceous arkoses, and silicic tuffaceous pyroclastic derived from the active western Cascade calc-alkaline volcanic arc. The incised-valley, meandering fluvial bar (rather than upper shoreface) depositional environment of the tuffaceous sandstones of the lower and upper units of the Toutle Formation in Olequa Creek to the north, was suggested by Payne (1998). This model is based on fining- and thinning-upward parasequences, filled channels, moderate-sorting, carbonized root-traces in growth position, coalified logs, abundant leaf imprints, and unidirectional high-angle trough cross-beds. Finer-grained, thinly-bedded to laminated clayey siltstones, mudstones, and interbedded tuffs and coal with abundant carbonized and imprinted plant material were interpreted as fluvial overbank floodplain deposits. Such fine-grained lithologies and facies associations suggest a broad floodplain (with meandering river channels) with the associated buildup of swampy plant debris. This floodplain was occasionally inundated by volcanic ash from the western Cascades in the form of airfall tuffs, and at times channelized debris/hyperconcentrated flows (Figure 35).

Local Toutle Formation Stratigraphy and Thickness

Within the study area, outcrops of tuffaceous, clayey sandstone, siltstone, and minor claystone of the Toutle Formation may occur stratigraphically above exposures of the Cowlitz Formation and Grays River volcaniclastics in Coal Creek, Clark Creek, Hazel Dell Creek, and also on Mt. Solo and the hills northeast of Kelso (Plate 1). Unfortunately, the possible contact between the Oligocene Toutle Formation and underlying middle and upper Eocene sedimentary and volcanic units was not discovered in outcrop anywhere within the study area. Although some of the Toutle Formation is

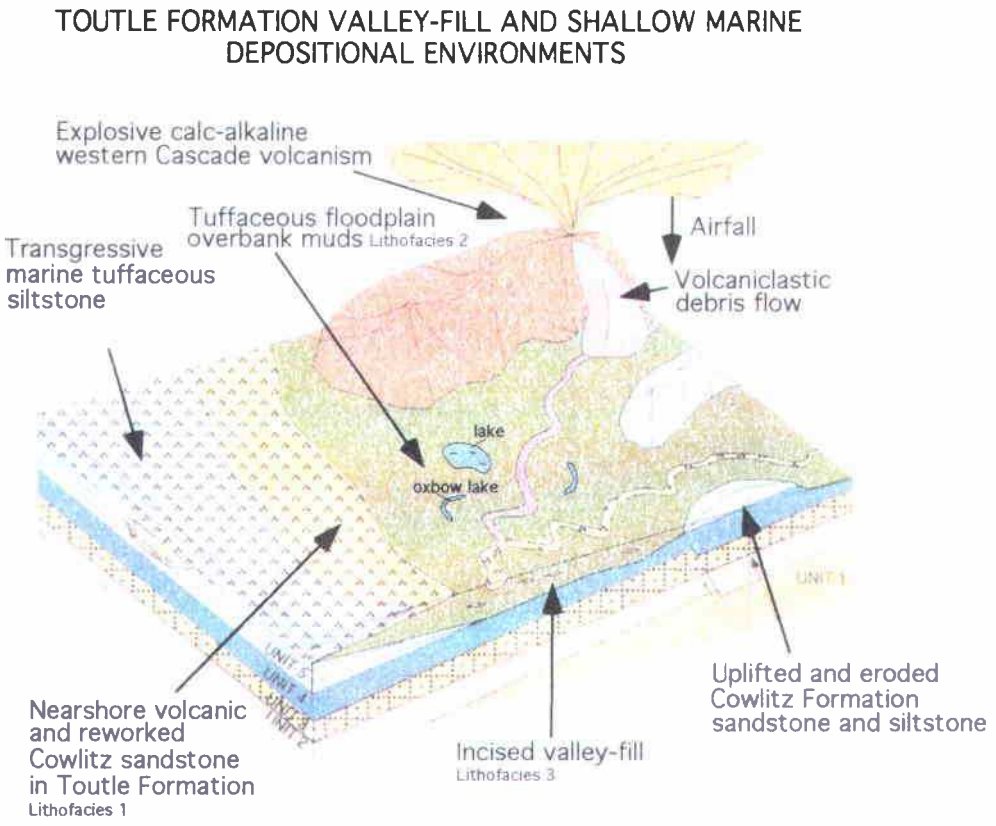

Figure 35: Paleogeographic reconstruction of the Toutle Formation showing depositional environments and unconformable stratigraphic relationship with the underlying Cowlitz Formation. Modified from Payne (1998).

arkosic and micaceous (resembling Cowlitz Formation beds, and accounting for previous mapping as Cowlitz Formation by other authors in the study area), several consistent lithologic characteristics allow differentiation of these formations in the field. Potential outcrops of the Toutle Formation are nearly universally lighter in color than the more orange or brown Cowlitz Formation arkosic beds and gray siltstone, ranging from nearly white to light tan or buff. Local orange, reddish, or brownish coloration generally can be attributed to staining by overlying iron oxide-rich soils leached from the Columbia River Basalt Group. Toutle Formation samples have abundant clay, even coarse-grained sandstones are commonly clay-rich. Samples are more weakly lithified than Cowlitz Formation sandstones and siltstones, and even the hardest samples are easily crushed or broken apart by hand, and due to the high smectite clay content, usually hold the new shape when compressed. Most of these semiconsolidated outcrops have abundant open burrows created by modern beetles, crickets, and wasps, as the soft sediment is easy for them to burrow through. Hand samples, even when wet, have noticeably lower specific gravity than Cowlitz Formation samples, resulting largely from the high clay content, but also from the relatively high percentage of pumice clasts in some samples, and relatively little cement. No samples collected are well indurated; all are either friable and/or clayey (many samples have the consistency of sandy chalk). The few molluscan fossils collected (invariably molds that rapidly crack and disintegrate when dry) and some trace fossils (unusual downwarping of laminae, see Figures 36 and 37) are unlike those described in the Cowlitz Formation in Coal Creek. Within the study area, plant fossils from the Cowlitz Formation are carbonized, whereas Toutle Formation leaves and other plant debris are nearly always (with the exception of one bed at Site 49) imprints or

molds with the carbonaceous organic material leached away. Three common characteristics of the Cowlitz Formation in Coal Creek: flaser-mud drapes, invasion by Grays River dikes and sills, and interbeds of highly molluscan fossiliferous, shallow marine Grays River volcaniclastic beds do not occur in the Toutle Formation.

Toutle Formation outcrops with the characteristics described above occur widely throughout the low hilly terrain stratigraphically beneath unconformably overlying Miocene Columbia River Basalts in the central and northern parts of the study area, apparently reaching a maximum thickness of 500 to 600 feet (~155 to 186 meters). Stratigraphically lower exposures (the lowermost ~30 to 40 meters) dominantly consist of massive, clayey, tuffaceous siltstone, and appear to be shallow marine, based on sparse molluscan molds (found only at Site 124, and years ago in an outcrop of "Olequa Clay" behind a house in Clark Creek, as described by the homeowner). Higher elevation outcrops of the upper portion of the Toutle Formation are commonly trough cross-bedded, channel-fill, clay rich arkosic sandstones, with overbank thinly bedded and laminated tuffaceous sandy siltstone with claystone and thin sandstone lenses. Three generalized lithofacies are recognized for this study: 1) mostly massive to thinly laminated, tuffaceous, clayey, bioturbated siltstone with sparse molluscan fossils (mostly the lower section, and may correlate to Payne's Toutle Formation marine unit B), 2) thinly bedded to laminated clayey siltstone and fine-grained arkosic sandstone with abundant leaf and twig imprints, almost entirely lacking carbonaceous material, and 3) cross-bedded, tuffaceous, highly friable, clayey, micaceous, arkosic sandstone, occasionally lined with dark gray or brown mudstone laminae (may correlate to Payne's upper unit C of his Toutle Formation).

Lithology and Outcrop Characteristics

Lithofacies 1, 2, and 3 occur throughout the area mapped as possible Toutle Formation in Plate 1. Most exposures occur as road cuts or excavations behind new houses, and are typically 3 meters or less in stratigraphic thickness, many are 1 meter or less. The thickest exposure occurs at Site 49 (NE ¼ of the NW ¼ of Sec. 5, T 8 N, R 2 W) where approximately 10 meters are exposed along a curved roadcut about 200 feet long on Columbia Heights Road North (Plate 1, Figure 36). Nearly 8 meters of continuous exposure occurs in the headscarp of a small 1997 landslide at Site 59 (NW ¼ of Sec. 31, T 9 N, R 3 W, Plate 1, Figure 38). Unfortunately, no exposures are continuous enough or of sufficient thickness to allow much detailed analysis of vertical facies changes or sequence stratigraphic analysis. In addition, due to the lack of induration of this unit, grasses and other vegetation quickly cover all new exposures.

Lithofacies 1 is most distinctive in its monotony and lack of well-preserved sedimentary structures in outcrop. This in part represents actual lithologic features, but is in part an artifact of poor exposure. Exposures range from massive to thinly-laminated, and are light colored, tuffaceous, clay-rich, and finely micaceous. Those sedimentary structures that do occur include micro-cross and wavy laminations, typically about 0.5-cm thick in both clayey sandstone and siltstone. The majority of outcrops of this lithofacies lack stratification and are mottled gray, tan, or buff. Mottling appears to be due in most cases to bioturbation (Sites 54, 105, 109, 113, 115, 116, 120, and 124). Site 54 (The West Side Quarry, SE ¼ of Sec. 4, T 8 N, R 2 W) includes vertical burrows 3-cm wide filled with coarse-grained tuffaceous sandstone. Sites 110 and 124 (SW ¼ of the NE ¼ of the SE ¼ of Sec. 35, R 3 W, T 9 N) have abundant sub-vertical, mudstone-lined

burrows ~1-cm wide and several cm long, and also produced two poorly preserved mollusk molds. Particularly at Sites 116 (center of Sec. 6, T 8 N, R 2 W), and 109 (SW ¼ of the NW ¼ of Sec. 36, T 9 N, R 3 W), mottled texture is due to large (0.5 to 1-cm wide) light gray to nearly white subangular pumice lapilli. Site 113 (SW ¼ of the SW ¼ of Sec. 24, T 9 N, R 3 W) is a fine siltstone to claystone with evenly distributed fine mica, and is likely a reworked air fall tuff. Site 115 (NW ¼ of the SE ¼ of Sec. 18, T 8 N, R 2 W) is a poorly exposed, medium- to coarse-grained arkosic sandstone that may be Cowlitz Formation immediately beneath the Toutle Formation contact. Lenses of highly altered volcanic coarse-grained sandstone to rounded pebble conglomerate occur infrequently in Toutle Formation exposures in the study area.

Lithofacies 2 is characterized by thinly-bedded to laminated clay-rich siltstone with thin lenticular laminae of fine- to medium-grained sandstone, and some lenses of claystone or mudstone. This lithofacies is best exemplified by Site 49 along Columbia Heights Road North (Figures 36 and 37, and Figures 75 and 76 of the structure section) where approximately 10 meters of thin-bedded to laminated tuffaceous clayey siltstone is exposed in a roadcut immediately beneath dark reddish Grande Ronde basalt soil (producing the reddish stain at this location). Most thin beds (remarkably uniform in thickness) are micro-cross to wavy-laminated, with the thickest low-angle cross-beds less than a few cm high. Individual laminae or thin beds are defined by coarser-grained and more micaceous siltstone or fine arkosic sandstone at the base, and finer-grained, more clay-rich siltstone at the top. Limonite staining also tends to define individual laminae, forming rims around grains in the more permeable, coarser-grained sandstone layers. Near the middle of this stratigraphic sequence discontinuous, dark gray, micaceous

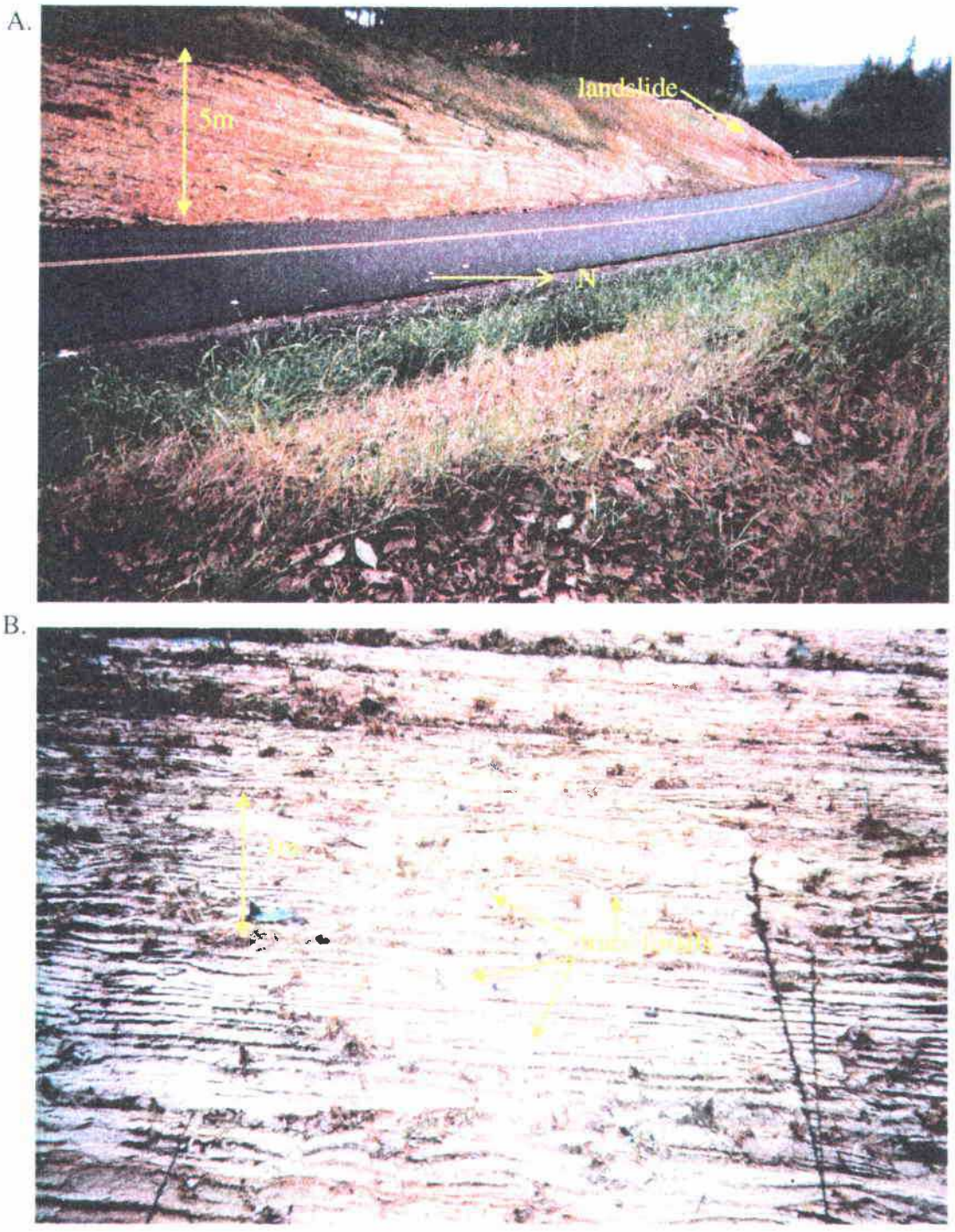

Figure 36: Thin-bedded to laminated, clay-rich siltstones and fine-grained sandstones of the Toutle Fm. (facies 2) at Site 49, atop the Columbia Heights Anticline.

A. View toward the northwest illustrating overall size and character of the exposure. Note dipslope landslide and iron oxide staining from overlying leached, reddish, reworked Grande Ronde basalt soils.

B. Tuffaceous, clayey siltstone with very thin beds or laminae of uniform thickness, interpreted to be floodplain overbank or shallow lake silt deposits.

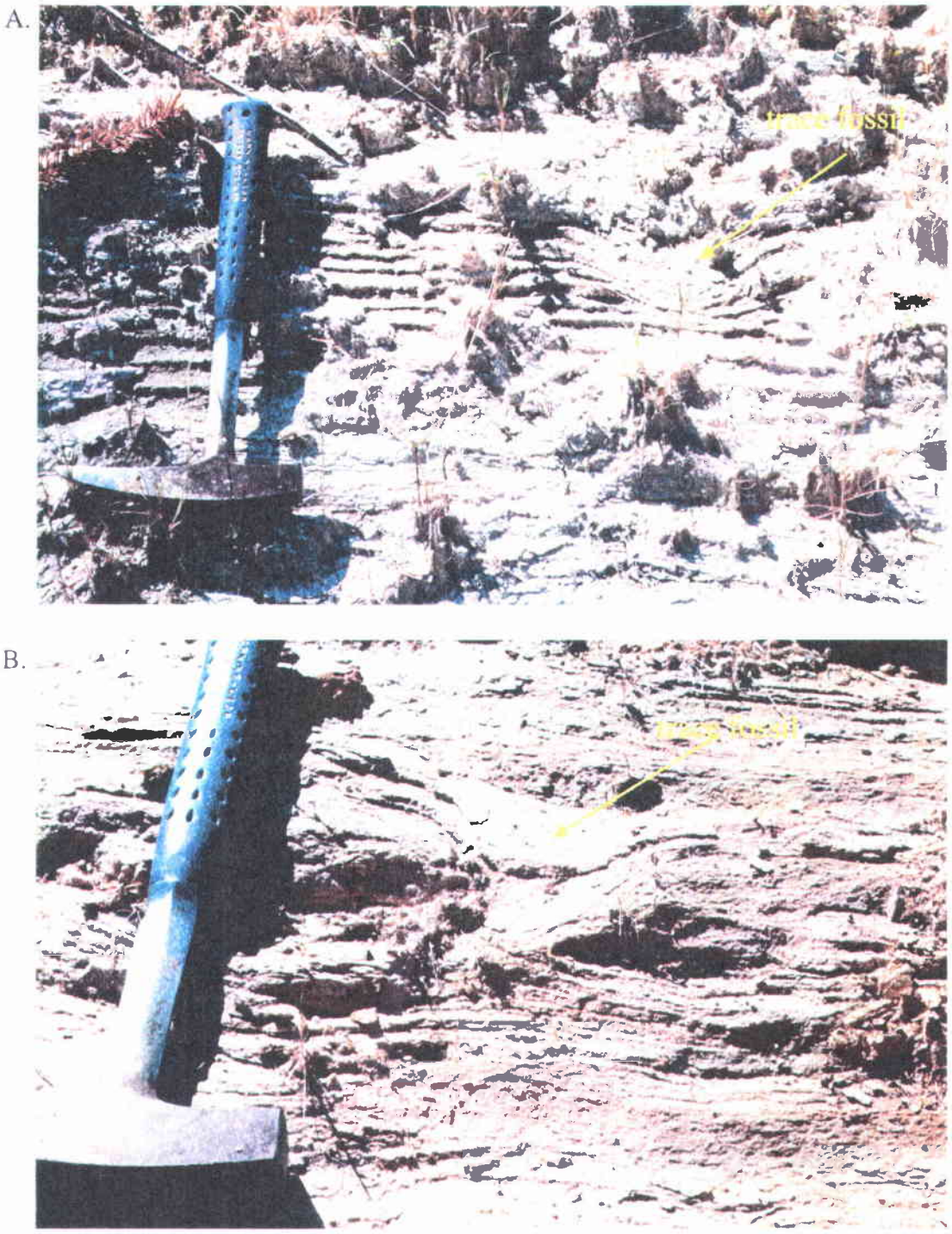

Figure 37: Unusual trace fossils of uncertain origin in clayey siltstones of the Toutle Formation at Site 49. These structures, unique in the study area, consist of downwarped siltstone laminae which tend to bend underlying laminae near the contact. Over 100 of these trace fossils were seen in the upper 10 meters of this stratigraphic sequence, and vary from 10 to 20 cm wide and 5 to 15 cm deep.

siltstone lenses only a few cm to 1 meter in length occur. Samples from this location are dominantly light in color, with the consistency of sandy chalk or diatomite (although no diatoms were found despite many attempts). One year after this outcrop was described for this study, the detail of the sedimentary structures had weathered away.

Site 49 is also characterized by abundant leaf imprints (with very little carbonaceous material), especially in the lower 10 meters. These leaf species are broad and undivided, characteristic of the more tropical climate that persisted through the Eocene and into the early Oligocene (Jeff Myers Western Oregon University, paleobotanist, personal communication, 2002). Unique features of this exposure are trace fossils of uncertain origin that consist of downwarped laminae up to 20 cm wide and 15 cm deep (Figure 37). These depressions often truncate underlying laminae, but in all cases underlying laminae are bent downward near the contact with the depression, commonly becoming tangential to it.

Lithofacies 3 is characterized by light colored, clay-rich, tuffaceous, trough cross-bedded sandstone, with current direction toward the southwest. These deposits may represent point bar channel-fill sequences exemplified by the landslide headscarp exposure at Site 59 (Figure 38). Here, medium- to coarse-grained arkosic and sparsely micaceous, unidirectional trough cross-bedded clay-rich arkosic sandstone at the base of the exposure grades upward through finer-grained sandstone into 2 meters of micro-cross-bedded and wavy-laminated clayey siltstone and fine sandstone of lithofacies 2 (Figure 38b). Coarser-grained sandstone beds at the base are commonly lined with dark gray or brown mudstone or sandstone with some disseminated carbonaceous debris. Similar channel-fill sandstone sequences occur elsewhere in the study area. Site 33 (S ½

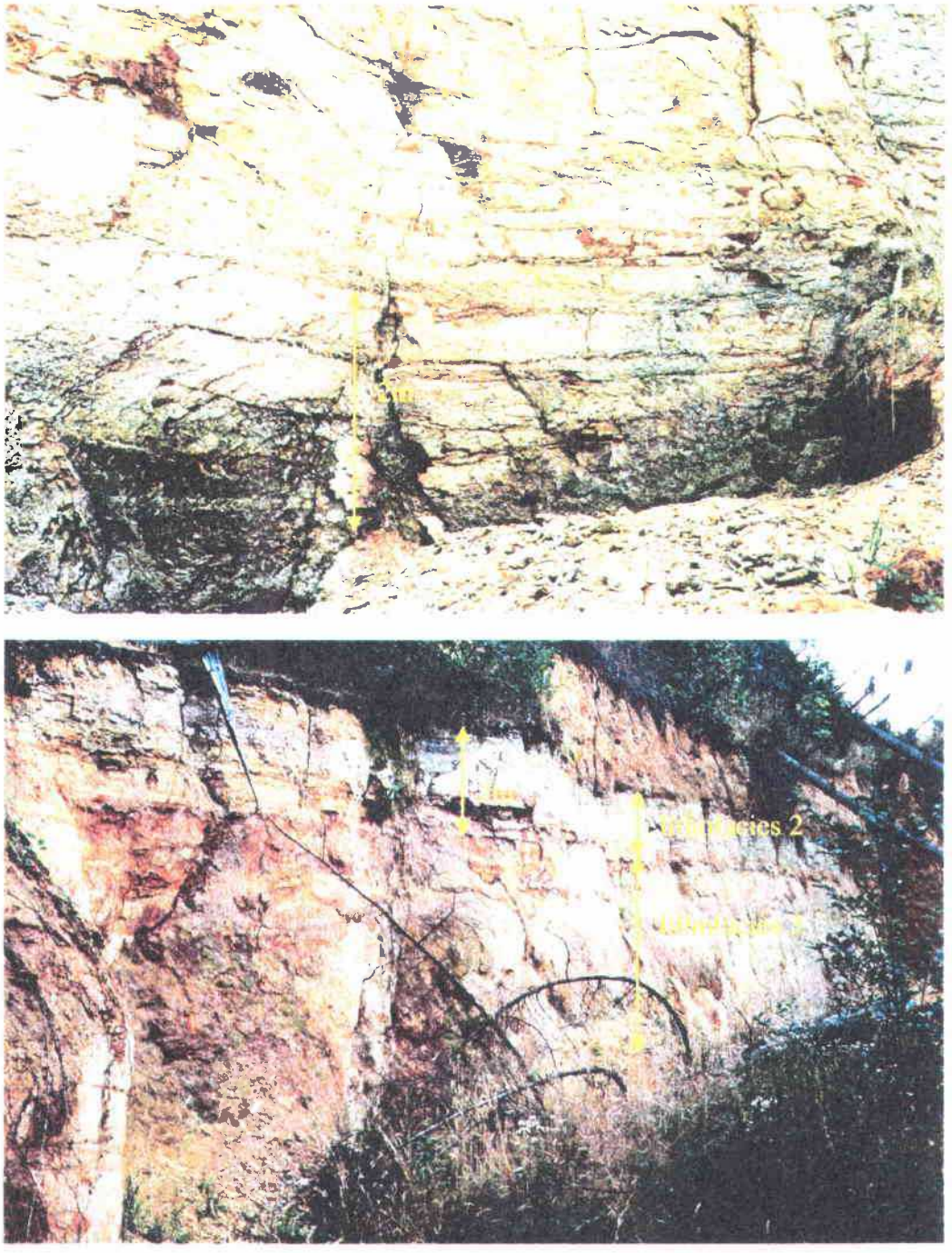

Figure 38: Sandstones and siltstones of the Toutle Formation exposed in the headscarp of a landslide at Site 59.

A. Unidirectional trough cross-bedded sandstone at the base of the exposure. Cross-bed sets become thinner-bedded upward, and sandstone gradually becomes finer-upward.

B. Side view of the scarp illustrating the transition from cross-bedded sandstone to parallel even bedded sandy siltstone in the uppermost 2 meters. This is interpreted to be a fining-upward point bar sequence.

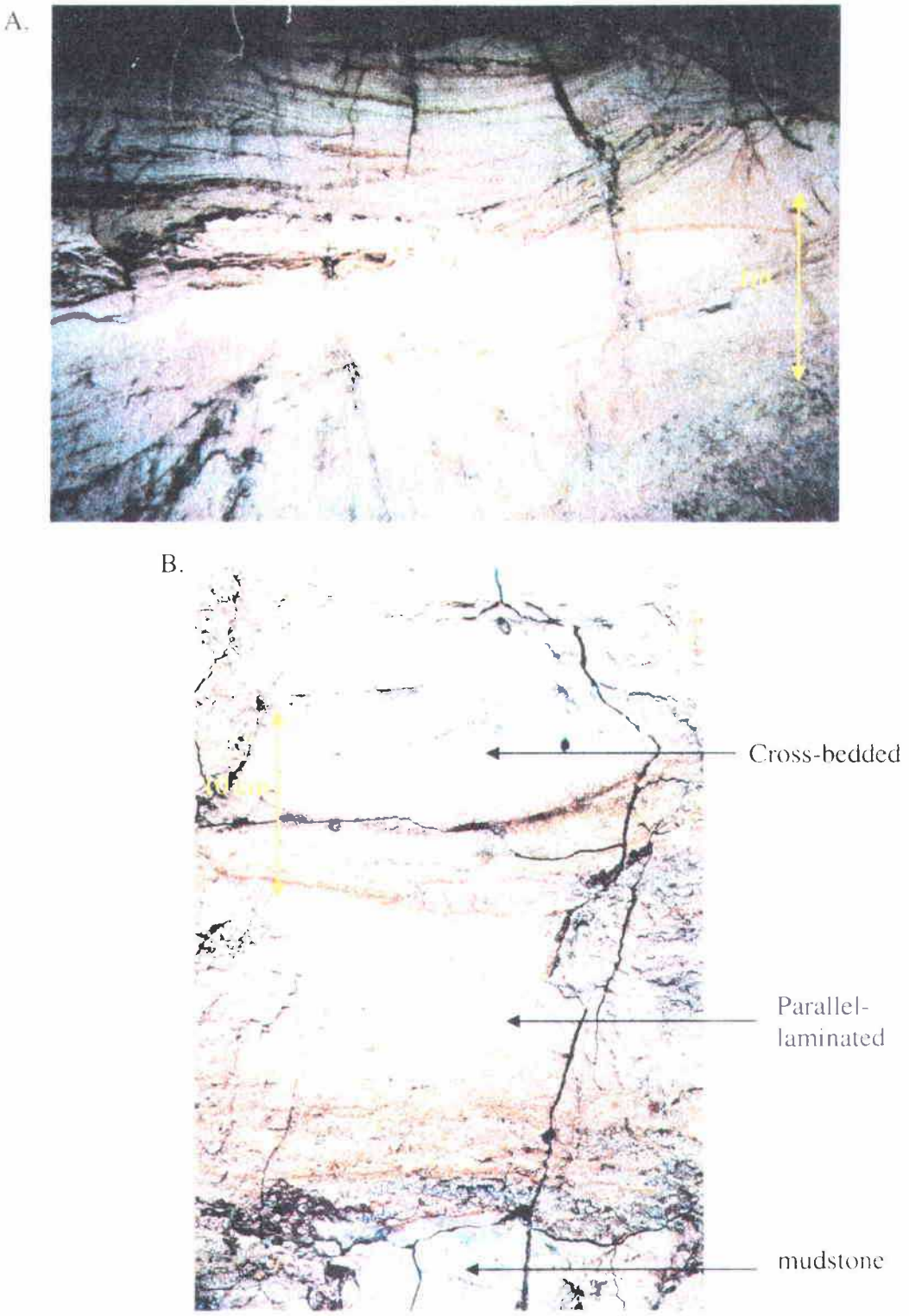

Figure 39: Cross-bedded arkosic sandstones, Toutle Formation lithofacies 3.
A. Channel-fill of trough cross-bed sets with cross-truncation at Site 33.
B. Pebbly tuffaceous sandstone from Site 51 (upper quarry) on Mt. Solo. These occur immediately below a Columbia River Basalt flow (Ortley unit 1).

of Sec. 12, T 8 N, R 3 W, Figure 39a) contains similar nested cross-bed sets in a roadcut on 50th Avenue, also with paleocurrent direction toward the southwest. At Site 51 (NW ¼ of Sec. 25, T 8 N, R 3 W), immediately beneath Miocene Columbia River Basalt (Ortley flow unit #1) on Mt. Solo, tuffaceous sandstone to pebbly volcanic conglomerate occurs, also with paleocurrent direction toward the southwest (Figure 39b).

Petrography

Toutle Formation sandstones and siltstones differ substantially from Cowlitz Formation samples is some aspects of composition. Toutle Formation samples display a much higher percentage of pumice, chert, and clay alteration products. Most samples consist of 50% or more of these three components. As a result, quartz, feldspars and micas of extrabasinal origin (i.e., reworked Cowlitz Formation grains) are reduced in abundance. In addition, the clay rim and sparry calcite cements that surround grains in Cowlitz Formation thin sections are nearly lacking entirely from Toutle Formation samples, as are calcareous molluscan fossil fragments. Also greatly reduced in percentage are the pilotaxitic and amygdaloidal Grays River basalt clasts so common in Cowlitz Formation clastic sediments. Carbonaceous plant fragments are also greatly reduced in abundance or lacking. Most of these compositional differences may alternatively be due to extensive weathering, leaching, and alteration of these exposures.

Thin section from Site 60 (NE ¼ of the SE ¼ of Sec. 30, T 9 N, R 2 W, Figure 40a) is from a thinly-bedded to laminated sample of lithofacies 2, consisting of coarse- to fine-grained sandstone with sparsely bioturbated siltstone laminae. This sample consists of approximately 50% chert, 20% reworked Cowlitz Formation clasts (~10% quartz, 9% plagioclase feldspar, 1% mica), 10% pumice (mostly long-tube), 5% basalt, and 10-15%

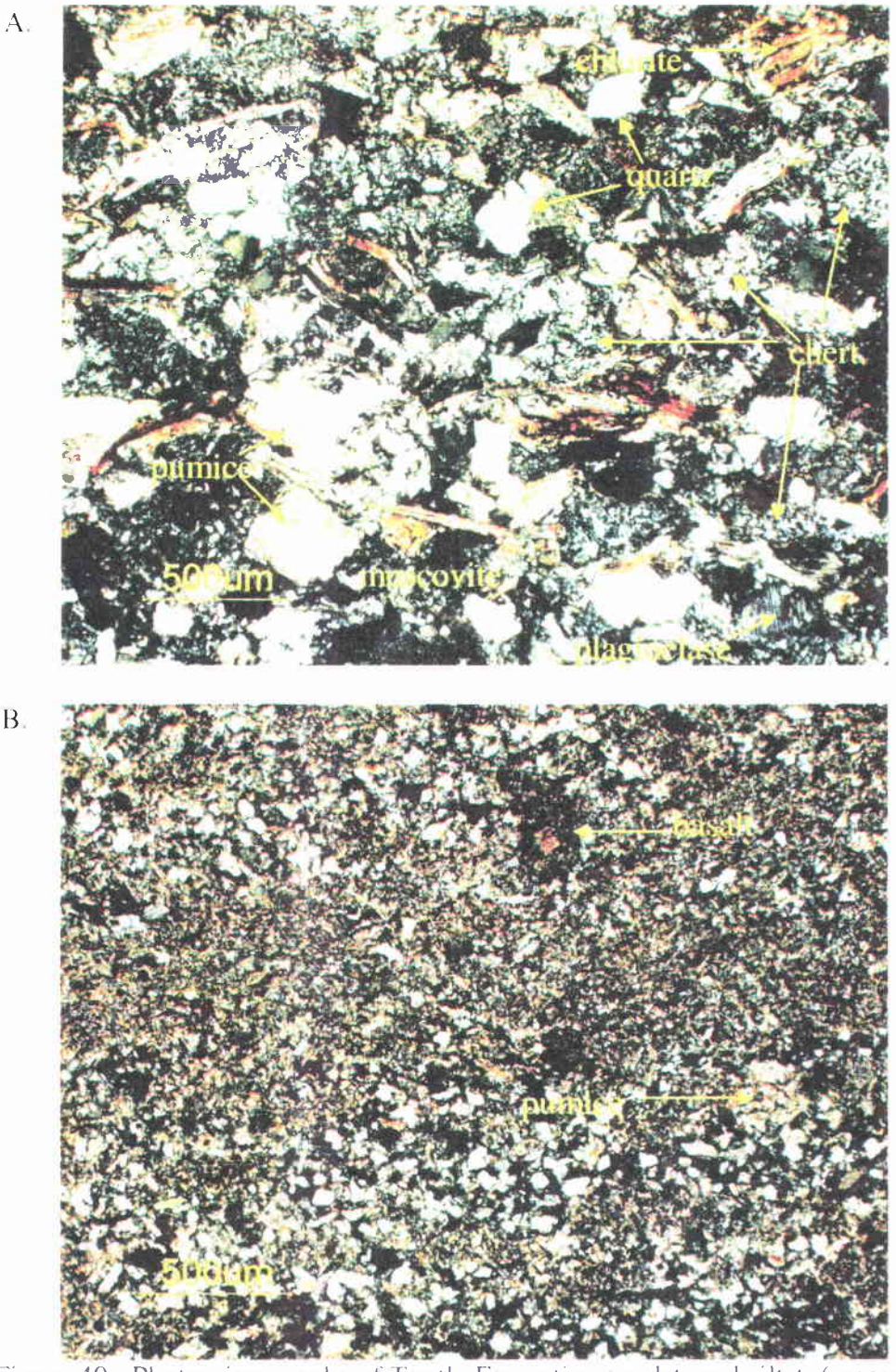

Figure 40: Photomicrographs of Toutle Formation sandst. and siltst. (crossed-nicols).

A. Sample from Site 60. This image is a coarse-grained sandstone interbed from an otherwise siltstone-dominated exposure. Note high percentage of chert, chlorite, and long-tube pumice fragments.

B. Sample from Site 62, a clay-rich quartzofeldspathic siltstone. Note that the central lamina is approximately 90% smectite clay and chlorite.

clay. Biotite has mostly been altered to chlorite, and smectite clay forms a thin rim around some clasts. Some pumice fragments have been altered to greenish smectite. The high percentage of chert is likely due to altered silicic volcanic fragments of western Cascade origin. Evidence for this can be seen in some pumice grains that have been partially altered to chert, but some may originate from altered dacite.

Thin section from Site 62 (SE ¼ of Sec. 26, T 9 N, R 3 W) is from a thinly-laminated, sparsely bioturbated, quartzofeldspathic, micaceous, clayey siltstone. This locality also produced well-preserved leaf impressions and, like many Toutle Formation exposures, is the site of a landslide, due to high clay content and poor induration. This thin section (Figure 40b) consists of approximately 60-70% smectite or sericite clay, 20% quartz, 5% plagioclase feldspar, and the remainder mica and lithic clasts.

X-ray diffraction

Two Toutle Formation samples were analyzed by x-ray diffraction to help identify mineral composition, and help unravel the diagenetic history. The sample from Site 60 (Figures 41 and 42), a clayey siltstone shows strong quartz and muscovite peaks in the <15μm fraction. Some chlorite is also present, but the sample is very low in feldspar relative to Cowlitz Formation samples. The sample from Site 49 is much the same (Figures 43 and 44), but has slightly more chlorite. The clay fraction (<2μm) for these samples is rich in smectite, illite, and chlorite, illustrating the high percentage of clay that gives much of this formation its clayey character, makes it prone to landslides. Figure 40 shows this high clay content in thin section.

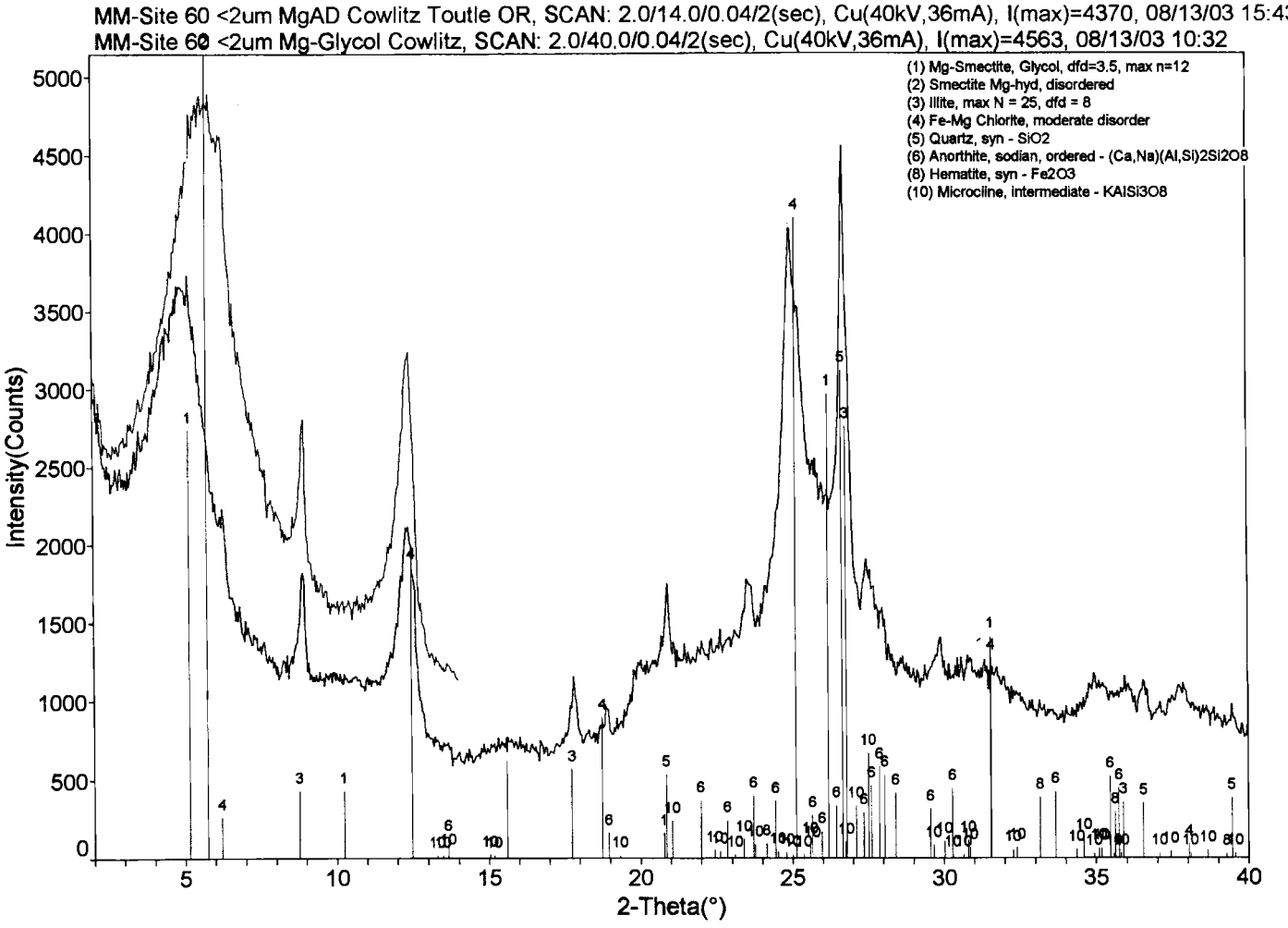

Figure 41: < 2 micrometer fraction of Toutle Formation from Site 60.

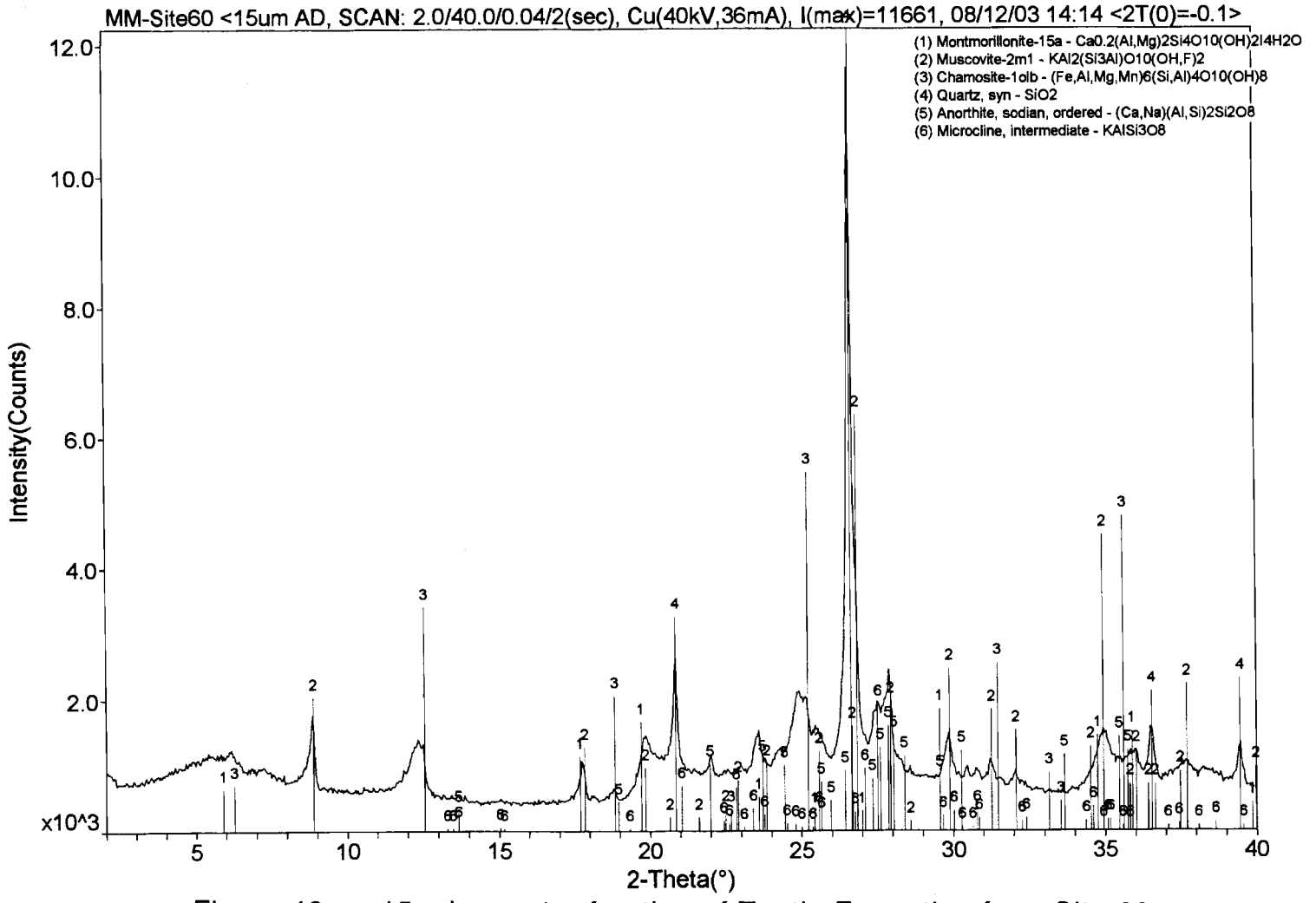

Figure 42: < 15 micrometer fraction of Toutle Formation from Site 60.

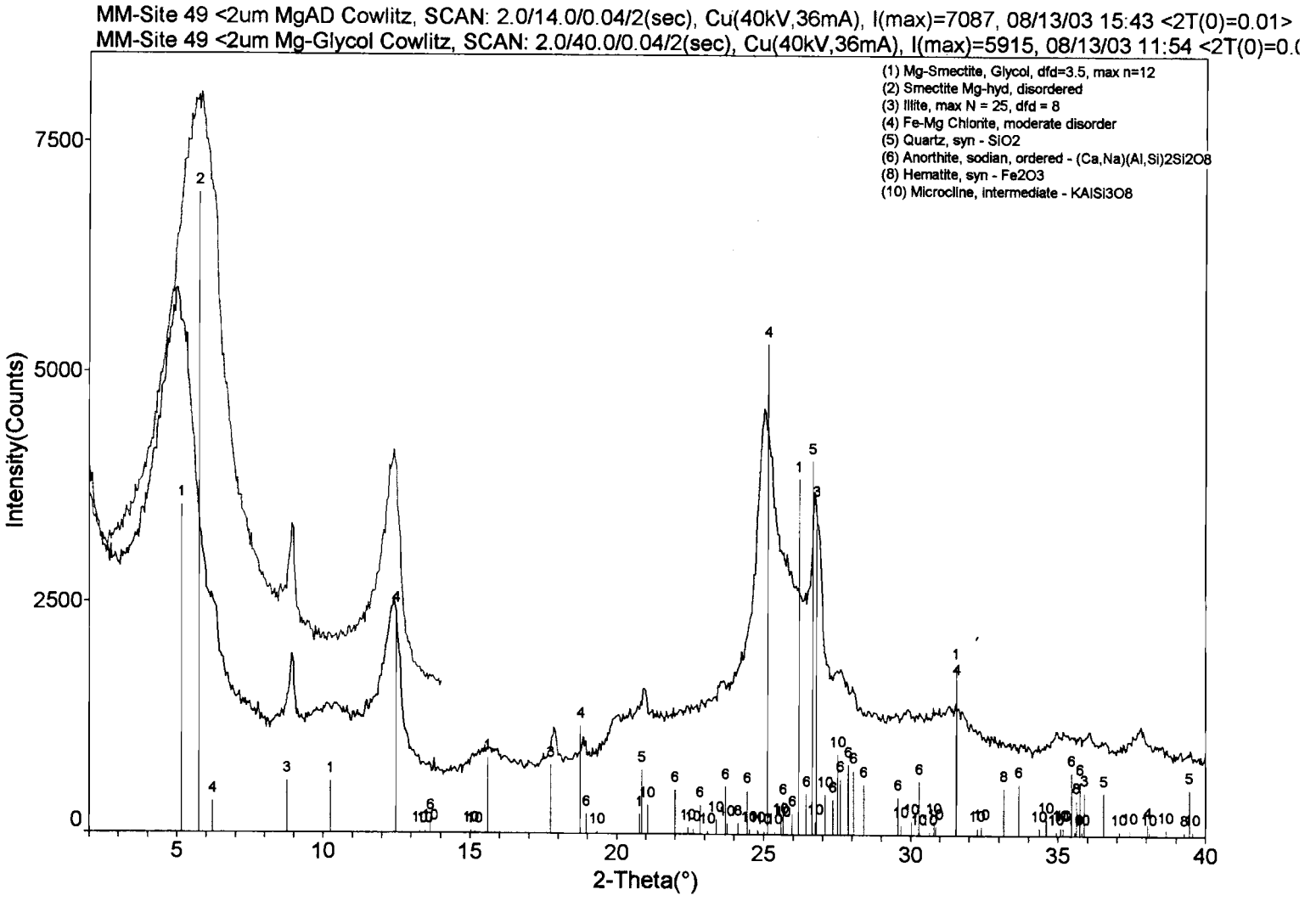

Figure 43: < 2 micrometer fraction of Toutle Formation from Site 49.

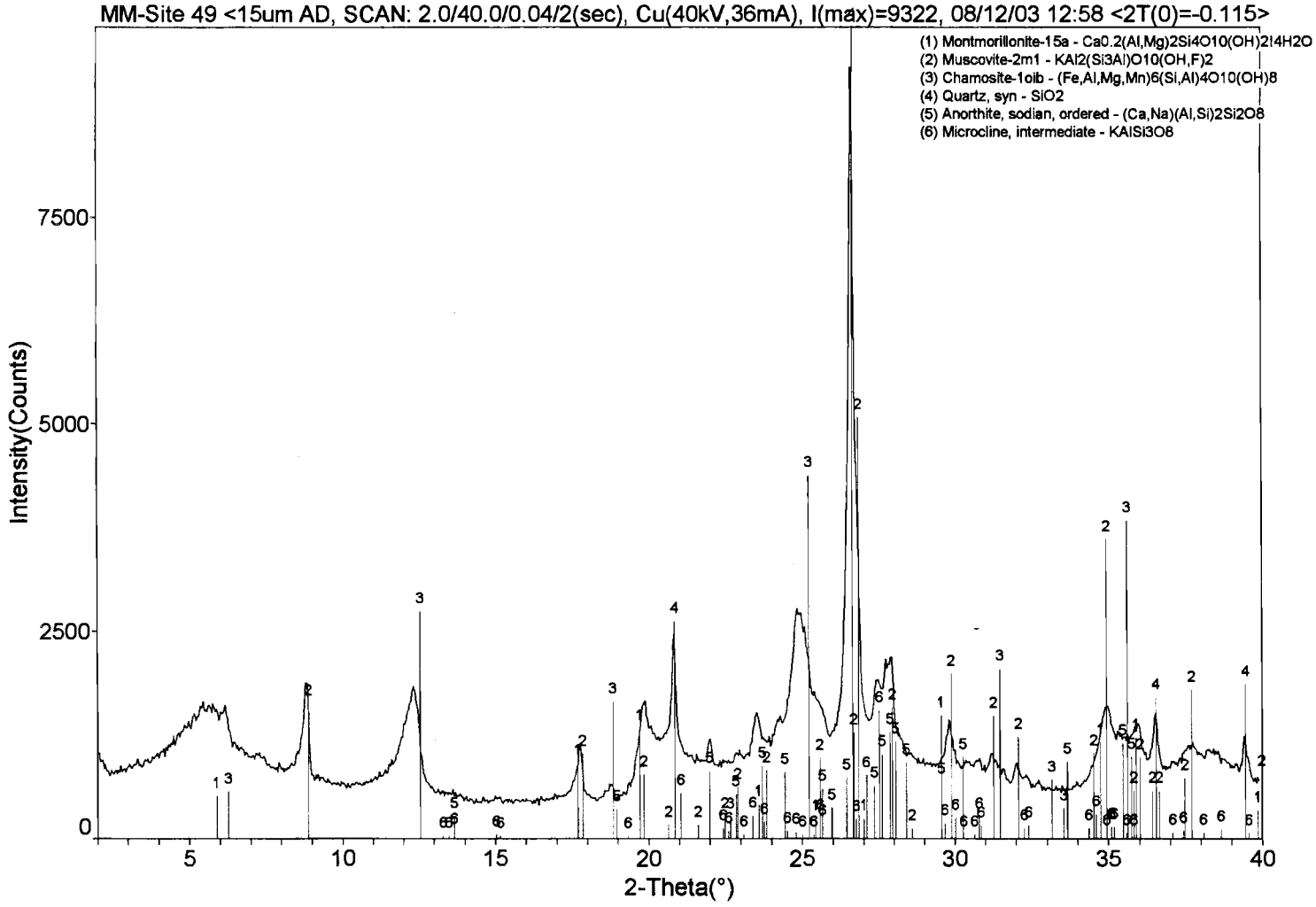

Figure 44: < 15 micrometer fraction of Toutle Formation from Site 49

Depositional Environments

Fluvial channel-fill, micaceous, arkosic litharenites and lithic wackes of the Toutle Formation (lithofacies 3) were likely deposited as part of a meandering river system. The best evidence of this interpretation is found at Site 59 (Figure 38), where unidirectional, moderately-sorted, trough cross-bedded sandstones gradually thin and fine upward. This sequence terminates in approximately 2 meters of tuffaceous, parallel-bedded siltstones and fine-grained sandstones of lithofacies 2 that likely represent fluvial overbank and floodplain deposits, or top of a point bar. Further evidence for this interpretation are the lithofacies 2 mudstone lenses and abundant leaf imprints at Sites 49 and 62, where sandy tuffaceous siltstones contain sandstone lenses. These fine-grained, plant fossil-rich facies with associated meandering channel-fill facies suggests a broad coastal floodplain environment including high sinuosity rivers and possibly shallow lakes on the floodplain, where frequent explosive western Cascade silicic volcanic eruptions would periodically inundate the area with air fall tuffs and debris/hyperconcentrated pumiceous flows (Figure 35).

A shallow marine or estuarine depositional environment is indicated for some exposures of the Toutle Formation, particularly in the stratigraphically lower outcrops in the study area (lithofacies 1), as suggested by poorly preserved pelecypod molds, and mudstone-lined burrows. It is interesting to note that locations with abundant leaf imprints lack molluscan fossils and tubular burrows. Those containing molluscan fossils and/or burrows do not have associated leaf imprints. These features as well as the point bar sequences differentiate shallow marine from non-marine lithofacies. As shown in Figure 35, these tuffaceous nearshore marine siltstones and fine-grained sandstones can

be thought of as upper to middle shoreface, wave-reworked Cowlitz Formation sand and silt, supplying the arkosic and micaceous component of the Toutle Formation. The incised valley (produced by a relative sea level fall) with meandering channel-fill sands and plant fragment-rich overbank siltstones may have been contained in the study area by the remaining topographic volcanic highs to the northwest and southeast that originally resulted in deposition of tide-dominated, estuarine sediment of the middle Eocene Cowlitz Formation prior to the sea level fall in the late Eocene/early Oligocene.

VOLCANICS

Grays River Volcanics

During the late-middle and late Eocene, nearly 3,500 meters of Grays River Volcanics in southwest Washington and Tillamook Volcanics in northwest Oregon were erupted into the forearc basin of Cascadia. These high-titanium tholeiitic units are petrologically and chemically similar (Rarey, 1986; Kenitz, 1997), but can be distinguished based on location, stratigraphic position, and age, with Tillamook flows ranging in age from 46 to 42.5 Ma, and the younger Grays River flows ranging from 42.4 to 36.8 Ma. These flows erupted from several volcanic centers, producing coalescing submarine tholeiitic basalt shield volcanoes that eventually built up above sea level to become oceanic islands. The lower flows consist of high TiO_2 and Fe_2O_3 tholeiitic submarine hyaloclastite and pillow basalts and subaerial tholeiitic basalt, but differentiate upward to become plagioclase- and augite-phyric, platy, subaerial basaltic andesites, andesites, and some dacites in the subaerial upper portion (Rarey, 1986; Mumford, 1988). Both units are characterized by plagioclase microlites arranged into a pilotaxitic (sub-parallel) flow texture, in a black, glassy groundmass (Nelson, 1985; Berkman, 1990; Payne, 1998; Kleibacker, 2001).

Eruption of both Tillamook and Grays River lavas may be due to middle to late Eocene right-lateral shear and tensional opening of the forearc basin, resulting from changes in the relative motion of the Farallon and North American Plates (Armentrout, 1987). The volcanic edifices produced in this way subdivided the forearc into smaller basins (Niem and others, 1992), into which nearly 2,500 meters of marine and marginal marine mudstones, siltstones, and deltaic sandstones with interbedded volcanic units were

deposited. Kenitz (1997) and Robertson (1997) in subsurface stratigraphic studies in northwest Oregon concluded that the Tillamook Volcanic flows are stratigraphically lower than the Grays River flows. In northwest Oregon, the Tillamook Volcanics underlie the Eocene Hamlet and Cowlitz Formations, whereas the younger Grays River Volcanics are interbedded with the Clark and Wilson sandstone member of the Cowlitz Formation in the northern Mist Gas Field. Similarly, Grays River Volcanic sedimentary units interfinger with Cowlitz sandstones and siltstones in Coal Creek and several other locations within the study area (Plates 1 and 2).

A possible Grays River eruptive center may exist nearly 20 km (~13 mi) due west of Longview, north of the Columbia River, identified by a Bouguer gravity anomaly of over 50 milligals (Finn et al., 1991; Figure 45). Various authors have interpreted this anomaly in different ways. Wells and Coe (1985) and Stanley et al. (1996) have suggested that the gravity high may be related to thickened oceanic crust of the underlying Crescent Formation (Siletz Terrane) resulting from relict seamount topography. Alternatively, gravity anomalies above 10 milligals may define the discrete, fault-bounded crustal blocks of the Siletz Terrane. Kenitz (1997) points out that the Champlin Puckett 13-36-5 well, on the south bank of the Columbia River in the core of the anomaly (Figure 45), and on the southwest flank of the gravity high, drilled through about 1700 meters of Grays River basalt flows, and thus, is a likely candidate for a Grays River Volcanic edifice. Outcrops of Grays River Volcanics flows have recently been identified near this well site near the town of Clatskanie in northwest Oregon by Eriksson (2002), in Mt. Solo (this study), and across the bridge from Longview in Rainier, Oregon.

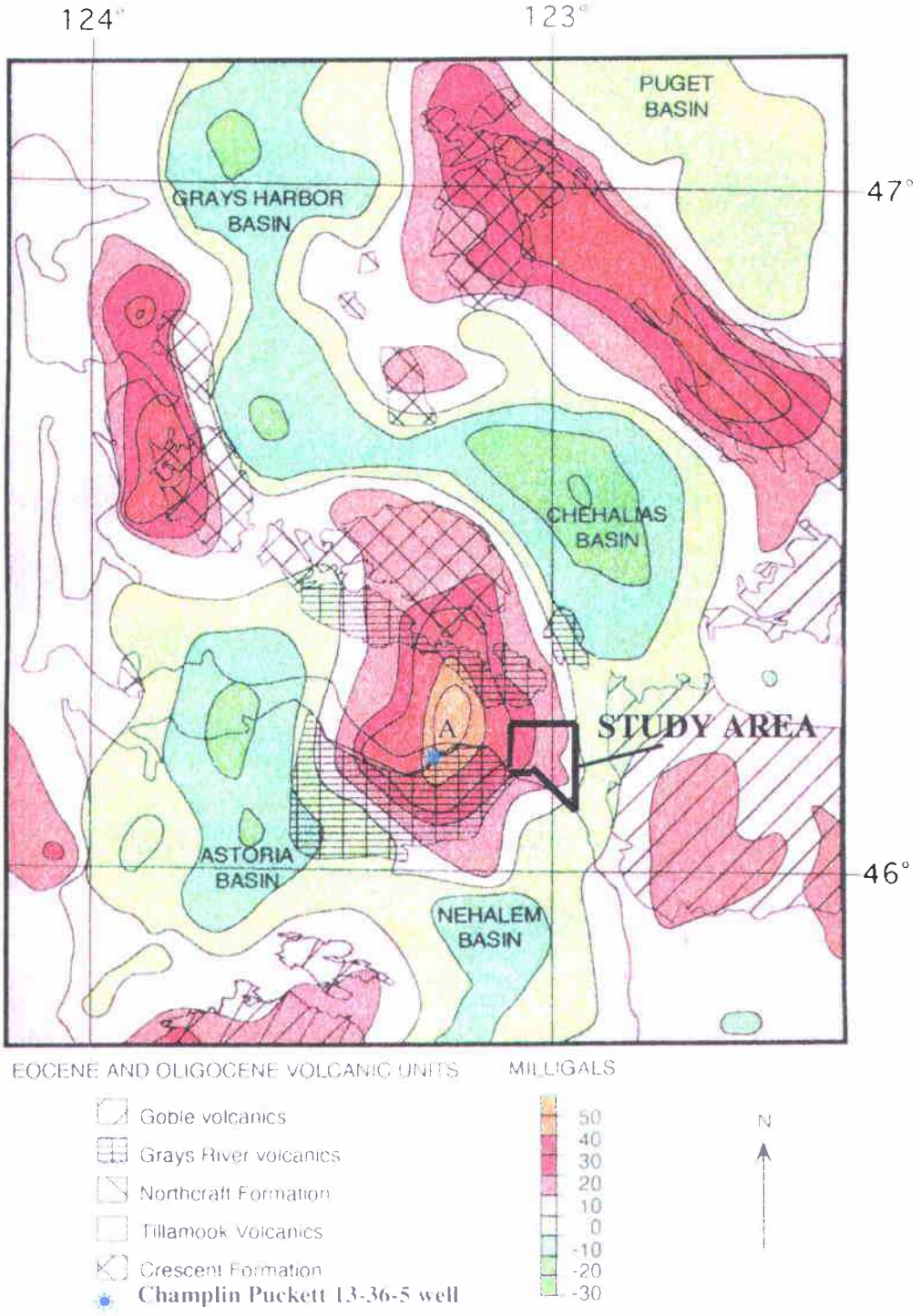

Figure 45: Residual wavelength-filtered gravity anomaly map and volcanic geology map superimposed to show relationship of shallow crustal features and surface geology. The large anomaly (A) centered on Grays River Volcanics may be the eruptive center. Modified from Payne, 1998; Finn et al., 1991; and Walsh and Phillips, 1987.

A localized gravity anomaly of this magnitude may be the result of a combination of these factors.

Age

Kleibacker (2001) postulated in his master's thesis that in the area immediately to the north and west of the study area, two separate Grays River volcanic piles occur, separated by an intra-formational unconformity that he dated at about 39 Ma. In Germany Creek (~6km northwest of the study area), subaerial Grays River basalt flows conformably overlie the middle Eocene Cowlitz Formation, and were $^{40}Ar/^{39}Ar$ dated at about 40 Ma. A Grays River basalt dike intruding interval 44 of the Coal Creek section was dated by Irving et al. (1996) to be about 40 Ma, similar to Grays River dikes in Kleibacker's (2001) thesis area (Figure 46), beneath the unconformity. Payne (1998) describes a younger subaerial Grays River subunit from Abernathy and Bebe Mountains 10 km farther to the north, that overlies the older Grays River unit. This younger unit was $^{40}Ar/^{39}Ar$ dated at between 36.85 and 38.64 Ma, and is the same age as and continuous with the upper flow unit in Kleibacker's thesis study area. $^{40}Ar/^{39}Ar$ dates reported by Payne (1998) from this upper Grays River subunit show a general decrease in age toward the northeast. Regionally $^{40}Ar/^{39}Ar$ radiometric dates of the Tillamook and Grays River Volcanics from northwest Oregon and southwest Washington show an age progression from southwest to northeast (Figure 46), possibly showing a northeastward progression of the tensional regime within the forearc basin from 42.4 to 36.8 Ma. However, an $^{40}Ar/^{39}Ar$ date of 36.98 ± .78 Ma acquired for this study from Site 7 on Mt. Solo does not fit this age progression model, indicating that Grays River volcanism in the study area occurred over a 3 million year period from ~40 to ~37 Ma.

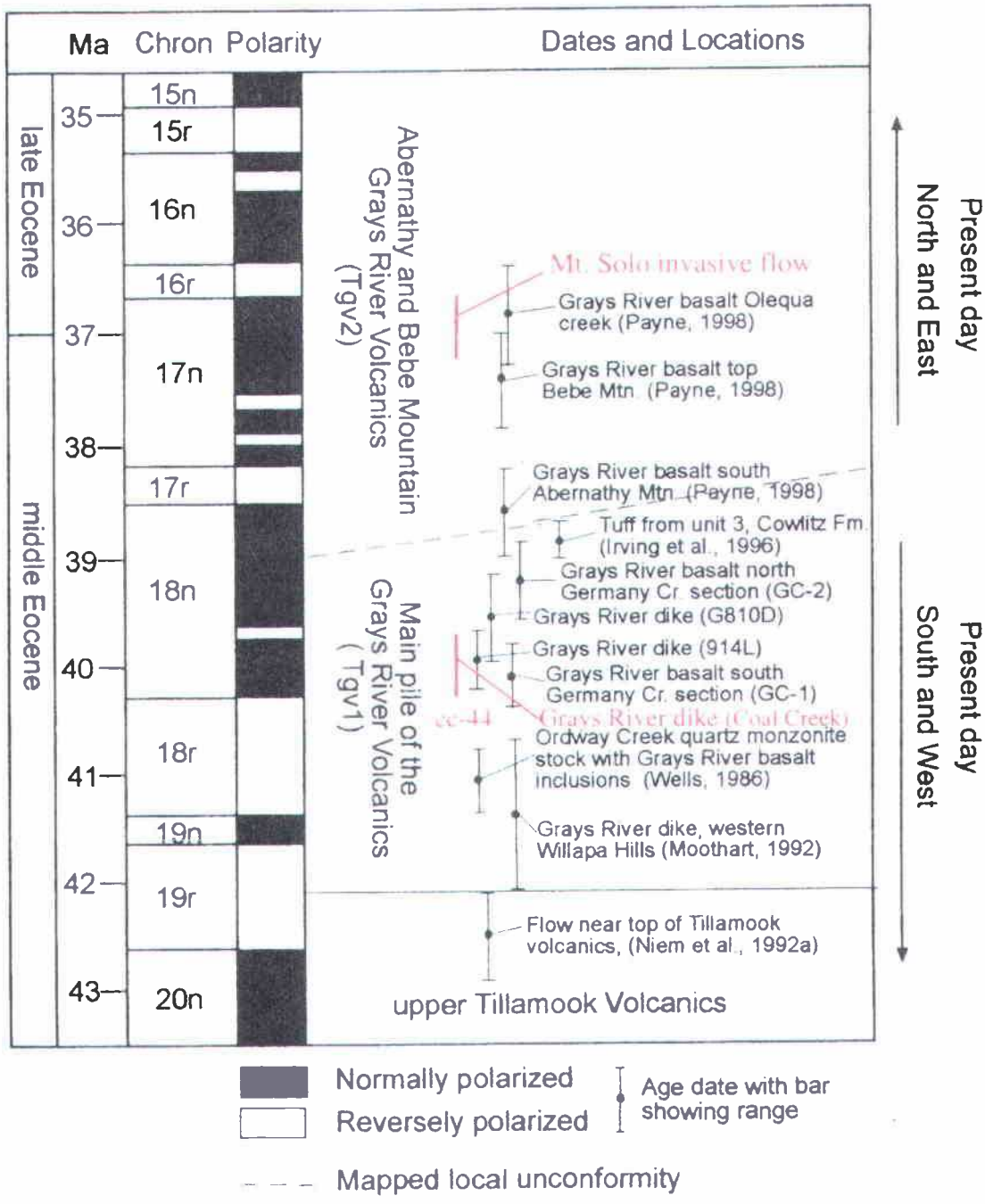

Figure 46: Magnetic polarity stages and Ar^{40}/Ar^{39} age-date diagram of Grays River Volcanics. Note decreasing age of the Grays River Volcanics toward the present-day northeast, and that the ~37 Ma date from Mt. Solo is anomalous. Modified from Kleibacker (2001). Coal Creek interval 44 Grays River dike in red. Samples GC2, G810D, 914L, and GC-1 are from Kleibacker (2001).

Distribution and Stratigraphy

Volcanic rock units of Grays River chemical composition occur in many parts of the study area (Plate 1). Subaerial Grays River flows (map unit Tgv1) are exposed in three locations on or near the margin of the Cowlitz River. Exposures occur in roadcuts along a 0.6 km stretch of the southern portion of Columbia Heights Road (N ½ of Sec. 27, T 8 N, R 2 W, Site 1a), and in cuts along the railroad tracks on the west bank of the Cowlitz River (Site 1b, S ½ of Sec. 22, T 8 N, R 2 W). Poor exposures also occur in cuts along West Side Highway (Sec. 15, T 8 N, R 2 W), east of the Beacon Hill housing subdivision. Excellent exposures of columnar Grays River flows occur on the east bank of the Cowlitz River in railroad cuts and roadcuts in the north and west sides of the two small hills known as Rocky Point (Sites 2 and 4, SW ¼ of Sec. 14, T 8 N, R 2 W, Plate 1). Another good exposure is in the Terra Firma Quarry on the southwest flank of Mt. Solo (E ½ of Sec. 26, T 8 N, R 3 W, "FQ" samples). Grays River flows are also exposed in three small fault-controlled hills (Plate 1), rising above the alluvium in parts of Sec. 13 and 24, T 8 N, R 3 W, and Sec. 18 and 19, T 8 N, R 2 W.

Shallow marine (and in part subaerial) basaltic Grays River breccia and basalt conglomerates (map unit Tgvs1, Plate 1) occur overlying and interfingering with the subaerial flow unit (Tgv1) in lower elevation areas in the eastern part of Mt. Solo (Sites 6 and 7, Sec. 24, 25, and 26, T 8 N, R 3 W), along Pacific Way in a large roadcut beneath the power lines (Site 32, NW ¼ of Sec. 13, T 8 N, R 3 W), in thick deposits on both the west and east sides of the Cowlitz River, and at elevations reaching 700 feet in the Columbia Heights area. This breccia/conglomerate Grays River Volcanic unit is faulted against Cowlitz sandstone and western Cascade basaltic andesite flows in the northern-

and southern-most exposures at Site 9 (Carrolls I-5 exit) along Old Pacific Highway (N ½ of Sec. 12, T 7 N, R 2 W, "CR" samples). Particularly good exposures occur at Site 7 in the eastern part of Mt. Solo, Site 32 along Pacific Way, a roadcut at Site 105 (NW ¼ of Sec. 3, T 8 N, R 2 W), a roadcut along Interstate 5 at Rocky Point (Site 5, SW ¼ of Sec. 14, T 8 N, R 2 W), and a large roadcut along Main Street in Kelso (Site 14, SW ¼ Sec. 26, T 8 N, R 2 W).

Younger shallow marine, mollusk-bearing Grays River volcaniclastic conglomerate, sandstone, and siltstone interbeds within the Cowlitz Formation (map unit Tgvs2) are well exposed in both Coal Creek and Clark Creek (see Plates 1 and 2, and descriptions in the Coal Creek section of this text), but sparsely represented in exposures of the Cowlitz Formation elsewhere (one example in Site 77 near Ostrander). Younger Grays River dikes (map unit Tgvid) and two Grays River sills (map unit Tgvis) occur in Cowlitz Formation sandstones and siltstones in Coal Creek, and invasively intermingled with Grays River volcaniclastics on the south side of Mt. Solo (particularly Site 7).

Throughout the study area, a consistent relationship exists between the four Grays River units (Figure 47). At the base is the Grays River subaerial flow unit (Tgv1), well exposed in the Terra Firma Quarry at the base of Mt. Solo where a minimum of 20 meters of basalt flow occurs. Approximately 15 meters of dark gray massive to blocky basalt flows are overlain by about 5 meters of channelized, matrix-supported, subrounded to rounded, porphyritic boulder-cobble conglomerate (base of Tgvs1, Figure 48a), with the largest clast (near the upper right-center of the photograph) measuring approximately 3-4 meters in diameter. Grays River flows in this quarry also contain a nearly 10-meter

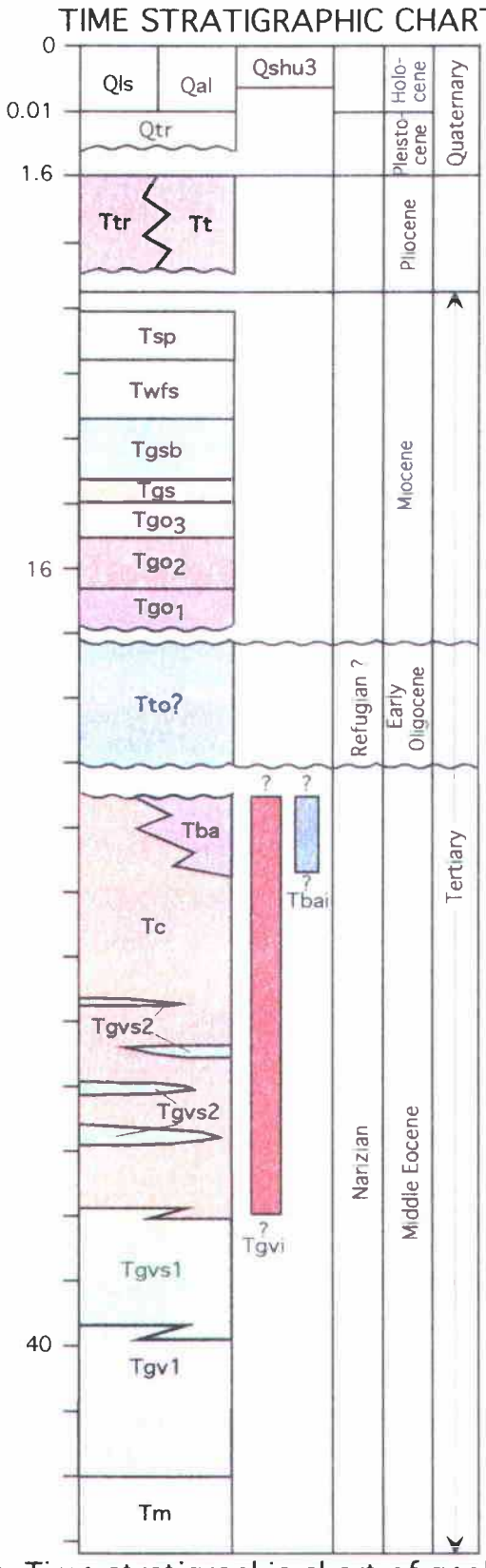

Figure 47: Time stratigraphic chart of geologic units within the study area.

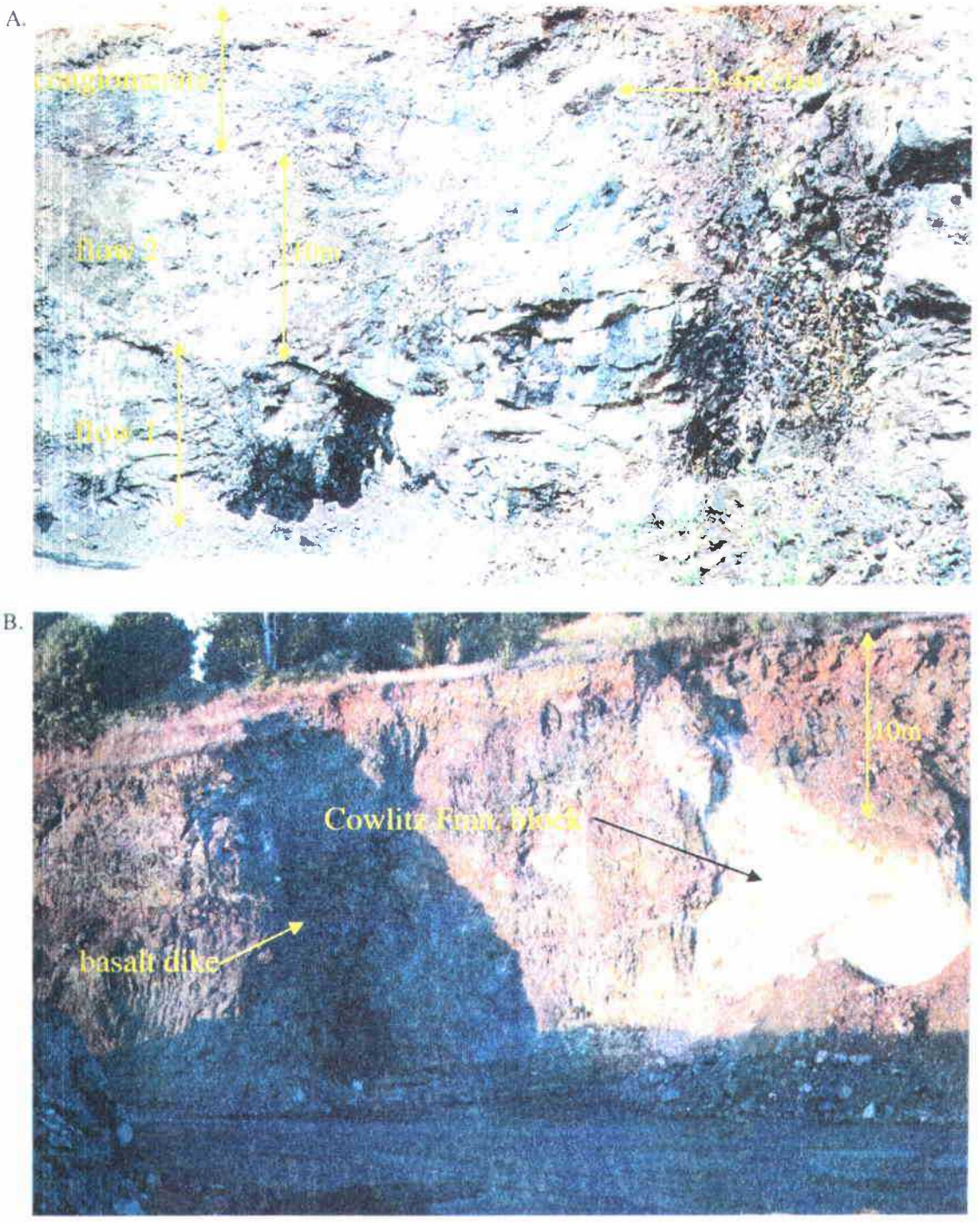

Figure 48: Grays River flows in the Terra Firma Quarry on the south side of Mt. Solo.

A. Central part of the quarry showing at least two Grays River flows (Tgv1) with overlying boulder conglomerate channel-fill of Tgvs1. Several well-rounded boulders are over 1 meter in diameter, the largest is nearly 4 meters.

B. Eastern part of the Terra Firma Quarry. A large (20-meter diameter) block of Cowlitz Formation arkosic sandstone is caught-up in this flow, showing that at least some Cowlitz Formation predates these lower Grays River flows, and suggests that the flow is possibly invasive.

diameter block or xenolith of yellowish gray Cowlitz arkosic sandstone (Figure 48b), indicating that at least some Eocene sandstone was already in place (and already somewhat consolidated) before this eruption, suggesting that the flow may be partly interbedded (or possibly invasive or intrusive) within the Cowlitz Formation. The same relationship of basaltic flow unit Tgv1 overlain by volcaniclastic breccia or conglomerate can be seen at Site 1, and at Rocky Point (Plate 1). Site 7 at the southern tip of Mt. Solo contains several discordant, irregularly-shaped autoclastic dike-like bodies, with columnar jointing in several orientations, intermingled with brecciated basalt (Figure 49), possibly flow breccia, with the lava and volcaniclastic forming nearly at the same time. The 36.98 ± .78 Ma date from this site is anomalously young given its position stratigraphically beneath the Cowlitz Formation in this area. This is further evidence that one or more Grays River flows at Mt. Solo are invasive. Similar autoclastic breccias and associated dikes occur in submarine Miocene Columbia River Basalts at Big Creek in northwest Oregon (Murphy, 1981; Niem personal communication 2003).

The thick volcaniclastic unit (Tgvs1) described above as overlying or co-mingled with Grays River lava (Tgv1) underlies Cowlitz micaceous arkoses (map unit Tc) at several locations. The contact is exposed at Site 16 (SW ¼ of Sec. 14, T 8 N, R 2 W), and at Site 129 (NE ¼ of Sec. 26, T 8 N, R 2 W). Interbeds of Cowlitz arkose in Grays River basalt pebble and cobble conglomerate occur at several locations, including volcaniclastic beds in Coal Creek. Site 15 (SW ¼ of Sec. 23, T 8 N, R 2 W) is also an excellent example of this relationship, where a 2-meter thick arkose interbed can be seen from Interstate 5. Basaltic conglomerate underlying Cowlitz Formation micaceous

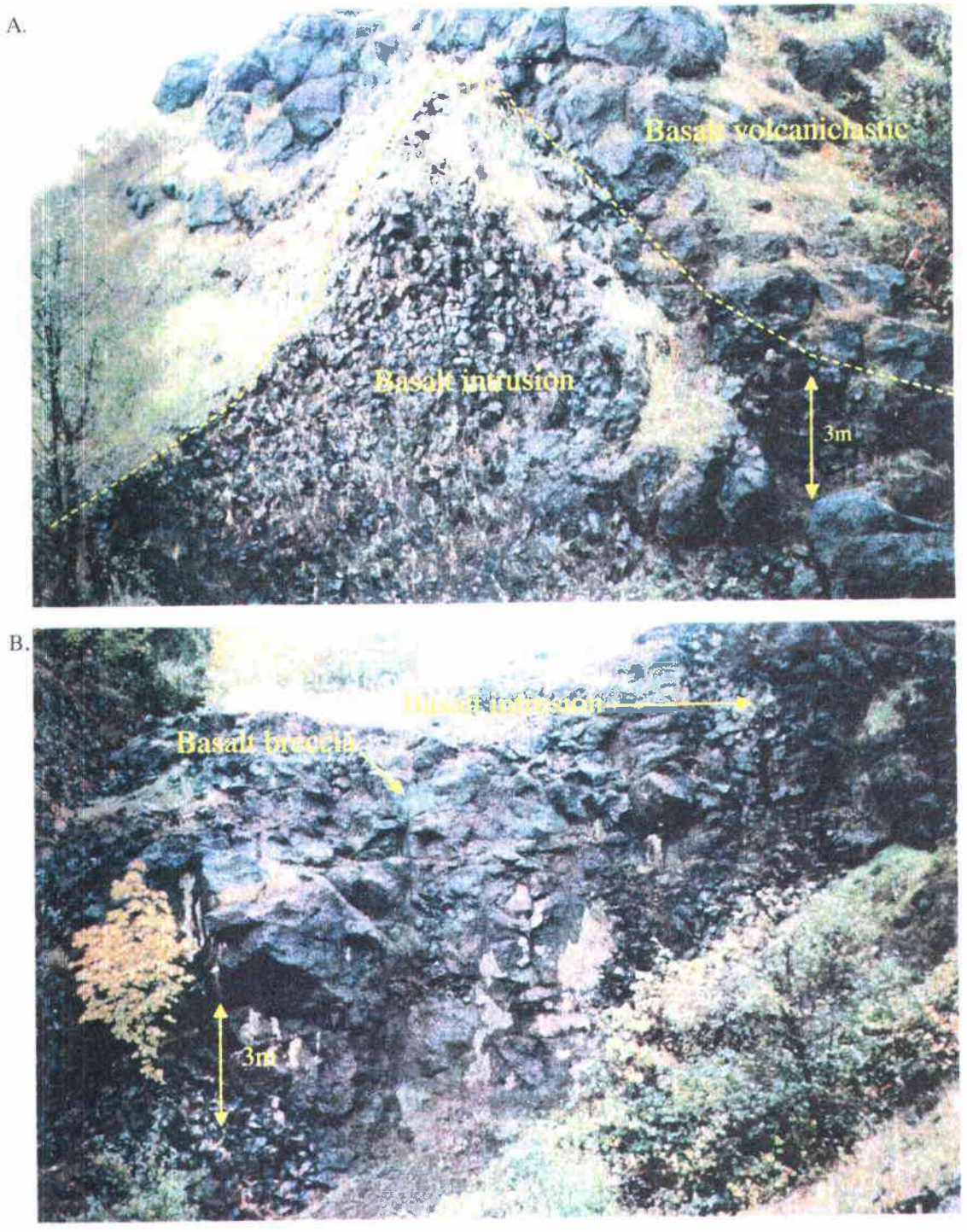

Figure 49: Quarry at Site 7, on the south side of Mt. Solo, illustrating the intermingling of Grays River lava (Tgv1) and associated lower Grays River autoclastic breccia (Tgvs1).

A. Western wall of the quarry showing an irregular-shaped lower basalt intrusion with hexagonal jointing projecting upward into basaltic autoclastic breccia.

B. Eastern wall of quarry showing autoclastic basaltic breccia intruded by irregular autoclastic columnar jointed basalt dikes.

arkoses can also be inferred based on strike and dip of these units throughout the map area (see cross section A-A' and B-B', Plate 1).

Younger shallow marine, mollusk-bearing Grays River volcaniclastics (Tgvs2) interfinger with Cowlitz Formation micaceous arkosic sandstones and siltstones throughout the 640-meter Coal Creek section (see Plate 2, Figure 47, and the lithologic descriptions in the Coal Creek section of the text). A particularly thick (~35 meter) subunit consisting of interbedded Grays River pebble conglomerate, sandstone, and siltstone occurs 100 meters from the base of the section, and may be the more marine facies of the thick volcaniclastic unit Tgvs1. Many Cowlitz Formation sandstone and siltstone intervals that are dominated by micaceous arkose also have a high percentage of Grays River basaltic clasts, and are shown as arkose in Plates 1 and 2 if less than 50% basalt fragments. Grays River composition basaltic dikes and sills intrude portions of the entire Coal Creek section (Figure 50a) and are therefore in part younger than much of the section. An invasive (?) ~5-7 meter thick Grays River sill is exposed at Site 9 ("IS" samples, Figure 50b) along Coal Creek Road (SE ¼ of the NW ¼ of Sec. 11, T 8 N, R 3 W). The dike that intrudes between intervals 7 and 10 in the Coal Creek section is peperitic, as is the sill along the road to the Storedahl and Sons Quarry (NW ¼ of the NE ¼ of Sec. 15, T 8 N, R 3 W), immediately below the Miocene Columbia River Basalt flows. These intrusions, in some of the stratigraphically highest beds of Cowlitz Formation exposed in the area, probably intruded the Cowlitz units when they were still wet and unconsolidated, suggesting these Grays River intrusions may have occurred shortly after deposition of the uppermost Cowlitz beds.

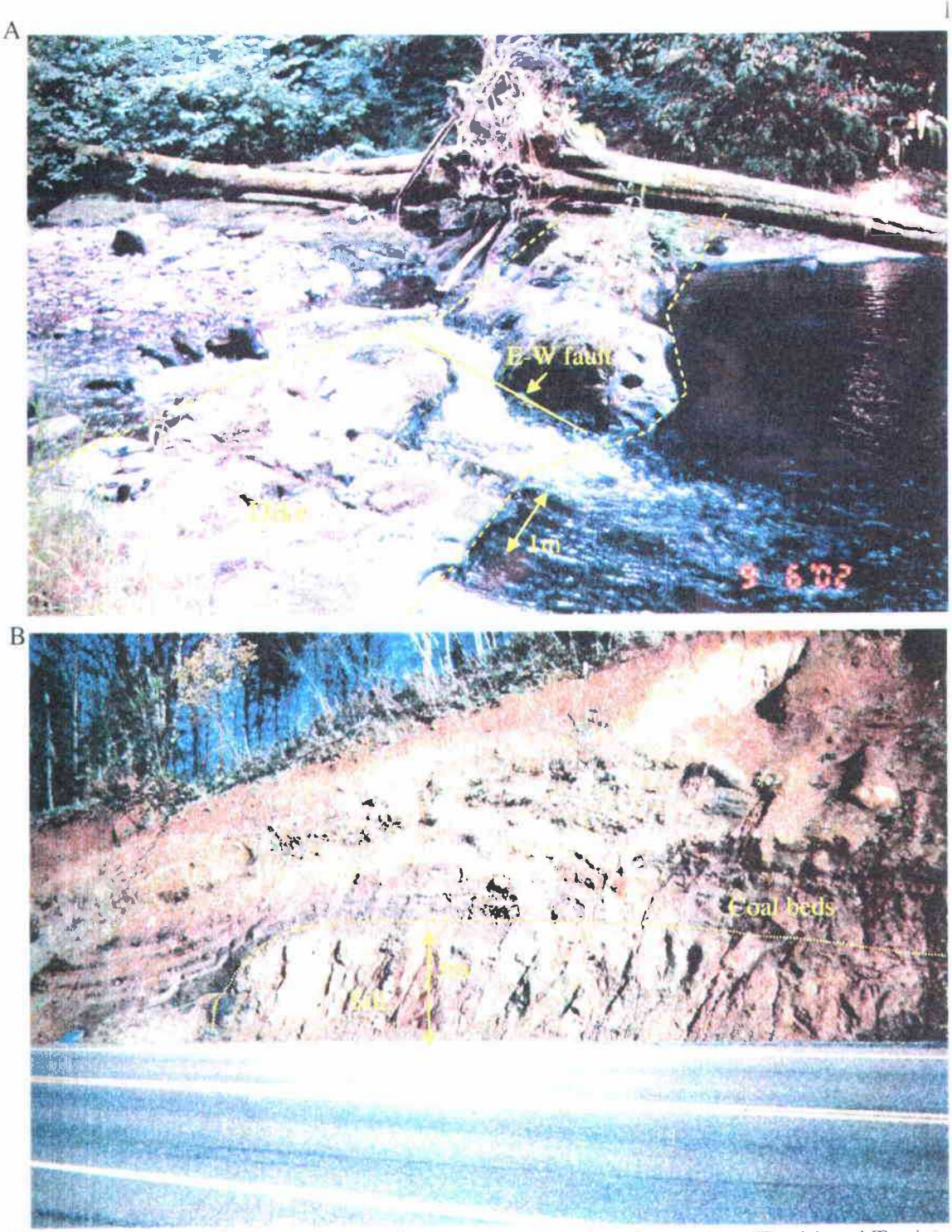

Figure 50: Grays River basalt intrusions into the Cowlitz Formation (Tgvid and Tgvis).

A. Nearly vertical two-meter wide Grays River dike intruding interval 21 in Coal Creek. Over 60 such dikes, most trending northwest, intrude the Cowlitz Formation only in Coal Creek. Note E-W fault offsetting the dike.

B. Roadcut along Coal Creek Road (Site "IS") exposing a Grays River sill. Note the displacement of overlying tuff and coal beds, suggesting a possible invasive relationship. This offset could also be entirely due to faulting.

Petrology

Seventeen thin sections were produced from Grays River Volcanics samples collected in the study area. These samples were selected because they illustrate the range in mineralogy and texture of the four Grays River units (thin section locations are identified in Plate 1). Three thin sections are Grays River basaltic lava flows (Tgv1; Sites 1a, 2a, and 7). Nine thin sections are from the thick, partly subaerial lower volcaniclastic unit (Tgvs1; Sites 5, 6, 7a, 7b, 14, 15, CR-2, CR-7, and FQ clast). Four thin sections are from the shallow marine Grays River basalt volcaniclastic unit interbedded with Cowlitz Formation arkoses described in the Coal Creek section (Tgvs2; CC-45, 54, 77, and 93). One thin section was made from a dike intruding interval 44 in the Coal Creek section (Tgvid; CC-44). Eleven Grays River Volcanics samples were analyzed with financial assistance from Karl Wegmann of the Washington Department of Natural Resources for major oxide and trace element geochemistry using x-ray fluorescence (XRF) by the Washington State University GeoAnalytical Laboratory (Appendix III). Six of these samples are from the Grays River subaerial basalt flows (Tgv1; Sites 1b, 2a, 7c, 7d, 63, and 101). Two samples are from the partly terrestrial lower volcaniclastic unit (Tgvs1; Site 5 and FQ clast). Three samples are from dike intrusions into the Cowlitz Formation in Coal Creek (Tgvid; CC-9, 44, and 63).

Grays River Flows

Grays River basalt flows in the Longview-Kelso area appear to be largely subaerial, and can be either massive or show well-developed columnar jointing. Flows at the Terra Firma Quarry at the base of Mt. Solo, and Site 1b, are massive to columnar-jointed. Those at Sites 1a, 2, and 4 are mostly columnar-jointed, and are medium to dark

gray, but weather to medium brown or medium brownish orange. No individual flow in the area can be studied from top to bottom in its entirety, so flow thickness cannot be precisely ascertained, but they are at least several meters thick. Flows seem to be dominantly sheet-like, but individual flows cannot be traced laterally for much distance, so some may be partly channelized or intracanyon. At Site 1b, nearly horizontal joints are likely boundaries between flows (flow joints). Toward the north of this outcrop and slightly upsection, the flow top becomes amygdaloidal (vesicles filled with both calcite and zeolite), suggesting one of the flows is over 10-meters thick. No instance of reddish oxidized flow tops or paleosols as observed by Payne (1998) and Kleibacker (2001) in younger Grays River flows were observed in the study area.

Fresh hand samples are typically augite-, olivine-, and labradorite-phyric, but are less commonly microphyric to aphyric. Feldspar glomerophenocrysts consisting of several labradorite feldspars range in size up to nearly 2 mm, but average less than 1 mm. Individual euhedral augite phenocrysts can reach 5 mm, but are more typically nearly 1 mm. Weathered and often clay-altered olivine phenocrysts are rounded and appear brownish or greenish in hand sample. The most highly porphyritic hand samples are ~30% visible phenocrysts and ~60% black glassy groundmass consisting of aligned plagioclase microlites (pilotaxitic flow texture).

One sample was chosen to represent each of the three major exposures of Grays River Volcanics flows within the study area, and thin sectioned for petrographic study; Site 7 (Mt. Solo), Site 1a (the core of the Columbia Heights Anticline, Plate 1), and Site 2a (Rocky Point, east of the Cowlitz River). Site 7 flows are intermingled with flow breccia and may represent the transition from basal autoclastic flow breccia to the basalt

flow itself. These are sparsely porphyritic, with nearly 75% of the sample consisting of greenish clay altered groundmass with sub-aligned lath-like plagioclase microlites, and small and less abundant augite microlites that average 100-200 micrometers (Figure 51a). Labradorite glomerophenocrysts average 1-2 mm and commonly include augite and olivine phenocrysts of similar size (figure 51b). About 5% of Site 7 flows consists of albite-twinned plagioclase laths, 2-3% altered olivine/augite microlites, 8% large phenocrysts or glomerophenocrysts of labradorite, and 9% glomerophenocrysts of augite. Augite crystals are commonly equant and have brown clay-altered margins.

Subaerial basalt flows from Site 1a are highly porphyritic, and have a clay altered groundmass constituting about 75% of the sample, containing randomly oriented plagioclase microlites and globular opaque ilmenite. Larger phenocrysts comprise about 25% of the sample, augite accounting for 15% (Figure 52a), labradorite accounting for 10%, and a minor ~3% amount of olivine. Secondary white sparry calcite fills microfractures and accounts for about 1% of the total sample. Augite phenocrysts are equant, fractured, and have partially resorbed margins, as do some of the plagioclase microlites and larger labradorite phenocrysts. Both of these minerals form abundant glomerophenocrysts throughout the flow. Site 2a (Figure 52b) from Rocky Point contains phenocrysts set in a pilotaxitic groundmass consisting of aligned plagioclase microlites (100-200 micrometers), and smaller interstitial augites, olivines, and opaque ilmenite crystals averaging about 50 micrometers (together constituting about 80% of the sample). Larger labradorite phenocrysts, commonly forming glomerophenocrysts several mm in diameter (Figure 52b), constitute about 16-17% of the basalt. The remainder is iddingsite-altered olivine phenocrysts. Only one sizeable augite occurs in this sample,

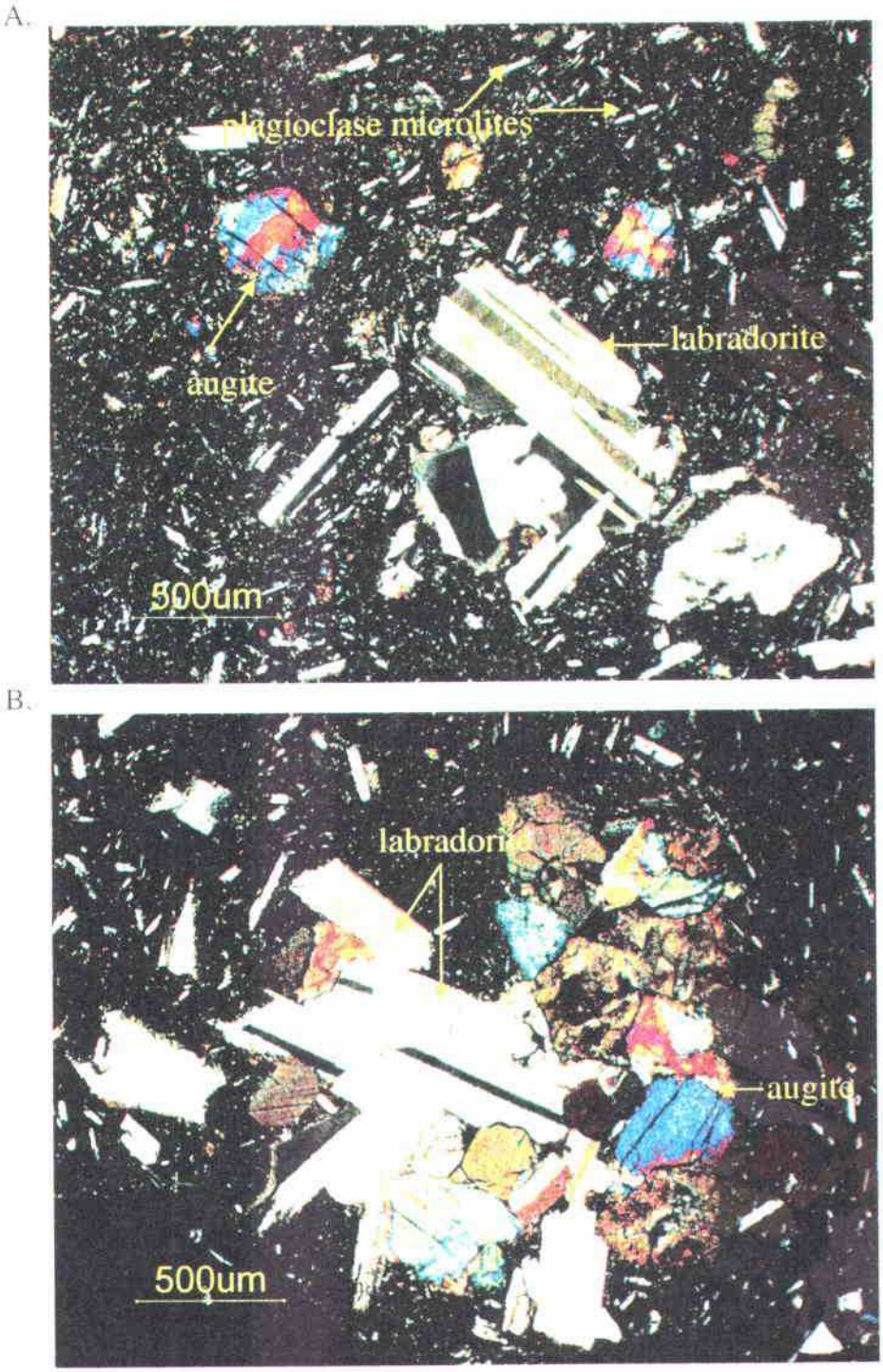

Figure 51: Photomicrographs of Grays River flows from the south side of Mt Solo.
A) Porphyritic Grays River flow with labradorite glomerophenocryst in clay-altered groundmass with sparse plagioclase microlites showing weak pilotaxitic flow texture (Site 7, crossed-nicols).
B) Porphyritic Grays River flow showing combined labradorite and augite glomerophenocryst (Site 7, crossed-nicols).

A.

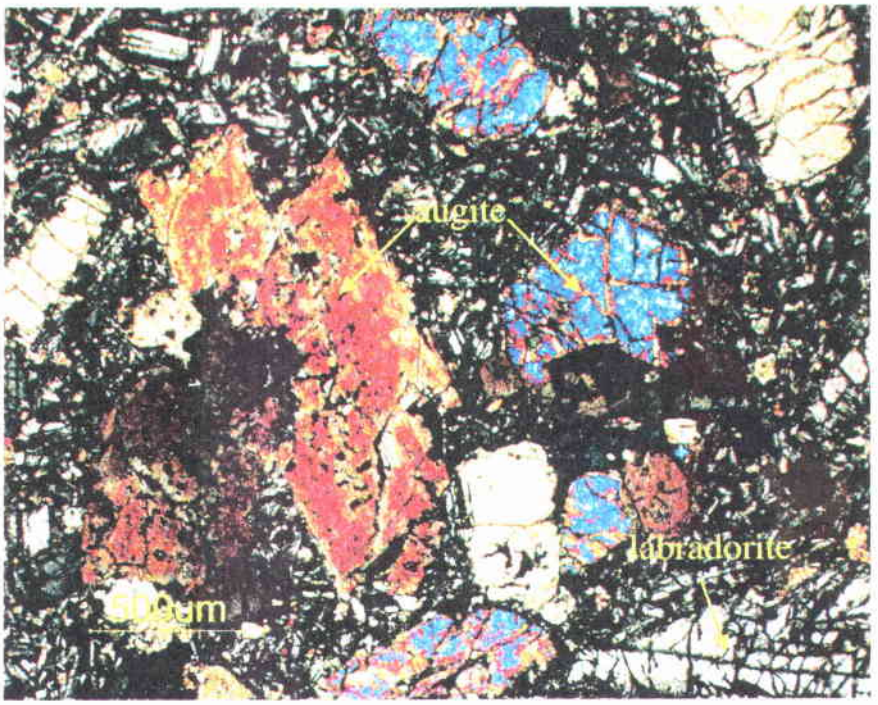

B.

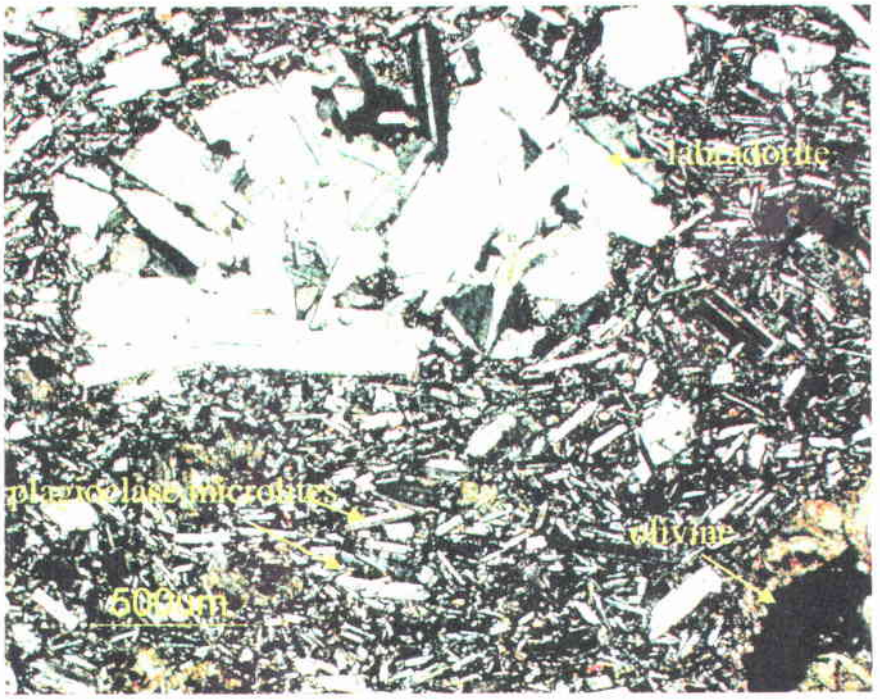

Figure 52: Photomicrographs of Gray River flows from near the Cowlitz River (crossed-nicols).

A) Large partially resorbed and clay-altered augites from Site 1a (Plate 1).

B) Labradorite glomerocryst and highly iddingsite-altered olivines set in a pilotaxitic groundmass consisting of aligned plagioclase microlites, from Rocky Point (Site 2a, Plate 1).

equant with altered margins. These Grays River basalt flows are similar in most respects petrographically to Grays River flows described by Payne (1998) and Kleibacker (2001), except that Longview-Kelso area flows are apparently not texturally differentiated from top to bottom as described in Payne's m.s. thesis area ~10 km to the north.

Dikes

Over 30 basalt dikes and two sills of Grays River basalt were mapped along Coal Creek and roadcuts adjacent to the creek (Plate 1, and Coal Creek inset Plate 2), where they intruded perpendicular to the bedding of Cowlitz Formation micaceous arkoses or marine Grays River volcaniclastics. The dikes (of normal polarity according to the fluxgate portable magnetometer) range in width from 0.5 to 6 meters, and are generally sub-parallel, trending between N 40 W and N 60 W. Dikes less than 0.3 meters across were not mapped. They are largely parallel to, and commonly associated with, the dominant northwest-trending joint and fault pattern in the creek. Many dike outcrops have well-developed sub-vertical slickensides on their planar margins. These intrusive bodies generally parallel the strike of Cowlitz Formation beds in the creek, and dip at right angles to the dip of the sedimentary beds. If these Cowlitz beds were returned to their original horizontal position, the dikes would have to have been emplaced vertically, and were later tilted (5-30 degrees) along with the beds into which they intruded to their present orientation. As previously mentioned, the basalt dike intruding between intervals 7 and 10 in the Coal Creek section is peperitic (consisting of basalt with fragments of medium-grained micaceous, arkosic sandstone), and may have been emplaced shortly after deposition of these beds when they were still wet and unconsolidated, also applying

to the sill exposed on the road to the Storedahl and Sons Quarry. The sill intruding Coal Creek interval 22, exposed in the "IS" roadcut along Coal Creek Road, seems to invade between and displace formerly adjacent baked coals, sandstones, and thin tuff beds (Figure 50b).

Most dikes are plagioclase- and augite-phyric, with phenocrysts accounting for about 20% of the volume. They are medium to dark gray fresh, weathering to medium brown. Larger dikes (>3 meters) are compositionally zoned with phenocryst size increasing slightly toward the interior. These coarsely crystalline dikes also display a microphyric groundmass toward the interior, but an aphyric clay altered groundmass toward the margins. About 50% of the basaltic dikes are somewhat vesicular, and a few (particularly the Coal Creek peperitic dike mentioned above) are amygdaloidal, with the calcite- or zeolite-filled, spherical to ovoid, 1-5 mm diameter amygdules reaching a maximum of 10% of the total sample.

A fresh sample of the 3-meter wide dike intruding interval 44 of the Cowlitz Formation (Plate 2) in Coal Creek was thin-sectioned for petrographic analysis. The dike is labradorite- and augite-phyric, with plagioclase microlites (averaging about 250 micrometers in length), augites, and opaque ilmenite phenocrysts randomly oriented, and constituting approximately 40% of the sample (Figure 53a). Larger labradorite phenocrysts are as large as 3 mm, and constitute about 10% of the sample (Figure 53a). Calcic albite and carlsbad twinned plagioclase feldspars show a high degree of absorption along the margins so that over 50% of the phenocrysts are no longer euhedral. Approximately 30% of the sample is composed of interstitial augite and olivine microlites, and ~5% are globular opaques. Another 5-10% is clay-altered interstitial

A.

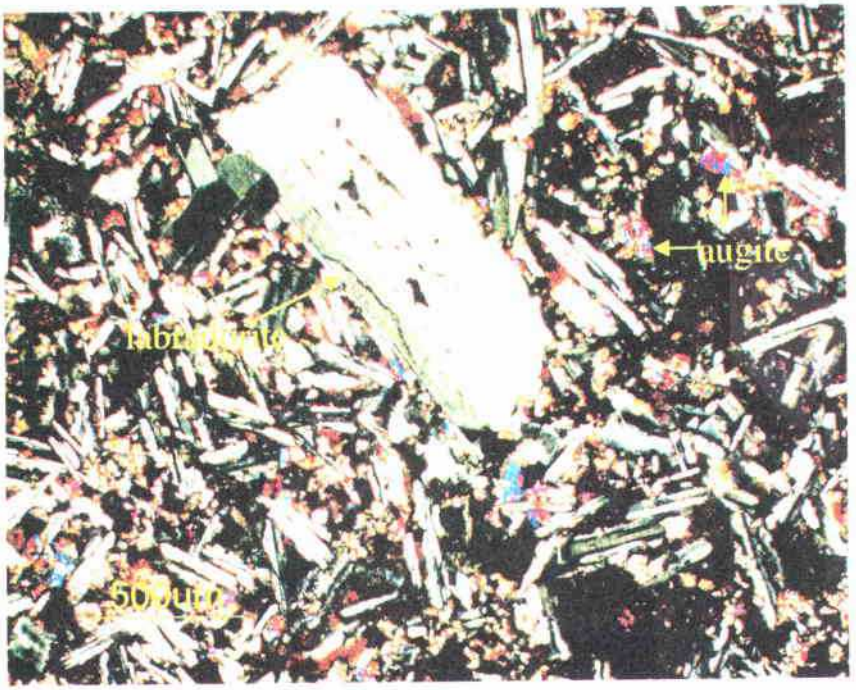

B.

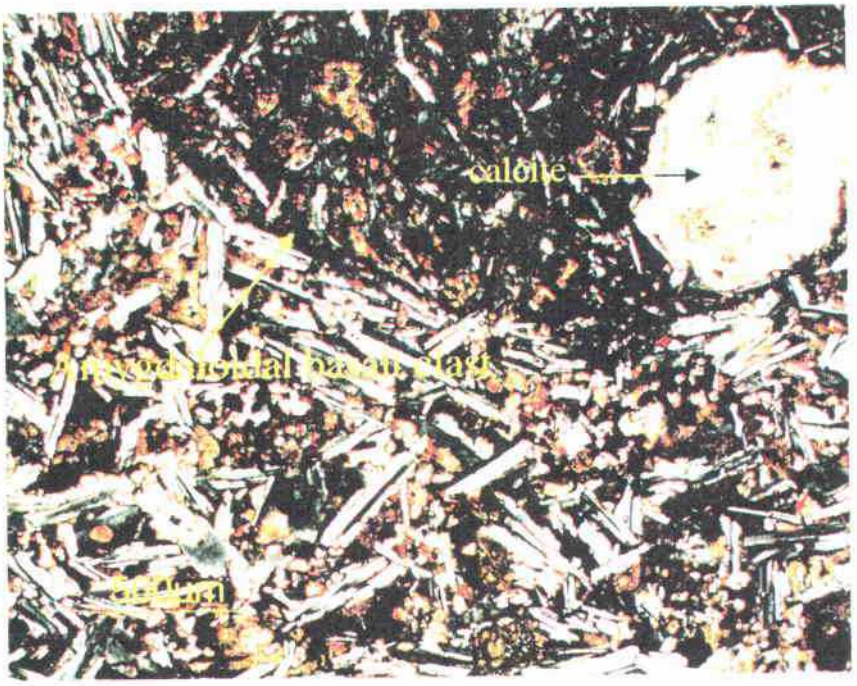

Figure 53: Photomicrographs of a Grays River dike from Coal Creek (CC-44)
A) Intersertal texture consisting of randomly oriented plagioclase microlites and large labradorite phenocryst with a high degree of embayment along the margins (crossed-nicols).
B) Spherical xenolith of amygdaloidal Grays River basalt within CC-44. Note smaller vesicles filled with brown clay and large vesicle filled with sparry calcite (crossed-nicols).

groundmass between crystals. Large augite phenocrysts with embayed margins constitute about 1%. This sample also contains well-rounded amygdaloidal xenoliths of older Grays River basalt flows that have pilotaxitic flow texture (Figure 53b). The dikes are petrographically like the subaerial Grays River basalt flows except they lack the pilotaxitic flow texture of aligned plagioclase microlites. Large vesicles are filled with calcite, smaller vesicles are filled with brown chlorophaeite clay.

Lower Volcaniclastics

The Lower Grays River Volcaniclastic unit (Tgvs1, Plate 1) varies in lithology throughout the study area from basaltic breccia to pebble-boulder conglomerates and basaltic sandstones, and at Site 105 (Plate 1) is interbedded with western Cascade-derived lithic pumice lapilli tuffs. These tuffs are thinly bedded and contain spherical accretionary lapilli. Five facies of this unit are recognized within the study area: 1) fluvial channel-fill clast- or matrix-supported, cobble to boulder conglomerates, 2) very poorly-sorted debris flow deposits derived from *en mass* movement of volcanic material, 3) hyperconcentrated flow deposits consisting of moderately- to poorly-sorted, massive to thickly-bedded volcanic breccia to cobble conglomerate, 4) scoriaceous hyaloclastite base surge deposits from phreatomagmatic eruptive centers (e.g., Rocky Point and Mt. Solo), and 5) basal autoclastic flow breccias intruded by irregular basalt dikes. At Mt. Solo this unit conformably overlies, and is partially interbedded with flows of Grays River composition (facies 5). It also conformably underlies, and is partially interbedded with micaceous lithic arkosic sandstones and siltstones of the middle Eocene Cowlitz Formation (facies 3). The occurrence of micaceous Cowlitz Formation arkose interbeds in this unit shows that it is also in part shallow marine. Similar (but mostly younger)

Grays River volcaniclastics north and west of the study area do not contain as high percentage of scoriaceous clasts as those from the study area (Kleibacker, 2001). The thickness of Tgvs1 also widely varies throughout the study area. In the vicinity of Mt. Solo, an up-thrown fault block, the unit has a minimum thickness of 350 feet (~110 meters). Over 500 feet (~150 meters) of basaltic conglomerate and underlying Grays River flows have been uplifted in the southern core of the Columbia Heights Anticline (Plate 1, cross section A-A'). East of the Cowlitz River, within and north of the city of Kelso, roughly 200 feet (70 meters) is exposed beneath conformably overlying arkoses of the Cowlitz Formation. An unknown thickness of this unit is covered by Quaternary alluvium of the Columbia and Cowlitz Rivers beneath the cities of Longview and Kelso.

The wide variation in thickness of this unit in the study area, and the apparent lack of thick exposures of this volcaniclastic unit in the thesis areas of Payne (1998) and Kleibacker (2001) to the north, indicates that it is highly localized. The thickest and coarsest-grained deposit seems to lie along an axis that generally trends along a line from Mt. Solo toward the Columbia Heights suburb of Longview, and Rocky Point (Plate 1). The unit apparently rapidly thins toward the northwest and southeast. If this thick partly subaerial volcaniclastic is correlative to the thickest mollusk-bearing shallow marine basalt volcaniclastic unit in Coal Creek (Tgvs2, Plate 2), which has similar lithology, then it has thinned to roughly 100 feet (30 meters) in that direction. If it is not correlative to Tgvs2, then it has either pinched out in that direction or underlies 2000 feet (~650 meters) of Cowlitz Formation. Toward the southeast, the deposit is at least 10 meters thick where it is faulted into the large roadcut at the Carrolls I-5 exit (Site 9).

Maximum clast size of the basalt cobble-boulder conglomerate portion of Tgvs1 decreases toward the northeast, and upsection. In the Terra Firma Quarry on the southwest flank of Mt. Solo, in the paleo-channels in the upper part of the cliff face (facies 1, Figure 48a), several boulders are over 1 meter in diameter, and the largest is 3-4 meters. Paleocurrent direction based on the cross sectional shape of the channel would have been toward the east-northeast (nearly directly into the cliff face), suggesting a substantial paleo-topographic high was toward the west (where the gravity anomaly occurs, Figure 45). At the small canyon in the west half of Sec. 22, T 8 N, R 2 W (low in the section), well-rounded, large clasts are over 10 cm, and the largest clast is 30 cm (facies 2 or 3). At Site 123 (SW ¼ of Sec. 16, T 8 N, R 2 W), elongate basaltic boulders nearly 1 meter in diameter are widely scattered in a matrix of well-rounded basalt cobbles a few centimeters in diameter (facies 2). At Site 105 (NW ¼ of Sec. 3, T 8 N, R 3 W), average clast size has decreased to 3 cm, with the largest 8 cm (facies 3). A sufficient amount of time to deposit 1-3 meter-thick air fall tuffs had to elapse between these individual hyperconcentrated flows. At Site 9 (along Old Pacific Highway, Carrolls I-5 exit) the largest clast size is about 6 cm. No clasts over 3 cm were found in the high elevation exposures of this unit.

Grays River volcaniclastic natural outcrops in the study area (i.e., Mt. Solo) are typically cliff-formers since they are well-indurated due to extensive calcite cement. Roadcuts or railroad cuts are slow to weather relative to less indurated Cowlitz Formation sandstones and form prominent cliffs (e.g., roadcuts at Sites 5, 7, 9, 14, and 33). Outcrops are highly fractured with some degree of alteration. Clasts typically have a

weathered rind, and spaces and fractures are commonly filled with limonite and manganese oxide, or with calcite, analcime (Site 7), or zeolite.

The only exposures of true volcaniclastic breccia, containing few or no rounded clasts (and no arkosic component in places), are the two quarries on the south side of Mt. Solo (facies 5). Here, massive and poorly sorted breccias of angular porphyritic basalt are intermingled with columnar-jointed Grays River flows and irregularly shaped intrusions. At Site 7 (Figure 49), columnar-jointed projections (irregular dikes) of Grays River basalt of various shapes, sizes, and angles intrude the breccia. The variety of shapes, including the curvature, and in places the open honeycomb nature of some of the columnar bodies, indicates that these are not intruding previously fractured or faulted older volcaniclastic breccias that were already in place. It is more likely that these are basal or top flow breccias, produced at the same time as the lavas, which then injected autoclastic dikes and irregular intrusions into the flow breccia pile. Basaltic clasts at Site 7 are very angular, and some are nearly 0.5 meter in diameter. Fragments can be plagioclase- or augite-phyric, aphanitic, vesicular, or amygdaloidal. Breccias can be either clast- or matrix-supported, with the matrix consisting of smaller fragments of porphyritic and aphyric basalt and euhedral plagioclase (labradorite) and augite. Some euhedral augite crystals are over 1-cm long. Breccias higher in the section and farther east on Mt. Solo (e.g., Site 6) have a substantial percentage of stream reworked subrounded clasts and grade into poorly-sorted cobble conglomerate, possibly indicating a transition from a debris flow or lahar (facies 2) to hyperconcentrated fluvial flows (facies 3). Fractures, pore spaces, and amygdules at these locations are dominantly filled with white analcime and zeolite. Elsewhere on Mt. Solo, sparry calcite is more common

or the dominant fracture- and void-filling mineral. Both breccias and conglomerates of this unit are typically massive, or bedding is thicker than the height of the outcrop, characteristics of both debris flows and the lower portion of thick hyperconcentrated flows.

A roadcut exposure where 38th Street in Longview is cut through the eastern part of Mt. Solo (Site 6), consists of highly fractured, dark gray, monotonous, non-graded, somewhat sorted (lacking significantly larger than average clasts), massive to thickly-bedded volcaniclastic basalt hyperconcentrated flow (facies 3) to phreatomagmatic surge deposits (facies 4). Many clasts are sub-rounded, enough for this part of the unit to be considered a stream-reworked, poorly-sorted, clast-supported volcanic conglomerate, rather than a volcanic flow breccia. However, the high percentage of scoriaceous clasts indicates a phreatomagmatic origin for most clasts. This exposure is transitional between the two facies, and may represent reworked older phreatomagmatic clasts. Fracture sets may be crude bedding. Like Site 7, Site 6 contains euhedral augite crystals, some nearly 1 cm long, and abundant scoriaceous clasts. Two km to the northwest, the large roadcut beneath the power lines (Site 32) has virtually the same lithology, but is laterally discontinuous, with the nature of the contact with adjacent units uncertain. This could be a block faulted into the Cowlitz Formation, or a channelized hyperconcentrated flow.

Three thin sections of the basalt volcaniclastics from Mt. Solo were studied: two from Site 7, and one from Site 6 (Plate 1). Samples from Site 7 are from the scoriaceous conglomerate/breccia portion of the unit. They consist of subrounded to well-rounded porphyritic basaltic clasts of varying basalt lithologies (Figure 54a). About 70% are amygdaloidal (scoriaceous) with abundant spherical vesicles filled with greenish fibrous

A.

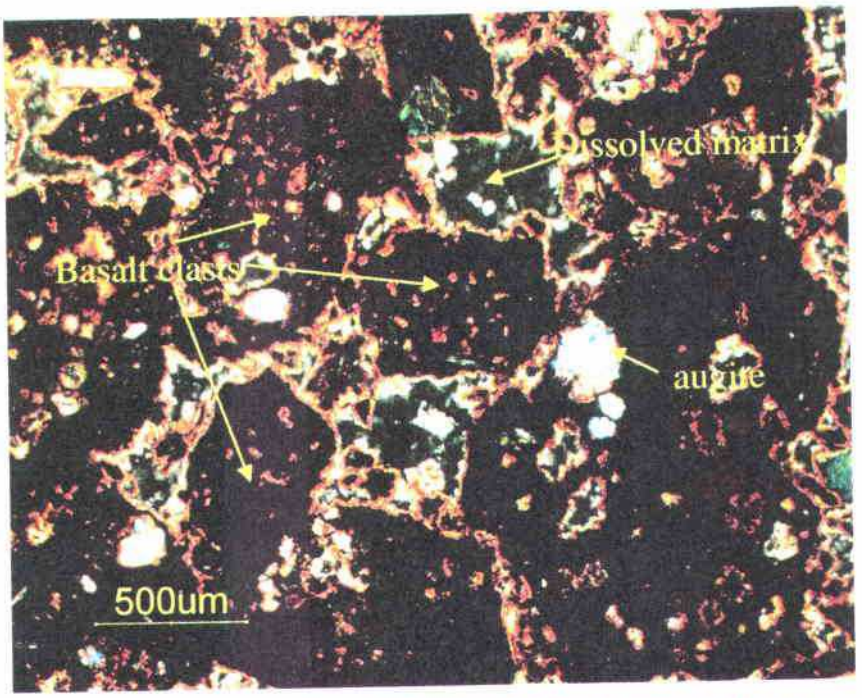

B.

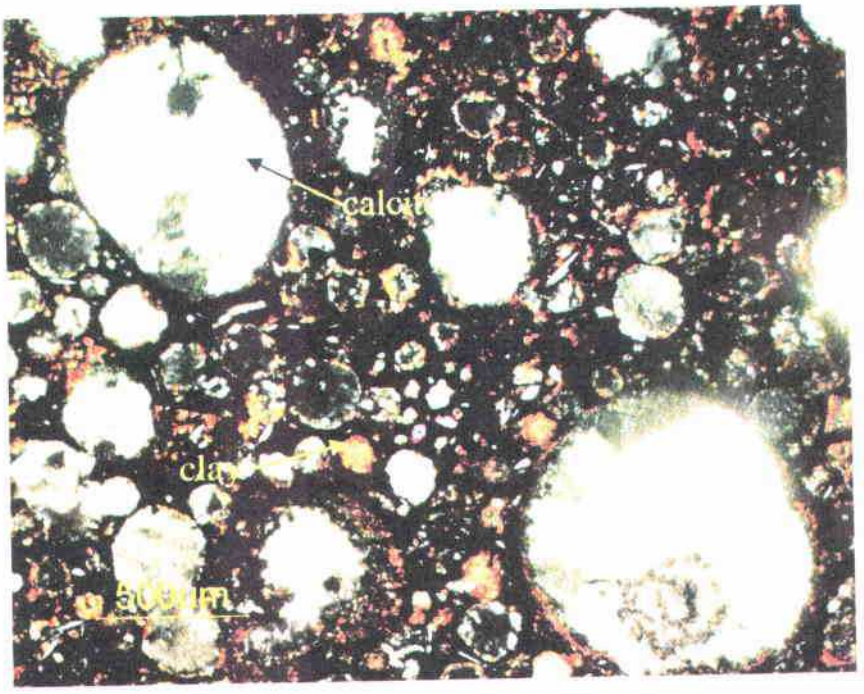

Figure 54: Photomicrographs of Lower Grays River Volcaniclastic (Tgvs1) from Mt. Solo (facies 4, Plate 1)(crossed-nicols).

A) Scoriaceous basalt pebble conglomerate/breccia from Site 7. Note the smectite-altered margins, and that the matrix has largely dissolved.

B) Scoriaceous basalt clast typical of conglomerate at Site 6. Amygdules are filled by celadonite, nontronite, and sparry calcite. Note similarity to Grays River dike xenolith from Figure 53b.

clay, likely celadonite and nontronite. About 20% of the sample consists of much darker, rounded, porphyritic basalt clasts, with nearly opaque clay-altered basaltic glass groundmass. Many plagioclase phenocrysts have been altered to brownish clay, which also fills the vesicles in the basalt clasts. Augite phenocrysts are still largely unaltered. Another ~10% consists of relatively unaltered pilotaxitic and aphyric basalt clasts, with aligned albite twinned plagioclase microlites still largely intact. Some clasts are highly altered, and some sparry calcite (<1%) fills the pore spaces. Much of the calcite that originally filled the pore spaces has been dissolved, leaving about 10% pore space. Green, fibrous celadonite or nontronite clay lines voids and rims all clasts as a widespread cement that has destroyed much of the primary porosity and permeability.

In thin section, Site 6 is also a scoriaceous basalt conglomerate/breccia (Figure 54b). Approximately 90% of the subrounded clasts are scoriaceous or amygdaloidal, some vesicles filled with calcite (~10%), some filled with smectite clay (~20%), the rest rimmed with fibrous nontronite or celadonite clay but otherwise empty. About 90% of the sample as a whole is brownish due to extensive clay alteration. A few pilotaxitic lava clasts are identifiable. This thin section from Site 6 contains a small (~5%) component of arkose (i.e., angular monocrystalline quartz, mica, potassium feldspar), suggesting this thick basaltic volcaniclastic, despite being stratigraphically lower than most of the Cowlitz Formation in the area, is coeval with this formation rather than pre-dating it. This conclusion is supported by the large arkosic xenolithic Cowlitz block within Grays River flows at the Terra Firma Quarry, and the arkose interbed at Site 15. The arkosic clasts, in addition to the scoriaceous clasts, indicate that this could be a hyperconcentrated channelized flow entering the deltaic environment, reworking older

basalt phreatomagmatic and lava flow clasts and mixing in Cowlitz micaceous arkose. Alternatively, arkosic clasts and older flows could have been incorporated into a deposit from a phreatomagmatic eruption occurring in place within the delta front.

Basalt lava clasts from Site 6 appear to have undergone a period of diagenetic alteration before emplacement, since few sodic plagioclase feldspar clasts of Cowlitz Formation origin are altered, but most (more calcic) plagioclase phenocrysts within the Grays River clasts are highly altered. This, along with the rounding and poor sorting of the basalt clasts, suggests that the clasts had been transported by stream some distance prior to deposition, perhaps in a hyperconcentrated flow. Some augites are completely altered to brownish clay, others have only an altered clay rind. This conglomerate/breccia is a collection of volcanic clasts of different textural maturity.

Three Grays River basalt pebble to cobble conglomerates are exposed at Site 9 ("CR" samples) at the Carrolls I-5 exit on Old Pacific Highway, at both the north (CR-1 and 2) and south (CR- 13) ends of this 100-meter long roadcut that exposes three north-south trending faults (part of the Kelso Fault Zone, Plate 1). Another volcaniclastic unit faulted into this outcrop is CR-7. This pumiceous lapilli tuff/pebble conglomerate is massive, light to medium gray, and highly fractured with substantial alteration and spheroidal weathering. Basaltic Grays River exposures have fractures filled with white zeolite and calcite and, especially in thin section CR-1, abundant manganese oxide. These poorly-sorted conglomerates (facies 3) are mainly basaltic sand matrix supported, with clasts typically cobble-sized, but some are over 10 cm in diameter. Most clasts are rounded to subrounded. The outcrop at the south end of the roadcut is similar, but has a higher percentage of coarse-grained basaltic sandstone-sized clasts, and graded bedding

occurs over 1-meter intervals (Figure 55a). According to Smith and Fisher (1986) these graded beds are consistent with finer-grained, normally graded deposits found in the upper part of hyperconcentrated flows. Hand samples from these outcrops have abundant and clearly visible dark green euhedral augite crystals, and few visible white plagioclase feldspars.

Three thin sections were prepared for petrographic analysis of outcrops from the Carrolls interchange (Site 9, samples CR-1, 2, and 7). Only in thin section is the degree of alteration of CR-1 and CR-2 apparent (Figure 55b). Before alteration, the framework clasts were rounded, porphyritic pebbles of clay altered Grays River basalt, with large labradorite and augite phenocrysts apparent throughout the sample. The basaltic sandy matrix, however, has been replaced by a mesh-like network of opaque manganese oxide (formerly the interstitial spaces) and calcite replaces some of the basaltic clasts. This is the most extensive diagenetic alteration observed in any Grays River unit within the study area, with only large phenocrysts remaining.

Adjacent to this conglomerate in the Carrolls Interchange roadcut is another coarse, matrix supported, poorly-sorted basaltic conglomerate (facies 3), that is far less scoriaceous than samples in or near Mt. Solo (thin section CR-2). All components appear to be derived from Grays River lavas. Approximately 5-10% of the clasts are angular slivers of plagioclase (labradorite) with a few small interstitial augite crystals (tending to form the matrix). The remainder of the sample is composed of Grays River lava clasts in various states of chemical alteration and rounding. Some are altered nearly to clay and appear brownish next to the less altered clasts. About 90% of the clasts are subangular to subrounded, and about 50% are aphanitic or contain randomly oriented plagioclase

A.

B.

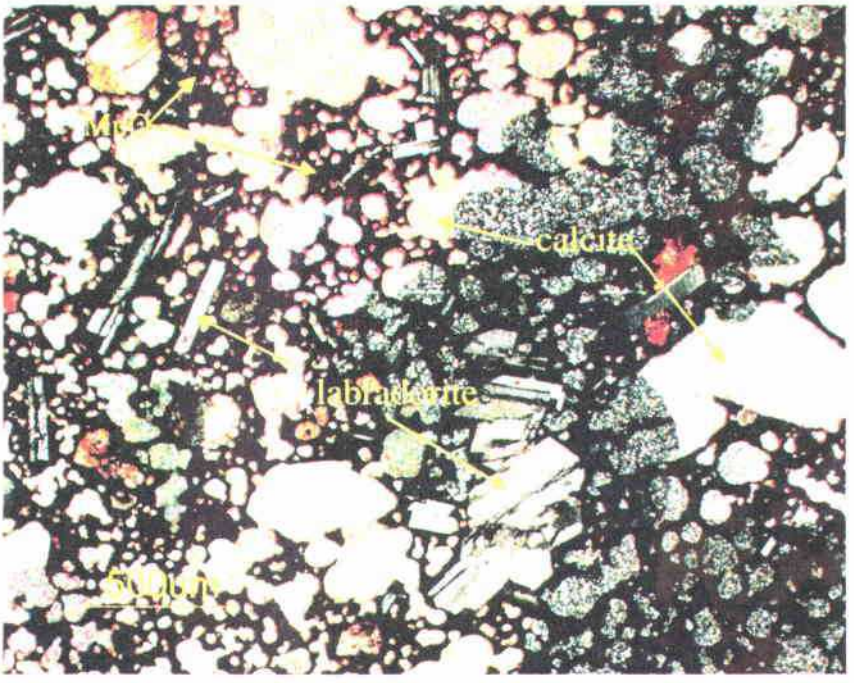

Figure 55: Lower Grays River volcaniclastics from Site 9. 55b is a photomicrograph with (crossed-nicols).

A) Graded beds about 1-meter thick at the south end of the outcrop, consisting of basaltic conglomerate alternating with coarse sandstone.

B) Highly altered basaltic conglomerate (sample CR-1). Rounded clasts have almost completely dissolved away and been replaced by sparry calcite and MnO, only larger labradorite phenocrysts remain.

microlites, and about 50% display pilotaxitic flow texture of plagioclase microlites, augite, and opaque ilmenite. About 25% are scoriaceous. Both sparry calcite cement (especially around the larger clasts) and fibrous clay rim cement are present in this sample. Thin section CR-7 is a reworked pumiceous basaltic tuff, containing ~40% pumice clasts, and only about 10% of the basalt clasts are pilotaxitic. This unit is also clay cemented and contains hydrothermal vein quartz, and some black carbonaceous plant debris occurs.

Outcrops of thick-bedded basalt pebble to boulder conglomerate and breccia in the Columbia Heights area are variable in lithology. Exposures lower in the section are generally coarser-grained or have larger maximum-sized clasts. The two small canyons mentioned earlier to the south and west of Beacon Hill (Sec. 15 and 22, T 8 N, R 2 W) expose coarse-grained, relatively unaltered, poorly-sorted basaltic cobble to boulder conglomerates with clasts approaching 1 meter in diameter (facies 2). Farther to the north at Site 43 (SE ¼ of the SW ¼ of Sec. 33, T 9 N, R 2 W), Site 44 (SW ¼ of the SE ¼ of Sec. 33, T 9 N, R 2 W), and Site 37 (E ½ of Sec. 3, T 8 N, R 2 W) grain size averages nearly 1 cm (facies 3). These outcrops are in various states of weathering, the most altered being Site 37, where clasts are very light tan due to clay alteration. The Tgvs1 outcrop at the highest elevation in the study area is Site 22, exposed in a small gully on the side of Columbia Heights Road. This light brown conglomerate exposure is nearly completely altered to clays.

A very thick-bedded, 10-meter high roadcut on Main Street near downtown Kelso (Site 14) appears indistinguishable from similar exposures described above; highly fractured and spheroidally weathered, poorly-sorted, matrix supported

conglomerate/breccia, massive with abundant alteration, and large euhedral augite clasts (facies 3). One thin section was produced from this location (Figure 56a), and it classifies as a basalt wacke and, unlike the other exposures, this has a substantial arkosic component. About 15% is monocrystalline quartz, 5% polycrystalline quartz, ~6% potassium feldspar, 3% sodic plagioclase and/or labradorite, 1% mica (both muscovite and biotite flakes), 2% clinopyroxene, 1% quartzite, 1% chert, 25% silt-sized basaltic matrix, 10% pilotaxitic basalt, and 30% randomly oriented basalt. Approximately 30% of basalt clasts are scoriaceous. The arkosic minerals are angular to subangular; the relatively less resistant basaltic clasts are subrounded to well-rounded, very poorly-sorted, and compositionally immature, but texturally mature (i.e., moderately rounded and lack of detrital clay matrix). Some basaltic clasts are heavily altered, nearly entirely to smectite clay. Potassium feldspars (orthoclase) are also highly altered to sericite mica, and the cement is exclusively clay. Like Mt. Solo samples, this sample is important because, being 1/3 arkosic in composition, it demonstrates the co-existence of extrabasinal Cowlitz micaceous arkoses and intrabasinal Grays River volcanic sources. This deposit could have been produced by hyperconcentrated flows that entered the deltaic environment upstream, mixing basaltic and micaceous arkosic components as it moved.

Nearly 2 km north of Site 14 on the east side of Interstate 5 is Site 15 (facies 3), which appears in outcrop to be lithologically similar to Site 14. However, at this site there is a 2-meter thick micaceous arkosic sandstone interbed near the base. Thin section shows this to be a poorly-sorted, fine basaltic pebble conglomerate with a high percentage of arkosic minerals. In thin section, most rounded clasts that appear to basalt

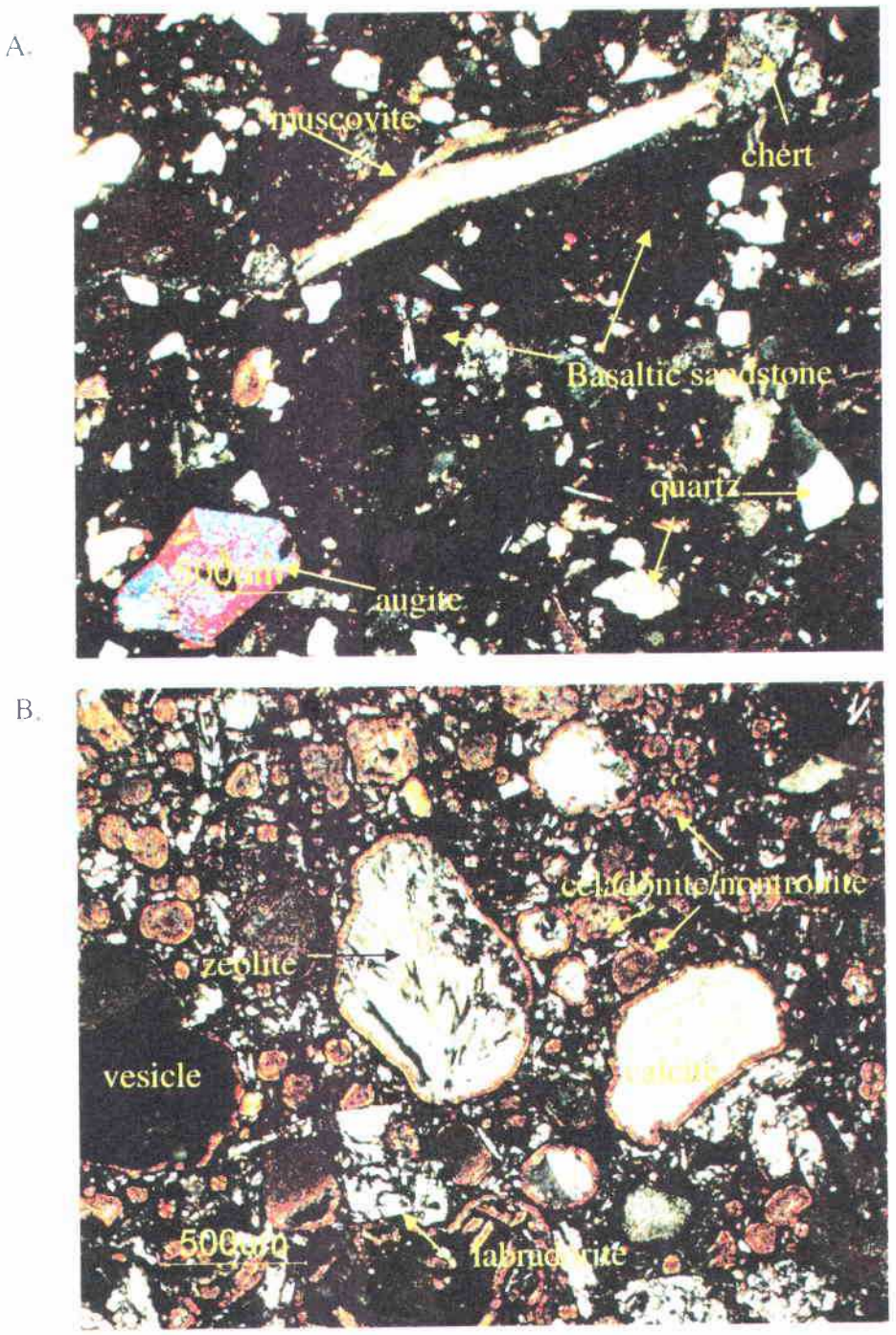

Figure 56: Photomicrographs of two Lower Grays River Volcaniclastics (Tgvs1). (crossed-nicols).

A) Basalt lithic wacke from Site 14. Note high percentage of quartz, muscovite, and chert clasts.

B) Amygdaloidal conglomerate/breccia clast from Rocky Point (Site 5). Note clay filled vesicles (amygdules), and celadonite or nontronite clay rim around zeolite or calcite-filled vesicles (amygdules).

in hand sample have a micaceous arkosic component contained within them, as if they are rounded clasts of a lithology similar to Site 14 (i.e., the clasts are rounded basalt lithic sandstone rather than basalt). This sample is composed of ~15% monocrystalline quartz, 5% polycrystalline quartz, 1% mica (mostly muscovite), <1% clinopyroxene, 5% potassium feldspar, 1% plagioclase, 3% chert, 3% carbonaceous plant material, and 60% rounded clasts of fine-grained arkosic and basaltic sandstone. The sample is poorly-sorted, compositionally immature, and clay cemented.

A roadcut along I-5 through the eastern part of Rocky Point (Site 5) is a lithologically unique example of Grays River volcaniclastics. These are phreatomagmatic hyaloclastites (facies 4) that appear mottled light brownish gray and dark gray. The light colored portion are moderately-sorted, rounded vesicular basalt clasts that are fairly uniform in size, from 0.5 cm to 1.5 cm. In thin section these are apparently calcite and zeolite filled scoriaceous clasts (Figure 56b). The entire outcrop is highly weathered, with the phenocrysts altered to such an extent that no calcic plagioclase feldspars remain. Some augite crystals are also heavily altered to brownish clay. Secondary pore and vesicle filling varies. A thin greenish clay rim surrounds all grains and partly infills all pores. About 15% of remaining pore space is filled with sparry calcite, 75% with greenish smectite or celadonite clay, and 10% with white zeolite. Intergranular primary porosity is roughly 15%. Most pore throats are filled with greenish clay, suggesting low effective porosity and permeability in these tightly cemented volcaniclastics. This basalt volcaniclastic consisting exclusively of scoriaceous clasts, with no arkosic component or clasts of Grays River flows, is evidence that the two small hills that form Rocky Point are phreatomagmatic volcanic centers (cinder cones) erupting

into the shallow marine environment. A roadcut on the west side of Rocky Point near the train tunnel exposes red basaltic cinders, suggesting part of the eruption may have been subaerial.

Geochemistry

Eleven Grays River Volcanic samples were analyzed for major oxide and trace element geochemistry (with financial assistance from Tim Walsh and Karl Wegmann of the Washington Department of Natural Resources) by the Washington State University GeoAnalytical Laboratory using x-ray fluorescence (XRF, Appendix III). Of these, 3 are basalt dikes intruding the Cowlitz Formation in Coal Creek (Tgvid), 3 are Grays River flows (Tgv1), 2 are from the Lower Grays River Volcaniclastic unit (Tgvs1), and three are ambiguous as to whether they are invasive flows or intrusive dikes. All of these samples were crushed and the freshest non-amygdaloidal chips were handpicked and cleaned to ensure the most accurate results. SiO_2 content ranges from 42.71% to 50.34%. The 42.71% result from a dike intruding Coal Creek interval 44 likely represents an altered or weathered specimen, 46.54% should probably represent the low end (Figures 57 and 58). Total alkalis ($K_2O + Na_2O$) range from 2.25% to 4.5%, averaging 3.44%. TiO_2 varies widely from 1.4% to 4.1%, with anomalously low TiO_2 flows (varying from 1.4% to 1.9%) occurring only near Rocky Point (Sites 1b, 2a, and 5, Figure 58), suggesting that these samples represent a localized flow that combines geochemical features of Grays River basalt and Cascade-derived basaltic andesite. Elsewhere Grays River samples vary from 2.8% to 4.1%. Total FeO varies from 10.5% to 17.5% with the lower readings from near Rocky Point and a clast from the Terra Firma Quarry, and the

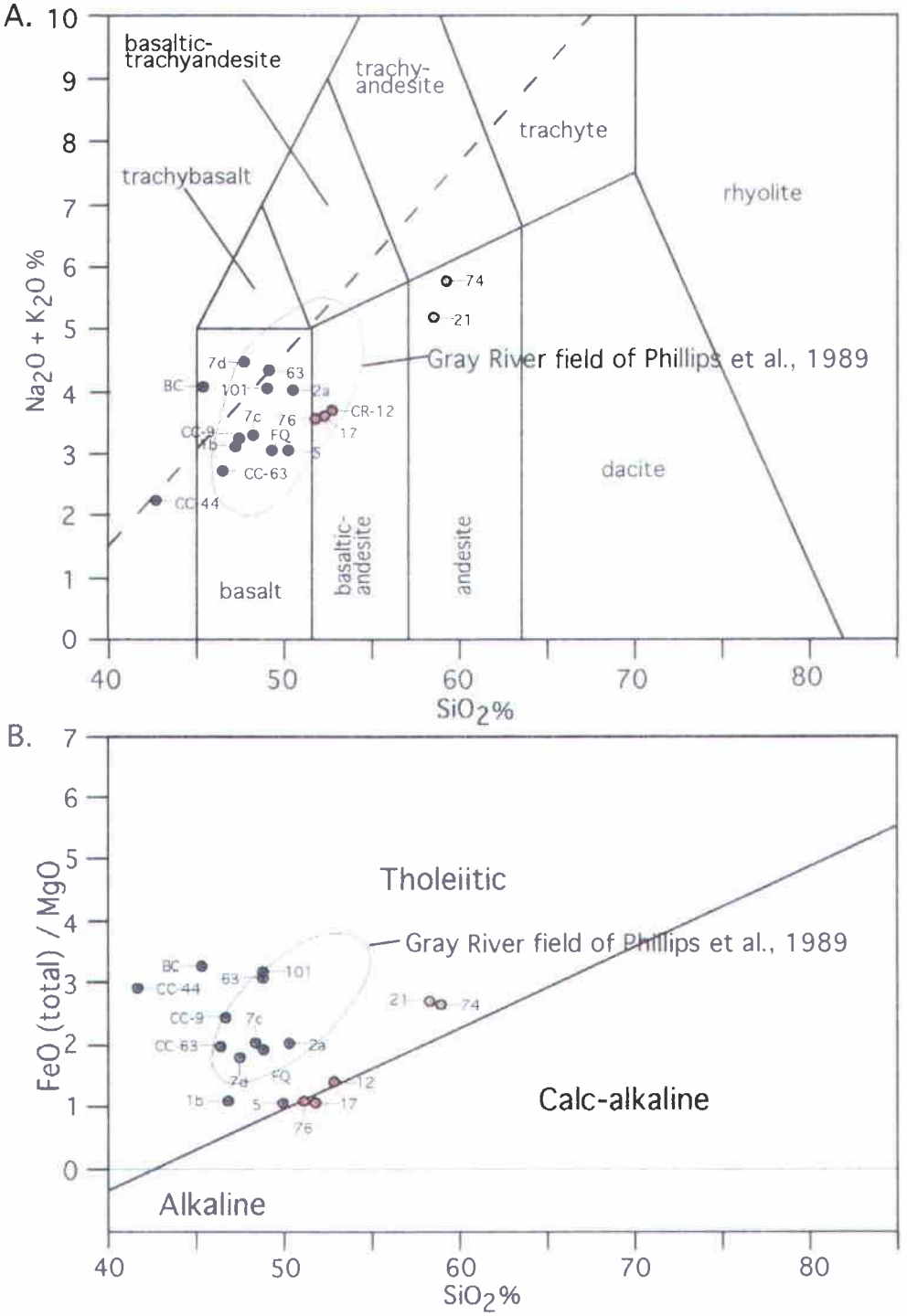

Figure 57: A) Grays River Basalts, western Cascade basaltic andesite, and western Cascade andesite dikes and possible flow from the study area plotted on total alkali vs. SiO_2 (TAS) diagram. Based on IUGS classification scheme of Le Bas et al., 1986. Dotted line separating alkaline vs. subalkaline volcanic rocks from Irvine and Baragers (1971) classification.
B) Same samples plotted on the Iron enrichment diagram of Miyashiro (1974). Note western Cascade basaltic andesite samples are borderline calc-alkaline, and that Rocky Point flows (samples 1b and 5) plot low for FeO_2/MgO.

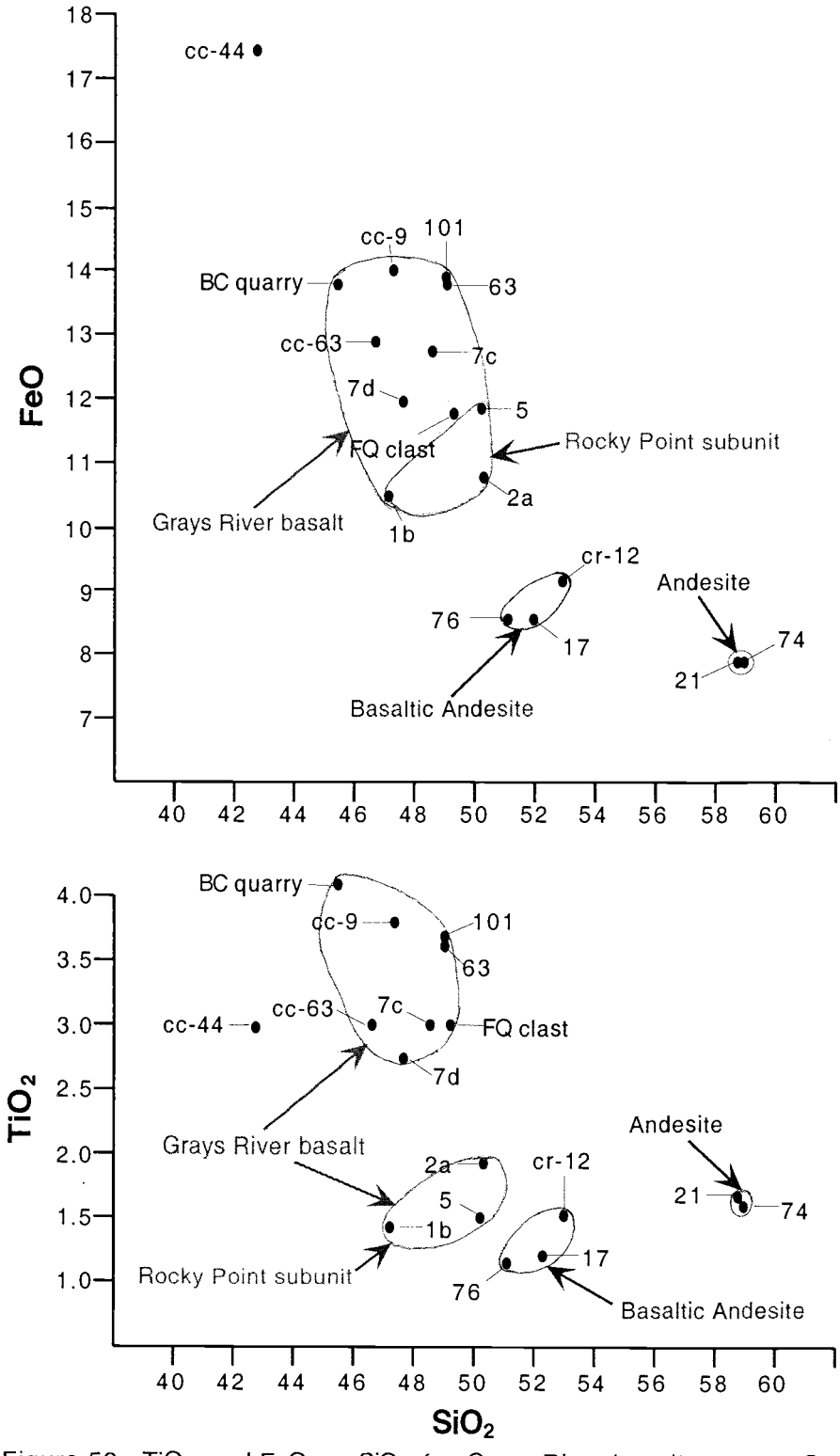

Figure 58: TiO_2 and FeO vs. SiO_2 for Grays River basalt, western Cascade Basaltic Andesite, and western Cascade Andesite. Rocky Point Volcanics appear to be a low TiO_2 Grays River/western Cascade Basaltic Andesite mixture.

highest reading from a Coal Creek dike (CC-44) at 17.5% (again, likely due to alteration or weathering, Figure 58).

Using Irvine and Barager's (1971) classification (Figure 57), all but samples 7d and BC clast (from Mt. Solo) plot as subalkaline basalt. Site 7d plots as alkaline basalt and CC-44 is marginally alkaline. Note that all but CC-44 and BC clast plot within the Grays River field as defined by Phillips et al. (1989). This is likely the result of some degree of alteration or weathering in those samples. The iron enrichment diagram of Miyashiro (1974) show that all but four of the samples (BC clast, CC-44, Site 1b, and Site 5) plot within the field of Phillips et al. (1989) as tholeiitic basalts. The BC clast and CC-44 are tholeiitic basalts that plot slightly lower in SiO_2 than the Phillips et al. fields. On both diagrams, samples from the study area tend to plot lower than average for SiO_2.

On both FeO and TiO_2 vs. SiO_2 diagrams (Figure 58), Grays River samples generally plot near each other, and are separate from western Cascade basaltic andesite and western Cascade andesite flows and intrusions within the study area. Grays River samples are relatively higher in FeO and lower in SiO_2 than the other volcanic units, and typically higher in TiO_2. However, flows and volcaniclastics from the vicinity of Rocky Point (Sites 1a, 2b, and 5) plot significantly lower in TiO_2, and relatively low in FeO than other Grays River units. Given this geochemical difference, and that Rocky Point appears to be an isolated phreatomagmatic eruptive center, Grays River Volcanic deposits associated with Rocky Point should be considered a separate relatively low TiO_2 and FeO subunit of Grays River Volcanics (or possibly a separate unit entirely), occurring only in the study area.

Grays River Volcaniclastic Depositional Environments and Paleogeographic Reconstruction

Eocene sedimentary rock units in the Longview-Kelso area of southwest Washington are the result of a complex interplay of extrabasinal micaceous, arkosic Cowlitz Formation deltaic/estuarine sediment derived from a Rocky Mountain source (e.g., the Idaho Batholith), and intrabasinal basalt flows and basaltic volcaniclastics derived from nearby Grays River volcaniclastic highlands. Most Coal Creek lithic arkoses have at least a minor component of Grays River basalt clasts, and most Grays River volcaniclastic units have a component of mica, quartz, and feldspar clasts (see petrography section). The position of the study area on the southeast flank of the gravity anomaly presumed to be the Grays River shield volcano (Figure 45) suggests that at the time of deposition of the Cowlitz Formation deltaic sediments, volcanic highlands would have dominated the area immediately to the west, with a smaller Rocky Point volcanic pile to the east (Figure 59). Dominant paleocurrent direction in Cowlitz Formation sigmoidal cross-beds in Coal Creek is toward the southwest. Allowing for some (up to 45 degrees) post-Eocene clockwise tectonic rotation of Cowlitz Formation strata, the ancestral Columbia River (source for Cowlitz sediment) was locally flowing from the north or northeast. This scenario is as expected given that the course of the ancestral Columbia River would have been deflected toward the south or southwest, due to the volcanic high (Figure 45).

In the study area, the main distributary channels and tidal channels would have been oriented south southwest-north northeast before tectonic rotation, with a Grays River high to the west. Delta front sands would have prograded toward the south and

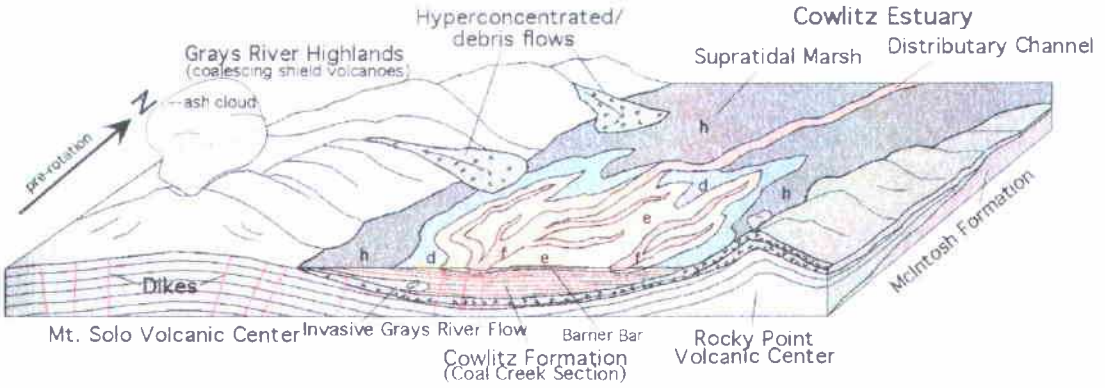

Barrier Bar
Tidal Channel Sandstone (Flaser-draped megaripples, lithofacies f)
Tidal Rythmites (Heterolithic Sandst. and mudst., lithofacies e)
Bay Mud (lithofacies d)
Supratidal Marsh (Coal & carbonaceous shale w/ interbedded tuffs, lithofacies h)
Cowlitz Formation undifferentiated
Grays River Volcaniclastic (Tgvs1, basalt conglom. & breccia)
Grays River Basalt Flows
McIntosh Formation (Shelfal siltstone/mudstone)
Grays River Dike

Figure 59: Paleogeographic reconstruction of Grays River Volcanics and Cowlitz Formation shoreface to supratidal facies associations. The Colwitz Formation section in Coal Creek is tide-dominated due to the confined geometry of the estuary between the Grays River highlands to the west, and thick Grays River flows and volcaniclastics to the east. Rocky Point is an isolated phreatomagmatic cinder cone.

southwest, in the direction of the Mist Gas Field. Surrounding the tidal channels (lithofacies f) were extensive tidal flats, an environment similar to modern Willapa Bay (Figure 20), depositing the mud flaser-draped cross-beds of lithofacies f, the tidal rhythmites of lithofacies e, and micaceous bay muds of lithofacies d. Toward the northeast and between distributary channels were extensive supratidal marshes producing the coals of the Coal Creek section (lithofacies h, Figures 20 and 59).

The basaltic fraction of Cowlitz micaceous arkoses deposited in the environments described above has two plausible origins. It could be the result of nearby Grays River volcanic detritus entering the Eocene Columbia River immediately upstream and adjacent to the delta via tributary streams, debris flows, or hyperconcentrated flows derived from the adjacent erupting volcanic highlands to the southwest (and possibly Rocky Point to the east). In addition, mixing of deltaic micaceous arkosic sediments and Grays River basaltic sediments could have resulted from strong tidal currents, storm wave surges, or (less common) tsunamis entering the delta or estuary, mixing micaceous arkose with offshore basaltic sands and gravels. Offshore volcanic highland sources for basaltic sediment have been verified in this study because of several small Grays River basalt tongues and storm wave-lag, recorded throughout the Coal Creek section, deposited shallow marine fossils and associated coarse-grained shallow marine basaltic sediment (Tgvs2) over arkosic tidal facies and delta front sands. Most basalt clasts mixed with Cowlitz micaceous arkoses are well-rounded grains of Grays River basalt lava fragments rather than scoriaceous clasts, suggesting some Grays River highland source upstream.

Periods of larger influxes of fresher basaltic sediment in the form of hyperconcentrated or debris flows into the area are apparent based on the thick, poorly-

sorted, matrix-supported basalt pebble, cobble, and boulder conglomerates and breccias of the Lower Grays River Volcaniclastic unit (Tgvs1). These debris flows, derived from the nearby volcanic highlands (Figure 59), would have catastrophically rushed downslope and into the ancestral Columbia River deltaic mouth, mixing with the river and estuarine water to become channelized hyperconcentrated flows, and enter the delta via distributary channels where mixing with extrabasinal micaceous arkosic sediment occurred. Hyperconcentrated flows in the study area are massive to thick-bedded and consist of subrounded to well-rounded basalt lava clasts with variable amounts of scoriaceous clasts, and contain a percentage of mica, quartz, and feldspar from a Cowlitz extrabasinal source. High energy debris flow deposits occur in the study area, consisting of much larger basalt boulders in a poorly-sorted matrix of coarse basalt sand and well-rounded to angular, pebble to cobble-size clasts (e.g., Site 123). These deposits represent catastrophic volcanic or tropical flood events, possibly from a local source such as the eruptive center of which Mt. Solo is a remnant.

These periods of heavy influx of Grays River volcaniclastic sands and gravels into the deltaic/estuarine environment via debris and hyperconcentrated flows occurred before the bulk of the Cowlitz Formation in the area had been deposited. The thick (up to 600 feet) Tgvs1 unit, where exposed, occurs stratigraphically beneath the Cowlitz Formation (Plate 1, cross sections A-A' and B-B'). These deposits are thickest along a northeast-southwest axis from the Columbia Heights/Rocky Point area toward Mt. Solo. The large paleo-channel cross section exposed in the Terra Firma Quarry on the south flank Mt. Solo containing clast-supported boulder conglomerate with several clasts over 1-meter in diameter (facies 1, Figure 48a), has a paleocurrent orientation directly out of or into the

cliff, toward the northeast or southwest. Mt. Solo appears to be an upfaulted remnant of a growing volcanic eruptive center based on the autoclastic breccia and associated basalt intrusions. The boulder conglomerate channel-fill shows that there was considerable topographic relief toward the west, in the direction of the gravity high. This could then have been the source of this thick Tgvs1 volcaniclastic deposit, flushed into the basin by a series of hyperconcentrated flows toward the northeast. Once deposited, this thick volcaniclastic pile would have effectively channelized the ancestral Columbia River into an incised valley between the volcaniclastic pile and Rocky Point, and the Grays River highlands to the west. Cross section A-A' shows this relationship, and explains why over 2000 feet of Cowlitz Formation was deposited in the Coal Creek area, but very little was deposited in the Columbia Heights area, or at least little remains after late Eocene uplift (folding and faulting) and erosion. The 35-meter thick volcaniclastic unit low in the Coal Creek Cowlitz Formation section at the base of unit B (Plate 2) likely represents the shallow marine equivalent of these catastrophic volcanic pulses.

The large (~20 meter diameter) block of micaceous, arkosic Cowlitz Formation caught up in a Grays River flow exposed in the Terra Firma Quarry (Figure 48b) is evidence of an invasive relationship between this flow and older Cowlitz Formation arkosic micaceous sandstones. From west to east on Mt. Solo, Grays River units range from lower invasive and subaerial flows, into an autoclastic upper flow breccia with lava dikes, which then grades into phreatomagmatic scoriaceous deposits, which further grade into hyperconcentrated flood deposits with a substantial component of Cowlitz arkose. All this evidence supports the model of a (possibly isolated) growing volcanic edifice,

with lava flows entering the sea, causing massive steam (phreatomagmatic) explosions and some flows invading the underlying sediment (Figure 59).

Predominantly scoriaceous, and in places red oxidized, volcaniclastics from Rocky Point indicate that this is an isolated phreatomagmatic to subaerial eruptive center (Rocky Point subunit). Furthermore, basaltic flows and hyaloclastites from this site are anomalously low in TiO_2 (refer to Figure 58), indicating a different magmatic source than the other Grays River units, or possibly mixing with magmas of a western Cascade source. Rocky Point was, thus, likely an isolated cinder cone erupting into the water saturated delta. All of this evidence combined allows for a plausible paleogeographic reconstruction (Figure 59). Grays River Volcanic highs or shield volcanoes exist to the north and west of the study area. Debris flows, and (more commonly) hyperconcentrated floods in this tropical Eocene setting would periodically rush downslope and into the deltaic incised estuarine depositional environment of the arkosic Cowlitz Formation. The distributary channels of the ancestral Columbia River mouth, and their associated estuarine tidal channels and tidal bars, would have been surrounded by tidal flats, and supratidal swamps landward. In such areas as Mt. Solo, the Terra Firma Quarry, and possibly the IS roadcut along Coal Creek Road, Grays River basalt flows invaded wet and unconsolidated Cowlitz sediments, and in the case of Mt. Solo, displaced and transported a house-size block of Cowlitz micaceous, arkosic sandstone. Mt. Solo, initially a center of phreatomagmatic activity, eventually built up to include subaerial flows, hyperconcentrated flows, and at least one large channel flowing down the side of the edifice toward the northeast. Erupting into this setting to the east was the Rocky

Point cinder cone, a phreatomagmatic eruptive center producing dominantly scoriaceous (red and black) cinders.

Western Cascade Basaltic Andesite

High hilly topography east of the Cowlitz River within the study area is due to the erosional resistance of a minimum of 600 feet (~180 meters) of western Cascade Basaltic Andesite (map unit Tba, Plate 1). This thick volcanic unit was assigned to the Goble Volcanics by Livingston in 1966, as part of a 1500-meter thick, westward-thinning wedge of late Eocene/early Oligocene lava overlain by younger Tertiary sedimentary rock in northwest Oregon, and overlying and possibly interfingering with the Eocene Cowlitz Formation in the Longview and Kelso area and northwest Oregon. However, a problem with assigning these flows to the Goble Volcanics on the southwest Washington side of the Columbia River has developed in recent years. According to Evarts and Swanson (1994) and Evarts (2002), the overlying Tertiary marine sedimentary formations (e.g., Keasey and Pittsburg Bluff Formations), which define the stratigraphic position of this volcanic unit in northwest Oregon, do not extend east of the Columbia River. Therefore, on the Washington side the top of this mafic volcanic unit is impossible to define, and instead becomes just the lower part of a thick pile of Tertiary, volcanic arc flows that underlie the majority of the western slope of the southwest Washington Cascade Range. Lacking the overlying marine sedimentary units, this unit is considered here to be the basal part of late Eocene-Oligocene, western Cascade arc derived basaltic andesite that is partly correlative to the Goble Volcanics of northwest Oregon (Evarts, 2002).

Geochemistry

Geochemistry samples were taken of this unit in the hills above Ostrander (Sites 17 and 76, just east of the Kelso quadrangle, Plate 1) and from a portion of a flow down-faulted into the long roadcut on Old Pacific Highway at the Carrolls interchange (CR-12, Site 9, Plate 1). The samples plot as basaltic andesite in Irvine and Barager's (1971) classification, chemically distinct from the Grays River Volcanics in containing a slightly higher percentage of SiO_2 (Figures 57 and 58). However, these flows fall within the broad Grays River field as defined by Phillips and others (1998). In Miyashiro's (1974) iron enrichment diagram these samples straddle the line between tholeiitic and calc-alkaline compositions (Figure 57b). Due to the chemical and lithologic differences between these flows and those of the Grays River Volcanics within the study area, particularly the low TiO_2 (1.2% to 1.5%) and FeO values (8.5% to 8.9%, Figure 58), they are treated here as separate units. These samples are geochemically (and petrologically) consistent with the lower SiO_2 samples of the basaltic andesite unit described by Evarts from the Deer Island, Oregon quadrangle (2002). FeO and TiO_2 percentages are consistent with those of Goble/Cole Mtn. basalts as described by Rarey (1986) in northwest Oregon. The possibility exists that these higher elevation flows east of the Cowlitz River are stratigraphically higher flows in a chemically differentiated Grays River sequence, but unlikely given the low TiO_2 values and other similarities with basaltic andesite/Goble/Cole Mtn. samples as described above.

Lithology and Petrography

Columnar-jointed basaltic andesite flows within the study area are typically spheroidally weathered and altered, but the three sample locations mentioned above

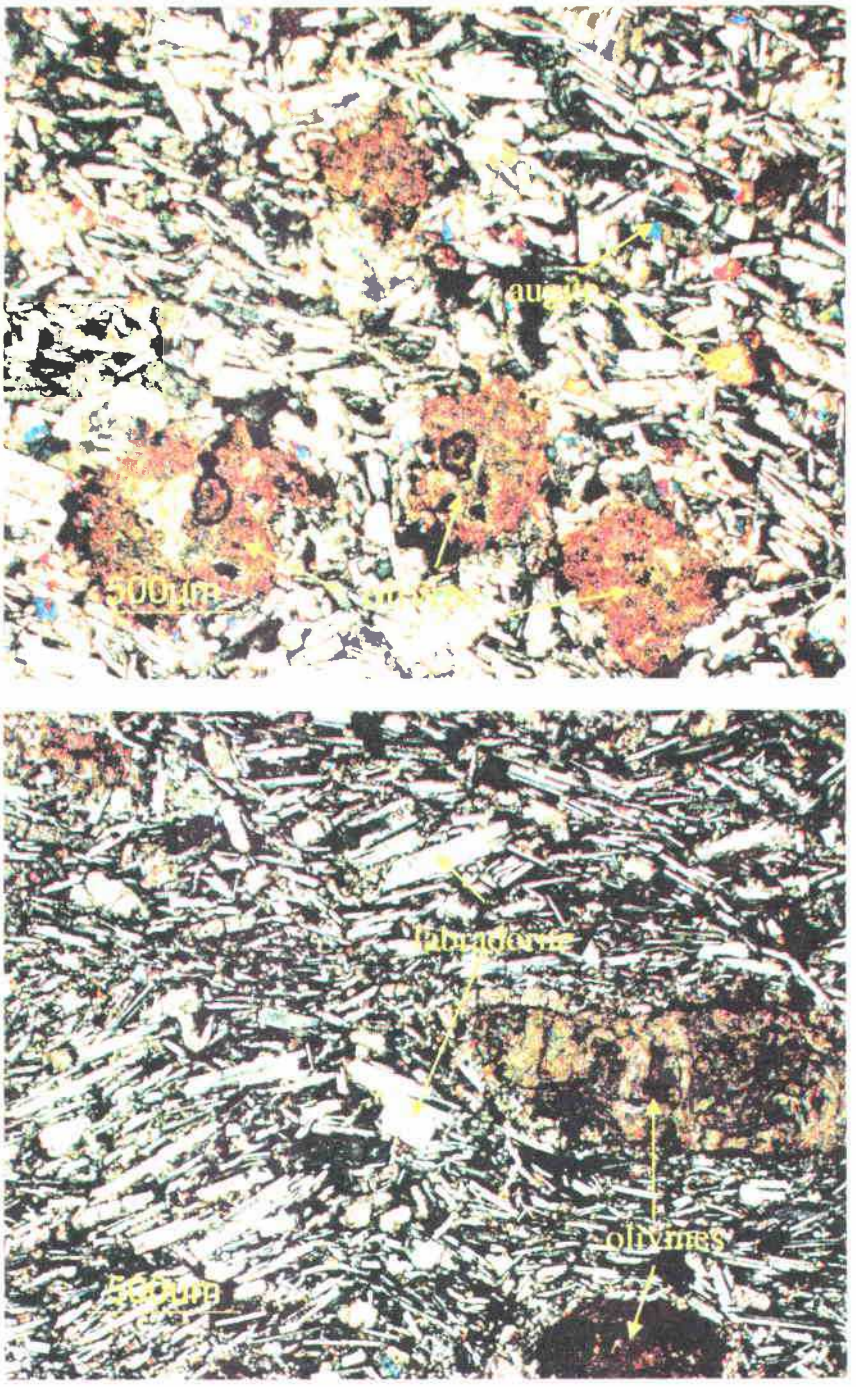

Figure 60: Photomicrographs of basaltic andesite flows (Tba, Plate 1).
A) Site 17, porphyritic with a high percentage of plagioclase microlites, and large iddingsite-altered olivine phenocrysts (crossed-nicols).
B) Site 9 (Sample CR-12), pilotaxitic flow texture around altered olivines (crossed-nicols).

produced useful fresh samples. Like the Grays River basalts, these basaltic andesite augite- and plagioclase-phyric flows are also olivine-phyric (similar to basaltic andesite flows described by Evarts, 2002), with some phenocrysts over 5 mm in length. In the weathered exterior of the basaltic andesite outcrops, the olivine crystals are weathered away. In thin section (Figure 60a) Site 17 is noticeably more porphyritic than Grays River basalt samples, with larger olivines, and consists of about 80% flow-aligned (pilotaxitic), albite-twinned plagioclase (labradorite). About 5% is untwinned feldspar, and 10% unaltered euhedral augite crystals, small relative to Grays River clinopyroxenes, and not glomeroporphyritic. Large (1-2mm) iddingsite-altered olivines constitute about 10% of the sample. This flow does not have true groundmass, but is instead almost entirely phyric. Site 76 shows virtually the same lithology, but olivines are slightly more altered, some almost entirely dissolved away. Plagioclase feldspars in Site 76 are not flow-aligned, and augites are larger and more abundant. Sample CR-12 from Site 9 is similar overall (Figure 60b) but has pilotaxitic texture, with flow-aligned plagioclase and altered olivines up to 3 mm long.

Western Cascade Andesite Dikes

Geochemistry and Field Characteristics

Two parallel dikes and an apparent small flow in Sec. 25, T 9 N, R 2 W (Sites 21 and 74, Plate 1) were chemically analyzed and plot as significantly more silicic (SiO_2 values range from 58.6% to 59%) and slightly more alkaline (i.e., higher total NaO + K2O values ranging from 5.2% to 5.8%) in the Irvine and Barager (1971) diagram, plotting as calc-alkaline andesites (Figure 57a). In the iron enrichment diagram of Miyashiro (1974), the dikes plot as higher in SiO_2 and away from both Grays River

Volcanics and basaltic andesite fields (Figure 57b). Total FeO and TiO_2 vs. SiO_2 plots (Figure 58) also show these samples to be lower in total FeO (~7.9%) than other volcanic units in the study area, and relatively low in TiO_2 (~1.7%). These dikes are over 10-meters wide (although actual width is not known due to incomplete exposure), lack columnar jointing, and are planar-sided and nearly vertical. They intruded Eocene Cowlitz Formation arkoses, and their high resistance to erosion has produced a west-northwest topographic ridge parallel to the trend of the dikes (Plate 1). This intrusive unit is noticeably more silicic (vitreous) and lighter gray in fresh sample than the other volcanic units, and breaks with a weak conchoidal fracture. In hand sample the dikes are sparsely feldspar porphyritic.

Petrography

The two geochemical samples described above were also thin-sectioned for the purpose of determining if the intrusion exposed along Interstate-5 (Site 21) is the same unit as the dikes themselves (Site 74). The thin section from Site 21 (Figure 61a) is pilotaxitic, with microlites of albite twinned plagioclase feldspar flowing around larger plagioclase and augite phenocrysts, creating a unique "swirly" effect. This sample is ~85% albite twinned plagioclase microlites and larger labradorite laths, 1-2% untwinned feldspar, 3-4% very small augites, and 1% cubic opaques (magnetite). About 10% of the sample is glassy groundmass, transparent in normal light, but nearly opaque in crossed nicols. The pilotaxitic flow texture of this sample suggests that this sample from along the interstate is a minor flow rather than an intrusion.

The thin section from Site 74 (Figure 61b) is similar to Site 21, but with opaque greenish brown clay as the groundmass, constituting about 20% of the sample. Also,

A.

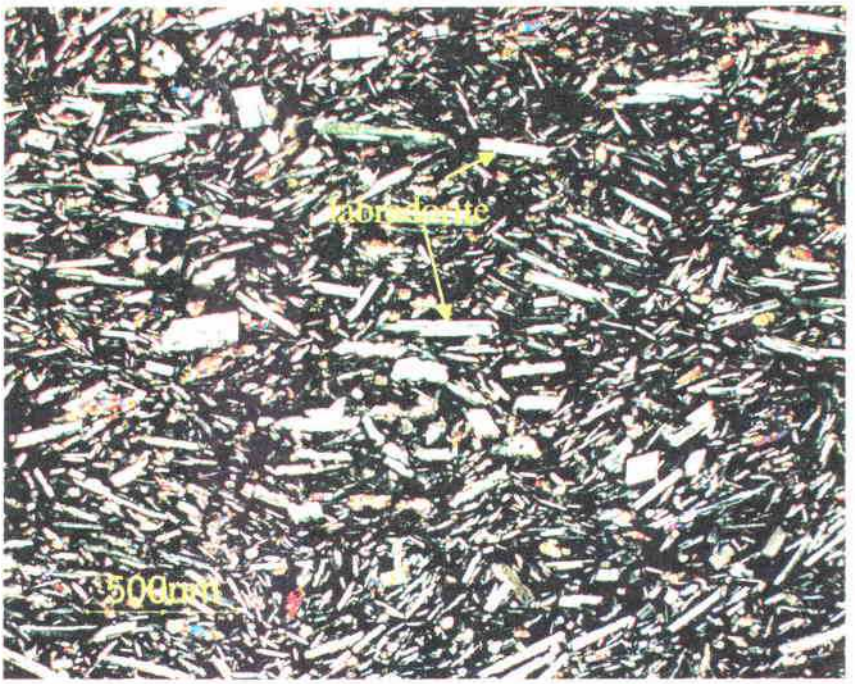

B.

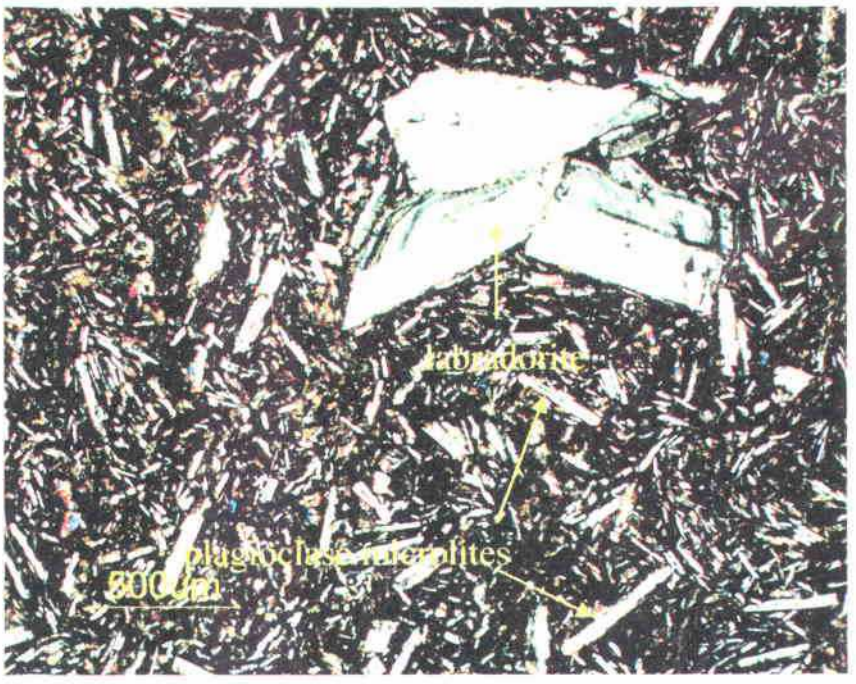

Figure 61: Photomicrographs of andesite unit (Tai) from east of the Cowlitz River.
A) Site 21 along Interstate-5. Pilotaxitic texture suggests this may be a small andesite flow (crossed-nicols).
B) Site 74 andesite dike. Note randomly oriented plagioclase microlites and large labradorite glomerophenocryst (crossed-nicols).

about 75% of the sample is randomly oriented plagioclase microlites and larger labradorite phenocrysts. One to four percent of the sample consists of small augites randomly scattered throughout the groundmass. One 3-mm diameter augite and labradorite glomerocryst occurs in this thin section. About 1% consists of cubic or globular opaque magnetite.

Columbia River Basalt Group

Introduction

The Columbia River Basalt Group (CRB) is a thick sequence of tholeiitic flood-basalts that erupted from fissures on the Columbia Plateau in parts of northeast Oregon, southeast Washington, and western Idaho in the early to late Miocene (Taubeneck, 1970). These eruptions produced approximately 200,000 km^3 of basalt (Swanson and Wright, 1978), covering an area of about 163,700 km^2 (Tolan et al., 1989). Due to the large volume of these flood basalts, some were able to flow out of the Columbia Plateau, and down the drainage of the ancestral Columbia River, a path not substantially different from the present Columbia River Gorge, and into western Oregon (as far south as Salem) and southwest Washington. Most Columbia River Basalt units were confined to the Columbia Plateau (Beeson and Moran, 1979), but some flows (initially erupted hundreds of miles to the east) reached the Miocene coastline. Here, the lavas formed submarine basalt piles, and invaded the Tertiary coastal sediment, forming invasive dikes and sills, and in places emerged again at the surface in localized marine eruptive centers (Beeson et al., 1979; Rarey, 1986; Reidel and others, 1989). Three Columbia River Basalt units reached as far west as southwest Washington and northwest Oregon; the Grande Ronde Basalt, the Frenchman Springs Member of the Wanapum Basalt, and the Pomona Member of the Saddle Mountain Basalt.

The early to middle Miocene Grande Ronde Basalt Formation (~15.6-16.5 Ma) is typically aphanitic, and was erupted during two normal and two reversed polarity intervals, which from oldest to youngest are R_1, N_1, R_2, and N_2. According to Reidel et al. (1989), these basalts have a narrow compositional range, with 52-57 normalized

weight percentage of SiO_2, and MgO ranging from 3-6 normalized weight percent. They are also enriched in FeO and incompatible elements relative to mid-ocean ridge basalts (MORB). Six units of Grande Ronde Basalt reached west of the Cascades (Reidel and others, 1989). From oldest to youngest these units are: the Wapshilla Ridge unit (R_2), Grouse Creek unit (R_2), Ortley unit (N_2), Umtanum unit (N_2), Winter Water unit (N_2), and the Sentinel Bluffs unit (N_2). The middle Miocene Frenchman Springs Member of the Wanapum Basalt Formation (15.3 Ma) is divided into six major units which include at least 21 different flows (Beeson and Tolan, 1985), of which only 11 separate flows of the Ginkgo and Sand Hollow units reached the Pacific Coast (Beeson and others, 1989; Reidel and others, 1989). These flows are usually sparsely plagioclase-phyric. The late Miocene Pomona member of the Saddle Mountains Basalt Formation (~12 Ma) is typically glomeroporphyritic and only one flow (confined to the Columbia River paleo-channel) reached southwest Washington. All of these Columbia River Basalt units can be differentiated by varying abundance of major elements, particularly MgO, TiO_2, and P_2O_5 (Reidel and others, 1989).

Local Distribution

Within the study area, Columbia River Basalt outcrops and deeply weathered red soils occur at several locations, including elevations above 300 feet on Mt. Solo, where flows occur above the Toutle (?) Formation. Here, a basalt flow is well exposed with a pillow base in a quarry (Site 51, E ½ of Sec 25, T 8 N, R 3 W), and overlying flows occur as reddish soils and as slide blocks. Above 600 feet, Grande Ronde basalt flows underlie the high elevation part of Columbia Heights area, and their resistance to erosion is largely responsible for the high topography. In one large quarry (Site 54, the West

Side Quarry near the center of Sec. 4, T 8 N, R 2 W), red oxidized soil horizons, and basalt slide blocks allowed for mapping and study of the flow distribution in that area. Erosional remnants of weathered Columbia River Basalt flows (reddish soils) cap the hills 2 to 5 km west and northwest of the Columbia Heights area above 600 feet. Resistance to erosion of these basalt flows is again largely responsible for the high topography of these isolated hills (Plate 1).

Excellent, fresh exposures of the four lowest flows in the study area, and interbeds between them, are found in both the north and south walls of the Storedahl and Sons Quarry (NW ¼ of the NE ¼ of Sec. 15, T 8 N, R 3 W) near Eufaula, where stratigraphy and approximate thickness of the Grande Ronde Basalt flows was determined (Figures 62 and 63). Other good exposures of the Grande Ronde Basalts in the general area west of Coal Creek can be found along Highway 4 in the N ½ of Sec. 15, T 8 N, R 3 W, in and around the small community of Eufaula (Sec 10, R 8 N, T 3 W), and in the steep cliffs immediately west of Coal Creek. Other Grande Ronde exposures occur in road cuts and in a small quarry (Site 104, E ½ of Sec. 28, T 9 N, R 3 W) along the northernmost part of Coal Creek Road within the study area. No exposures were found in the northeast portion of the study area, or anywhere east of the Cowlitz River.

Frenchman Springs and Pomona basalt flows are not well exposed in the study area west of Coal Creek due to extensive deep weathering to red soils. One Frenchman Springs outcrop just west of the study area consists of large uniform colonnade with sparse labradorite laths approximately 1 cm long. They are mapped (Plate 1) based on better exposures to the west of the study area and reddish soils within the study area, and were mapped into the study area by Wells (1981).

Grande Ronde Stratigraphy

For this study, Grande Ronde Basalt flow units were identified and distinguished by geochemistry, petrography and field characteristics, and magnetic polarity. Once these distinctions were made, areas where outcrops were poor or lacking were extrapolated from known outcrops, and mapped based on soil color, elevation, and unit thickness. Characteristics of sedimentary interbeds (e.g., cobble conglomerate or tuffaceous siltstone) were also useful tools in flow identification and correlation. Over 30 hand samples were collected for lithologic and geochemical study in the laboratory; many were oriented in the field for determination of normal or reverse polarity using the portable fluxgate magnetometer. Six samples from the Grande Ronde stratigraphic section in the Storedahl and Sons Quarry were chosen for petrographic analysis, and sent to San Diego Petrographics for thin sectioning, for the purpose of describing the local Grande Ronde stratigraphy. From oldest to youngest these are BC-1, BC-4, BC-5, BC-8, BC-10, and BC-13 (Figures 62 and 63). Six samples from these same Grande Ronde flow units in the quarry (as well as 7 other samples from the study area, for a total of 13) were chosen for major oxide and trace element geochemistry (Appendix III).

The geochemical and fluxgate polarity analysis of a sample from the only really good exposure in the Columbia Heights area (Site 54, the West Side Quarry) was important in that identification of the stratigraphically lowest unit in this area would allow mapping of that area once the Grande Ronde stratigraphy was established. Similarly Site 51, the lowest flow on Mt. Solo (also the only good outcrop in that area), was chemically analyzed and its magnetic polarity was determined for correlation to the known stratigraphic section in the Storedahl and Sons Quarry. In the Columbia River

Figure 62: Two views of the Storedahl Quarry where recent excavation has exposed four Grande Ronde Basalt flows and their sedimentary interbeds. The lower 3 flows are of the Ortley unit, flow #4 is a high MgO Sentinel Bluffs unit. Stratigraphic location of samples (BC) from this exposure are shown.

Basalt-dominated area west of Coal Creek, four other samples were prepared for chemical analysis, three near Eufaula (Sites, 102a, 102b, and 103), and one from the small quarry at Site 104 (Plate 1). Sites 63 and 101 were chemically analyzed to determine if this unit was Columbia River Basalt, as it appeared in hand sample, or Grays River Basalt as mapped by Wells (1981). High titanium and other characteristics (e.g., augite and plagioclase phenocrysts) suggest that it is a Grays River flow or sill (Plate 1, Figures 58 and 64).

Flow Units Correlation and Geochemistry

Using all available data (geochemistry, field characteristics, and magnetic polarity) 6 individual Columbia River Basalt flow types have been identified and mapped within the study area (Plate 1). They are 3 N_2 low MgO Ortley flows, overlain by one N_2 high MgO Sentinel Bluffs flow, and possibly Frenchman Springs and Pomona flow units. Figure 63 is a composite section of the six flow units, and the flow unit to which each rock sample number is assigned. Using stratigraphic position, normal magnetic polarity, and geochemical similarity, the lowest Ortley flow in the Storedahl and Sons Quarry, the lowest Ortley aphyric flow on Mt. Solo, and the Ortley flow beneath the thin interbed in the small quarry near the town of Eufaula are correlative (Sample BC-1, Site 51, and Site102a respectively, Plate 1), and the lowest flow in the area (Flow #1). The next Ortley flow #2 (the thickest one in the Storedahl and Sons Quarry), is represented by BC-4 (at the bottom of the flow), BC-5 (at the top of the flow), the lower flow in the West Side Quarry (Site 54), and the thick Ortley flow above the interbed at Site 102(b) near Eufaula. Aphyric N_2 Ortley Flow #3 chemical samples BC-8 and BC-10, near the top of the cliffs in the Storedahl and Sons Quarry correlate to Site 104 in the northwest corner of

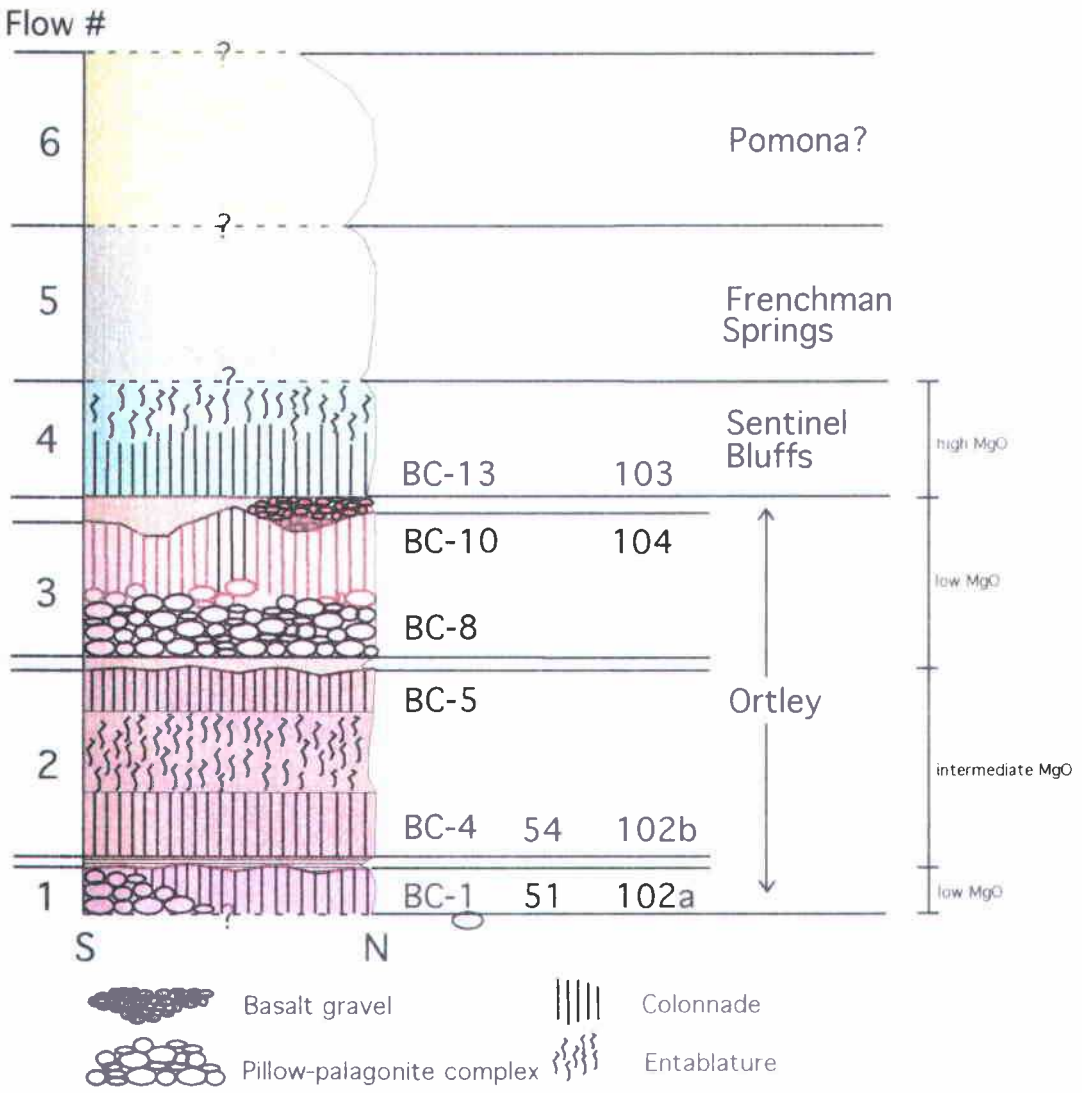

Figure 63: Composite section of Columbia River Basalts and interbeds in the map area.

the study area. A high MgO N_2 Sentinel Bluffs flow (#4) in the Storedahl and sons Quarry (sample BC-13) occurs stratigraphically above a thick basalt conglomerate/tuffaceous siltstone interbed and correlates to sample Site 103, a similar medium-crystalline basalt with well developed colonnade that overlies a similar, thick basalt conglomerate interbed across Harmony Drive from the (former) Eufaula Store (SW ¼ of the NW ¼ of Sec. 10, T 8 N, R 3 W). Outcrops of N_2 Frenchman Springs and Pomona units above these four Grande Ronde flows consist of deeply weathered basalt and thick red soil. A combination of soil color, topography, stratigraphic position, and the previous regional map by Wells (1981) was used to re-map these units (Plate 1).

Basalt samples of Ortley flow #1 have normal magnetic polarity, and plot very near each other on TiO_2 vs. MgO and P_2O_5 vs. MgO diagrams (Figure 64). They fall within or close to the rectangular boundaries of the Ortley flows established on the Columbia Plateau by Reidel and others (1989)(R), and for western Oregon by Beeson and others (1989)(B). These are low titanium and low MgO Grande Ronde flows, with MgO values that range from 3.5 to 3.7 weight percent, P_2O_5 values range from 0.30 to 0.34 weight percent, and TiO_2 values range from 1.93 to 2.14 weight percent. Other major oxides and trace elements in Ortley flow #1 samples are similar in abundance. Geochemical samples BC-1 and Site 51 are especially chemically similar. Basalt sample 102a was taken from the vesicular and slightly weathered uppermost meter of the flow, likely accounting for the relative decrease in soluble MgO and P_2O_5, and the relative increased concentration of less mobile TiO_2. On the corrected binary chemical plot diagram of TiO_2 vs. P_2O_5 (Figure 65), these flow #1 samples fall in or very near to the Ortley and Grouse Creek rectangular fields of Reidel and others (1989) on the Columbia

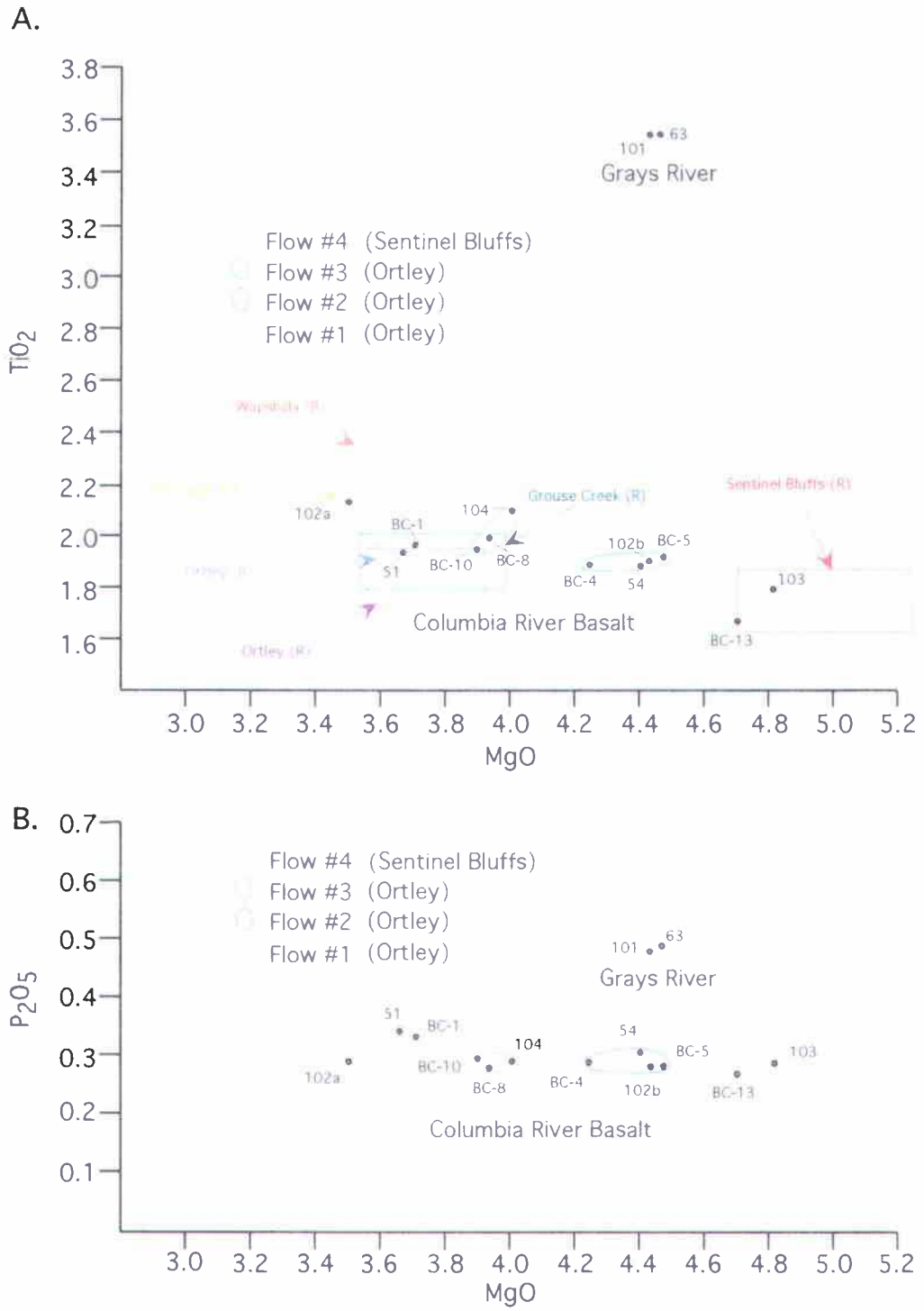

Figure 64: TiO_2 and P_2O_5 vs. MgO for Grande Ronde Basalt flow units1-4. Columbia River Basalt rectangular fields of Beeson and others (1989) and Reidel and others (1989). Chemistry for this study adjusted with MgO, TiO2, and P2O5 correction factors and rectangular fields provided by Russ Evarts (2003 written communication).

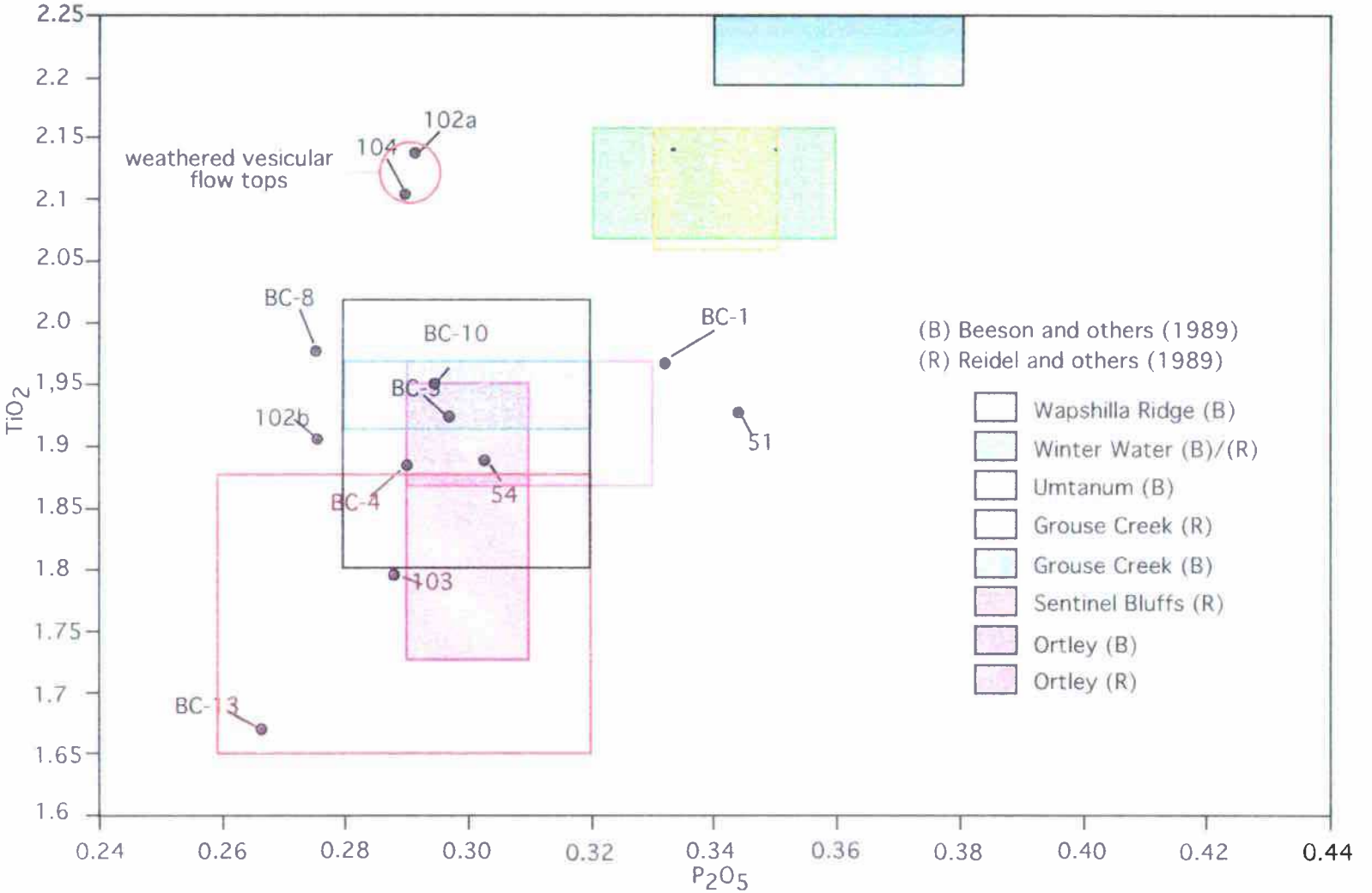

Figure 65: P_2O_5 vs. TiO_2 for Grande Ronde basalt samples (shifted)
(Rectangles show geochemical variations for CRB units in western Oregon (Beeson and others, 1989), and for the Oregon Columbia Plateau (Reidel and others, 1989).

Plateau and by Beeson and others (1989) for western Oregon. Since Grouse Creek is reversely polarized, and Ortley is normally polarized, it is concluded that this lower flow is an Ortley unit flow.

All basalt samples taken from Ortley flow #2 have normal magnetic polarity, and plot near each other on both TiO_2 vs. MgO and P_2O_5 vs. MgO diagrams (Figure 64). This flow is low TiO_2 but intermediate MgO, with values ranging from 4.2% to 4.5%. P_2O_5 values range from 0.28% to 0.30%, and TiO_2 values range from 1.89% to 1.92%. Other major oxides and trace elements in Ortley flow #2 are similar (Appendix III). It is interesting to note that on both of these binary chemical plots, there is far less chemical difference between Site 54b, Site 102b, and BC-5 (widely separated from each other), than there is between the bottom and top of the same flow (comparing BC-4 and BC-5). This may be due to chemical differentiation of the flow. On the TiO_2 vs. P_2O_5 diagram (Figure 65), these samples plot near the Ortley and Grouse Creek fields established by Beeson and others (1989), and Reidel and others (1989). On the MgO vs. TiO_2 diagram (Figure 64a) these samples plot in similar positions, but anomalously higher in MgO than either Ortley or Grouse Creek. Since the polarity is normal and the overlying flow (#3) also plots near the Ortley field, it seems likely that despite relative enrichment in MgO, this is an intermediate MgO Ortley unit flow.

All basalt samples collected from Ortley flow #3 have normal magnetic polarity, and have less variation in MgO than the other flows analyzed (Figure 64). They are also low MgO and low TiO_2. MgO ranges from 3.78% to 3.90%, P_2O_5 ranges from .322% to .340%, and TiO_2 ranges from 2.052% to 2.211%. Values for other major oxides and minor elements are similar, especially BC-8 and BC-10 since they represent the bottom

and top of the same flow in the Storedahl and Sons Quarry, respectively (Figures 62 and 63). However, BC-8 and BC-10 are greatly enriched in Ba (nearly 600 ppm) versus site 104 from the same flow (220 ppm). These three samples cluster together on TiO_2 vs. MgO and P_2O_5 vs. MgO diagrams, and in or very near the corrected Ortley and Grouse Creek fields on both TiO_2 vs. MgO and TiO_2 vs. P_2O_5 (Figures 64 and 65). This also appears to be an aphyric Ortley unit flow, because these samples have normal polarity, and not reversed, as the Grouse Creek flows are. These three N_2 Ortley flows are separated from the overlying high MgO Sentinel Bluffs flow by a 3- to 4-meter thick basalt conglomerate/tuffaceous siltstone interbed (described in the CRB interbeds section). Both samples from flow #4 have normal polarity and cluster together, and away from the other samples on the TiO_2 vs. MgO, P_2O_5 vs. MgO, and TiO_2 vs. P_2O_5 diagrams. High MgO values range from 4.31% to 4.58%, P_2O_5 ranges from .313% to .334%, and TiO_2 ranges from 1.773% to 1.898%. On all diagrams, this unit lies in or just below the high MgO field for Sentinel Bluffs.

Lithology and Petrography

Geochemistry and magnetic polarity were the main tools used to correlate and identify the Grande Ronde flows in the study area. Lithologic and textural characteristics of individual flows in outcrop and thin section helped in additional verification of flow identities. Some widely spaced flows with the same chemistry and polarity varied considerably in field characteristics. These differences are the result of vertical variation within a single flow (entablature top vs. colonnade bottom, vesicular vs. non-vesicular), whether the flow entered a body of water (e.g., pillow lava), and effect of paleotopography on flow thickness.

The upper four meters of flow #1 (low MgO, Ortley unit, sample BC-1) were exposed in the lowest portion of the Storedahl and Sons Quarry (Figure 62b) only during the summer of 1999, before it flooded, and was eventually filled in 2001. As a result, the total thickness of this unit is not known, but it overlies Cowlitz Formation arkosic sandstone and an invasive Grays River sill that are exposed along the access road to this quarry. Exposures of this lowermost flow in this quarry were in part massive, and in part poorly developed colonnade, dark gray, aphanitic, and moderately vesicular. The uppermost meter of this flow is also exposed at Site 102a, beneath a thin silty sedimentary interbed in an outcrop at the entrance to the quarry (unnamed) on Harmony Drive near Eufaula. Here, even the freshest samples are lighter in color (medium gray) than in the Storedahl and Sons Quarry due to minor weathering or alteration, and were of marginal usefulness for chemical analysis. At this location, the flow is also aphyric with sparse transparent plagioclase microlites about 0.25 mm long, and nearly 30% of the rock body consists of vesicles. On Mt. Solo, this basal N_2 Ortley flow and the overlying carbonaceous siltstone interbed are exposed in a 50-meter long Quarry (Site 51, Figure 66), where it forms a ~7-meter thick lava delta, consisting of basalt pillows in the lower half and poorly developed subaerial colonnade above. The flow is up to 30% vesicular, and aphyric to sparsely plagioclase-phyric, similar to exposures in the Storedahl and Sons Quarry and along Harmony Drive. In thin section (Figure 66b), this flow exhibits intersertal texture consisting of randomly oriented plagioclase microlites and augite in a black glassy groundmass. The sample is nearly 50% black opaque glassy groundmass (sideromelane), 40% calcic plagioclase (labradorite), ~8% small augite microlites, and

A.

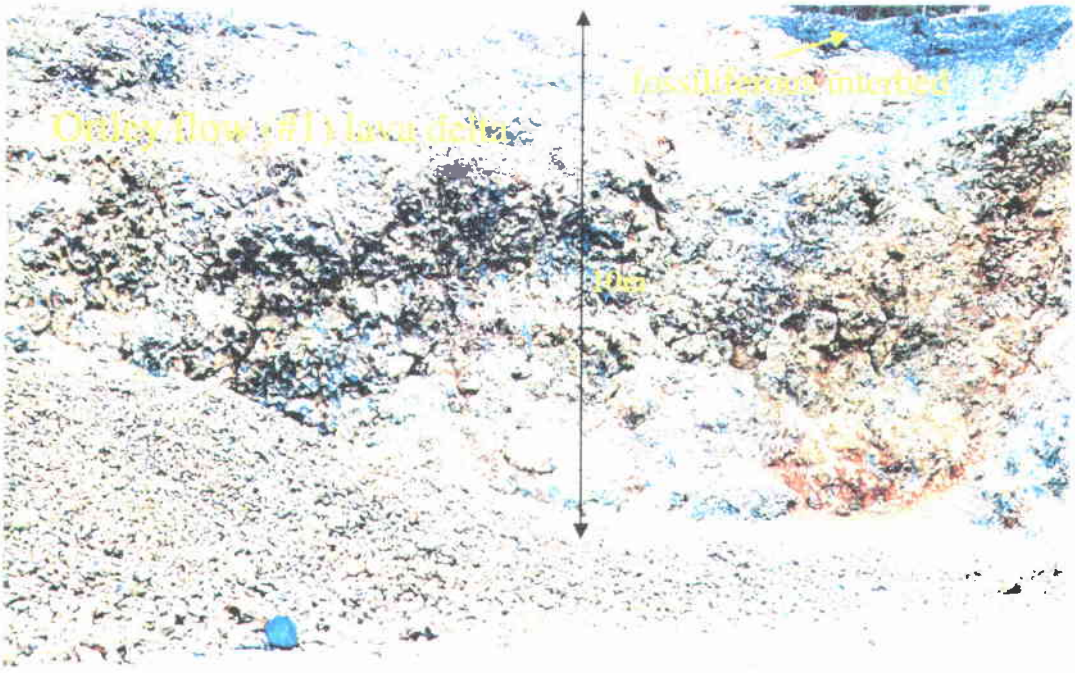

B.

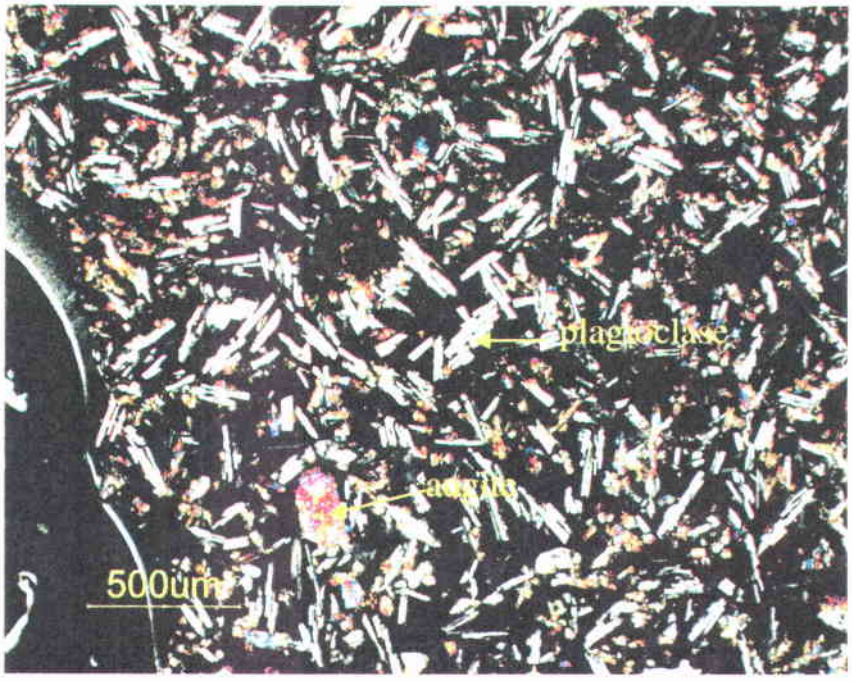

Figure 66: A) Ortley flow #1 lava delta in an unnamed quarry on Mt. Solo (Site 51). The interbed exposed above is a fossil leaf- and wood-rich shale.
B) Photomicrograph of Grande Ronde Ortley flow #1 (Sample BC-3) from the Storedahl Quarry. This sample consists largely of randomly oriented plagioclase microlites in a glassy groundmass (crossed-nicols).

~2% opaque magnetite. This basal Ortley flow is absent from the Columbia Heights area (see geochemistry section).

Ortley flow #2 is exposed in its entirety in the south wall of the Storedahl and Sons Quarry (Figure 62). The lower ~8-9 meters consists of well-developed colonnade, the overlying ~10-11 meters is partly massive and partly entablature, and the uppermost ~8-9 meters consists of poorly-developed colonnade (Figures 62 and 63). This same jointing pattern and relative thickness of the three layers occurs in the West Side Quarry, where low MgO Ortley N_2 flow #1 is missing, and contact between intermediate MgO flow #2 and the underlying medium gray clayey siltstone is exposed in the wall at the northern end of the quarry (Figure 67a). At this location, the flow filled an incised channel, resulting in tilted colonnade. These lower colonnade and overlying entablature of similar thickness also form a quarry wall at Site 102b along Harmony Drive, above the frothy upper part of Ortley flow #1 at Site 102a on the road.

Flow #2 is uniform in hand sample lithology throughout the study area, and is vesicular or aphyric to microphyric depending on which horizon of the flow is sampled. Sample BC-5 from the upper part of the flow in the Storedahl and Sons Quarry (Figures 62 and 63) is ~15% vesicular, with a substantial amount of secondary brownish goethite filling the vesicles. All other exposures are mostly aphanitic to microphyric. All specimens appear "sparkly" in hand sample due to some larger lath-like plagioclase (labradorite) microlites. Thin section BC-4 from the lower colonnade (Figure 67b) consists of 60% randomly oriented plagioclase microlites with some larger labradorite micro phenocrysts. Augite crystals constitute roughly 10% of the sample, some as large as the labradorite microphenocrysts (1-1.5 mm). Thirty percent of the sample is basaltic

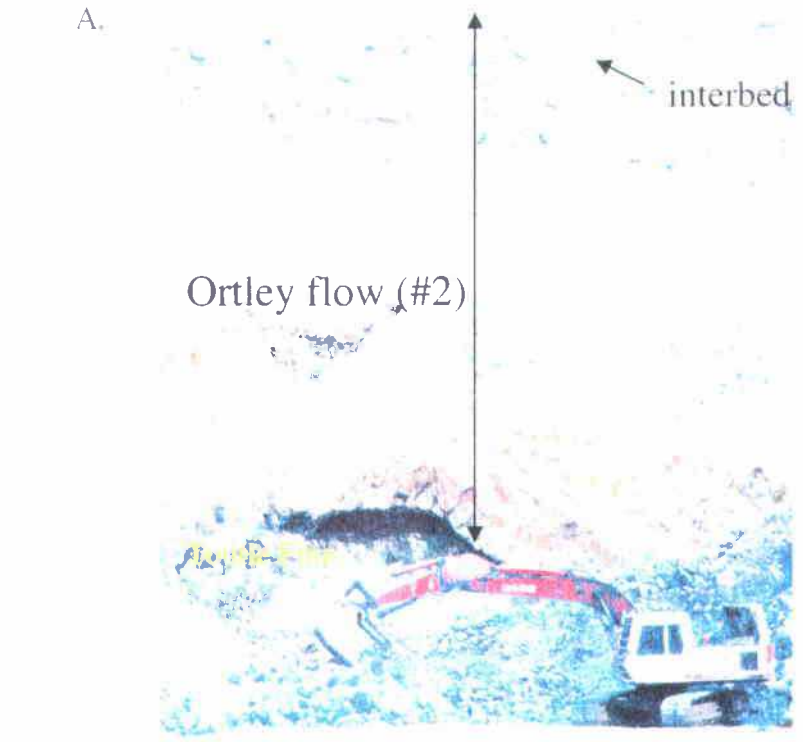

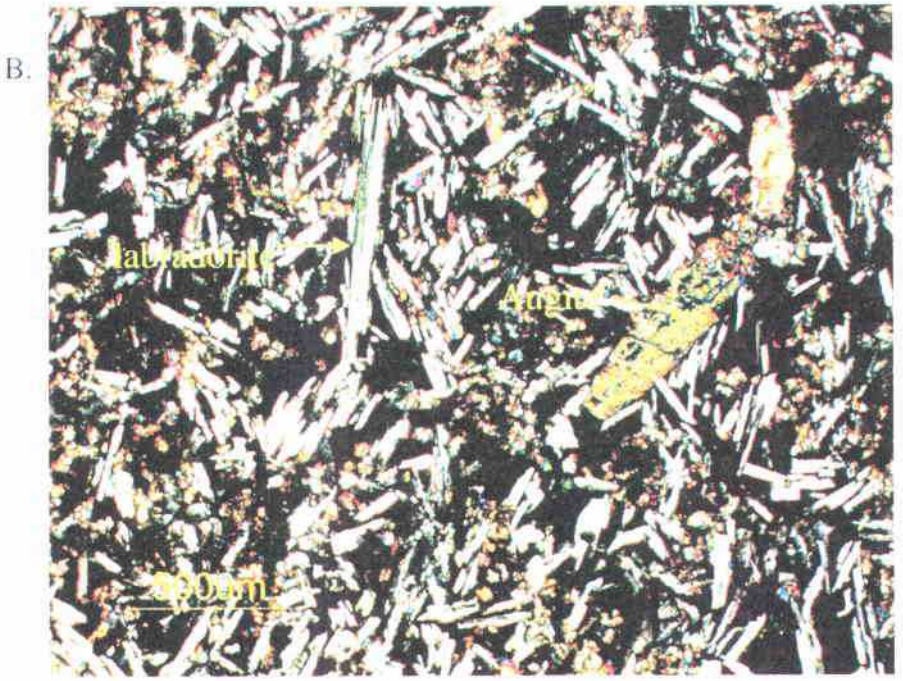

Figure 67: A) Contact of Ortley flow #2 and the underlying Toutle Fm. (Site 54).
B) Photomicrograph of Grande Ronde Ortley flow #2 (Sample BC-4) from the lower colonnade in the Storedahl Quarry (crossed-nicols).

glass groundmass (tachylite/sideromelane), and 1-2% is white sparry calcite filling the cracks. Thin section BC-5 from the upper colonnade contains few vesicles and has about 15% pore space. Approximately fifty-five percent consists of randomly oriented plagioclase microlites and microphenocrysts of labradorite, and 30% micro-glomerocrysts of augite, unusually uniform in size.

Flow #3 is a low MgO flow of N_2 Ortley composition (see geochemistry section). Exposures in both the north and south walls of the Storedahl and Sons Quarry show approximately 6-7 meters of elongate basalt pillows 1-3 meters long with radial jointing in a yellow palagonite clay matrix constituting a lava delta (BC-8, Figure 62). Gradationally overlying this is about 8 meters of variously poorly- or well-developed colonnade with vesicular upper portion (BC-10, Figure 62). Within this quarry wall, the pillow palagonite complex thins to the west and abruptly pinches out near the west wall, apparently representing the western extent of the 6-7 meter deep body of water (lake or river) in which the pillow basalts formed. Exposure in the north wall shows the opposite, the pillow structures pinch out abruptly to the east, putting further constraints on the paleogeography of this lake or river. This uppermost Ortley unit flow in the Storedahl and Sons Quarry has substantial paleotopography preserved on its upper surface (Figure 62). Since no soil or basalt gravel horizon is apparent, just horizontal tuffaceous laminated mudstone fill, this feature is more likely the wavy irregular upper surface of the flow (i.e., pressure ridges), rather than a product of subsequent erosion before deposition of the tuffaceous interbed. Site 104 in the northwest corner of the study area along Coal Creek Road exposes only about 5 meters of well-developed, uniform-sized basalt columns of Ortley flow #3.

Hand samples are dark gray and appear largely aphyric. Some larger (0.5 mm) plagioclase microphenocrysts are visible. BC-8 samples have a somewhat glassy luster, likely the product of rapid chilling in water, producing a tachylite glassy rind. Thin section BC-8 consists of ~80% dense, dark basaltic glass (tachylite or sideromelane, Figure 68a), and ~10% pore space (microvesicles). About 10% is randomly oriented plagioclase (labradorite), and 1% augite. Thin section BC-10 is largely the same, but contains 10-20% less basalt glass and larger augite crystals.

The uppermost flow exposed in the Storedahl and Sons Quarry (sample BC-13, Figures 62 and 63), and in the town of Eufaula (Site 103, Plate 1) geochemically plots in or close to the high MgO Sentinel Bluffs field (Figures 64 and 65), and consists of 1 to 5 meters of colonnade in its lower portion and up to 5 meters of entablature in its upper portion. Due to erosional upper contact with Troutdale gravels, the total thickness of this flow is not exposed in the study area, and is therefore not known. A maximum of 4 meters is exposed in the quarry, and 2 meters exposed at Site 103 in the town of Eufaula. In both locations, the lower colonnade is mostly spheroidally weathered and light gray, and fresh samples occur only within the remnant cores. Samples appear microphyric to medium-crystalline due to a high percentage of larger plagioclase microlites. A unique feature of this N_2 high MgO flow is the 0.5-1 mm micro-vesicles (diktytaxitic texture) that account for about 5% of the sample. In thin section, these vesicles are very nearly circular, and therefore, not likely a secondary weathering feature. Thin section BC-13 (Figure 68b) consists of about 70% randomly oriented, white, albite twinned plagioclase (labradorite) laths, 20% smaller augite (~50-100 micrometers), and the remainder consists of ~3% basaltic glass, magnetite, and some secondary white sparry calcite.

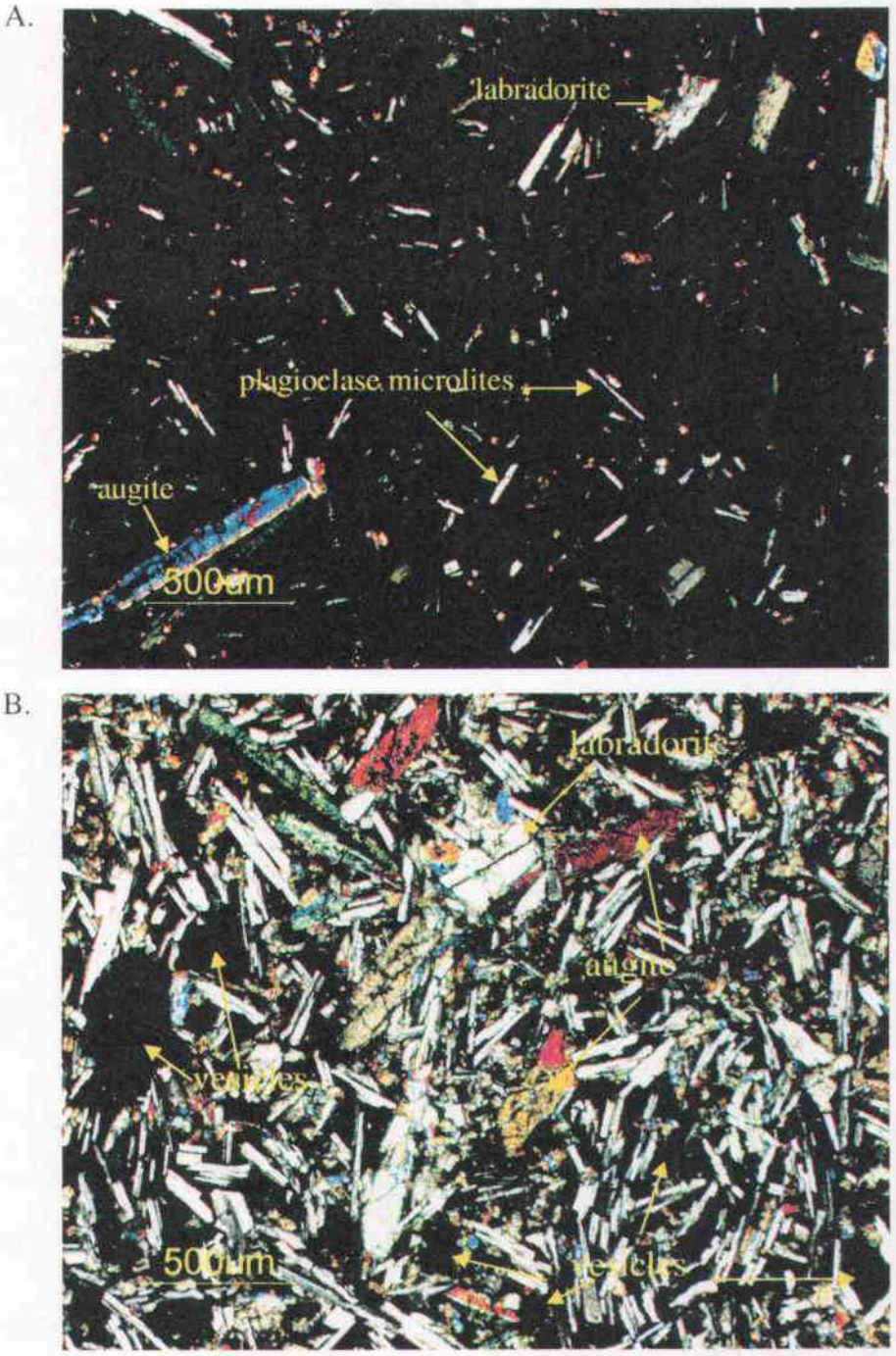

Figure 68: A) Photomicrograph of Ortley low MgO flow #3 (Sample BC-8) from the Storedahl Quarry. This sample from a basalt pillow is about 80% opaque basaltic glass (crossed-nicols).
B) Photomicrograph of high MgO Sentinel Bluffs flow #4 (Sample BC-13) from the Storedahl Quarry. Note relatively large feldspars and micro-vesicles (crossed-nicols).

Interbeds and Contact Relations

At least three interbeds occur within the study area between the four N_2 Grande Ronde Basalt flows that are locally traceable between outcrops (Plate 1). The interbed between Ortley unit flows #1 and #2 has a consistent lithology between widely scattered outcrops. In the Storedahl and Sons Quarry (Figure 62) this interbed consists of approximately 1.5 meters of dark gray to black, carbon rich, massive, hackly mudstone to silty mudstone. Bedding, when present, is indistinct. This mudstone is highly indurated and fracture ranges from hackly to nearly conchoidal. The interbed in the same stratigraphic position (above flow #1 and below flow #2) on Mt. Solo (Site 51, Figure 66a) is a well-stratified brown to medium gray shale or silty mudstone containing abundant carbonaceous debris in the form of carbonized twigs, roots, whole leaves, and flattened logs (apparently burned in one case). This interbed varies from two to three meters thick (although the entire thickness was not exposed) and is micro-cross laminated in places. At Site 102, this interbed separates the highly vesicular lower Ortley flow #1 (102a) and the lower colonnades of 102b, and is a carbonaceous siltstone with a baked and blackened upper surface. The plant species, sedimentary structures, and fine-grained nature of this unit suggest a low energy, lacustrine or swampy depositional environment.

The thicker interbed between Ortley flows #2 and #3 is exposed in the Storedahl and Sons Quarry and in the West Side Quarry in the Columbia Heights area (Site 54, Figure 67a). In the Storedahl and Sons Quarry (Figure 62), this interbed is well exposed immediately beneath the pillows of the lava delta of Ortley flow #3 (BC-8, Figure 69a). The bed thickness varies from 1 to 3 meters, and consists of distinct upper and lower lithologies. The lower ~1 meter ranges from gray tuffaceous silty clay to dark gray,

extremely carbon-rich, silty mudstone. This lower portion of the interbed contains abundant leaf and twig material, and some flattened branches and roots, possibly a paleosol. The upper 1-2 meters is a massive to micro-cross laminated, basaltic, tuffaceous, and carbonaceous siltstone, with a high percentage of clay. The uppermost 0.3 meter is a coarse basaltic breccia to palagonitized hyaloclastite, produced by steam explosion and basalt fragmentation along the advancing front of the basalt delta. In Figure 69b, glassy pillow rinds and yellow-brown hyaloclastite (fragmented basalt) between the pillows have been altered to yellow brown palagonite.

In the West Side Quarry (Site 54) this interbed between Ortley flows #2 and #3 shows a different contact relationship. Here, parallel beds within the sedimentary unit are contorted, and undulate to conform to the irregular upper top of the flow (Figure 70a). Another unique feature is that it is the lower (rather that the upper) 0.3 meter of the interbed that is dark gray or black. This relationship is similar to baked contacts described by Eriksson (2002) and Dr. Robert Bentley (emeritus professor at Central Washington University, personal communication, 2000), as first theorized by Beeson et al. (1979). It appears that in wet or marshy areas of Oregon and Washington during the middle Miocene, Columbia River Basalts invaded the relatively unconsolidated sediments to produce invasive intrusive bodies. In places along the Miocene coastline, the lava re-erupted at local volcanic centers along the coastline and shelf. Bentley (personal communication, 2000) has suggested the Columbia River Basalts invaded wet and semiconsolidated sediments, and carried the sediments along the top of the flow as a raft, baking the base and contorting the bedding. This theory explains this contact relationship in the West Side Quarry.

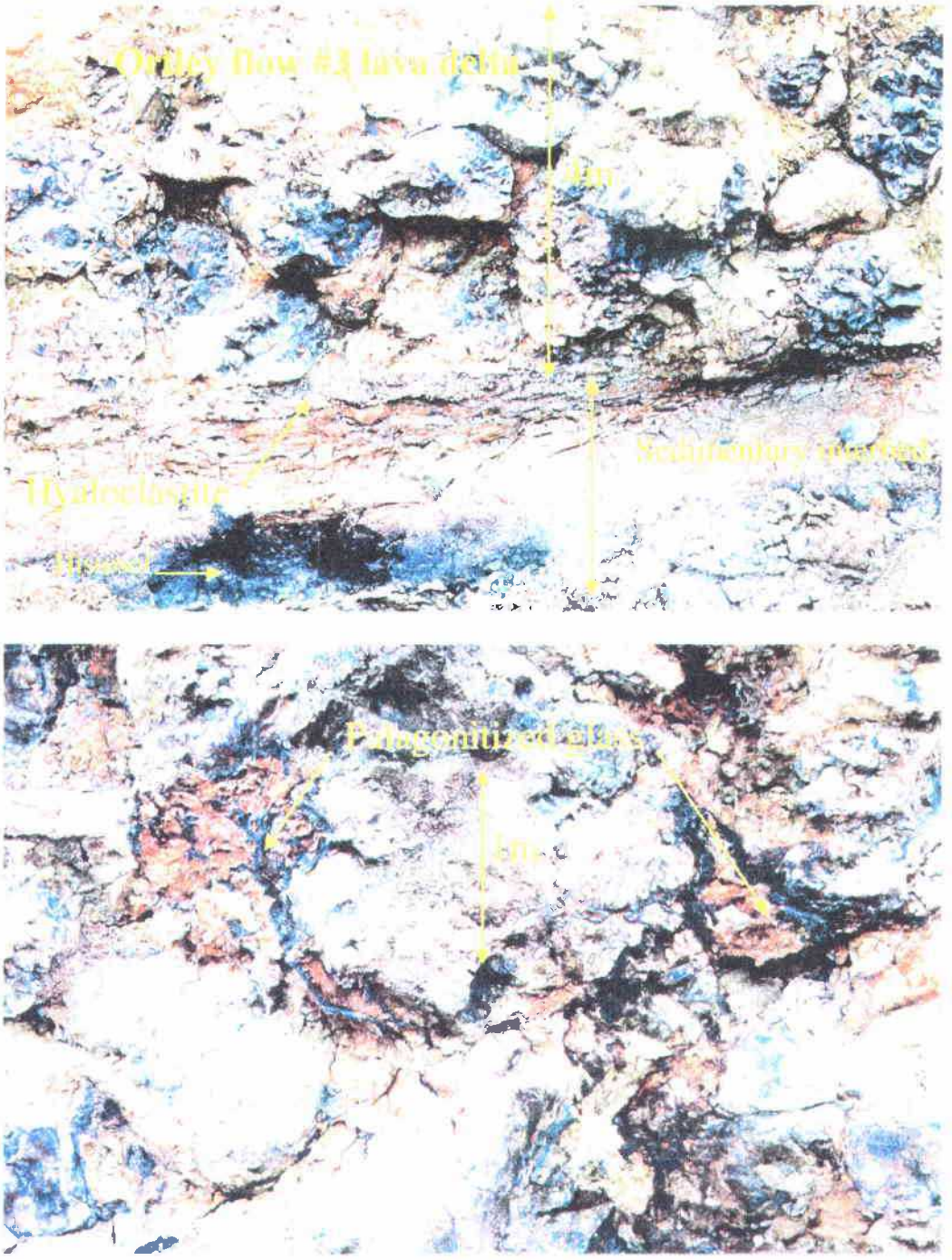

Figure 69: Closely packed pillows in Ortley flow #3 lava delta in the Storedahl Quarry.
A. Lower 4 meters of flow #3 and underlying sedimentary interbed. Note well-developed basalt pillow structures immediately overlying a 0.3 meter-thick basal hyaloclastite, and dark gray A-horizon histosol at base of interbed.
B. Close-up of the same horizon farther east in the quarry. Note the palagonitized basalt glass between pillows.

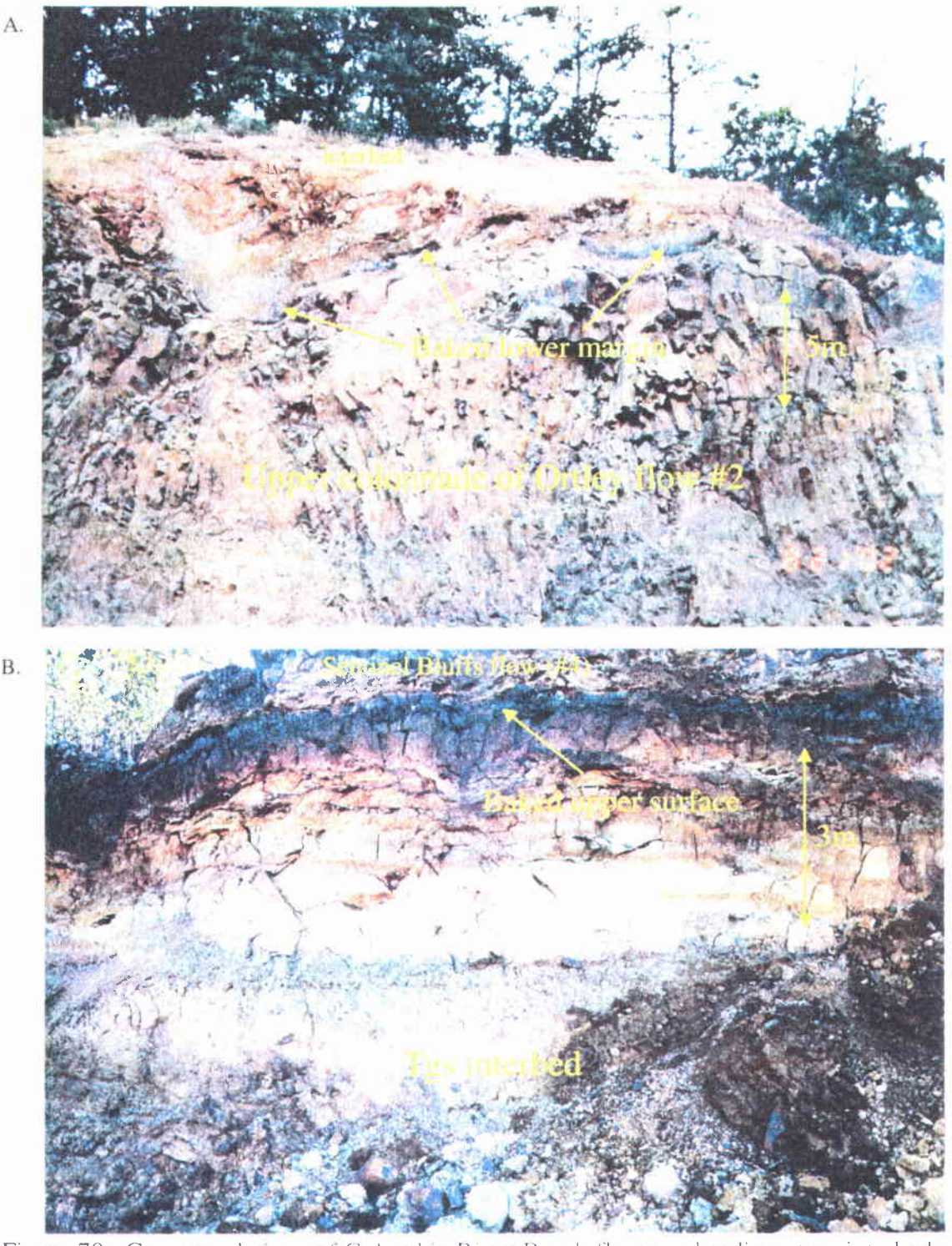

Figure 70: Contact relations of Columbia River Basalt flows and sedimentary interbeds.

A. Flow #2 and overlying interbed in the West Side Quarry (Site 54). Note baked lower surface and convolution of the beds to conform to the shape of the upper surface of the flow. These characteristics suggest an invasive contact.

B. Thick interbed between flows #3 and #4 in the Storedahl Quarry (Tgs) consisting of tuffaceous mudstones and siltstones with burrows. Note baked upper surface.

The uppermost interbed between low MgO Ortley flow #3 and high MgO Sentinel Bluffs (flow #4) is the thickest and most variable in the study area (map unit Tgs, Plate 1). In the south wall of the Storedahl and Sons Quarry (Figures 62 and 70b) this interbed varies in thickness from 0 to about 5 meters, and individual horizons can be traced throughout the quarry walls. The lower meter is a very light gray tuffaceous siltstone with abundant carbonaceous plant debris, especially root traces (a subaerial paleosol). The next 0.5 to 1 meter is a light to medium gray, basaltic, tuffaceous, silty to sandy mudstone with abundant sub-vertical burrows and carbonized root traces, in places comprising a high percentage of the exposure (Figure 71a). This bed acts as discontinuous underclay for a thin (~10 cm) black lignitic coal bed preserved in small paleo-depressions. The overlying gray floodplain mudstone is 1-2 meters thick, very light brown or gray, basaltic, tuffaceous, clayey mudstone/siltstone, again with abundant carbonized root traces. Ten to twenty cm thick bands of yellow orange iron oxide staining also characterize this interval. In most exposures in the quarry this tuffaceous bed is overlain by a 0.3 to 0.5-meter thick gray mudstone beneath a 0.5 to 1- meter thick tuffaceous, clayey siltstone with root traces. The uppermost 0.5 to 1 meter is a highly carbonaceous, tuffaceous A-horizon paleosol, baked by the overlying Sentinel Bluffs flow.

The majority of this interbed in the north wall of the Storedahl and Sons Quarry is similar to the south wall. However, this mudstone/paleosol interbed becomes a basalt conglomerate in the easternmost part of the wall and in exposures just to the north (Figure 71b), where it is a channelized pebble and cobble basaltic conglomerate with a maximum thickness of 5 meters. All clasts observed are Columbia River Basalt. This

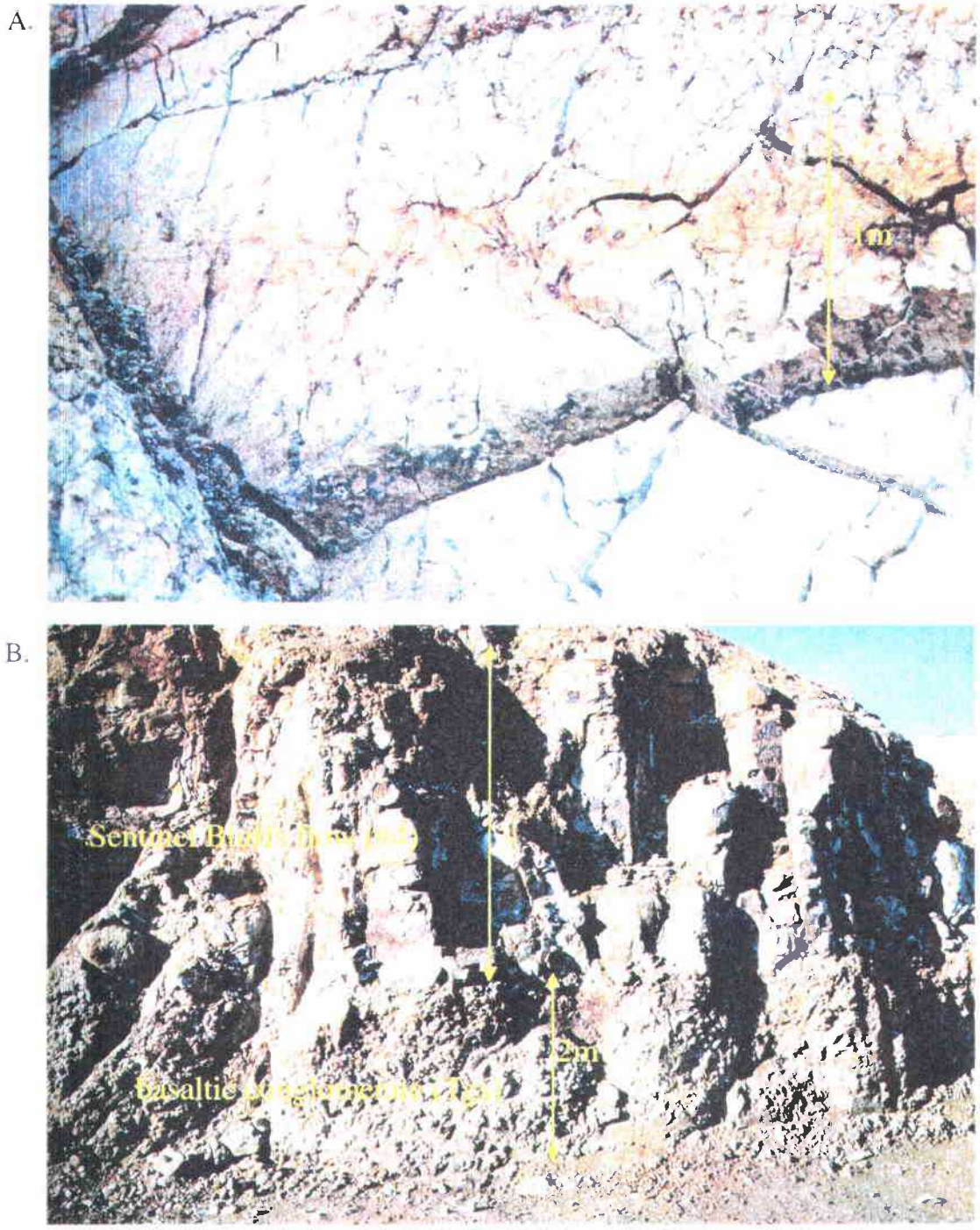

Figure 71: Two facies of the Columbia River Basalt interbed (Tgs) in the Storedahl Quarry.

A. Tuffaceous siltstone showing abundant vertical burrows. This is the dominant facies in the south wall of the quarry, and represents a shallow floodplain depositional environment. Carbonized leaves, twigs, and logs are also common in this facies.

B. Contact between the Sentinel Bluffs flow (#4) and underlying basalt conglomerate of map unit Tgs in the north wall of the quarry. This conglomerate likely represents a fluvial channel gravel, and can be correlated to Site 103 in the town of Eufaula.

fluvial channelized deposit is moderately well-sorted and rounded, clast supported, and relatively unconsolidated, with cobble clast size averaging about 4 cm. This channelized conglomeratic facies of this interbed is also present beneath the high MgO Sentinel Bluffs flow at Site 103 across Harmony Road from the Eufaula Store in the town of Eufaula. This interbed is consistently found beneath the Sentinel Bluffs flow and above the Ortley #3 flow, and is extrapolated to exist in some form throughout the study area, and is mapped as such (Plate 1). Lithofacies in this unit seem consistent with a depositional environment consisting of a substantial fluvial channel and adjacent floodplain with stagnant-water lakes or coaly marshes. The basalt clasts are too weathered for geochemical analysis, but are likely derived from the underlying Ortley #3 flow.

TROUTDALE FORMATION AND PLIOCENE ANDESITIC TERRACE GRAVELS

Introduction

The Portland Basin, which began to form in the middle Miocene and continued to subside into the Pliocene, filled with fluvial and lacustrine sediments transported westward through the Cascade calc-alkaline volcanic arc and into the forearc basin by the ancestral Columbia River (Beeson and others, 1989). This sediment mixed with lesser amounts of sediment derived from local tributaries draining surrounding volcanic highlands to produce the Troutdale Formation, as first described by Hodge (1938). This unit consists dominantly of well-rounded, light colored pebbles and cobbles of quartzite, granite, and schistose metamorphic rocks (derived from an extrabasinal source, most likely the Rocky Mountains of Montana and Idaho), but also contains some clasts of Columbia River Basalt, and more volcanic silicic material derived from the western Cascades.

In the type area for the Troutdale Formation, near Troutdale, Oregon (east of Portland) the unit consists of three sediment types: basalt clast conglomerate, arkosic sandstone, and vitric sandstone (Hodge, 1938). The vitric sandstone consists of poorly-sorted, coarse-grained, palagonitized hyaloclastic debris, similar in composition to Pliocene basaltic andesite flows in the Columbia River Gorge (Beeson and others, 1989). The lithic arkosic sandstone contains some Columbia River Basalt and western Cascade clasts, but is otherwise similar to the Cowlitz Formation in composition, with quartz, feldspar, mica, and metamorphic and granitic clasts of extrabasinal origin. Recent work by Howard (2002) and Evarts (2002), in mapping the Deer Island Quadrangle 20 miles southeast of the study area, shows that the Troutdale Formation consists of two

lithologically similar units that are separated by a slight angular unconformity. The older conglomerate tends to be exposed at higher elevations and the younger unit at lower elevations. Evarts (2002) has mapped the upper sheet-like upper conglomerate as an informal unnamed conglomerate in the Deer Island Quadrangle. Since the near-horizontal gravels in the study area rest unconformably on more steeply dipping Paleogene sedimentary and volcanic rocks, they are considered Troutdale gravels in this study.

Local Distribution and Lithology

Within the study area, Troutdale Formation river terrace gravels crop out at several locations near the Columbia River and lower Cowlitz River (Plate 1). Sand and gravel deposits up to 200 feet thick occur in the Columbia Heights suburb of Longview, on the southeastern portion of the Columbia Heights Anticline, overlying Grays River lava flows (Tgv1), Lower Grays River Volcaniclastics (Tgvs1), and to a lesser extent Cowlitz Formation micaceous arkoses (Tc). The hills north and east of Kelso contain Troutdale gravels and sandstone lenses up to 250 feet (~ 80 meters) thick (Plate 1). These semiconsolidated gravels are in places clast supported and quite coarse-grained with an average clast size of several centimeters (e.g., pebbles to boulders). In this area, gravels overlie Lower Grays River Volcaniclastic pebble and cobble conglomerates and breccias, Cowlitz Formation micaceous arkoses, and at higher elevations, overlie Toutle Formation clayey siltstones and sandstones. In the hills south of Kelso and east of I-5, in the Davis Terrace and Aldercrest neighborhoods, Troutdale Formation gravels up to 350 feet (~110 meters) thick constitute most of the volume of the hill. In this area, Troutdale gravels are overlain by at least 4 meters of coarse-grained, trough to sigmoidally cross-

bedded arkosic sand (Figure 72a), and overlie Cowlitz Formation arkosic, micaceous sandstone. Granitic and quartzite pebbles spilling into the Storedahl and Sons Quarry from the west side attest to at least a thin remnant river terrace deposit of Troutdale Formation above the quarry (not mapped).

Paleocurrent direction in the coarse-grained cross-bedded sand at the top of the headscarp produced by the Aldercrest-Banyon Landslide (Figure 72a) is dominantly toward the northwest. The poorly-sorted, well-rounded cobble to boulder gravel exposed in this cliff face (with the largest clast observed about 0.5 meter) indicates that this is the paleo-thalweg of the Columbia River during the Pliocene, running northwestward as it does at present for much of its length immediately south of the study area. Troutdale quartzite-bearing, pebble, cobble, and boulder gravel also were once well-exposed at Site 9 (the Carrolls I-5 exit), above the faulted Grays River volcaniclastics and Cowlitz Formation sedimentary rocks (Niem, personal communication 2003). Terrace gravels in the area near Kelso have a higher percentage (up to 50%) of porphyritic andesite clasts. This area near Kelso during the Pliocene was a point where Cascade-derived andesitic clasts from the Cowlitz River mixed with extrabasinal granitic and metamorphic clasts from the Columbia River, as they do today. Terraces of pebble and cobble conglomerate and sandstone lenses at higher elevations north of Rocky Point are dominantly to exclusively porphyritic andesite pebble to cobble gravels (Figure 72b), and have been mapped in this study as a separate unit, Pliocene Andesitic Gravel Terraces (Ttr, Plate 1). The change in clast lithology between these two units is gradational. Andesite gravel terraces occur at elevations from 200 to 400 feet, representing several periods of stability

A.

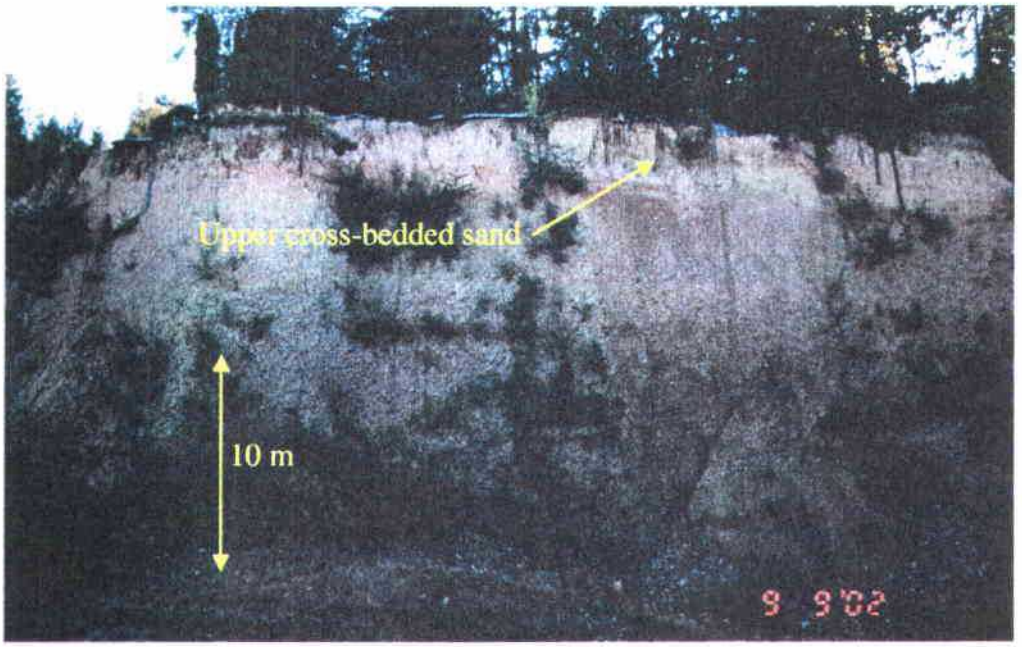

B.

Figure 72: A. Headscarp of the Aldercrest-Banyon Landslide. The lower ~20 meters consists of Troutdale cobble to small boulder gravel with mostly granitic and quartzite metamorphic clasts derived from the Rocky Mountains. The upper 4-5 meters consist of arkosic cross-bedded sand. This is the Pliocene thalweg of the ancestral Columbia River. B. Locally derived Pliocene gravel terrace deposit from east of the Cowlitz River (Ttr). Note that nearly all rounded pebble and cobble-sized clasts consist of well-rounded western Cascade andesite (usually porphyritic). These terraces are contemporaneous with Troutdale gravels but were produced by the ancestral Cowlitz River, with a western Cascade source for the sediment.

in the Cowlitz River valley between periods of uplift and downcutting over a prolonged period of time.

QUATERNARY UNITS

Quaternary units within the study area include Pleistocene through Holocene sand and gravel terraces at elevations of 50 to 150 feet along the Cowlitz and Coweeman Rivers, landslide deposits occurring within several Tertiary map units, alluvium along major rivers and streams, and Mt. St. Helens lahar deposits of May, 1980 along the Cowlitz River. Recent landslide mapping by Karl Wegmann of the Washington Department of Natural Resources in the Kelso and Rainier quadrangles was generously offered and used to assist in this study, and many (especially smaller) slides mapped in the study area particularly are a result of his work (Plate 1). In addition, the work of Roberts (1958) on the Pleistocene terraces in the area was relied upon heavily for this study.

Pleistocene-Holocene Terraces

Matrix supported cobble and pebble gravels produce terraces along most of the length of the Cowlitz and Coweeman Rivers in the study area (map unit Qtr, Plate 1). Particularly widespread deposits occur at housing developments in section 22, 23, and 27 of T 9 N, R 2 W and in the Pleasant Hill housing development area in section 2 of T 8 N, R 2 W and sections 26, 27, 35 and 36 of T 9 N, R 2 W. Much of Interstate 5 is also built on these flat, raised terraces (Plate 1). They are erosional remnants left as the Cowlitz River downcut due to broad regional uplift of the Coast Range. In the study area these deposits consist of thick-bedded, matrix to clast supported, pebble and boulder polymict gravels up to 150 feet thick, with coarse-grained sandstone matrix. Well-rounded pebble and cobble clasts, as well as coarse-grained sand clasts, consist of western Cascade porphyritic andesite and aphanitic Columbia River Basalt or western Cascade basaltic

andesite. A minor component consists of granitic and metamorphic (mostly quartzite) clasts.

A plausible explanation for this coarse-grained, matrix-supported unit that contains extrabasinal granitic and metamorphic clasts well up into the Cowlitz drainage is that these are deposits of the cataclysmic outburst floods of Lake Missoula (Roberts, 1958). The floods were produced by a series of failed ice dams (producing large lakes in Montana on the Missoula River behind them) during periods of glacial retreat, and flowed down the Columbia River drainage. Hydraulic constriction in the relatively narrow lower part of the Columbia River valley just south of the study area could have produced ponding of the floodwater in the Portland Basin (Evarts, 2002). In that area gravels were deposited as bedload, and fine-grained silts were deposited as slack-water suspension. In the study area, the coarse lithic sand and poorly-sorted, rounded gravel comprising the terraces are interpreted to be bedload deposited as these flood waters rushed up the Cowlitz River, as the Columbia River rounded the bend at Longview and Kelso (Waitt, 1994). Radiocarbon dating places most of these floods, possibly as many as 100, between 15.5 and 12.7 Ka. Boulders as large as 3 meters in diameter composed of extrabasinal rock types were rafted as ice-bound erratics into the Portland basin (Wilkinson and others, 1946).

Landslides

Landslides were recognized on aerial photographs and topographic maps by scarps and hummocky topography. Landslides occurring in several different Tertiary bedrock units and terrace deposits are common features throughout the study area (map unit Qls, Plate 1), and are particularly common in the unconsolidated to loosely

consolidated Troutdale Formation gravels (including the 1999 Aldercrest-Banyon Landslide, Figure 81). Landslides are also particularly common in the Toutle Formation, which being poorly consolidated and having a high percentage of clay matrix is particularly prone to slumping (Plate 1). A roadcut at Site 49 along Columbia Heights Road North in the Toutle Formation (NE ¼ of the NW ¼ of Sec. 5. T 8 N, R 2 W) began to slide along the dip slope almost immediately after being bulldozed (which removed support of the toe of the slide). Slides in both the Toutle Formation and the Cowlitz Formation commonly include pronounced headscarps where they have included the overlying Miocene Grande Ronde Basalts of the Columbia River Basalt Group. Much of the apparent tectonically produced fault structure throughout the study area may be the result of such large translational slides. The east-west trending faults at Site 49 display rotation of adjacent blocks relative to the fault plane, and faults within meters of each other have opposite senses of motion (some are reverse and some are normal). These features are commonly associated with landslides on the Oregon coast and elsewhere in the Pacific Northwest (Niem personal communication, 2003).

Particularly large-scale landslides occur in the Columbia Heights area, where the resistant, nearly horizontal Grande Ronde Basalt flows capping the hill have allowed oversteepening of the surrounding slopes. One large translational landslide in sections 9 and 16 of T 8 N, R 2 W trends southeastward and has produced a large bowl-shaped valley and prominent Grande Ronde head scarp. This slide has transported large semiconsolidated blocks of Toutle Formation, and likely some Cowlitz Formation arkosic sandstone blocks some distance. Another Columbia Heights slide trends northeastward in sections 32 and 33 of T 9 N, R 3 W and section 4 of T 8 N, R 3 W (Plate 1), and has

also produced a prominent Columbia River Basalt scarp, and a pronounced hummocky toe on which is built a trailer park community. The toe undoubtedly temporarily dammed Hazel Dell Creek immediately after the slide event. This landslide also has numerous ponds and closed contours just beneath the headscarp (and farther downslope) and a substantial slide block about 200 feet long of Grande Ronde Basalt at the N ½ of the NW ¼ of Sec. 4. Smaller slides occur around the periphery of the Grande Ronde erosional remnant that caps the Columbia Heights area, and it is likely that many of the Columbia River Basalt cliffs in the Columbia Heights area are landslide headscarps. J-shaped ("pistol butt") tilted tree bases, and soils with chaotic mixtures of red weathered Grande Ronde blocks and tan Toutle Formation blocks are common.

Another large translational landslide occurs between Clark Creek and the lower portion of Coal Creek. This slide occupies an area of about 3 km^2 and also includes prominent Columbia River Basalt scarps on the east side, as well an numerous ponds and closed contours of a hummocky topography. The IS roadcut along Coal Creek Road (Figure 77, Plate 1) may be part of this extensive slide and marks its northernmost boundary in the Coal Creek drainage. The segment of Coal Creek road at the slide has been rebuilt several times, and the toe in Coal Creek is loaded with basalt boulder riprap. The faults in this exposure are listric and have an unusual orientation (more north-trending) for faults in Coal Creek beds. They may be landslide slip planes. Large isolated Columbia River Basalt blocks occur on Niemi Road (NW ¼ of Sec. 14, T 8 N, R 3 W), and here deep soils are mottled red and tan from slide blocks of weathered CRB and Toutle Formation respectively. Roadcuts and natural exposures on the west side of Clark Creek are composed of clayey, fractured blocks of Toutle Formation where the toe

of the landslide has overridden Cowlitz Formation arkoses and basaltic siltstone and sandstone of the Upper Grays River Volcaniclastic unit (Tgvs2), interbedded within Cowlitz Formation micaceous arkoses.

Another substantial translational landslide occurs north of Raglund Road in Goose Hollow. Jumbled blocks of Toutle Formation sandy siltstones occur in the toe of this slide along Raglund Road (E ½ of Sec. 35, and W ½ of Sec. 36, T 9 N, R 3 W). A much smaller landslide occurs at the S ½ of Sec. 26, T 9 N, R 3 W where a new housing subdivision was built during the summer months of 1999 and 2000 in a bowl-shaped drainage slope uphill from Coal Creek Road. Multiple landslides occur in the Cowlitz Formation, Toutle Formation, and Troutdale Formation gravels and sandstones in the southeast part of the study area, east of Interstate 5 (Plate 1). In the Davis Terrace/Aldercrest area (more detailed description in the geologic hazards section), most Troutdale gravels have slumped to some degree, and reactivated slides occurring within previous Pleistocene landslides are also common. Bowl-shaped drainages occur throughout this area along I-5. No less than 35 slides occur in the hilly area north of Kelso, south of Ostrander, and east of Rocky Point (Plate 1). Most of these are small-scale surficial slope failures without well-defined headscarps or toes.

Mt. Helens lahar deposit, May 18th, 1980

Lahar or pyroclastic debris flow deposits from the May 18th, 1980 eruption of Mt. St. Helens (Qshu3) occur in scattered remnants along the Cowlitz River particularly on the inside of meanders. At least 15 separate deposits occur in the study area, and a large berm pile produced by dredging of the Cowlitz River near its confluence with the Columbia River occurs on the Cowlitz River's east bank just out of the map area. This

lahar entered the Cowlitz River drainage from the South Fork of the Toutle River ~20 km to the north of the study area. Drainage of the Cowlitz River was blocked at the town of Castle Rock where tremendous damage occurred as a result of the lahar. The lahar entered the Columbia River at the mouth of the Cowlitz River and produced a pyroclastic delta that blocked the shipping channel for weeks. Within the study area Mt. St. Helens deposits, most of which are less than a few meters thick, consist mostly of poorly-sorted, massive gray mixtures of andesitic to dacitic boulder and cobble gravel and pumice lapilli suspended in fine gray volcanic ash (glass shards and crystal matrix). A. Niem (OSU professor emeritus, personal communication, 2003) noted that the lahar had mixed with river water and had become hyperconcentrated slurries with 2 to 3 meter standing waves near the Carrolls I-5 exit south of Kelso on the Columbia River.

Holocene and Late Pleistocene Alluvium

Alluvium of Holocene and Pleistocene age (Qal) form thick flat lying unconsolidated deposits in local drainages within the study area including Coal Creek, Clark Creek, and Delameter Creek in the west half of the area, and in the east half of the area in tributaries of the Cowlitz River, including Hazel Dell, Ostrander, and Coweeman Creeks (Qal, Plate 1). Both the Cowlitz and Columbia Rivers have alluvium in the form of gravel, sand, silt, and wood, which according to local well logs range from 10 to 200 feet in thickness. Most of the vast, alluvium-filled valley around Mt. Solo is part of the historical flood plain and paleochannel of the Columbia River. Dams on the Columbia River today prevent major flooding of the lower Columbia River region. Local marshy and swampy areas are the sites of organic-rich mud and silt deposition today, including meandering streams that wind through much of Longview north and south of Mt. Solo.

Another swampy area is along the Cowlitz River east and south of the Pleasant Hill community built on late Pleistocene terraces. Lake Sacajawea (in the middle of downtown Longview, Plate 1) is a dredged oxbow lake nearly 2 miles long that likely was formerly a part of a meander of the Columbia or Cowlitz River. It was dredged in order to construct a protective levee that stretches along the length of Longview to protect against flooding.

STRUCTURAL GEOLOGY

Introduction

The Coast Range Province, in which the study area lies, began its complex structural history with the accretion of the oceanic Siletzia Terrane in the early-middle Eocene (Wells et al., 1984). This volcanic terrane, termed the Crescent Formation in Washington and the Siletz River Volcanics in Oregon, consists of tholeiitic to alkalic, subaqueous pillow lava and breccia to subaerial basalt flows, and may have originated as remnants of an oceanic seamount province. It could have alternatively been erupted nearly in place as a result of rifting due to oblique subduction of the Farallon Plate beneath the North American Plate along a leaky transform fault (Wells et al., 1984; Snavely, 1987; Ryu and Niem, 1992). After emplacement of this thick, buoyant volcanic pile in western Washington and Oregon, the early-middle Eocene subduction zone was clogged and forced to jump westward to near the edge of the Eocene continental margin. Because of the oblique subduction and northeast motion of the Farallon Plate relative to the North American Plate, a northeast-southwest transpressional and transtensional wrench tectonic stress regime with associated dextral shear was formed, controlling the dominant trend of regional faults, folds, and uplift in the Oregon and Washington Coast Range.

Oblique subduction has caused the Siletzia Terrane (the basement rocks of the region) to fracture into several discrete crustal blocks up to 30 km wide, bounded by northwest-trending dextral shear zones (Wells and Coe, 1985). This dextral shear of

basement blocks, and overlying sedimentary and volcanic units, has produced varying degrees of clockwise rotation of crustal blocks in the Cascadia volcanic arc of Washington and Oregon. According to Simpson and Cox (1977), paleomagnetic studies show that as much as 75 degrees of clockwise rotation has occurred is some middle Eocene blocks of the Oregon Coast Range. Wells and Coe (1985) demonstrated much less rotation (approximately 22 degrees) in the Washington Coast Range. Substantially higher rotation (~103 degrees) in the Cowlitz Formation has been suggested by Kleibacker (2001) and Prothero and others (2001) for the area immediately to the north of this study. Wells and Coe have also suggested that these clockwise rotations could be the result of shear coupling along transcurrent fault zones. Such shear is the result of partial coupling of the forearc (Coast Range) with the obliquely subducting Farallon Plate (Rarey, 1986), and the relative movement of adjacent blocks is accommodated by secondary conjugate shear sets (Riedel shear) which rotate in response to the external shear couplet (Wells and Coe, 1985). In parts of northwest Oregon, northwest-trending conjugate shears occur with oblique right-lateral shear (Olbinski, 1983; Peterson, 1984; Nelson, 1985; Rarey, 1985; Niem and others, 1992). Rarey (1986) suggested that this shear-coupling model can explain much of the present structure of the Oregon and Washington Coast Range. Northwest-trending right-lateral faults would be the dominant expression of simple dextral shear, and northeast-trending left-lateral faults result from Reidel shears that have accommodated the clockwise rotation.

Continuation of northeastward oblique subduction and simple dextral shear produced a dominant northeast-southwest tensional fault system along which the Eocene

Grays River Volcanics may have erupted, and also produced tension on the overlying Eocene sedimentary units. In the late-early Miocene, a compressional period of deformation began in the Coast Range producing a series of folds and reverse (transpressional) faults (Wells and Coe, 1985). Compression and oblique dextral shear along northwest-trending faults continued throughout the Miocene, uplifting and deforming the Columbia River Basalt Group in the Coast Range (Armentrout, 1987). Compressional uplift in the form of oblique slip wrench faulting and folding continues today (i.e., continued uplift of the Oregon Coast Range producing coastal terraces, and oblique slip reverse faulting such as the Corvallis Fault, and the Portland Hills Fault consisting of an anticline bordered by a reverse fault to the northeast) (Wong and others, 2001).

Local Structure

General

The structural geology of the study area, like all of southwest Washington, is complex, consisting of folds and faults with wide ranges in the extent of deformation, and produced by tensional and compressional forces acting in several directions, and at different periods of geologic time. Two features dominate the structure of the study area: 1) two parallel northwest-trending folds, the Columbia Heights Anticline and the Hazel Dell Syncline, likely resulting from the same compressional (or transpressional) event, and 2) a prominent northwest-trending system of faults (Plate 1). These features combined with the down-cutting of the Columbia and Cowlitz Rivers, have led to the exposure of older units (middle Eocene Grays River Volcanics, map units Tgv1 and

Tgvs1) in the core of the Columbia Heights Anticline. These stratigraphically lowest volcanic units are also exposed at the base of Mt. Solo, an isolated up-thrown fault block surrounded by Quaternary alluvium of the Columbia River (Plate 1). The Cowlitz River, Coal Creek, and Clark Creek have eroded down to expose the Eocene Cowlitz Formation (Tc) and the interbeddded younger Grays River volcaniclastics (Tgvs2). Younger units such as the Miocene Columbia River Basalt flows and the Troutdale gravels (deposits of the thalweg of the Pliocene Columbia River, map unit Ttr) are still largely horizontal, but have undergone considerable broad uplift, attesting to the ongoing tectonic activity of the area through the Neogene.

Eocene and Oligocene (?) Volcanic units east of the Cowlitz River (e.g., Grays River Volcanics and western Cascade basaltic andesite) generally dip from 5 to 35 degrees to the east or east-southeast, making the west-facing slopes of the hills anti-dip slopes (cross section A-A', Plate 1). Middle Eocene and Oligocene units in the hills containing the Columbia Heights Anticline generally dip away from the axis by 5 to 30 degrees, and toward the axis of the Hazel Dell Syncline by 5 to 15 degrees. It is important to note that Columbia River Basalts throughout the area are nearly flat-lying. Beds on Mt. Solo gently dip about 5 degrees to the northwest. Cowlitz Formation beds exposed in the southern third of Coal Creek dip relatively steeply (from 5 to 30 degrees) toward the southwest, gently toward the north in the middle third of the creek, and gently (0 to 15 degrees) southwest in the northern third (Plate 1). In several Coal Creek intervals, local dip increases steeply due to drag along faults. The northern-central part of the study area consists of beds of varying orientation, related to minor faults and folds.

Determination of faults and folds in this lushly vegetated area relied primarily on exposures of fault planes in creek beds, or in railroad or road cuts, but also on repetition of beds, field reconnaissance of lineations on aerial photographs, topographic maps, side-looking airborne radar (SLAR) images, and digital elevation model (DEM) images and grouping of consistent attitudes of beds into fault blocks. Some strike and dip data on bed orientations collected by Livingston in the mid-1960's were collected from exposures that are no longer accessible or no longer exist. Many of Livingston's bed attitudes have been incorporated into this study. Some of the apparent structure (e.g., fault trends) of the study area may be the result of unidentified landslides. This study, and recent work by Karl Wegmann of the Washington Department of Natural Resources (personal communication, 2002), has resulted in mapping dozens of slides within the area (Plate 1), particularly prominent in the clayey and loosely-consolidated Oligocene Toutle Formation (?), and the largely unconsolidated thick gravels of the Pliocene Troutdale Formation. Landslides are also common in the Cowlitz Formation (see natural hazards section).

Columbia Heights Anticline and Hazel Dell Syncline

Field work conducted for this study has further corroborated the existence of the northwest-trending Columbia Heights Anticline, and the adjacent and parallel Hazel Dell Syncline, first mapped by Livingston in 1966. Evidence for these structures consists of fairly consistent strikes and dips of Eocene and Oligocene (?) units in the limbs of each structure, and of the position and orientation of units within each fold of a known stratigraphic sequence (i.e., older Grays River Volcanic units in the core of the anticline).

Since the older units occur along the axis of each structure in their southeastern-most exposures, both structures may plunge somewhat toward the northwest (Plate 1). Alternatively, this apparent plunge may simply be an artifact of topography, older units exposed at lower elevation area along the Cowlitz River. The relative position of the Cowlitz Formation and underlying Lower Grays River Volcaniclastic unit in the southeastern part of the Hazel Dell Syncline indicates a plunge to the northwest. Another indication is that dips toward the axis of the syncline are angled slightly to the northwest. The northwest orientation and position of Hazel Dell Creek is likely due to these folds.

The eastward dip of pre-Pliocene units east of the Cowlitz River may be a continuation of the northeast dipping limb of the Columbia Heights Anticline west of the river. Beds in the northeastern limb (those that are reliably not the result of slope-failure) tend to dip more east than northeast. If better resolution were possible, the orientations on opposite sides of the river might not differ substantially. Resolution of true strike and dip is poor west of the river because beds there consist of Lower Grays River Volcaniclastics (Tgvs1) which are largely massive. Also, the N 75 E dip of the anticline limb (essentially a dip-slope) would require only a slight eastward bend in order to conform to dips east of the river. Bed orientations across the Cowlitz River from the Hazel Dell Syncline are more problematic, and may indicate a hidden fault beneath the alluvium of the river (see Kalama Structure Zone section).

Some constraints can be put on the timing of these large folds. Referring to cross-sections A-A' and B-B' (Plate 1), Eocene and Oligocene units (Cowlitz Formation, Grays River Volcanics, and Toutle Formation) within the Columbia Heights Anticline are

substantially tilted, whereas the Miocene Grande Ronde Basalts are nearly horizontal, and therefore overlie the older Tertiary strata in angular unconformity. This same pattern occurs throughout the study area where Columbia River Basalt flows occur. Thick Columbia River Basalt flow units west of Coal Creek (e.g., in the Storedahl and Sons Quarry, Figure 62) are within 5 degrees of horizontal, apparently unaffected by the more intense deformation of the underlying middle Eocene Cowlitz Formation in Coal Creek. The same is true of the erosional remnants of Columbia River Basalts that cap the hills east of Coal Creek. Incomplete exposure of Columbia River Basalts, and shallow dip of underlying Paleogene sediments on Mt. Solo make it difficult to determine if angular unconformity exists there. The interbed above Ortley flow #1 (Figure 66) is not perceptibly tilted. Although stratigraphically lower Grande Ronde Basalt flows differ in present elevation from ~600 feet (180 meters) to nearly sea-level, this broad post-late Miocene Columbia River Basalt differential uplift has resulted in very little tilting of the basalt.

The absence of the lowermost Ortley flow #1 above the Columbia Heights Anticline could indicate that broad differential uplift had already begun in this area at the time of emplacement of the lower flow. This could have resulted in an erosional paleotopographic high that directed the lowermost Ortley flow around it. Because of the lack of good bedding surfaces for strike and dip in the lower Grays River Volcaniclastic unit in the Columbia Heights Anticline, it is difficult to determine if this deformation had begun between the time of deposition of the Cowlitz Formation and Grays River volcaniclastics, and the overlying Toutle Formation. Evidence collected along Coal

Creek, and in the Hazel Dell Syncline is also inconclusive as to whether angular unconformity exists between the Cowlitz and Toutle Formations, or if the broad-scale folding and faulting in the area occurred entirely after deposition of both units. The latter is more likely since large-scale compressional deformation of these units in the region had not begun until the early Miocene. Cowlitz Formation dikes in Coal Creek do not occur in the overlying Toutle Formation, but no evidence was found to indicate if this unconformity is angular.

The N 30 W orientation of the axis of these folds is an unusual trend for the area. Gentle folds within the strata of Coal Creek are oriented east-west, apparently resulting from north-south (post-rotational) compression. Other small folds to the north and west of the study area are oriented N 45-70 W. The Arkansas Anticline in Arkansas Creek between Abernathy & Bebe Mountains described by Kleibacker (2001) in the adjacent thesis area to the north, trends approximately N 50 W, and is interpreted to be the eastward extension of the Willapa Hills uplift described by Payne (1998) and Wells and Coe (1985), which does not affect the Longview-Kelso area. Major northwest-trending faults in the study area, and areas to the north and west, trend more westerly (Figure 73, see northwest fault section). Two structures in the study area that trend in similar directions are the Coal Creek Fault trending N 40-45 W, and the Kelso Fault system trending N 20-25 W. The possible relationships between these structures will be described in later sections.

N 50-70 W-Trending Faults

Northwest-trending faults, in addition to the large-scale northwest folding described above, are prominent structural features in the study area (Plate 1). Deformation from this faulting, which trends N 50-70 W, can be found in all geologic units in the study area older than the Pliocene Troutdale gravels, suggesting they formed in the late Miocene. Northwest-trending lineations are prominent on topographic maps, aerial photographs, and SLAR and DEM images (Figure 74) and have had great influence on the orientation of drainage systems in the immediate area. These faults in the study area are extensions of a much larger system of northwest-southeast trending faults occurring throughout southwestern Washington (Wells and Coe, 1985, Figure 73) and northwest Oregon (Niem and others, 1992; Meyer and Niem, 2002), related to oblique subduction and differential clockwise rotation of small crustal blocks in the Coast Range. From south to north, this system of faults in the Longview-Kelso area change orientation to progressively trend more westerly (Figure 73, Plate 1). The Abernathy Fault just west of the study area trends N 20 W, and two unnamed faults farther east trend N 45 W. Throughout the thesis area they range from N 50 W in the Eufaula Fault, N 52 W in the Rottweiler Fault, to N 60 W in the Goose Hollow Fault (Plate 1). Northward in the study area of Kleibacker (2001), the Germany Creek and Loper Creek Faults trend N 65 W. These faults appear to be a system of splays dispersing stresses into several smaller oblique slip, right-lateral faults, rather than one or two as is the case 3 km to the northwest where these splays converge (Figure 73).

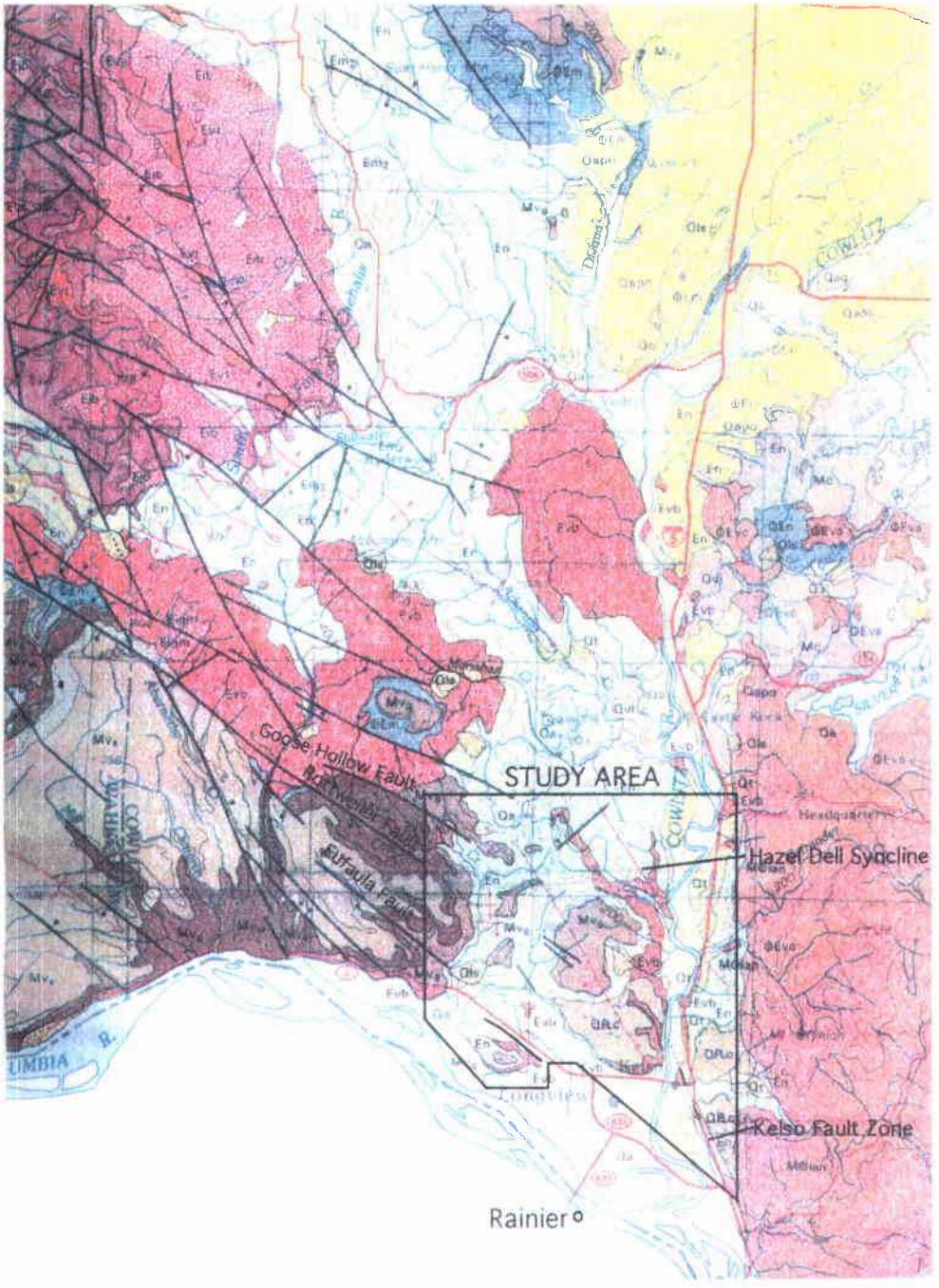

Figure 73: Portion of southwest Washington State Geologic map by Walsh and Phillips (1981). Note system of northwest-trending oblique slip faults and associated folds (red). Study area outlined in black.

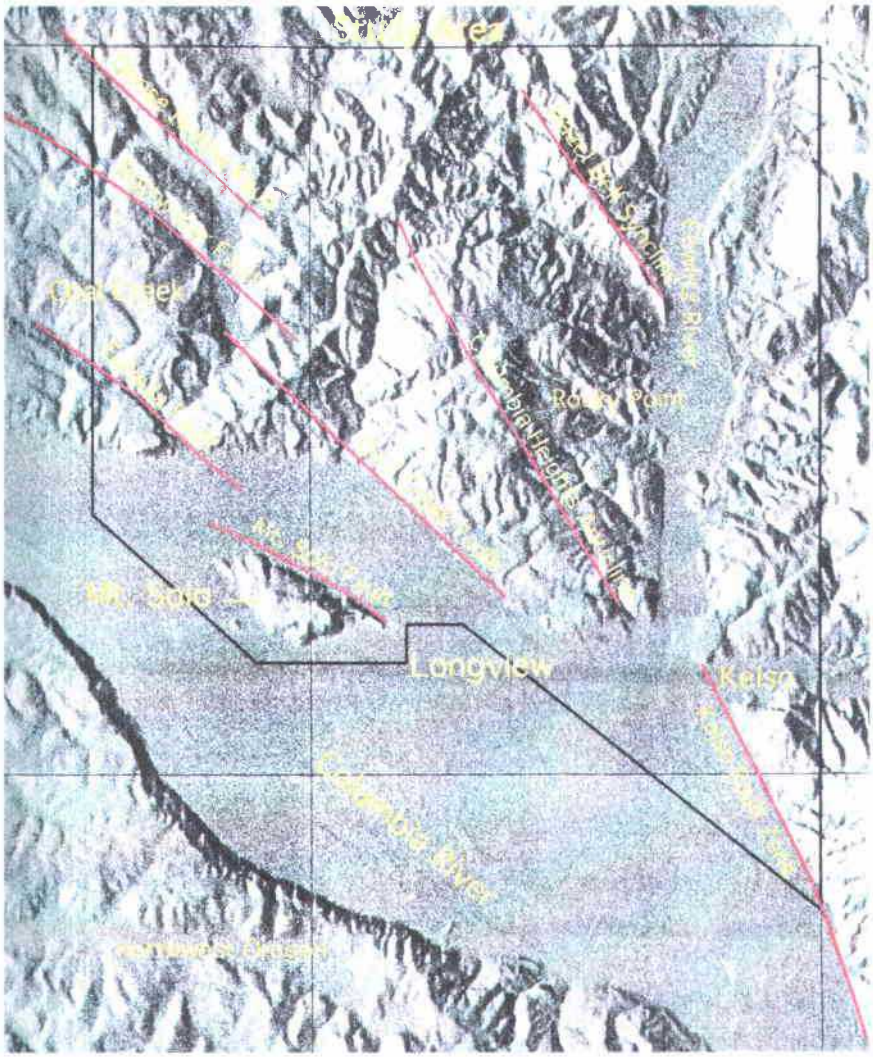

Figure 74: Digital elevation model (DEM) of the Longview-Kelso area (lighting from the south). Major oblique slip faults are apparent as fault scarps or linear drainages. Scale 1:100,000. Courtesy Phil Dinterman USGS to A. Niem, 2003.

For this study, northwest trending faults mapped by Livingston (1966), and later by Wells (1981), have been extended based on exposures of fault planes and joint systems discovered in Coal Creek, and new measurements of orientations found throughout the map area (Plate 1). In addition, several smaller-scale faults (< 30 meters of offset) and fractures were documented, particularly along Coal Creek, where hundreds of small faults with centimeters of offset, most normal but some reversed, occur along with thousands of fractures of this orientation. Coal Creek has also exposed more than 60 late-middle Eocene Grays River basalt dikes that have intruded along both faults and fractures ranging from nearly east-west to N 75 W, but most are close to N 60 W (Plate 1). Most other fresh exposures show this system of faults, suggesting that if exposures were better, this northwest signature would be seen as pervasive throughout.

With the exception of the major fault bounding Mt. Solo to the north (Mt. Solo Fault, Figure 74, Plate 1, cross section B-B') all major faults of this northwest orientation within the study area are up to the north. The next major fault to the north, the Eufaula Fault, juxtaposes Columbia River Basalt to the south against fine arkosic sandstone of the Cowlitz Formation to the north (Plate 1). This represents at least 20 meters of offset. The next major northwest fault to the north (excluding the N 40 W Coal Creek fault described in the next section) is the Rottweiler Fault, also up to the north, which causes several unusual steep strikes and dips within Coal Creek, and produces a 30+ meter repeat section of some intervals of the Coal Creek stratigraphic section (cross section C-C'). The discovery of this fault in Coal Creek also allowed extrapolation of this fault system to include a set of small northwest-trending faults offsetting middle Miocene

Grande Ronde Basalt flows above the Columbia Heights Anticline. The next large fault to the north, the Goose Hollow Fault, juxtaposes Grande Ronde Basalt against clayey siltstones of the Toutle Formation, an offset of at least 20 meters. This fault appears to die out to the southeast. All other northwest-trending faults documented for this study are up to the north, but Kleibacker (2002) described the Germany Creek and Loper Faults in his study area to the north as being up to the south. This post-Columbia River Basalt stair-stepping of fault blocks upward to the north, culminating in the block north of the Goose Hollow Fault, explains the progressive increase in elevation of the Columbia River Basalt flows in the area toward the northeast, accounting for their differential uplift. The south to north progressive up-faulting of blocks, then stepping down again in Kleibacker's study area, suggests that the entire system of northwest-trending splays is a complex northwest-trending horst. Likewise, the valley north and west of Mt. Solo can be described as a small pull-apart graben (Plate 1, cross-section B-B').

There is evidence of both extension and compression within this wrench fault system. The northwest-trending middle Eocene Grays River dikes intruding the Cowlitz Formation in Coal Creek, ranging from 0.3 to over 6-meters wide and largely paralleling the larger faults in the area, are viewed as resulting from late Eocene extensional forces. Normal faults associated with extension are thought to provide a low-pressure route for lava to rise toward the surface. Since most faults of this trend in Coal Creek are normal, this is a reasonable explanation. Slickensides on the margins of these dikes (faults) show a minor oblique-slip component, but are largely vertical. Today this would indicate

tension in the direction of N 30 E and S 30 W. However, some northwest-trending faults in the study area are reverse, and a regional pattern of anticlines and synclines (indicating compression) trend northwest and nearly parallel adjacent normal faults (Figure 73). Clearly, this fault system is also associated with compressional forces. The Goose Hollow Syncline, affecting Cowlitz Formation and Grays River volcaniclastic beds in the northern half of Coal Creek, almost exactly parallels both the Rottweiler and Goose Hollow Faults (Plates 1 and 2). This fold pattern indicates that the northwest-trending fault set is also associated with a compressional stress regime, despite the evidence from most of the Coal Creek normal faults and extensional dikes.

A reasonable explanation for these fault data is that a normal fault horst and graben system produced by an earlier extensional regime in middle to late Eocene, occurring prior to folding or reverse faulting and producing the Grays River dikes in Coal Creek, was later reactivated in late-middle Miocene by a compressional wrench tectonic regime acting in a N 20-40 E direction, producing the dozens of folds, and many of the reverse and normal faults that trend N 50-70 W. Since most northwest-trending faults are normal, many were not reactivated in the later compressional event(s). The initial tensional event in the middle to late Eocene, perhaps related to the magmatic inflation and distension of the oceanic crust and eruption of the Grays River Volcanics, may have determined the general orientation and location of the faults, joints, and dikes that would later become the northwest-trending fault system reactivated during Miocene compression and extension associated with wrench tectonic faulting. This pattern of late-middle Eocene northwest-trending horst and graben faulting followed by late-middle

Miocene to Pliocene reactivation and clockwise rotation in a wrench system also occurs in the Mist Gas Field (Niem personal communication, 2003).

Evidence also exists within the study area for right-lateral shear along these faults. Many Coal Creek dikes show evidence of a horizontal, as well as vertical component to the offset, confirmed by non-vertical slickensides. These also show that the horizontal component of the northwest-trending faults is right-lateral. Slickensides on other small faults in the creek and elsewhere show more horizontal component than vertical. This pattern is similar to the northwest-trending simple dextral shear described by Rarey (1986). In this model, the northeast-trending fault in the north-central part of the map area near the headwaters of Hazel Dell Creek (Plate 1), and several faults with similar northeast trends described by Kleibacker (2001), could be explained as Riedel shears formed by these northwest-trending oblique-slip faults in a wrench tectonic system (Payne, 1998; Kleibacker, 2001). Lack of a substantial number of these northeast-trending faults in the Longview-Kelso area could be evidence that not much rotation has taken place there. Additional evidence for this is in the southwest-trending paleocurrent directions recorded in Coal Creek and elsewhere in the study area, averaging S 50 W. If clockwise rotation of even 45 degrees had occurred, the original paleocurrent direction prior to rotation would have been from the north or northwest, an unlikely scenario given Eocene paleogeographic reconstructions. If rotations described by Kleibacker (2001) immediately to the north (~103 degrees) applied to the Coal Creek section, original paleocurrent direction would have been from the west-northwest, a seemingly impossible paleogeographic model given deltaic models for the Cowlitz Formation and the thick pile

of Grays River Volcanics in that direction. This field evidence is in contrast to recent paleomagnetic studies of the Cowlitz Formation and Grays River Volcanics (Wells and Coe, 1985; Prothero and others, 2001). If in fact not much rotation has occurred in the Longview-Kelso area, but significantly more has occurred just a few km to the north in Kleibacker's study area, small block rotation could explain the northeast (rather than northwest) trend of the Grays River dikes in Germany Creek, a clockwise difference of ~110 degrees from the study area. The similarity of fault and fold directions throughout the immediate area, and between the two areas, makes this substantial difference in rotation, especially over such a short distance, unlikely. More likely is the scenario that dikes in Kleibacker's area resulted from northwest-southeast late-middle Eocene extension along conjugate faults related to Riedel shear, but resulted from magma upwelling and distension in the study area, perhaps related to its possible position on the flank of the Grays River volcanic edifice.

Coal Creek Fault

The abrupt change in strike and dip directions of middle Eocene Cowlitz Formation beds in Coal Creek, from a southwest dip averaging about 20 degrees to a north dip averaging 2-5 degrees at the S ½ of Sec. 2, T 8 N, R 3 W was interpreted by Weaver (1937) and Livingston (1966) as resulting from an anticlinal axis at that location. Weaver, while traversing the creek from south to north, measured and described approximately 2000 feet (~610 meters) of Cowlitz Formation while moving downsection through the southwest-dipping southern third of the creek. After crossing what he considered to be the axis of an asymmetrical anticline, he began measuring upsection, and

included these units within the stratigraphic section he had already measured, correlating units based on stratigraphic position within the measured section, rather than by stratigraphic correlation. Abrupt changes in dip in the northern two-thirds of the creek were also interpreted as being related to synclines and anticlines.

A different interpretation is being proposed here. While traversing the creek from south to north for this study (Plate 2), it was noted that the nearly flat-lying, cliff-forming Cowlitz sandstones and siltstones north of Weaver's anticlinal axis are of a unique lithology not encountered in the ~600 meter measured Cowlitz section south of the anticlinal axis. These beds represent stratigraphic intervals lower in section than the lowest beds encountered south of the change in dip. The location in the creek where the change in dip occurs is also highly fractured and faulted, with a dominant trend toward the northwest. Cowlitz sandstone and siltstone units in the 100 meters of creek bed south of the major change in dip, besides being highly fractured, also change strike and dip frequently, with a dip of 40 degrees toward the southeast right at the edge of the fault (the steepest recorded in the creek). Given that 1) beds close to the structure cannot be correlated across the structure, 2) the change in bed orientation is sudden and severe, not gradual and decreasing toward the axis as would be expected from an anticline, and 3) beds immediately to the south of the structure are highly fractured and faulted, this structure is considered here to be a northwest-trending reverse fault that is up to the north. Further evidence for this interpretation is that a thick volcaniclastic interval in Coal Creek near the base of the southern section is again encountered moving upward through the northern section (Plate 2, cross section C-C').

Much evidence for this major fault exists beyond Coal Creek. Abrupt changes in dip similar to those described in Coal Creek exist along the projected trend of the fault at Site 68 (up N 50th Avenue beneath the power lines, NE ¼ of the SW ¼ of Sec. 12, T 8 N, R 3 W, Plate 1). This is within a probable modern landslide block that moved slightly downhill *en mass* (i.e., translational slide and left bedding largely in tact). At SE ¼ of NE ¼ of Sec. 13, T 8 N, R 3 W, Livingston (1966) mapped a fault plane of this orientation and along trend toward the southeast, with the fault plane dipping 60 degrees toward the northeast (Plate 1). Two fault-controlled blocks in parts of Sec. 13 and 24, R 3 W, T 8 N, and Sec. 18 and 19, R 2 W, T 8 N trend in this direction and are adjacent to the projected fault plane beneath Columbia River alluvium. In addition, the trend of this fault projects along the southwest limb of the Columbia Heights Anticline, suggesting that this quite linear feature may be fault-controlled.

The Coal Creek Fault is part of the extensive deformational event that largely occurred before emplacement of the Miocene Columbia River Basalts, as it does not offset these flows in the study area. The N 40 W orientation of this structure is similar to the trend of the Columbia Heights Anticline and Hazel Dell Syncline, indicating that all of these features could have resulted from the same compressional or wrench tectonic event. The Coal Creek Fault could be the western expression of the same forces that folded units to the east. The Columbia Heights Anticline bordered by the Coal Creek Fault to the south is in some ways analogous to the relationship between the Portland Hills Anticline bound by the Portland Hills Fault to the north (Wong and others, 2001). In this view, the block north of the Coal Creek Fault in Coal Creek is part of the same

uplift affecting the Columbia Heights Anticline, and the steeply southwest dipping block south of the fault could have been tilted by drag.

East-West-Trending Faults

Fresh bedrock exposures throughout the study area of pre-Pliocene formations contain fault and fracture sets trending within 15 degrees of due east-west (Plate 1). Along Coal Creek, fractures or small-scale faults of this trend offset the middle Eocene Cowlitz Formation and all other fracture sets, including the prominent N 60 W fault set and its associated Grays River dikes. Figure 50a of the volcanic section shows an example of this offset. Associated small-scale anticlines and synclines in Coal Creek also trend east-west. The largest offset observed from this east-west fault set is at most 3 meters. A common and unusual feature of this set is that small fault blocks are rotated relative to the fault plane, producing the illusion that beds change thickness across the fault. Another feature shared by the N 60 W fault set is that some are normal (indicating tension) and some are reverse (indicating compression). Fault planes only a few meters apart can have opposite motion. This fault set also contains examples of small-scale thrust faulting.

A nearly 100-meter long roadcut along Columbia Heights Road North (Site 49) at N ½ of Sec. 5, T 8 N, R 2 W displays several features of the east-west fault set in the Toutle Formation. This roadcut inside a 60 degree turn on Columbia Heights Road North on the Columbia Heights Anticline was bulldozed in 1998 due to partial landslide slope failure. The next year, most of the structural features in this friable siltstone and sandstone exposure had been covered with talus and soil, and grass almost completely

covered the outcrop. Twelve east-west faults in this roadcut hint at the extent of deformation by this stress regime. In Figure 75a two normal faults and one fracture are visible. Offset on fault #1 is about 0.7 meter and about 1 meter on fault #2. Drag folds on either side of these normal faults clearly show relative motion. In Figure 75b, ten meters north of Figure 75a and trending the same direction, two small faults with 0.3-meter offset (faults #3 and #4) are reverse. In Figure 76a, a due east-west normal fault with 45 degree dip is an example of block rotation relative to the fault plane. The block on the left is rotated toward the viewer, making it difficult to match beds across the fault. A small N 30 W thrust fault is also visible on the right, a product of the compressional event that produced the Columbia Heights anticline. In Figure 76b a thrust fault offsets beds by less than 1 meter. Offset appears greater because the block on the left is rotated about 20 degrees relative to the block on the right. An alternative view of these faults may be shallow extensional and compressional slip planes associated with the recent landslide in this weakly consolidated, clayey and tuffaceous unit. Similar compressional and tensional faults are observed in large translational slides along the central Oregon Coast (Niem personal communication, 2003). However, east-west normal and reverse faults in the bed of Coal Creek must be tectonic since the creek bed would be base level for any landslides in the valley walls above.

North-South-Trending Faults

Faults and fractures that trend within 30 degrees of north are present throughout the study area (Plate 1). An excellent example of this fault system is exposed at Site "IS" along Coal Creek Road (Figure 77), where N 20 W-trending normal listric faults with variable (1-3 meter) offset displace coals and yellow gray sandstones and siltstones of

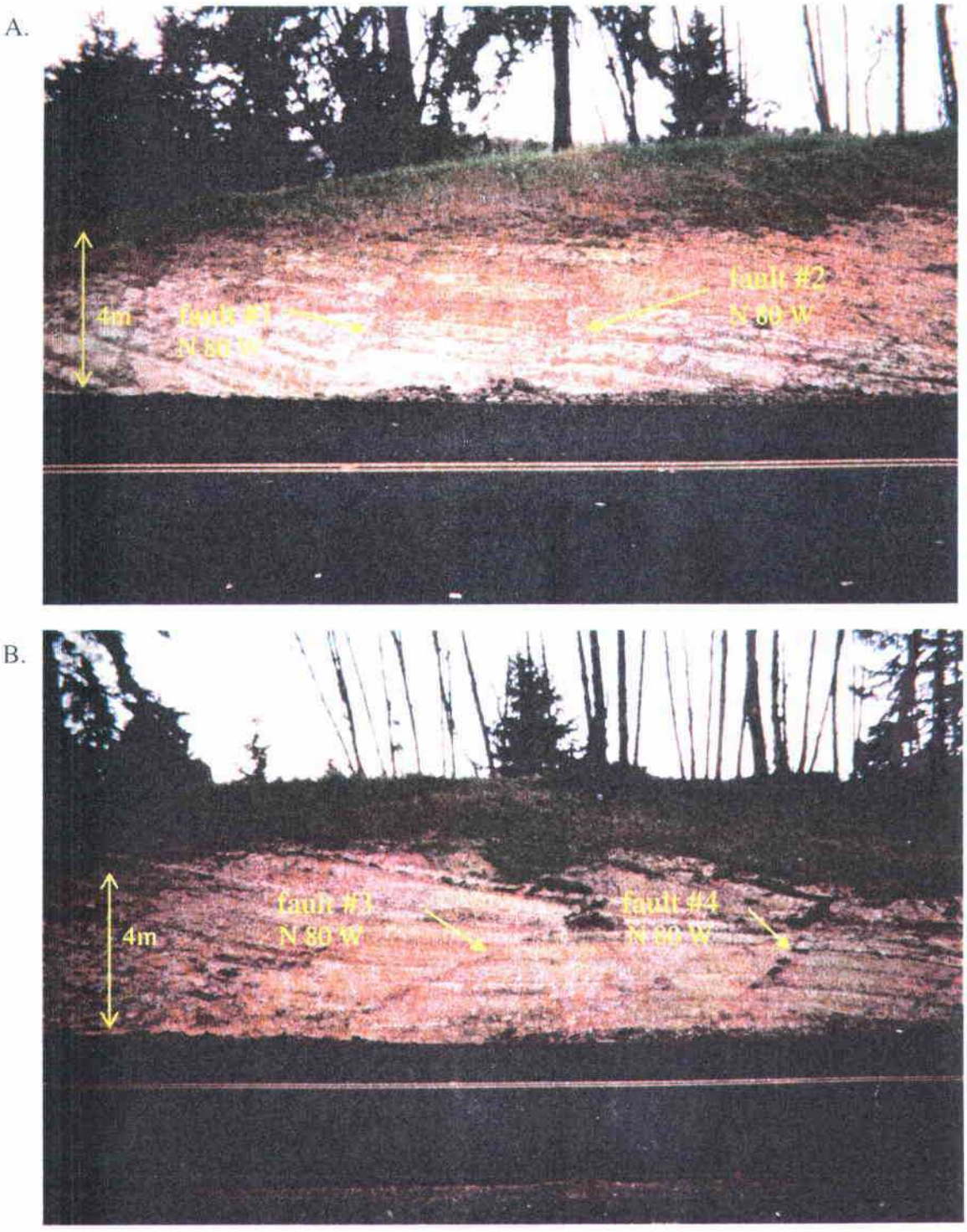

Figure 75: East-west trending faults from Site 49 in Toutle Formation clayey siltstones.
A. Two normal faults trending N 80 W with offsets of 1 meter or less.
B. Two reverse faults trending N 80 W with offset of less than 1 meter, located about 10 meters north of faults #1 and #2 (could be slump related).

A.

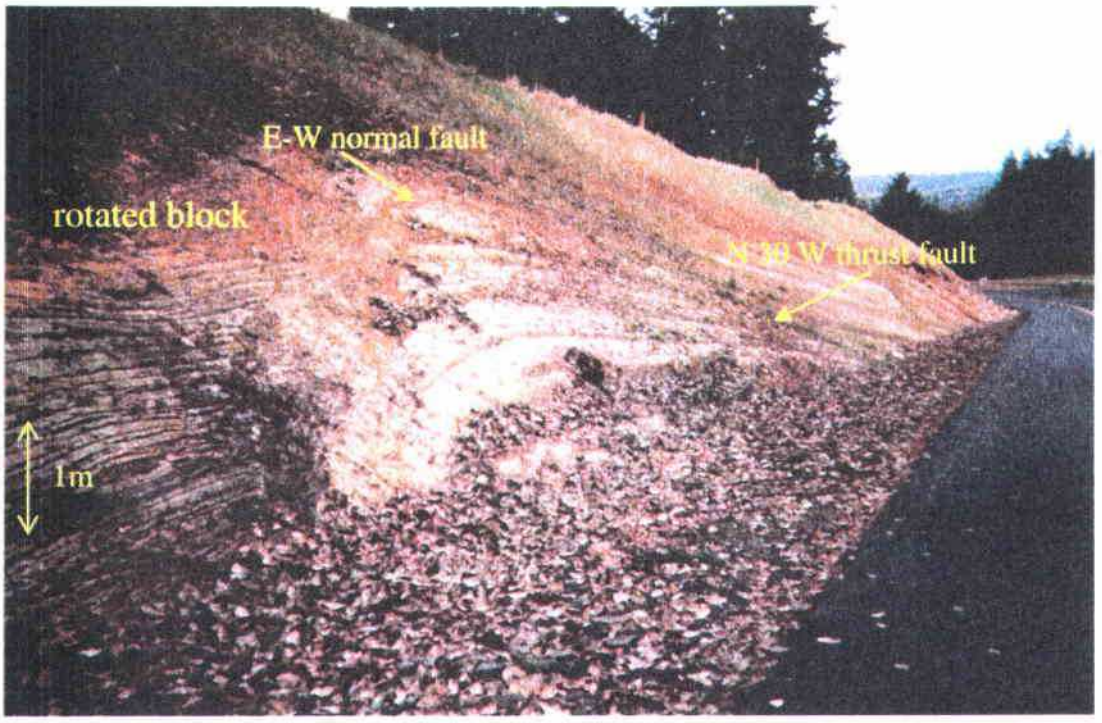

B.

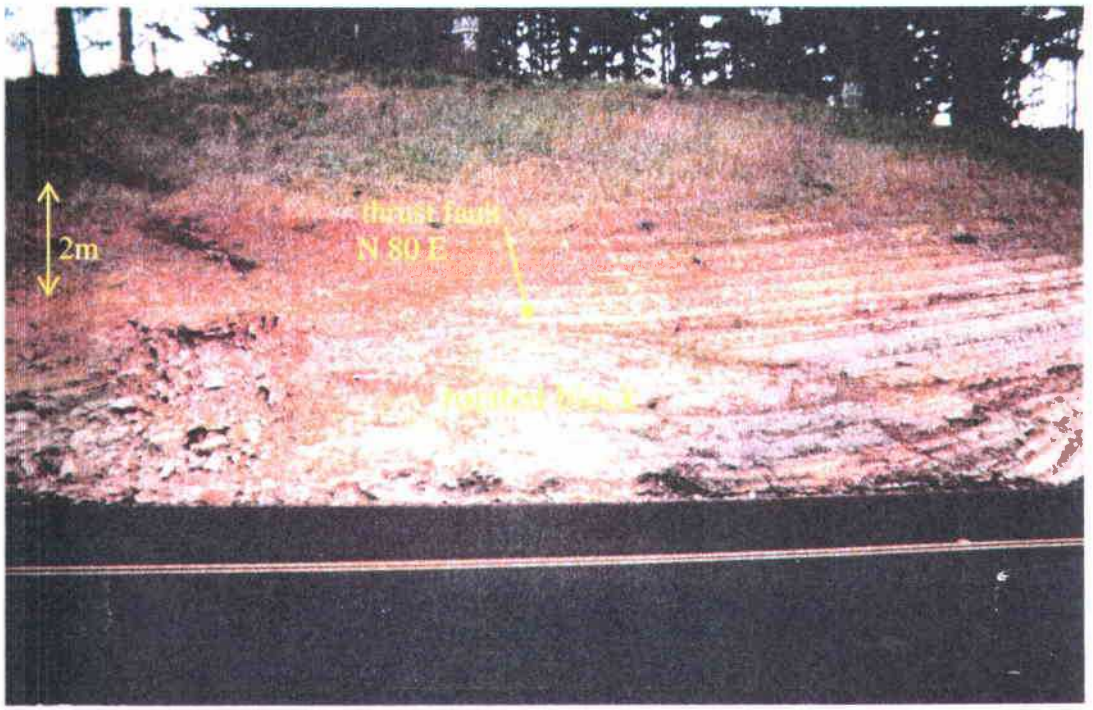

Figure 76: East-west trending faults from Site 49 in Toutle Formation clayey siltstones.

A. A due east-west trending normal fault with about 1 meter of offset. Note anticlinal drag fold in the right block, and rotation of the left block.

B. Thrust fault illustrating drag and rotation of the block on the left. Note slope failure in the far left part of the photograph. These may all be slump related structures.

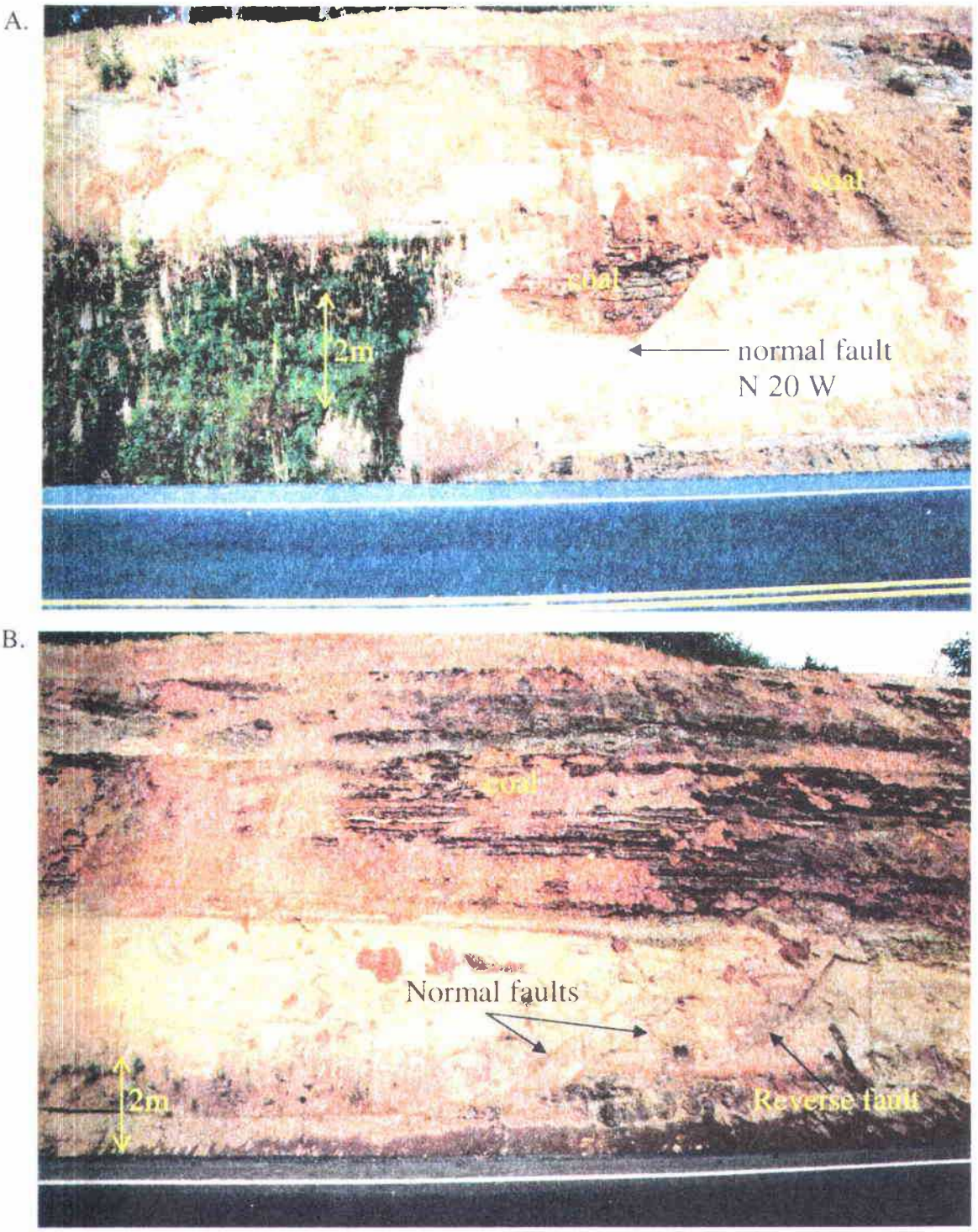

Figure 77: N 20 W faults exposed at Site "IS" in Coal Creek interval 22 of the Cowlitz Formation, along Coal Creek Road. These faults produce variable amounts of displacement, and can be either reverse or listric normal. These slip planes may be related to slumping.

interval 22 of the Coal Creek section (Plate 2), as well as a Grays River basalt sill. Alternatively, since this roadcut is part of an active landslide, these fractures may be listric shallow slip planes associated with the slide.

Kelso Fault Zone

At Site 9, a 100-meter long roadcut on Old Pacific Highway (the Carrolls I-5 exit at the center of Sec 12, T 7 N, R 2 W), three major and several minor faults and fractures occur with this northward trend, juxtaposing Grays River, Cowlitz Formation, and western Cascade basaltic andesite units that must have originally had tens of meters vertical separation. This outcrop with its north-trending faults has been included as part of the Kelso Fault Zone, which has created a linear fault scarp along I-5 in the southeastern corner of the study area, trending N 20 W (Plate 1, Figure 74). These faults have both normal and right-lateral strike-slip components, and many are difficult to decipher. It is clear that the beds and fault planes within this outcrop have undergone a considerable degree of deformation and alteration. The three north-trending faults and one east-west fault have been labeled 1 through 4 from north to south for this discussion.

Fault #1 (Figure 78a) consists of two fault splays that join at the top of the outcrop, with a near vertical wedge of Cowlitz Formation in between. The fault splay to the north has the more substantial offset of the two, trending N 20 E, the fault splay to the south trends N 20 W. The block to the north of this fault exposure consists of nearly horizontal thick beds of highly altered dark gray to grayish brown basaltic conglomerate (Tgvs1, thin section CR-1, Figure 55b of volcanic section); the block to the south consists of nearly vertical yellow gray, clean, friable Cowlitz micaceous arkose. The wedge caught

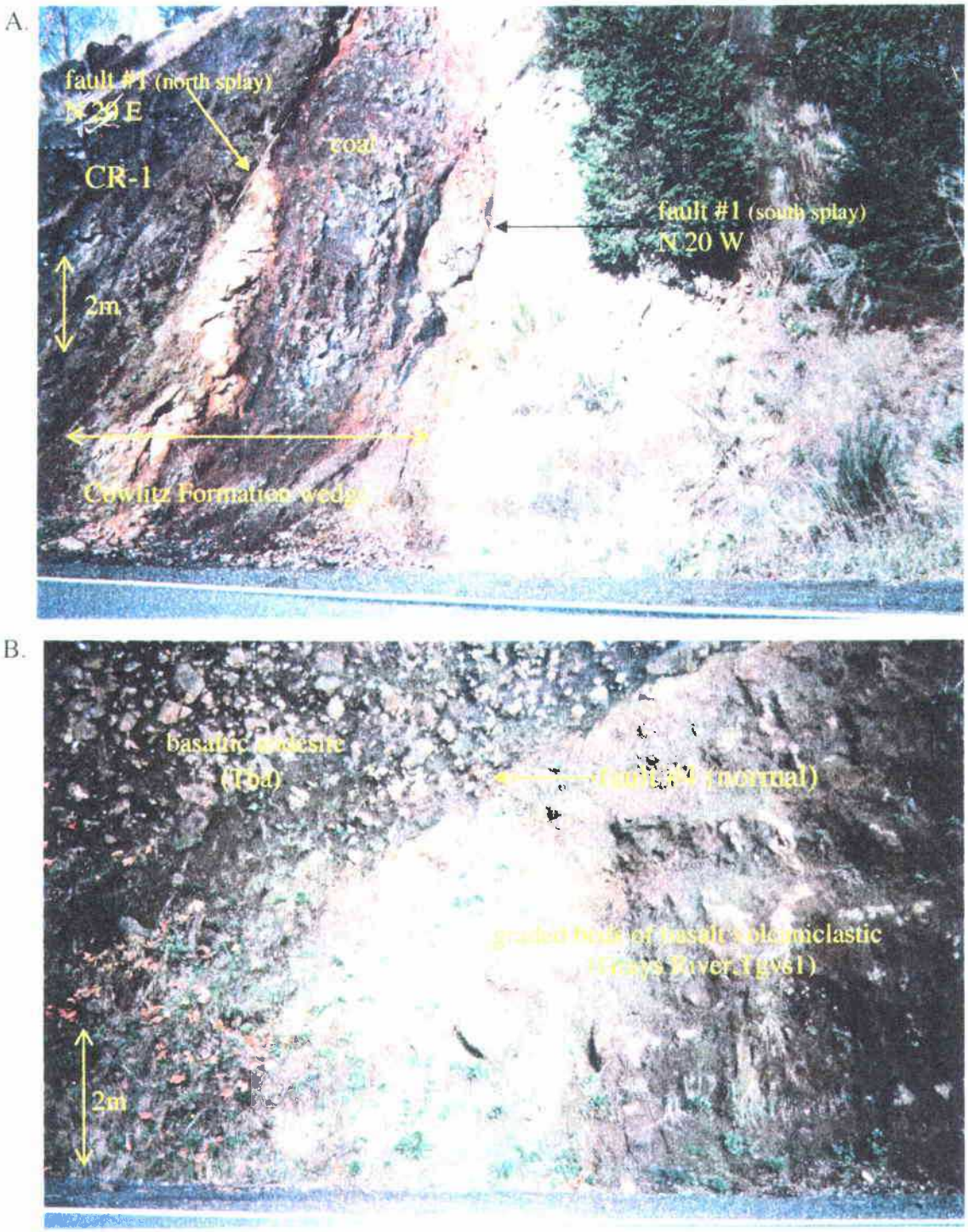

Figure 78: Exposures of the Kelso Fault Zone at Site 9, a long roadcut along Old Pacific Highway, near Interstate 5 (Carrolls I-5 exit).

A. Reverse N-trending fault with two splays converging at the top of the outcrop. Note that Cowlitz Formation beds have been tilted to dip steeply westward.

B. Normal east-west trending fault dropping western Cascade basaltic andesite down against graded beds of Grays River basalt volcaniclastic.

between the fault splays consists of a 2-meter thick light colored tuff, a 2-meter thick coal, and a dark gray basaltic sandstone dipping 65+ degrees toward the west. Slickensides in these faults are nearly vertical, but show an oblique-slip component (80 degree rake). Throughout the study area, the Grays River volcaniclastics unit north of the fault consistently occurs stratigraphically lower than Cowlitz Formation micaceous arkoses and coals, indicating this is oblique-slip fault is largely reverse. The steep dip of the Cowlitz Formation beds also indicates drag due to compressional deformation.

Fault #2 occurs about 10 meters south of fault #1 and trends N 30 W with a dip of 75 degrees toward the east-northeast. This fault consists of three main sub-parallel splays, and juxtaposes highly altered, light gray pumiceous and basaltic tuff/breccia (Tgvs1, thin section CR-7) against an altered, well-bedded basaltic sandstone (Tgvs2 ?) near the base. These relationships do not provide strong evidence as to relative motion of the two blocks. However, the oxidized reddish colored basaltic sedimentary unit south of the fault has been folded into a broad asymmetrical anticline, with an axis trending nearly due north, and this fold contains several small, nearly vertical faults and shear zones trending northward, indications that the fault resulted from compression from the direction of S 60 W. Fault #3 (Figure 79) juxtaposes the highly altered east-dipping limb of the anticline of Grays River basaltic sediments against a down-dropped block of the western Cascade basaltic andesite unit (thin section CR-12). This fault trends N 30 E and

Figure 79: N 30 E normal fault juxtaposing the western Cascade basaltic andesite unit and Grays River basalt volcaniclastic at Site 9. This nearly vertical fault is part of the north-south trending Kelso Fault Zone, with offset here of tens of meters.

dips slightly to the east, a relationship that suggests a normal fault. A fault breccia defines the fault plane on the east side. Fault #4 (Figure 78b) is this outcrop trends nearly east-west, and is a very low-angle (33 degrees) normal fault juxtaposing western Cascade basaltic andesite to the north against well-bedded Grays River basaltic conglomerate/sandstone to the south. This south block probably consists of the same unit as the block between fault #2 and #3, and therefore, the basaltic andesite block is down-dropped between faults #3 and #4. This ~100-meter wide complex of high-angle faults and drag folds at the interchange suggests this is a major fault zone trending N 20 W that might have controlled the north-south course of the ancestral Columbia River, and mark the tectonic boundary of the subaerial western Cascades volcanic arc on the east, and the Coast Range Paleogene forearc deltaic sedimentary units on the west.

Kalama Structure Zone

Several authors in recent years have proposed that a complex major north-northwest-trending structural zone transects the crust beneath the lower Columbia River Valley (Pezzopane and Weldon, 1993; Blakely and others, 1995; Wells and others, 1998; Evarts, 2002) based on the incongruity of geologic features on either side of the river. This shear zone, termed the Kalama Structural Zone, is believed to be part of a set of north-south shear structures that has accommodated northward translation of the Oregon and Washington Coast Range relative to the Cascade arc due to oblique subduction during the Tertiary. Evarts (2002) in his recent description of the Deer Island quadrangle ~20 km to the south of the study area, noted that strikes and dips vary across the proposed structure which is buried in a north-northwest orientation beneath the Columbia River,

and that a southward-plunging anticlinal structure in the area has an anomalous orientation for the southwestern Cascade Range.

One of the purposes of this study was to evaluate the possibility that this north-south structural feature has affected the geology of the Longview-Kelso area, because the trend of the structure (and the Columbia River) is toward the study area. Evidence neither confirms nor denies the existence of this structure in the study area, but there is much evidence to support it. The N 20 W trend of the Kelso Fault Zone (Plate 1), and the fact that this system and its associated fault scarp are parallel to the Columbia River, strongly suggests that it is part of the Kalama Structure Zone. In addition, this fault system trends directly toward the Cowlitz River Valley, which trends northward. The thick Grays River volcaniclastic exposure at Site 14 (near the southern end of the Cowlitz River in the SW ¼ of Sec. 26, T 8 N, R 2 W) is fractured and possibly faulted with a trend of N 20 W. The west side of the Cowlitz River is very straight, particularly the resistant Grays River basalt flows (unit Tgv1, Plate 1) near Kelso. Bedding east of the Cowlitz River consistently dips eastward in contrast to the highly variable dips west of the river. This dip direction is slightly different than the dip in the northeast limb of the Columbia Heights Anticline, but substantially different than the southwest dipping limb of the Hazel Dell Syncline. In addition, the synclinal axis cannot be confidently extrapolated across the river. Miocene Columbia River Basalt flows occur only west of the river, and the arc-derived, western Cascade basaltic andesite flow unit occurs only east of the river (Plate 1). The western Cascade andesite dikes in the northeast corner of

the study area (W ½ of Sec. 25, T 9 N, R 2 W) also do not extend across the river west of this north-south fault zone, suggesting additional structural control of the river's course.

There are also many reasons to doubt that a large-scale structure is hidden beneath the Cowlitz River. The east dip of Cowlitz Formation and Grays River volcaniclastic units east of the river is similar to that of the northeast limb of the Columbia Heights Anticline. Cross section A-A' does not require a structural feature there to make sense, just a small shift in dip eastward. Similar Cowlitz Formation and Grays River units occur directly across the river from each other with rare exception, and the Toutle Formation occurs on both sides. The Kelso Fault Zone is similar in trend to the Columbia Heights Anticline and Hazel Dell Syncline, and the Coal Creek Fault. This coupled with the fact that the slickensides in the Kelso Fault Zone are mostly vertical, implies that all 3 faults may be part of the same pre-Miocene Columbia River Basalt compressional (transpressional) event. This does not preclude the Kelso Fault Zone from being a northern extension of the Kalama Structural Zone, and in fact, may show that the Columbia Heights Anticline and Hazel Dell Syncline are related to the Kalama Structural Zone. Importantly, other than the north-trending fractures at Site 14 (Plate 1) in Kelso, there is a striking lack of north-trending faults or fractures in scattered exposures along the Cowlitz River. If such a structure exists, Rocky Point (projecting into this structural zone) should have a strong imprint of north-trending structures, but instead, fracture sets there are largely east-west trending.

The Columbia Heights Anticline and Hazel Dell Syncline are located at the termination of two major fault systems within the study area and the surrounding region; the N 50 W to N 70 W fault system and the north-trending Kelso Fault Zone (part of the

Kalama Structure Zone). The large anticline and syncline are oriented 15 degrees to the northwest of the Kelso Fault Zone, 10 degrees northeast of the Coal Creek Fault, and 20 degrees (average) from the northwest-trending faults. Since the northwest-trending fault system dies out near Columbia Heights, and little evidence exists of the Kalama Structure Zone north of Kelso, the study area is clearly an area of transition from one fault set to another. Motion on the Kalama Structure Zone has been determined by Evarts (2002) and others to be an oblique-slip fault system with right-lateral offset, resulting from oblique subduction and wrench-style deformation. In addition to the normal component of the offset in the three north-trending faults at Site 9, there is also a strike slip component (with rake angles as low as 60 degrees). Based on drag folds on these faults, and the known stratigraphic sequence of units in the area, these faults appear to be reverse (transpressional), as is the similar-trending Coal Creek Fault.

Similar structures with similar orientations occur in Southern California as a result of wrench faulting (Figure 80). Here, right-lateral oblique-slip faults with reverse normal components are associated with folds trending less than 30 degrees to the northwest of the main fault, more often within 15 to 20 degrees. A similar pattern occurs in wrench tectonic settings in New Zealand and Venezuela where right-lateral wrench faults produce a series of *en echelon* folds with angles of 30 degrees or less. Small-scale east-west folds in Coal Creek (Plates 1 & 2) are oriented 30 degrees clockwise to the northwest-trending faults through this area. Indeed, theoretical and clay models predict that compression and associated folding would occur at the same angles found in the study area in a north-

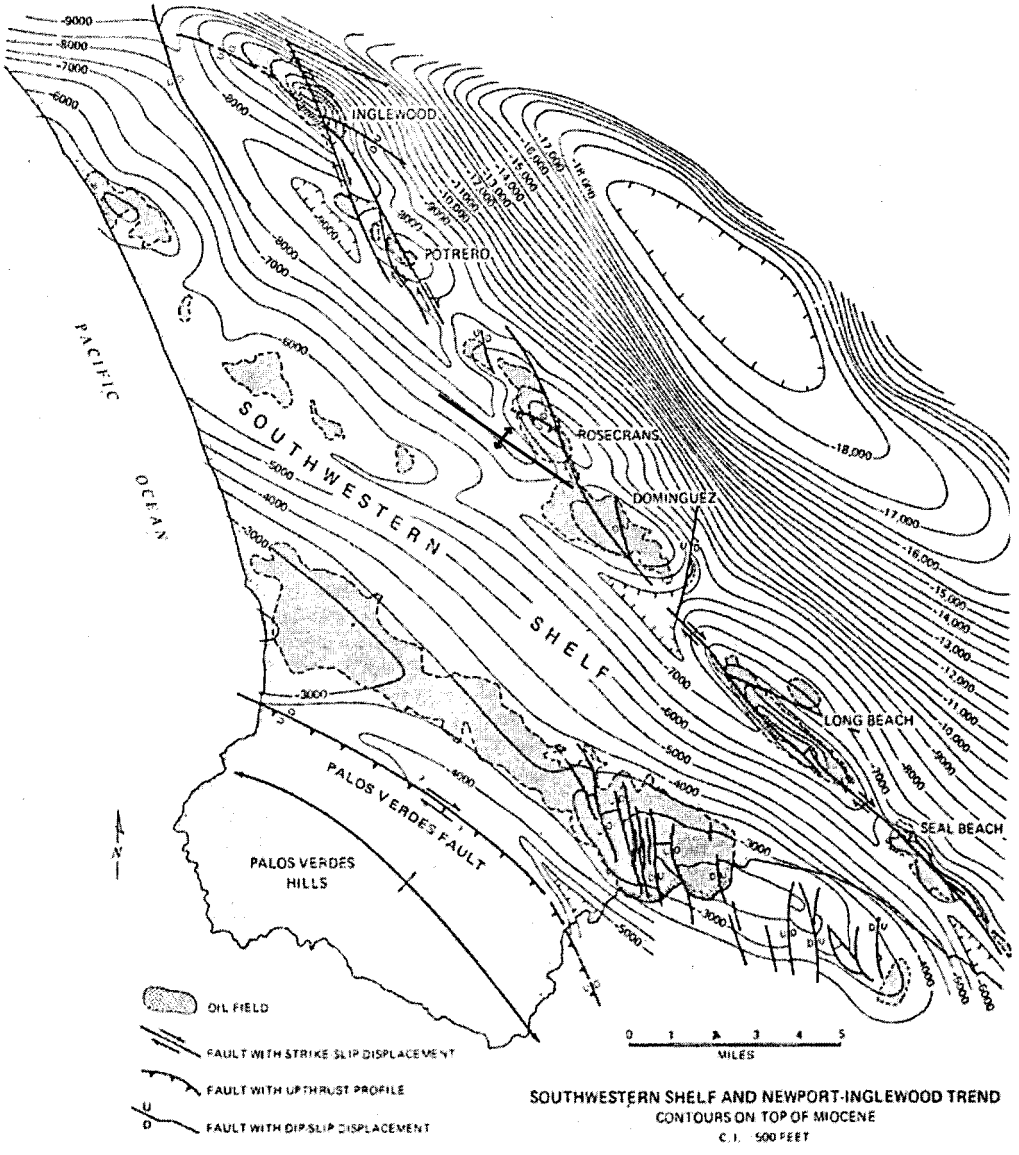

Figure 80: Structure of northwest and central part of Newport-Inglewood wrench fault zone (with oil fields named) and southwestern shelf of Los Angeles basin. *En echelon* step-over is accompanied by a fold, similar to the relationship between the Columbia Heights Anticline and wrench faults within the study area. (Modified from Harding, 1973).

trending, right-lateral fault system. For most wrench-fault experiments with clay, the angle between *en echelon* fold axes and the wrench fault is near 30 degrees, folds that form later during deformation have lower angles (Wilcox and others, 1973). By extrapolation from models, the axes of *en echelon* (right-handed when in association with right-lateral faults) should be at low angles (<30 degrees) in a counter clockwise direction.

Since the Kalama Structure Zone terminates in the southeast corner of the study area, the compressive force of northwest Oregon pushing into southwest Washington along this oblique-slip zone must be accommodated some other way. The series of northwest-trending faults in the study area and in the adjacent study area of Kleibacker (2001) to the north are also right-lateral oblique-slip faults, and could accommodate this motion. In this view, the study area is a step-over zone, where the Kalama Structure Zone essentially bends westward and splays into at least 7 smaller right-lateral wrench faults. This bend in the fault system could also explain why the Columbia Heights anticline and Hazel Dell Syncline (and the associated Coal Creek Fault) are positioned where they are, an area of concentrated compressional tectonic strain produced by the bend in the fault system. It is interesting to note that the Columbia River travels in nearly a straight line southeast of the study area because it follows the Kalama Structure Zone. At Longview and Kelso where the fault bend/stepover occurs, the river also bends westward following a nearly straight line that parallels the major northwest faults in the area (Plate 1). A similar pattern occurs in Southern California (Figure 80) along the Newport-Inglewood trend where an *en echelon* step-over is associated with a fold of similar orientation and scale, and also splays into at least 3 smaller faults.

HYDROCARBON POTENTIAL

With over 2000 feet (~650 meters) of potential Cowlitz Formation reservoir sandstone, coal methane gas source beds, structural traps, and seals, and a location approximately 16 km (~10 mi) northeast of the producing Mist Gas Field, the study area is a worthy target for future natural Gas exploration. Since first being drilled in 1979 by a joint venture between Northwest Natural Gas, Diamond Shamrock, and Reichold Energy Corporation (Olmstead, 1982), 70 BCF (billion cubic feet) of natural gas have been commercially produced from the Cowlitz Formation in the Mist field, worth an estimated $125 million. In the area of the Mist Gas Field specifically, natural gas was generated from deep-sea mudstones of the underlying Eocene Hamlet Formation, and to a lesser extent from carbonaceous mudstones, siltstones, and coal seams of the Cowlitz Formation itself. Carbon and oxygen isotopes suggest that the methane in the Mist Gas Field is both biogenically and thermogenically generated (Armentrout and Suek, 1985). The portion of the methane that was thermally produced is likely sourced from the Hamlet Formation and at least part of the overlying Cowlitz Formation in the hydrocarbon generation window, based on depth of burial and the local geothermal gradient (Armentrout and Suek, 1985). Much of the methane may also have originated from strata in the deeper Astoria or Nehalem basins, which are downdip, allowing gas migration updip into the Nehalem Arch where the Mist field is located. Flash heating by Eocene intrusions may also have generated gas (Stormberg, 1991).

The main reservoir for methane at the Mist Gas Field is the Clark and Wilson sandstone member of the Cowlitz Formation. These delta front reservoir sandstones can have permeabilities of up to 2 Darcies and porosity of 30 to 40% (Niem and others, 1992;

Robertson, 1997). In the field, upper Cowlitz Formation deep-marine mudstone and deep-marine tuffaceous Keasey Formation siltstone act as overlying stratigraphic seals. Hydrocarbons migrating laterally and upward are also stopped by normal fault traps developed in the late Eocene. In order for permeable sandstone to be an effective gas reservoir, there should be a four-way closure, typically defined by 2 to 4 impermeable fault planes. At the Mist Gas Field such traps occur as fault planes that define a series of horsts and grabens in the area that cut across the Nehalem arch. Gas is also trapped in small drag folded anticlines associated with these faults. These structures are commonly with northeast- and east-west-trending faults, that in northwest Oregon are secondary to the principal northwest-trending oblique-slip faults (Eriksson, 2002). These structures are along trend with the northwest-trending Portland Hills Fault Zone (Niem and Niem, 2002).

In the subsurface the arkosic C & W (Clark and Wilson) reservoir sandstone and the overlying stratigraphic seals (i.e., the upper Cowlitz mudstone) pinch out to the northwest and west. This results from onlapping and thinning of these Eocene sedimentary strata against the Grays River Volcanic paleo-high (large Grays River gravity anomaly presumed to the primary eruptive center, Figure 45) creating potential stratigraphic traps, and defining the northernmost extent of these units. The Champlin Puckett exploration well on the south bank of the Columbia River, 5 miles north of the Mist Gas Field (on the flank of the volcanic high, Figure 45), drilled through approximately 4400 feet (~1400 meters) of Grays River lava flows and volcaniclastics with no Cowlitz interbeds. However, the study area, as well as the study areas of Payne (1998) and Kleibacker (2001), also located on the eastern flanks of the Grays River

gravity high, contain thousands of feet of potential Cowlitz Formation micaceous lithic arkoses, associated mudstone seals, and methane-rich coals.

Even though no natural gas is currently being produced in southwest Washington, Johnson et al. (1997) have described the Cowlitz-Spencer gas play, which includes the study area. This play, which extends from the southern Puget Basin to the Oregon-Washington border, is based on the premise that methane generated from underlying middle Eocene marine mudstone or intraformational non-marine carbonaceous mudstone and coals, may have migrated into sandstone reservoirs in overlying or interbedded Eocene deltaic or estuarine shallow marine sandstones. The Mist Gas Field could be used as an analog for exploration in these Cowlitz Formation and older Eocene McIntosh units in southwest Washington. In and around the Chehalis Basin, 40 km north of the study area (Figure 3), 20 wells have been drilled to depths of 3000 feet or greater, without discovering commercial natural gas deposits, but many shows occur. Both the Chehalis basin of southwest Washington and the Mist Gas Field are used for storage of natural gas imported from Canadian gas fields (Niem and others, 1992)

Potential Local Hydrocarbon Generation

Based on the thick McIntosh Formation mudstones and siltstones described by Kleibacker (2001) in Germany Creek north and west of the study area, and also the presence of the McIntosh Formation in the Quigley no. 1 well just north of the study area, it is inferred that McIntosh Formation also underlies the Cowlitz Formation in the study area (Plate 1 cross sections). The deep-marine, organic-rich mudstones of this formation, which may be up to 3000 meters thick, are a marginal source for hydrocarbons. At the Mist Gas Field, natural gas generation was likely initiated about 33 Ma at burial depths of

3000 meters or more in the Nehalem and/or Astoria Basins based on the necessary geothermal gradient to mature these hydrocarbons and generate thermogenic natural gas (Armentrout and Suek, 1985). In southwest Washington, the limiting factor preventing development of large gas accumulations is the relatively low maturity of the source rocks (Johnson et al., 1997). The local thermal gradient would produce a maturation depth of approximately 3000 meters. That depth was probably attained in southwest Washington at the time of maximum burial during the early to middle Miocene, prior to the late Miocene transpressional event that produced regional faulting, folding, and uplift. At this time, it is also likely that the lower Cowlitz Formation (coal bearing units 1 and 2, Plate 2) was also within the window of hydrocarbon production. Today, it is likely that some of the lower bathyal marine mudstone of the McIntosh Formation is still beneath this 3000-meter limit in southwest Washington.

Cowlitz Formation coal seam and carbonaceous mudstone within the study area could likewise act as gas-prone source rocks for natural gas production. The Coal Creek stratigraphic section (Plate 2) differs from the type section described by Payne (1998) in having substantially more upper shoreface to delta plain sandstones and substantially less lower shoreface to bathyal mudstones and siltstones. Therefore, relatively thin mudstone interbeds are likely not a good source for hydrocarbons in this area. However, the Coal Creek section contains 8 substantial coal/carbonaceous shale horizons (coals A-H, Plate 2) that could act as sources for *in situ* biogenic and thermogenic methane. These low grade coals are typically lignitic to subbituminous, which typically have vitrinite reflectance values between 0.3 and 0.6 percent. Eocene intrusions of Grays River basaltic dikes and sills, and to a much lesser degree, western Cascade-derived andesite

dikes, could have produced narrow localized areas of thermogenic methane. In addition, the location of the study area so near the Grays River volcanic high, and with local eruptive centers such as Mt. Solo and Rocky Point active during Cowlitz deposition, the geothermal gradient may have been steeper in the study area than in surrounding areas.

Potential Local Hydrocarbon Reservoirs

Within the Coal Creek section, as well as elsewhere in the study area, several thick permeable and porous Cowlitz Formation sandstone units could act as natural gas reservoirs. Unit 1 upper shoreface to delta plain successions in the Coal Creek section (parasequences 1 through 4, Plate 2) have relatively few clean arkosic sandstones. Two intervals that are relatively clean are also relatively well-indurated with sparry calcite cement. The coarse-grained basalt volcaniclastic facies of parasequences 5 (lithofacies c1) is likewise well-cemented with calcite, and is thus a poor natural gas reservoir. Potentially good reservoirs (clean, friable, micaceous and arkosic sandstones) are comparatively rare throughout the Coal Creek section due to a heavy tidal influence during deposition (e.g., flaser-draped beds of lithofacies e and f) in this tide-dominated delta lobe or estuary. However, clean sandstones do exist in intervals 37, 33a and b, and 22, and are particularly common near the top of the section in the deep sea submarine channel facies (lithofacies j, Plate 2). If during the late Eocene transtensional or late Miocene transpressional events, horst and graben-style faulting downdropped blocks of Cowlitz Formation arkosic sandstones against McIntosh Formation mudstones, this could have allowed natural gas generated from the underlying McIntosh Formation to seep into these adjacent Cowlitz Formation potential reservoir sandstones. Some Cowlitz Formation sandstone exposures beyond Coal Creek in the study area are more friable and

clean, indicating that lateral facies changes of intervals in the Coal Creek section may include cleaner (i.e., more permeable and porous) delta front sandstones.

Petrographic work conducted for this study gives further insight into the varying reservoir potential of these Cowlitz Formation micaceous, lithic, arkosic sandstones. In general, medium- to coarse-grained Cowlitz sandstones from the study area are less friable (better cemented), contain more compacted carbonaceous debris, and contain more diagenetically susceptible volcanic lithic clasts than comparable sandstones from Kleibacker's (2001) or Payne's (1998) study areas to the north, or the Clark and Wilson sandstone in and near the Mist Gas Field to the south (Robertson, 1997). This is due to the tidal/estuarine influence of a large part of the Cowlitz Formation in Coal Creek and the close proximity of Grays River volcanic centers (Rocky Point and Mt. Solo), producing a higher basalt-lithic component in most lithic arkoses, and basalt volcaniclastic interbeds throughout the Coal Creek section. In contrast, the gas-producing C & W sandstone of the Cowlitz Formation is composed of dominantly storm wave-generated, hummocky bedded, delta front sandstones with few coals and very little basalt lithic component. The burial compacted carbonaceous, micaceous, and muddy flaser-draped laminae greatly reduce vertical and lateral migration of hydrocarbons. The Grays River volcaniclastic component of Cowlitz Formation lithic arkoses in the study area has the effect of locally reducing porosity and permeability, in that basalt clay alteration products (i.e., smectite) produce thin clay rims around most grains, causing moderate to heavy induration in most beds, and completely fill intergranular pore spaces in many lithic basaltic samples. Most basaltic samples studied petrographically have pore spaces clogged by these diagenetic clay minerals.

Sandstones with comparatively good porosity and permeability, particularly in the upper part of the section (unit 5), show maximum porosity of 15-20% estimated in thin section. This porosity is largely due to sand-size primary intergranular pores, with subsidiary porosity resulting from diagenetic dissolution of some glassy volcanic clasts, and also some potassium feldspars and calcareous fossil shell fragments. In these samples, porosity shows good interconnectivity. They also commonly show tangential framework grain contacts indicating that they have not undergone significant compaction. However, most Coal Creek sandstones do show significant burial compaction and resulting porosity reduction based on deformed micas, clay minerals, and carbonaceous material.

Potential Stratigraphic and Structural Traps

Within the Coal Creek section several potential stratigraphic traps and intraformational seals occur. Near the base of the section, two coals (A and B) and associated porous lithic arkosic sandstones and siltstones occur stratigraphically beneath a thick well-cemented Grays River basalt volcaniclastic. Toward the northern part of Coal Creek this unit becomes progressively dominated by well-cemented basaltic siltstone that could act as a seal. This arrangement of source rock (coals) and reservoirs (sandstones) underlying a well-indurated volcaniclastic seal could produce a good stratigraphic seal. Residential water wells drilled through this volcaniclastic into underlying lithic arkosic sandstones, carbonaceous siltstones, and coals produced water bubbling with methane. To this day, methane bubbles occur in at least one of these wells (SW ¼ of Sec. 27, T 9 N, R 3 W, the northernmost home on Coal Creek Road). Methane collected from this well for this study is biogenic biogenic rather than thermogenic

(Appendix V). Calcite-cemented Grays River basalt volcaniclastic and coal/carbonaceous shale beds could also act as local stratigraphic seals, as could sandstone stratigraphic pinch-outs of these subtidal sandstone channel and tidal bars.

Three other potentially good stratigraphic seals occur in the Coal Creek section. The maximum flooding surface at the base of parasequence 12 places lower shoreface mudstone with siltstone lenses (possible seals) over coarse-grained friable lithic arkosic sandstone of the upper shoreface (Plate 2). In addition, 7 of the 8 coals in the section (each a potential biogenic methane source) occur stratigraphically beneath this horizon. Another flooding surface at the base of parasequence 17 places middle shoreface siltstone stratigraphically above upper shoreface porous, clean, arkosic sandstone. In the uppermost unit (5) of the Coal Creek section, coarse-grained sandstones of lithofacies g or j are overlain by fine-grained, laminated, micaceous sandstone and siltstone of lithofacies k (a potential seal). Finally, in theory, anywhere delta front sandstone (including tidal channels) is overlain by tidal rhythmite facies or bay mudstone could be a potential reservoir and seal.

Potential structural traps occur within the study area in the form of oblique-slip transpressional and transtensional faults, and large-scale folding (Plate 1). The structural style of the Mist Gas Field, small Eocene (and late-middle Miocene) horst and graben fault blocks (Niem and others, 1992) is an analog for the study area. As described in the structure section of this text, the prominent set of northwest-trending faults in the study area has broken the sedimentary and volcanic units in the area into discrete blocks. Any one of the aforementioned stratigraphic traps and seals, in addition to these faults, could trap gas within reservoir sandstone. In addition, these fault blocks can be tilted relative to

each other, trapping gas in anticlinal drag folds against the fault (e.g., the Coal Creek Fault, Plate 1, cross section C-C'). Due to poor exposure in the northern part of the study area, it is uncertain if additional similar mapped structures are present in that area.

The Columbia Heights Anticline is another potential structural trap. This northwest-plunging fold capped by Grande Ronde basalt, has a core consisting largely of Grays River basalt flows and volcaniclastics, but also contains a substantial amount of Cowlitz and Toutle Formation sandstones and siltstones that project into the subsurface to the northwest. Natural gas generated in the McIntosh Formation or interbedded coals of the Cowlitz Formation could potentially migrate up the dip created by the Grays River Volcanics, and be trapped against Grande Ronde Basalt flows or interbeds at the top of the anticline (cross section A-A'). Smaller folds in the northern part of the study area could also act as potential structural traps (Plate 1). It is important to note that structural and stratigraphic traps are not necessary to retrieve small amounts natural gas from the study area. Dispersed coal bed methane molecules absorbed in coal cleats and other carbon-rich beds can be released by pumping ground water out of the pore spaces in these beds, thereby reducing the pore pressure within the sediment and allowing methane gas to come out of solution, and be pumped out in horizontal exploration wells.

The 1925 Quigley no.1 well, located approximately 1 km north of the study area, was drilled by the Castle Rock Oil and Gas Company to a depth of 2893 feet (~900 meters), and according to the well logs, the exploration hole had some encouraging results (Kleibacker, 2001). The well interval corresponds to a stratigraphic section from the upper McIntosh Formation deltaic sandstone (a potential reservoir) up to coal-bearing unit 1B of the Cowlitz Formation as described by Payne (1998). "Good show oil" was

reported in the drillers log from the upper McIntosh sandstone, and another "show oil" was reported from one of the lower Cowlitz Formation sandstones (Kleibacker, 2001). These well logs show that there is potential for hydrocarbons originating from underlying McIntosh Formation mudstones in the area. The large-scale northwest-trending complex horst running through the study area, with adjacent grabens in Longview and northward in the study area of Kleibacker (2001), may have juxtaposed Cowlitz Formation or upper McIntosh Formation sandstones against the underlying McIntosh Formation mudstones, leaking natural gas into the reservoirs.

Geologic Hazards

The Longview-Kelso area of southwest Washington is positioned in a tectonically and hydrologically active setting. Located only about 100 miles (~160 km) inland from the active Cascadia subduction zone, the potential exists for devastating great earthquakes of 8.0 or larger on the Richter Scale, and smaller forearc earthquakes (e.g., on the Seattle Fault). Such large-scale earthquakes would have devastating effects on old masonry buildings in the area, especially in Kelso and surrounding smaller towns where historic downtown districts are over 100 years old. To compound the problem, most communities in the area are built on floodplain alluvium and are less than 20 feet above sea level, and many are below 10 feet above sea level. This, in addition to the shallow groundwater level due to the proximity of the Columbia and Cowlitz Rivers, as well as the multiple small, meandering tributaries (with water saturated floodplain muds) that flow through much of Longview, drastically increases the threat of liquefaction. Shaking from the 1949 Seattle earthquake reportedly produced sand boils and sand volcanoes in the Longview-Kelso area. Most homes in the low-lying areas lack basements, since the water table is higher than the depth of the basements, even under normal precipitation conditions. High-water conditions coincident with a large earthquake could exaggerate the liquefaction effect. Even in low-lying areas not particularly prone to liquefaction (i.e., underlain by river gravels), housing developments are nevertheless built on unconsolidated alluvium, which would amplify the effects of an earthquake.

Flooding is another natural hazard that is particularly threatening to this part of the Pacific Northwest, due to high precipitation and proximity to large bodies of water. As previously mentioned, most of Longview is built on alluvium of the modern Columbia

River floodplain. Despite the protection against large-scale flooding provided by several Columbia River dams, the flood threat in this part of the lower Columbia River is great enough that material was dredged from Lake Sacajawea (an oxbow lake in downtown Longview) for the purpose of creating a 15-20-foot high levee along the Columbia River (that is maintained to this day) to protect the community. Several smaller communities such as Coal Creek and Ostrander are built on the 100-year flood plains of their respective creeks. These communities and others were affected during the unusually heavy precipitation runoff of the winter of 1996. Several newer and smaller housing developments are built on the floodplains of the Cowlitz River, some adjacent to marshes where both flooding and liquefaction are potential dangers. A further flood threat exists in this lower Columbia River area; if a Columbia River dam was compromised by earthquake or otherwise, nearly the entire city of Longview could be devastated, even if waters rose only 10 feet. In addition, Cascadia subduction zone great earthquakes are commonly associated with a sudden drop in elevation of a few feet in coastal areas (Peterson and others, 1993). Such an event could be devastating to the study area, possibly allowing Columbia River and ocean waters to inundate the heavily populated, lower elevation communities if subsidence occurred this far inland as well.

Volcanic activity is also a viable threat to the study area and surrounding region. The lahar produced from the May 1980 eruption of Mt. St. Helens inundated communities (e.g., Castle Rock) upstream along the Cowlitz River floodplain, and the potential exists for a similar occurrence in the Longview-Kelso area. The lateral blast and ensuing major landslide on the north face of Mt. St. Helens produced several large lahars that reached the mouth of the Columbia River via the Toutle and Cowlitz Rivers,

and created a pyroclastic delta that blocked the shipping channel in the Columbia River for several weeks until the Army Corps of Engineers cleared it away. Hyperconcentrated flows of Mt. St. Helens volcanic ash and debris were largely confined to the undeveloped flood plains and walled-in by natural levees, so damage to the Longview-Kelso area was minimal. Not only could lahar floodwaters back up at the confluence of the Cowlitz and Columbia Rivers, but a hydrologic obstruction such as the narrowing of the Cowlitz River drainage at Rocky Point could cause hyperconcentrated flows to back up north of this location, flooding communities upstream. In addition, the potential eruption and ensuing glacial melt off of Mt. Adams or Mt. Hood lahars could overwhelm flood control measures on the Columbia River. Air fall ash from any one of the large stratovolcanoes in the area could cause damage to both motor vehicles and crops, depending on the prevailing wind at the time of eruption. Volcanic ash did fall on the Longview-Kelso area during the May, 1980 eruption of Mt. St. Helens. Volcano-related earthquakes related to shifting magma might also cause minor damage in the area.

The greatest active danger to area residents and properties is the threat of landslides, particularly during severe storm events associated with high precipitation or snow melt off. Several geologic units in the map area (Plate 1) are prone to slope failure, especially semiconsolidated Troutdale Formation gravels and soft Toutle Formation clayey siltstones and sandstones, particularly where they dip parallel to the slope. The Aldercrest-Banyon landslide (described in the next section) is a reminder of this danger, as is the reactivated older slide in the Toutle Formation at Site 49 that failed almost immediately after being bulldozed and undercut. The marked increase in housing development in the area in recent years makes it all the more important to recognize the

landslide threat. Before any new building in the study area is constructed, careful consideration should be given to the geologic unit on which the structure is being built. As examples, dip slopes, bowl-shaped drainages, and hummocky topography in the Toutle Formation should be avoided, as should perhaps all future development on semi-consolidated Troutdale gravels. Consideration should be given as to whether trees in the area of development have J-shaped ("pistol butt") bases, or if springs, visible cracks in the ground or pavement, or slide-related ponds and poor drainage exist on or near the prospective property.

Aldercrest-Banyon landslide

The 1998 Aldercrest-Banyon Landslide, near the southeast corner of the study area (Sec. 36, T 8 N, R 3 W, Plate 1), is the second largest landslide disaster involving homes in the history of the United States (Burns and others, 2002). Unusually high precipitation over the previous three years led to reactivation of an ancient landslide that likely originally occurred during the Pleistocene Missoula Floods. The landslide occurred in permeable unconsolidated Troutdale Formation gravels and overlying sandstone, and slid over a paleosol developed on the less permeable Eocene Cowlitz Formation (Wegmann and Walsh, 2001). This disaster destroyed 60 homes (Figure 81) and threatened 77 more on the surrounding slopes and above the headscarp. The maximum slide movement in 1998 was approximately 15-30 cm/day, ultimately creating a headscarp 35 meters high (maximum) and 1000 meters in width. Damage to private property in this housing subdivision built in the early 1970s is estimated to be about $25.7 million, and damage to infrastructure another $6.2 million (Burns and others,

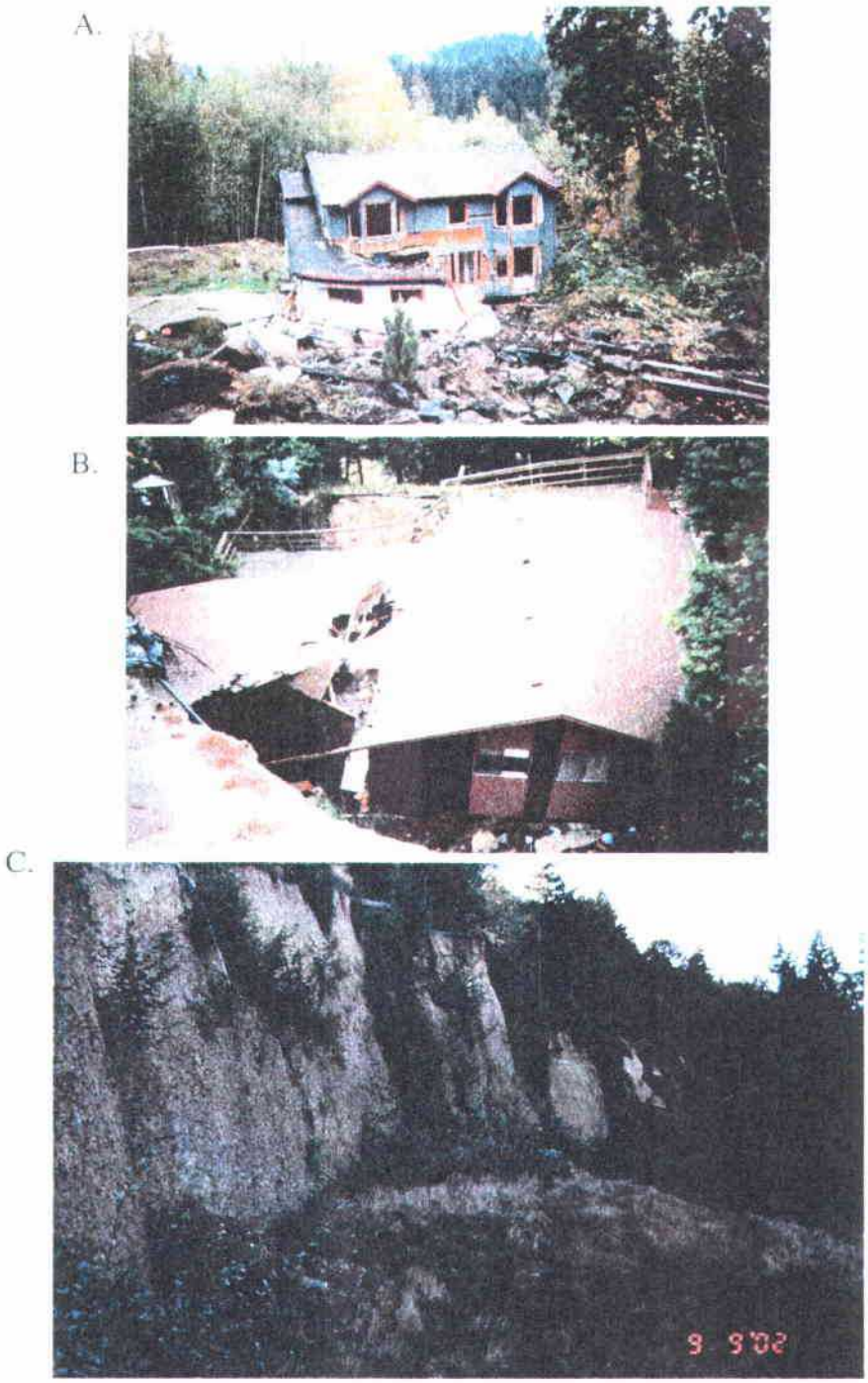

Figure 81: Aftermath of the 1998 Aldercrest-Banyon Landslide.
A.& B. Homes destroyed by the landslide. The house in photograph A was moved several meters from its original location. The house in photograph B came to rest about 20 meters beneath its own driveway (seen in the lower left). Photographs taken in 1999, both views toward the east.
C. Side view of the 20-30-meter high headscarp. The entire cliff consists of Troutdale Formation cobbles (lower ¾), and Troutdale cross-bedded semi-consolidated sandstone (upper ¼). Photograph taken in 2002.

2002). Reactivation of this slide was mostly due to the increased precipitation (increasing sediment pore pressure), but human activities may have helped initiate the process (Burns and others, 2002). At the time of the initial movement, an excavation across the lower part of the landslide to construct a road was underway, which may have led to the breakage of storm drains that added to the water content of the Troutdale gravels. In addition, a logging operation at the toe of the landslide was underway. To further illustrate the danger of building on Troutdale gravels, another landslide on the southwest side of the same hill has begun to reactivate (the Haussler Road-Apple Lane landslide). Eighty eight homes are in danger below the scarp, and another 42 above it.

.

GEOLOGIC HISTORY

During early-middle Eocene time, relative northeastern movement of the Farallon and Kula oceanic plates slowly moved the basaltic seamount chain of the Siletzia Terrane toward the subduction zone of western North America (Wells and Coe, 1985). Accretion of this terrane forced the subduction zone to jump westward, from approximately the current position of the Cascade mountain range, to near its present position off the coast on the continental slope. This event also produced northeast-southwest compression, and the production of a northwest-southeast fault and fold trend, with resulting uplift and erosion (Wells and Coe, 1985; Armentrout, 1987). Part of this was the Willapa Hills uplift approximately 20 miles (32 km) northwest of the study area. This compressional/subduction event was soon followed by a period of extension during the middle Eocene, producing a large forearc basin (~640 km long) that extended from the Klamath Mountains of southwest Oregon to Vancouver Island, Canada (Niem and Niem, 1984; Niem et al., 1992). Differential subsidence of the Siletzia Terrane (termed the Crescent Formation in southwest Washington and the Siletz Volcanics in Oregon) produced several smaller basins. One such basin formed to the north and east of the study area (the Chehalis Basin), immediately to the east of the Willapa Hills uplift (Figure 3).

Within the Chehalis Basin and elsewhere in the region, bathyal slope mudstones and thin turbidites of the lower McIntosh Formation began to cover the underlying basalts and gabbro intrusions of the Siletzia Terrane. This was deposited as a lowstand, transgressive, and high stand system tract and represents deposition by distal turbidity currents. McIntosh Formation mudstones, derived from erosion of Mesozoic continental

crust in Washington (i.e., Okanogan uplift, the Northern Cascades, and the Idaho Batholith)(Payne, 1998), onlap the Crescent Formation in the Willapa Hills (Wells, 1981), demonstrating that the hills were a paleo-topographic high in the late-middle Eocene, resulting either from compressional uplift from accretion (Wells and Coe, 1985), or remnant seamount topography (Stanley et al., 1994). In the type area of the Cowlitz Formation, slope to outer shelf siltstones and bathyal mudstones of the lower McIntosh Formation are overlain by shallow marine upper shoreface sandstones of the upper McIntosh Formation (Payne, 1998). Approximately one hundred thirty meters of shoreface sandstone and coal of the upper McIntosh was deposited on a wave-scoured erosional surface cut down into the underlying deep marine mudstones, representing a sharp sequence boundary between the two units (recording a relative sea level fall). This boundary has been correlated to the 42.5 Ma eustatic sequence boundary of Haq et al. (1987). Another marine transgression deposited a ~500-meter thick bathyal siltstone of the upper member of the McIntosh Formation, and the ensuing transgressive highstand system tract produced a prograding delta front sandstone that caps the formation (Payne, 1998).

Another sequence boundary separates the highstand mudstone of the upper McIntosh Formation and the comparatively shallow marine sandstone deposits of unit 1A of the Cowlitz Formation, ending 3rd order transgressive-regressive cycle 3 (Payne, 1998). In southwest Washington micaceous, arkosic sand of the Cowlitz delta prograded westward, covering the deep-marine facies of the upper McIntosh. The Cowlitz Formation is part of the large deltaic system of the Eocene Puget Group, produced from metamorphic and granitic sources transported into the forearc basin by the ancestral

Columbia River, from Rocky Mountain sources to the east. The Cowlitz Formation represents 3 transgressive-regressive 3rd order cycles (relative sea level fluctuations). The lowermost part of the type Cowlitz Formation as described by Payne (1998) was deposited during a regressive or lowstand event. This progradational phase ultimately produced several marginal marine and coal-bearing delta plain (shoaling or prograding) parasequences that form an aggradational parasequence set. In Coal Creek, 4 progradational parasequences define this lowermost portion of the Cowlitz Formation in the study area, correlative to unit 1B of the type section. Overlying the uppermost coal of unit 1 (coal B) is a ~35-meter thick Grays River basalt volcaniclastic, representing a major pulse of volcanic activity and erosion from the Grays River highlands to the west. This is likely part of the same pulse that produced the Lower Grays River Volcaniclastic breccias and conglomerates (Tgvs1) that underlies most of the arkosic Cowlitz Formation throughout the study area. A molluscan assemblage at the base of this volcaniclastic (overlying a coal) also shows that it represents a minor shallow marine transgression, marking the base of unit 2. This unit is defined by numerous Grays River volcaniclastic interbeds (Tgvs2), attesting to ongoing eruptive activity and erosion of the volcanic shield. Most of unit 2 consists of 7 progradational parasequences representing a largely aggradational parasequence set of shallow marine to delta plain successions, where most parasequences fine- and thin-upward and terminate in a thin coal or carbonaceous shale. Toward the top of unit 2, a major marine transgression occurs (a maximum flooding surface), above which lower shoreface to shelf mudstones and siltstones were deposited over delta front sands of the upper shoreface.

A sequence boundary at the top of parasequence 12 (top of unit 2, Plate 2) juxtaposes upper shoreface sandstone against middle shoreface storm- and wave-generated hummocky and swaley fine-grained sandstone of the middle shoreface. This defines the base of unit 3, which consists of 6 progradational parasequences of middle shoreface to delta plain successions, constituting 3rd order cycle 4 of a lowstand system tract. Thin deposits of deep marine facies above unit 3 may be remnants of deep marine unit 4 (3rd order cycle 4) of Payne (1998) in the type section. Scoured into the highstand distal turbidite facies of unit 4 (?) is the submarine channel facies of the lower part of unit 5, which forms an erosional parasequence boundary between cycles 4 and 5. This facies is overlain by distal turbidites. Western Cascade-derived airfall tuffs are preserved in several coal-bearing coastal plain deposits of the Coal Creek section, attesting to minor explosive activity of the Cascade volcanic calc-alkaline arc throughout the late-middle Eocene.

Grays River volcaniclastic interbeds in the Cowlitz Formation in the study area, as well as the underlying thick pile of Grays River volcaniclastics and flows, are part of the Lower Grays River Volcanics as described by Payne (1998) and Kleibacker (2001). This volcanic episode is associated with a period of northeast-southwest extension and emplacement of northwest-trending Grays River dikes beginning at about 40 Ma, and probably continuing throughout the duration of both the lower and upper Grays River eruptive episodes from ~40 to 36 Ma (which are separated by an unconformity north of the study area). The period of dextral transtension induced by volcanic inflation and continuing oblique subduction of the Farallon Plate, caused some clockwise tectonic rotation of crustal blocks, and produced horst and graben-style, northwest-trending

dextral oblique-slip faults and subordinate northeast-trending conjugate normal faults which offset these middle Eocene units. This late-middle Eocene transtensional period resulting from inflation of magma, produced uplift and an erosional unconformity (major sequence boundary II of Armentrout), which marks a period of reorganization of the Farallon Plate, affecting the tectonically active margin of North America and part of South America.

In the early Oligocene, during a lowstand period, the Cowlitz Formation sediments were overlain by a paleo valley-fill sequence, the Toutle Formation, consisting of meandering river sand channels incised into the upper deep-marine facies of the Cowlitz Formation (a sequence boundary at the top of unit 5)(Payne, 1998). These tuffaceous strata, including both marine and coastal plain fluvial facies, consist of a combination of wave- and stream-reworked micaceous and arkosic Cowlitz Formation sands, and tuffaceous, calc-alkaline silicic pyroclastic material derived from the Cascade calc-alkaline volcanic arc to the east. A broad coastal plain existed in the study area at this time, with meandering streams and shallow lakes on the floodplain (Figure 35), depositing cross-bedded sandstone point bar sequences and overbank tuffaceous, laminated siltstones.

The Paleogene volcanic and sedimentary units in the area (Crescent Formation, Grays River Volcanics, Cowlitz Formation, Toutle Formation, and upper Eocene basaltic andesite flows and andesite dikes derived from the western Cascades) were folded, faulted, and uplifted during the transpressional event starting in the late-middle Miocene. This wrench tectonic event produced the transpressional Coal Creek Fault, Kelso Fault Zone, and both the Columbia Heights Anticline and Hazel Dell Syncline. It also

reactivated many of the northwest-trending transtensional normal faults of the late-middle Eocene. Erosion of the paleotopography created from this compression produced low rolling hills. Into this environment Columbia River Basalt flows, erupting from fissures in eastern Oregon and Idaho during the early to middle Miocene (Reidel and others, 1989), flowed down the ancestral Columbia River drainage and into the study area. At least 6 Columbia River Basalt flows (3 Ortley, 1 Sentinel Bluffs, and at least 1 Frenchman Springs (Sand Hollow), and at least 1 Pomona flow (Saddle Mt. Formation) entered the area. Remnant erosional paleotopography of the Eocene and Oligocene units in the Columbia Heights fold forced the lower Ortley flow (#1) to go around, accounting for the lack of this unit there. Continued transpressional uplift along the northwest-trending faults produced faulting and differential uplift of the Columbia River Basalts and underlying sedimentary units into a complex horst in the study area.

Ancestral Columbia River gravels and sand, a mixture of local volcanic clasts and metamorphic quartzite and granitic rocks transported through the Cascades from eastern Oregon, Idaho, and Montana during the Pliocene (and possibly the latest Miocene), deposited the Troutdale Formation gravels. These nearly horizontal deposits are in angular unconformity with underlying Eocene and Oligocene units, and represent the coarse-grained thalweg deposits, and to a lesser degree overbank floodplain sand and silt, of the ancestral Columbia River. Similar age terraces along the Cowlitz River consist mostly of andesite gravel from a local western Cascade source. These semiconsolidated to unconsolidated formations in the study area, up to 300 feet thick, have been uplifted to form high terraces, attesting to continued broad uplift throughout the Pliocene and into the Quaternary. During the late Pleistocene, catastrophic Missoula Floods deposited

coarse gravels and sands up into the drainage of the Cowlitz River, and have since also been uplifted to form the Quaternary terraces along the Cowlitz River. Oversteepening of hillsides in the area, due to erosional resistance of Columbia River Basalts capping some of the hills, and also partly due to undercutting of units by the Missoula Floods, has produced several Pleistocene and Holocene landslide deposits within the study area. During the 1980 eruption of Mt. St. Helens, lahars rushed down the Toutle and Cowlitz Rivers, inundating some communities, depositing gray ash and gravel along the Cowlitz River, and creating a lahar delta at the mouth of the Cowlitz River.

CONCLUSIONS

Detailed lithological descriptions of a stratigraphic section of middle Eocene Cowlitz Formation in Coal Creek, and geologic mapping of the Longview-Kelso area of southwest Washington allowed interpretation of the geologic history of the area. The Cowlitz Formation was studied using biostratigraphy, magnetostratigraphy, lithostratigraphy, sequence stratigraphy, x-ray diffraction, and petrography. The goal was to interpret the diagenetic history, provenance, depositional environment, and hydrocarbon potential, and correlate the Cowlitz Formation in the study area to the type area in Olequa Creek to the north. Eocene and Miocene volcanic units in the area were identified, studied and mapped using lithology, petrography, geochemistry, and magnetic polarity. Another goal was to investigate the structural history and assess the natural hazard potential of the area through geologic mapping. In summary, the major results and interpretations of this study are:

1. The 650-meter thick stratigraphic section of the Cowlitz Formation in Coal Creek represents three 3rd order transgressive/regressive cycles and has been divided into 5 informal units in this study that correlate well to the Cowlitz Formation type section near Vader 20 km to the north. The lower 100 meters of the Coal Creek section (informal unit 1, Chron 18r) was deposited in a highstand system tract (HST) in the lower portion of 3rd order cycle 3. This micaceous/arkosic sandstone unit is dominantly tidal reflecting upper shoreface to lower delta plain/swamp depositional environments, and consists of 4 shoaling-upward (both coarsening- and thickening-upward, and thinning- and fining-upward) parasequences of an aggradational to retrogradational

parasequence set. The upper part of unit 1 contains two coal beds (A and B) that were used to correlate the complexly folded and faulted northern portion of Coal Creek. The overlying unit 2 (Chron 18n) is defined by abundant mollusk-bearing shallow marine Grays River basalt volcaniclastic interbeds that intertongue with Cowlitz Formation arkosic sandstone and siltstone, and represents the latter part of 3rd order cycle 3. The 7 parasequences that comprise this aggradational set are largely thinning- and fining-upward and terminate in thin upper coal beds, representing middle shoreface to lower delta plain successions. The base of unit 2 is a 35-meter thick Grays River basalt volcaniclastic tongue that is dominantly rounded basalt pebble conglomerate and coarse basalt sandstone to the south and dominantly graded thin beds of sandstone to siltstone to the north. A maximum flooding surface occurs near the high stand system tract top of unit 2. Unit 3 comprises 3rd order cycle 4 (Chron 17r), a lowstand system tract, and consists of 6 mostly fining-and thinning-upward parasequences of lower shoreface to delta plain coal-bearing facies associations. A sequence boundary separates unit 5 from a thin deep marine bedset that may be part of unit 4 of the type section Payne (1998). Unit 5 (Chron 17r) consists of deep marine facies. The mostly massive sandstone facies at the base is incised into the underlying units, and represents low stand system tract deep marine channel-fill. This is overlain by thinly-bedded to laminated overbank distal arkosic turbidites of unit 5 that define the top of the Coal Creek section.

2. A different interpretation of the Coal Creek section is being proposed in this study. Structural and lithological data suggest that the Coal Creek section is essentially two separate stratigraphic sections that are partially correlated by a distinctive 35-meter thick basalt volcaniclastic marker unit that occurs at the base of the southern section, and the top of the northern section. The northern section is an upfaulted sequence that contains different and older lithologic units than the southern section.
3. In this study, Grays River Volcanics within the map area have been differentiated into two units. The lower unit is over 150 meters thick and consists of basaltic subaerial flows, invasive flows, basalt dikes, some sills, and thick volcaniclastic breccias. The lower Grays River volcaniclastic unit overlies and is partially interfingered with Gray River flows in the study area and is subdivided into 5 informal facies: 1) channelized fluvial gravels, 2) matrix supported debris flow deposits, 3) hyperconcentrated flow deposits, 4) phreatomagmatic scoriaceous hyaloclastite, and 5) autoclastic flow breccia. The upper Grays River volcaniclastic unit consists of pebble and cobble volcanic conglomerate and coarse-grained basalt sandstone interbeds that interfinger with the Cowlitz Formation. These basaltic sedimentary interbeds commonly contain shallow marine to brackish water molluscan fossil and trace fossil assemblages and represent minor marine transgressive flooding surfaces or storm wave/tsunami wave-lag deposits.
4. Grays River basalt flows and intrusions are augite-, olivine-, and plagioclase-phyric, and are commonly glomeroporphyritic with a distinctive pilotaxitic

flow texture of aligned plagioclase microlites. Unless weathered, major element geochemistry of Grays River basalts from the study area falls within the fields defined by Phillips et al. (1989) and are high TiO_2 and iron tholeiitic basalts. Flows and scoriaceous bedded breccia from near Rocky Point, in the core of the Columbia Heights Anticline, also fall within these fields, but are anomalously low in TiO_2. Therefore, they are considered in this study to be a separate volcanic subunit. The two small hills that comprise Rocky Point are the remnants of an isolated phreatomagmatic tuff cone or cinder cone erupting into the middle Eocene Cowlitz arkosic estuary, and may represent mixing of the tholeiitic Grays River magma, and calc-alkaline magma of the nearby western Cascade arc. Over 60 originally near-vertical Grays River basalt dikes and sills intrude the Cowlitz Formation in Coal Creek, and are typically aphyric to glomeroporphyritic, but thicker dikes are somewhat zoned with coarser crystalline interiors. One dike intruding an interval low in the section has been dated at 40 ± 0.36 Ma.

5. Late Eocene western Cascade volcanism produced thick basaltic andesite flows and andesite dikes in the easternmost part of the study area. Basaltic andesite occurs as subaerial flows up to 100 meters thick, capping the hills east of the Cowlitz River. These flows, partly correlative to the late Eocene Goble Volcanics of northwest Oregon, are columnar-jointed, augite- and plagioclase-phyric, more porphyritic that Grays River flows and higher in SiO_2, and lower in FeO and TiO_2 than Grays River basalt flows and dikes. Two parallel western Cascade andesite dikes intrude the Cowlitz Formation

are significantly more silicic, more alkaline, and lower in FeO than Grays River basalt and western Cascade basaltic andesite flows.

6. Unconformably overlying Grays River Volcanics and the Cowlitz Formation in the study area are clayey and commonly tuffaceous siltstones, silty sandstones, and tuffaceous arkosic sandstones of the Toutle Formation. This unit is distinguished from the underlying Cowlitz Formation in that it is not intruded by Grays River dikes, does not contain mollusk-bearing Grays River volcaniclastic interbeds, contains significantly more clay and tuff, contains unusual trace fossils, and is noticeably lighter in color. The unit has been tentatively dated by leaf fossils as late Eocene/early Oligocene. This formation is divided into two informal facies in the study area. The lower shallow marine unit contains abundant vertical burrows and sparse molluscan fossil molds, but is otherwise mostly massive with few distinguishing characteristics. The upper unit consists dominantly of two lithologies: fining-upward, fluvial channel trough cross-bedded sandstone, and thinly bedded to laminated lacustrine and overbank clayey siltstones and silty sandstones, representing point bar sequences and overbank siltstones of a coastal plain with flood basins and oxbow lakes. The Toutle Formation sandstones and siltstones are a mixture of reworked Cowlitz Formation extrabasinal clasts (feldspar, quartz, mica, and granitic/metamorphic grains) and western Cascade silicic pyroclastic material in the form of pumice, andesite, and dacite fragments and clay-altered glass shards.

7. The early to middle Miocene Columbia River Basalt Group overlies these Paleogene sedimentary and volcanic units in angular unconformity. At least 6 separate Columbia River Basalt flows occur in the study area based on stratigraphic relationships, lithology, magnetic polarity, major oxide geochemistry, and weathered soil characteristics. The lowermost flow (N_2, low MgO, Ortley flow #1 of the Grande Ronde Formation) is absent from the Columbia Heights area (likely resulting from paleotopography at the time of the flow) and forms a pillow/palagonite complex in the upper quarry on Mt. Solo. It appears to be subaerial elsewhere. N_2, intermediate MgO Ortley flow #2 is the thickest in the study area (~30 meters) and is characterized by well-developed upper and lower colonnade. This flow appears to be locally invasive in one location. Overlying N_2, low MgO Ortley flow #3 is subaerial in the area except for the Storedahl Quarry where it forms a basal pillow palagonite complex where it flowed into a lake. A 0-5 meter-thick tuffaceous interbed overlies the 3 Ortley flows and underlies the Sentinel Bluffs flow of the Grande Ronde Formation. This interbed appears to occur throughout the study area, and is in part a tuffaceous siltstone with root traces and vertical burrows, and in part a pebble to cobble conglomerate. The N_2 Sentinel Bluffs flow is high in MgO. The Frenchman Springs (Sand Hollow) flow of the Wanapum Formation is poorly exposed in the study area and occurs only as an isolated exposure in the Eufaula Heights area west of Coal Creek. It is mapped largely by the occurrence of reddish soil, but one exposure of even-sized, large colonnade with sparse large labradorite phenocrysts identifies this

unit. Pomona flows are mapped based on the regional geologic map work of other authors.

8. Pliocene gravels and arkosic sand of the Troutdale Formation form terrace deposits up to 100 meters thick in southern parts of the study area, and represent the paleo-thalweg and overbank flood deposits of the ancestral antecedent Columbia River. Clasts are a mixture of extrabasinal granitic and metamorphic quartzite clasts from Rocky Mountain sources, and basaltic andesite and basalt from the western Cascades and backarc Columbia River Basalts. Troutdale gravels grade northward into gravel terrace deposits of the same age transported along the ancestral Cowlitz River, that are dominantly composed of andesite gravel and sand from the western Cascades. Lower terraces along the Cowlitz River are also dominantly andesitic clasts but have an extrabasinal component of granitic and metamorphic clasts. These are thought to be deposits of the late Pleistocene Missoula Floods. These unconsolidated to semiconsolidated Pliocene through Pleistocene terrace gravels and sands are prone to landslides. The devastating Aldercrest-Banyon landslide occurred in Troutdale Formation gravels at the impermeable weathered soil contact with the underlying Cowlitz Formation.
9. Forearc extension in the late-middle Eocene produced a northwest-trending set of oblique-slip normal faults along which Grays River dikes intruded. Starting in the early Miocene the region underwent transpressional wrench faulting, reactivating many of the northwest-trending faults in oblique-slip motion, and producing the Columbia Heights Anticline, Hazel Dell Syncline,

Coal Creek Fault, and Kelso Fault Zone. Topography produced from this event in the tilted Cowlitz, Grays River, and Toutle strata eroded down to a nearly flat plain before emplacement of the Columbia River Basalts. The Columbia River Basalts that filled the topographic lows were later faulted by continued activity along the northwest-trending faults, producing differential uplift. Continued post late-middle Miocene broad uplift of the Coast Range has resulted in incisement of the ancestral Columbia and Cowlitz Rivers, creating Pliocene through Pleistocene terraces.

10. The natural gas potential in the study area is low to moderate. This is due to breaching of the Cowlitz Formation sandstones and coals by erosion. Cowlitz Formation in the study area is unlikely to be a source rock for thermally mature hydrocarbons. Even though the McIntosh Formation may underlie the study area (the equivalent Hamlet Formation is the dominant source for thermogenic methane at the Mist Gas Field), thermal maturation of these strata in southwest Washington is poor. However, 8 substantial coals within the Coal Creek section could act as local sources for biogenic or coal bed methane. The lithic arkosic sandstones of unit 1 and associated thin coals have acted as a minor biogenic source rock and reservoir for methane. The ~35-meter thick overlying well-indurated Grays River basalt volcaniclastic beds act as a seal, and water wells through this stratigraphic trap have produced groundwater bubbling with methane. The Columbia Heights Anticline with overlying Columbia River Basalts could also act as a local structural trap. Lithic arkosic sandstones in the study area are dirty compared

to the C & W sandstone of the Mist Gas Field in northwest Oregon because of the heavy slack water tidal influence during deposition, with the associated flaser mud and carbonaceous debris. In addition, the comparatively high percentage of Grays River basalt lithic clasts and interbeds in the study area has led to decreased porosity and permeability of both the basaltic and arkosic units, due to diagenetic clay alteration of this basaltic detritus to form pore-clogging smectite rims and sparry calcite cement.

11. Geologic hazards include lahars, hyperconcentrated flows, and debris flows such as those from the May, 1980 eruption of Mt. St. Helens. Other hazards include potential liquefaction of water saturated silts and clays in heavily populated and industrial portions of Longview and Kelso during the seismic shaking of great earthquakes. 100-year winter and spring floods are another geologic hazard to low-lying areas. However, landslides represent the greatest and most common hazard, particularly to upland areas underlain by unconsolidated Troutdale Formation gravels.

REFERENCES

Armentrout, J.M., 1973, Molluscan paleontology and biostratigraphy of the Lincoln Creek Formation (late Eocene-Oligocene), southwestern Washington: Seattle, WA, University of Washington Ph.D. dissertation, 479 p.

Armentrout, and Suek, D.H., 1985, Hydrocarbon exploration in western Oregon and Washington: American Association of Petroleum Geologists Bulletin, v. 69, p. 627-643.

Armentrout, 1987, Cenozoic stratigraphy, unconformity bounded sequences, and tectonic history of southwest Washington, *in* Schuster, J.E., ed., Selected papers on the geology of Washington: Washington Department of Natural Resources, Division of Geology and Earth Resources Bulletin 77, p. 291-320.

Beeson, M. H., and Moran, M. R., 1979, Columbia River Basalt Group stratigraphy in western Oregon: Oregon Geology, v. 41, no. 1, p. 11-14.

Beeson, M. H., Perttu, R., and Perttu, J., 1979, The Origin of the Miocene basalts of coastal Oregon and Washington: An alternative hypothesis: Oregon department of Geology and Mineral Industries, Oregon Geology, v. 41, no. 10, p. 159-166.

Beeson, M. H., and Tolan, T. L., 1985, Regional correlations within the Frechman Springs Member of the Columbia River Basalt Group: New insights into the middle Miocene tectonics of northwestern Oregon: Oregon Geology, v. 47, p. 87-92.

Beeson, M.H., Tolan, T.L., and Anderson, J.L., 1989, The Columbia River Basalt Group in western Oregon; Geologic structures and other factors that controlled flow emplacement patterns: *in* Reidel, S.P., and Hooper, P.R., eds., Volcanism and tectonism in the Columbia River flood-basalt province: Geological Society of America Special Paper 239, p. 223-246.

Bentley, R.D., Professor Emeritus, Central Washington University: personal communication, 2000.

Berkman, T.A., 1990, Surface-subsurface geology of the middle to upper Eocene sedimentary and volcanic rock units, western Columbia county, northwest Oregon: Corvallis, Oregon, Oregon State University, masters thesis, 413 p.

Blakely, R.J., Wells, R.E., Yelin, T.S., Madin, I.P., and Beeson, M.H., 1995, Tectonic setting of the Portland-Vancouver area, Oregon and Washington: Constraints from low-altitude aeromagnetic data: Geological Society of America Bulletin, v. 107, p. 1051-1062.

Buckovic, W.A., 1979, The Eocene deltaic system of west-central Washington, *in* Armentrout, J.M., Cole M.R., and Terbest, J., Jr. eds., Cenozoic paleogeography of the western United States: Pacific Coast Paleogeography Symposium 3, SEPM Pacific section, p. 147-163,

Burns, S.F., Kuper, H.T., and Lawes, J.L., 2002, Landslides at Kelso, Washington, and Portland, Oregon: *in* Moore, G .W., Field guide to Geologic Processes in Cascadia: Oregon Department of Geology and Mineral Industries Special Paper 36, p. 257-272.

Chan, M.A., and Dott, R.H., Jr., 1986, Depositional facies and progradational sequences in Eocene wave-dominated deltaic complexes, southwest Oregon: American Association of Petroleum Geologists bulletin, v. 70, no. 4, p. 415-430.

Clifton, H.E., Phillips, R.L., and Anima, R.J., 1989, Sedimentary facies of Willapa Bay, Washington – a field guide: Canadian Society of Petroleum Geologists, Calgary, 9 p., 52 Figures.

Droser, M., and Bottjer, D., 1986, Ichnofabric indices: Journal of Sedimentary Petrology, v. 96, p. 558-559.

Duncan, R.A., 1982, a captured island chain in the Coast Range of Oregon and Washington: Journal of Geophysical Research, v. 87, p. 10593-10609.

Eriksson, A., 2002, Stratigraphy, Structure, and Natural Gas Potential, of Tertiary sedimentary and Volcanic Units, Clatskanie 7.5-Minute Quadrangle, Northwest Oregon: Corvallis, Oregon, Oregon State University, masters thesis, p. 1-215.

Evarts, R. C., and Swanson, D.A., 1994, Geologic transect across the Tertiary Cascade Range, southern Washington, *in* Swanson, D.A., and Haugerud, R.A., eds., Geologic field trips of the Pacific Northwest, 1994 Geological Society of America Meeting: Seattle, Washington, Department of Geological Sciences, University of Washington, v. 2, p. 2H-1-2H-31.

Evarts, R. C., 2002, Geologic map of the Deer Island quadrangle, Columbia county, Oregon and Cowlitz County, Washington: United States Geological Survey, Miscellaneous Field Map MF-2392, and accompanying pamphlet, 45 p.

Evarts, 2003, United States Geological Survey, Menlo Park, California: personal communication to A.R. Niem, 2003.

Farr, L.C., Jr., 1989, Stratigraphy, diagenesis, and depositional environments of the Cowlitz Formation (Eocene), northwest Oregon: Portland, Oregon, Portland State University, 169 p.

Finn, C., Phillips, W.M., and Williams, D.L., 1991, Gravity anomaly and terrain maps of Washington: United States Geological Survey Geophysical Investigations Map GP-988.

Folk, R.L., 1974, Petrology of sedimentary rocks: Austin, Texas, Hemphill, 182 p.

Haq, B.U., Hardenbol, J., and Vail, P.R., 1987, Chronology of fluctuating sea levels since the Triassic: Science, v. 235, p. 1165-1167.

Harding, T.P., 1973, Newport-Inglewood trend, California-an example of wrench style of deformation: American Association of Petroleum Geologists Bulletin, v. 57, No 1, p. 97-116, 15 Figures.

Henriksen, D.A., 1956, Eocene Stratigraphy of the lower Cowlitz River-eastern Willapa Hills area southwestern Washington: Washington Division of Mines and Geology, Bulletin 43, 122 p.

Hodge, E.T., 1938, Geology of the Lower Columbia River: Geological Society of America Bulletin, v. 49, p. 836-929.

Howard, K.A., 2002, Geologic map of the Battle Ground quadrangle, Washington: United States Geological Survey Miscellaneous Field Studies Map MF-2395, scale 1:24,000.

Irvine, T.N., and Barager, W.R.A., 1971, A guide to the chemical classification of the common volcanic rocks: Canadian Journal of Earth Sciences, v. 8, p. 523-548.

Irvine, A.J., Nesbitt, E.A., and Renne, P.R., 1996, Age constraints on earliest Cascade arc volcanism and Eocene marine biozones from a feldspar-rich tuff in the Cowlitz Formation, southwest Washington: EOS Transactions of the American Geophysical Union, v. 77, no. 46, p. F-814.

Jackson, M. K., 1983, Stratigraphic relationships of the Tillamook Volcanics and the Cowlitz Formation in the upper Nehalem River-Wolf Creek area, northwestern Oregon: Portland, OR, Portland State University master's thesis, 112 p.

Johnson, S.Y., Tennyson, M.E., Lingley, W.S, Jr., and Law, B.E., 1997, Petroleum geology of the state of Washington: United States Geological Survey Professional Paper 1582, 40 p.

Kenitz, S., 1997, Correlation of volcanic rocks within the middle-upper Eocene (Narizian Stage) sedimentary rocks in the Mist Gas Field area, Columbia County, Oregon: Portland, Oregon, Portland State University, masters thesis, p. 1-70.

Kleibacker, D.W., 2001, Sequence Stratigraphy and Lithofacies of the middle Eocene upper McIntosh and Cowlitz Formations, Geology of the Grays River Volcanics, Castle Rock-Germany Creek area, southwest Washington: Corvallis, Oregon, Oregon State University, masters thesis, p. 1-215.

Le Bas, M. J., Le Maitre, R. W., Streckeisen, A., and Zanettin, B., 1986, A chemical Classification of volcanic rocks based on the total alkali-silica diagram: Journal Of Petrology, v. 27, p. 745-750.

Livingston, V.E., 1966, Geology and mineral resources of the Kelso-Cathlamet area, Cowlitz and Wahkiakum Counties, Washington: Washington Division of Mines and Geology, Bulletin 54. p. 110.

May, D.J., 1980, The paleoecology and depositional environment of the late Eocene-early Oligocene Toutle Formation, southwest Washington: Seattle, Washington, University of Washington, masters thesis, 110 p.

Meyer, J, and Niem, A. R., 2002, An example of late Eocene/early Oligocene sea floor topography imaged by 3D seismic data, Mist Gas Field, and in outcrop, N. Coast Range, Oregon: Geological Society of America, Abstracts with Programs (Cordilleran section in Corvallis).

Mitchum, R.M., 1977, Seismic stratigraphy and global changes of sea level, Part 1, *in* C.E. Payton, ed., Seismic stratigraphy-applications to hydrocarbon exploration: AAPG Memoir 26, p. 53-62.

Miyashiro, A., 1974, Volcanic rock series in island arcs and active continental margins: American Journal of Science, v. 274, p. 321-355.

Moothart, S.R., 1992, Geology of the middle and upper Eocene McIntosh Formation and adjacent volcanic and sedimentary rock units, Willapa Hills, Pacific County, southwestern Washington: Corvallis, Oregon, Oregon State University, masters thesis, 265 p.

Mumford, D.F., 1988, Geology of the Elsie-lower Nehalem River area, south-central Clatsop and northernmost Tillamook counties, northwestern Oregon: Corvallis, Oregon, Oregon State University, masters thesis, 392 p.

Murphy, T. M., 1981, Geology of the Nicolai Mountain-Gnat Creek area, Clatsop County, northwest Oregon: Corvallis, Oregon, Oregon State University M.S. Thesis, 355 p.

Myers, J., Associate Professor, Western Oregon University, personal communication, 2001.

Nelson, D.E., 1984, Geology of the Fishhawk Falls-Jewell area, Clatsop county, Oregon: Corvallis, Oregon, Oregon State University, masters thesis, 360 p.

Nesbitt, E., 1995, Paleoecological analysis of molluscan assemblages from the middle Eocene Cowlitz Formation, southwest Washington: Journal of Paleontology, v. 69, no. 6, p. 1060-1073.

Nesbitt, E., Research Associate, Thomas Burke Memorial Washington State Museum written and personal communication, 1999.

Niem, A. R., and Niem, W.A., 1984, Cenozoic geology and geologic history of western Oregon, *in* Kulm, L.D., et al., eds., Western North America continental margin and adjacent ocean floor off Oregon and Washington: sheet 17.

Niem, A. R., MacLeod, N.S., Snavely, P.D., Jr., Huggins, D., Fortier, J.D., Meyer, H.J., Seeling, A., and Niem, W.A., 1992, Offshore-onshore geologic cross section, northern Oregon Coast Range to continental slope: Oregon Department of Geology and Mineral Industries continental Margin Transect OGI-26, 10 p., 1 plate.

Niem, W. A., Niem, A. R., and Snavely, P. D., Jr., 1992, early and Mid-Tertiary oceanic realm and continental margin – western Washington-Oregon coastal sequence; *In* Burchfiel, B. C., Lipman, P. W., and Zoback, M. L., eds., The Cordilleran Orogen: Conterminous U.S.: Geological Society of America The Geology of North America, v. G-3, p. 265-270.

Niem, A. R., and Niem, W. A., 2002, Bedrock architecture, natural resources, and geologic hazards of NE part of the Oregon Coast Range forearc: Geological Society of America, Abstracts with Programs (Cordilleran section in Corvallis).

Nio, S., and Yang, C., 1991, Diagnostic attributes of clastic tidal deposits: a review, *in* Smith, D.G., Reinson, G.E., Zaitlain, B.A., and Rahmani, R.A., eds., Clastic tidal sedimentology: Canadian Society of Petroleum Geologists, Memoir 16, P. 3-28.

Olmstead, D.L., 1982, Oil and gas exploration and development in Oregon, 1981: Oregon Geology, v. 44, p. 27-31.

Olbinski, J. S., 1983, Geology of the Buster Creek-Nehalem valley area, Clatsop County, Northwest Oregon: Corvallis, Oregon, Oregon State University M.S. thesis, 204 p.

Payne, C.W., 1998, Lithofacies, Stratigraphy, and Geology of the middle Eocene type Cowlitz Formation and associated volcanic and sedimentary units, eastern Willapa Hills, southwest Washington: Corvallis, Oregon, Oregon State University, masters thesis, p. 1-235.

Pezzopane, S.K., and Weldon, R.J., II, 1993, Tectonic role of active faulting in central Oregon: Tectonics, v. 12, p. 1140-1169.

Peterson, C. P. 1984, Geology of the Green Mountain-Youngs River area, Clatsop County, northwest Oregon: Corvallis, OR, Oregon State University master's thesis, 215 p.

Phillips, W.M., 1987, Geologic map of the Mt. St. Helens quadrangle, Washington: Washington Division of Geology and Earth Resources Open File Report 87-4, 63 p., 1 Plate, scale1: 100,000.

Phillips, W.M., Walsh, T,J., and Hagen, R.A., 1989, Eocene transition from oceanic to arc volcanism, southwest Washington: Proceeding of workshop XLIV; Geological, geophysical, and tectonic setting of the Cascade Range, United States Geological Survey Open File Report 89-187, p. 199-256.

Prothero, D.R., Nesbitt, E., Niem, A.R., and Kleibacker, D.W., 2001, Magnetic stratigraphy and tectonic rotation of the upper-middle Eocene Cowlitz and Hamlet Formations, western Oregon and Washington: Magnetic stratigraphy of the Oregon Coast Cenozoic: Pacific Section Society for Sedimentary Geology, Book 91, p. 75-95.

Rarey, P.J., 1986,Geology of the Hamlet-North Fork of the Nehalem River area, southern Clatsop and Southern Tillamook counties, northwest Oregon: Corvallis, Oregon, Oregon State University, masters thesis, 457 p.

Reidel, S.P., Tolan, T.L., Hooper, P.R., Beeson, M.H., Fecht, K.R., Bentley, R.D., and Anderson, J.L., 1989, The Grande Ronde Basalt, Columbia River Basalt Group; stratigraphic descriptions and correlations in Washington, Oregon, and Idaho: Geological Society of America Special Paper 239, p. 21-53.

Roberts, A.E., 1958, Geology and coal resources of the Toledo-Castle Rock district, Cowlitz and Lewis counties, Washington: United States Geological Survey Bulletin 1062, 71 p., 6 Plates.

Robertson, C.L., 1997, Surface-subsurface facies and distribution of the Eocene Cowlitz and Hamlet Formations, northwest Oregon: Corvallis, Oregon, Oregon State University, masters thesis, p. 1-158.

Ryu, I.C., Niem, A.R., and Niem, W.A., 1992, Schematic fence diagram of the southern Tyee basin, Oregon Coast Range, Oregon Department of geology and Mineral Industries Oil and Gas Investigation 18, Portland, Oregon, 28 p., 1 plate.

Shaw, N. B., 1986, Biostratigraphy of the Cowlitz Formation in the upper Nehalem River Basin, northwest Oregon: Portland, OR, Portland State University master's thesis, 110 p.

Simpson, R.W., and Cox, A., 1977, Paleomagnetic evidence for tectonic rotation of the Oregon Coast Range: Geology, v. 5, p. 585-589.

Smith, G.A., and Fisher, R.V., 1986, Sedimentation in volcanic settings: Society for Sedimentary Geology, Special Publication no. 45, 257 p.

Snavely, P.D., Jr., 1987, Tertiary geologic framework, neotectonics, and petroleum potential of the Oregon-Washington continental margin, *in* Scholl, D.W., Grantz, A., Vedder, J.G., eds., Geology and resource potential of the continental margin of western North America, and adjacent ocean basins- Beaufort Sea to Baja California: Circum-Pacific Council for Energy and Mineral Resources, Earth Sciences Series, v. 6, p. 305-335.

Stanley, W.D., Johnson, S.Y., and Nuccio, V.F., 1994, Analysis of deep seismic reflection and other data from the southern Washington Cascades, United States Geological Survey Open File Report 94-159.

Stanley, Johnson, S.Y., Qamar, A.I., Weaver, C.S., and Williams, J.M., 1996, Tectonics and seismicity of the Southern Washington Cascade Range, Bulletin of the Seismological Society of America, v. 86, no. 1A, p. 1-18.

Stormberg, G.L., 1991, The Mist Gas Field, N.W. Oregon: source rock characterization and stable isotope (C,H,N) geochemistry: Corvallis, Oregon, Oregon State University, masters thesis, p. 1-191.

Swanson, D. A., and Wright, T. L., 1978, Bedrock geology of the northern Columbia Plateau and adjacent area; *in* Baker, V. R., and Nummendal, D., eds., The Channelized Scabland: N.A.S.A., Planetary Geology Program, p. 186.

Swanson, D.A., Wright, T.L., Hooper, P.R., and Bentley R.D., 1979, Revisions in stratigraphic nomenclature of the Columbia River Basalt Group: United States Geological Survey Bulletin 1457-G, 59 p.

Taubeneck, W.H., 1970, Dikes of the Columbia River Basalt in northwest Oregon, western Idaho, and southeastern Washington, *in* Gilmore, E.H., and Stradling, D., eds., Proceedings of the 2nd Columbia River Basalt Symposium: Cheney, Eastern Washington University Press, p. 73-96.

Timmons, D. M., 1981, Stratigraphy, lithofacies, and depositional environment of the Cowlitz Formation, T 4 and 5 N, R 5 W, northwest Oregon: Portland, OR, Portland State University master's thesis, 89 p.

Tolan, T.L., Reidel, S.P., Beeson, M.H., Anderson, J.L., Fecht, K.R., and Swanson, D.A., 1989, Revisions to the estimates of the aerial extent and volume of the Columbia River Basalt Group: *in* Reidel, S.P., and Hooper, P.R., eds., Volcanism and tectonism in the Columbia River flood basalt province: Geological Society of America Special Paper 239, p. 1-20.

Van Wagoner, J. C., 1985, Reservoir facies distribution as controlled by sea-level change, abstract: Society of Economic Paleontologists and Mineralogists Mid-Year Meeting, Golden, Colorado, August 11-14, p. 91-92.

Van Wagoner, J. C., Mitchum R.M., Campion, K.M., and Rahmanian, V.D., 1992, Siliciclastic sequence stratigraphy in well logs, cores, and outcrops: American Association of Petroleum Geologists Methods in Exploration Series 7, 55p.

Waitt, R. B., Jr., 1985, Case for periodic, colossal jokulhaups from Pleistocene glacial Lake Missoula: Geological Society of America Bulletin v. 96, no. 10, p. 1271-1286.

Walsh, T.J., Korsec, M.A., Phillips, W.M., Logan, R.L., and Schasse, H.W., 1987, Geologic map of Washington-southwest quadrant: Washington Division of Geology and Earth Resources Geologic Map GM-34, 2 pl., 28 p.

Warren, W. C., Norbisrath, H., and Grivetti, R.M., 1945, Geology of northwestern Oregon, west of Willamette River and north of latitude 45 15': United States Geological Survey Oil and Gas Investigation Preliminary Map 42, scale

Warren, W. C., and Norbisrath, Hans, 1946, Stratigraphy of upper Nehalem River Basin, northwest Oregon: American Association of Petroleum Geologists Bulletin, v. 30, no. 2, p. 213-237.

Weaver, C. E., 1912, A preliminary report on the Tertiary paleontology of western Washington: Washington Geological Survey Bulletin 15, 80 p.

Weaver, C. E., 1937, Tertiary stratigraphy of western Washington and northwest Oregon: University of Washington publications v. 4, Seattle, 166 p., 15 Pls.

Wegmann, K. W., and Walsh, T. J., 2001, Landslide hazards mapping in Cowlitz County-A progress report: Washington Geology, v. 29, no. ½, p. 30-33.

Wegmann, K., Washington Department of Natural Resources, personal and written communication, 2001-2003.

Wells, R.E., 1981, Geologic map of the Eastern Willapa Hills, Cowlitz, Lewis, Pacific, and Wahkiakum Counties, Washington: United States Geological Survey Open File Report 81-674, scale 1:62,500.

Wells, R. E., Engebretson, D. C., Snavely, P. D., Jr., and Coe, R. S., 1984, Cenozoic plate motions and the volcano-tectonic evolution of western Oregon and Washington: Tectonics, v. 3, p. 275-294.

Wells, R. E., and Coe, R.S., 1985, paleomagnetism and geology of Eocene volcanic rocks of southwest Washington, implications for mechanisms of tectonic rotation: Journal of Geophysical Research, v. 90, no. B2, p. 1925-1947.

Wells, R. E., Weaver, C. S., and Blakely, R. J., 1998, Fore-arc migration in Cascadia and its neotectonics significance: Geology, v. 26, p. 759-762.

Wilcox, R.E., Harding, T.P., and Seely, D.R., 1973, Basic wrench tectonics: American Association of Petroleum Geologists Bulletin, v. 57, p. 74-96.

Wilkinson, W.D., Lowry, W.D., and Baldwin, E.M., 1946, Geology of the St. Helens quadrangle, Oregon: Oregon Department of Geology and Mineral Industries Bulletin 31, 39 p., scale 1:62,500.

Williams, H., Turner, F. F., and Gibert, C. M., 1954, Petrography: W. H. Freeman and Co., San Francisco, 460 p.

Wong, I.G., Hemphill-Haley, A., Liberty, L.M., and Madin, I.P., 2001, The Portland Hills Fault: An earthquake generator or just another old fault?: Oregon, v. 63, p. 39-50.

APPENDICES

MACROFOSSIL IDENTIFICATION

THE BURKE MUSEUM OF NATURAL HISTORY AND CULTURE

4/9/99

Dear Mark

I have finally identified your specimens from Coal Creek and the information is below (sorry it took so long). Two bivalves make their first appearance in the Cowlitz Formation – both are common in the Coaledo and Spencer Formations. And the little limpet may be a new species—I still have some work to do on that one. The environmental information is not startling, but shows a nice mix of very shallow normal marine, delta embayment, true brackish water, and even a freshwater locality. An asterisk * marks the assemblages described in my 1995 Journal of Paleontology paper, which describes these in detail (more than you care for, I'm sure!)

In return I'd like a copy of your section with these fossil localities marked. Do you want the fossils back, or should I included them in the Burke Museum collection? With the strat. column they make a very useful and valuable collection.

In reference to your comments:
I think that the reason you get fossils with basaltic sands is that these represent periods of transgressive sea – not big transgressions, just little onlaps. Under these circumstances waves are pushing shallow subtidal sediments, and fossils upwards. This doesn't really explain the phenomenon with the oyster bed (*Acutostrea*), but I assume if the shoreline is transgressing, so are the embayments. Then, the non-fossiliferous units are arkosic sands washed down by river floods, and either carry no organisms, or (much more likely) anything that could be preserved was leached out. This is typical of all sand units because the pore spaces are large enough to carry lots of ground water – and is almost ubiquitous in the Cowlitz sands. Does this make sense?

Looking forward to hearing back from you

Sincerely

Liz

Liz Nesbitt, Ph.D.
Curator of Invertebrate Paleontology

Coal Creek Section, Cowlitz Formation

Most of these fossils you'll find illustrated and named in Weaver, 1943, although t generic names may have changed. The generic and specific name follows the name of the person(s) who originally published the description of the fossil, - this is traditional in scientific literature.

ield #	Genera and species	Depositional environment
24	*Mytilus* species - looks like *Mytilus matthewsoni* Gabb which is Oligocene in age	Shallow marine, washed off intertidal rocks
27b	A lovely little limpet – I still have to identify it	Washed off rocks, I assume
27c	*Turritella uvasana stewarti* Merriam	These are marine, but pretty hardy, so can get washed up river
29	*Nuculana washingtonensis* (Weaver) *Septifer dichotomus* Gabb *Venericardia clarki* Weaver & Palmer *Acanthocardia (S.) breweri* Gabb *Pitar eocenica* Weaver & Palmer *Gari columbiana* (Weaver & Palmer) *Solena columbiana* (Weaver & Palmer) [1]*Spisula packardi* Turner *Tivelina vaderensis* (Dickerson) *Turritella uvasana stewarti* Merriam *Siphonalia sopenahensis* (Weaver) *Polinices nuciformis* (Gabb) *Colwellia bretzi* (Weaver) A limpet – perhaps *Acmaea*	This is the *Turritella-Solena** assemblage -must be the locality below the church parking lot. Many more species have been found here since I wrote that paper. Normal marine, shallow subtidal, close to rocks
30	*Acutostrea idriaensis* Gabb	*Acutostrea* assemblage* Soft sediment embayment
35b	*Acutostrea idriaensis* Gabb tube trace fossil	*Acutostrea* assemblage* Soft sediment embayment
38	*Acutostrea idriaensis* Gabb With rare *Pitar eocenica* Weaver & Palmer	This seems a common combination, so the *Pitar* could live in this shallow embayment environment
49	Nothing identifiable	

[1] Sand *Pachydesma* has not been found in the type area of the Cowlitz, but is common in the Coaledo and Spencer – so this makes a nice faunal link

52	*Batissa newberri* White	Freshwater clams – common in the Puget Group sediments
53	*Acutostrea idriaensis* Gabb With one *Pitar eocenica* Weaver & Palmer	Same as # 38
62	*Venericardia clarki* Weaver & Palmer *Turritella uvasana stewarti* Merriam *Pitar californiana* (Conrad) *Polinices nuciformis* (Gabb)	All of these are thick shelled and resistant to wear; so were washed in from the shallow, normal marine *Turritella* assemblage
63	*Pitar eocenica* Weaver & Palmer *Pitar californiana* (Conrad) *Pachydesma aragoensis* Turner	Normal marine, but low diversity – I suggest that they were displaced and washed together
67	*Acutostrea idriaensis* Gabb *Pitar californiana* (Conrad)	Same as # 38
68	*Corbicula cowlitzensis* Weaver	*Corbicula* assemblage* - typical marginal marine, brackish water
77c	*Glycymeris sagittata* (Gabb)	Marine sands – perhaps low intertidal to subtidal beach
77	*Acutostrea idriaensis* Gabb	
81	*Acutostrea idriaensis* Gabb *Pitar eocenica* Weaver & Palmer *Pitar californiana* (Conrad) *Pachydesma aragoensis* Turner *Spisula packardi* Turner *Gari columbiana* (Weaver & Palmer) *Tivelina vaderensis* (Dickerson) *Calyptraea diegoana* (Conrad)	normal marine, v. shallow – these are the thick shelled part of a *Turritella* assemblage, but all jumbled up by high energy
86	*Venericardia clarki* Weaver & Palmer *Siphonalia sopenahensis* (Weaver) *Polinices nuciformis* (Gabb)	normal marine, v. shallow - part of a *Turritella* assemblage
90	*Acutostrea idriaensis* Gabb	
92	*Glycymeris sagittata* (Gabb)	Marine sands – perhaps low intertidal to subtidal beach
99	*Acutostrea idriaensis* Gabb With burrow trace fossils	*Acutostrea* assemblage* Soft sediment embayment

APPENDIX II
Magnetic polarity of basalt samples

Columbia River Basalts

Site #	Polarity	Strength
BC-3	+	strong
BC-4	+	weak
BC-5	+	weak
BC-8	+	strong
BC-10	+	weak
Site 51	+	weak
Site 54	+	strong
Site 100	+	strong
Site 102a	+	weak
Site 102b	+	weak
Site 103	+	weak

Gray River Volcanics

BC-FQS (sill)	inconclusive	
Site 63	+	weak
Site 101	+	weak
FQ	-	weak
Site 1a	+	weak
Site 2a	+	weak
Site 7a	-	weak
Site 7b	-	weak

	WEG SI SITE 1b	WEG SI SITE 2a	WEG SI SITE 5	WEG SI SITE 7c	WEG SI SITE 7d	WEG SI SITE 17	WEG SI SITE 63	WEG SI SITE 74	WEG Si SITE 76	WEG CR -12
Date	22-Jul-00	22-Jul-00	22-Jul-00	22-Jul-00	22-Jul-00	22-Jul-00	22-Jul-00	22-Jul-00	22-Jul-00	22-Jul-00
LOI (%)			14.57							
	Unnormalized Results (Weight %):									
SiO2	47.26	50.34	50.26	48.52	47.69	52.27	49.03	58.98	51.91	53.07
Al2O3	14.81	17.85	14.76	14.22	13.64	16.51	13.77	15.93	16.59	16.73
TiO2	1.455	1.954	1.503	3.074	2.751	1.237	3.642	1.677	1.206	1.510
FeO	10.50	10.78	11.89	12.76	11.99	8.54	13.88	7.94	8.53	9.01
MnO	0.177	0.175	0.229	0.194	0.141	0.131	0.218	0.147	0.134	0.158
CaO	12.27	9.31	7.46	11.09	7.41	9.45	9.55	5.91	9.37	9.33
MgO	9.27	5.03	10.78	6.01	6.41	7.62	4.35	2.87	7.80	6.04
K2O	0.87	0.62	0.51	0.42	0.99	0.46	0.88	1.05	0.46	0.38
Na2O	2.31	3.42	2.54	2.88	3.51	3.16	3.50	4.73	3.12	3.35
P2O5	0.394	0.367	0.161	0.429	0.395	0.186	0.537	0.455	0.184	0.296
Total	99.31	99.85	100.10	99.60	94.93	99.57	99.35	99.69	99.30	99.87
	Normalized Results (Weight %):									
SiO2	47.59	50.42	50.21	48.71	50.24	52.50	49.35	59.16	52.27	53.14
Al2O3	14.91	17.88	14.75	14.28	14.37	16.58	13.86	15.98	16.71	16.75
TiO2	1.465	1.957	1.502	3.086	2.898	1.242	†3.67	1.682	1.214	1.512
FeO*	10.57	10.80	11.88	12.81	12.63	8.58	13.97	7.97	8.59	9.02
MnO	0.178	0.175	0.229	0.195	0.149	0.132	0.219	0.147	0.135	0.158
CaO	12.36	9.32	7.45	11.13	7.81	9.49	9.61	5.93	9.44	9.34
MgO	9.33	5.04	10.77	6.03	6.75	7.65	4.38	2.88	7.85	6.05
K2O	0.88	0.62	0.51	0.42	1.04	0.46	0.89	1.05	0.46	0.38
Na2O	2.33	3.43	2.54	2.89	3.70	3.17	3.52	4.74	3.14	3.35
P2O5	0.397	0.368	0.161	0.431	0.416	0.187	0.541	0.456	0.185	0.296
	Trace Elements (ppm):									
Ni	136	63	302	61	67	185	11	1	178	142
Cr	299	47	242	114	128	338	23	7	336	196
Sc	37	25	28	29	30	20	32	26	30	19
V	313	248	153	337	299	193	344	165	203	193
Ba	288	117	103	173	172	113	228	245	117	121
Rb	26	7	8	9	20	5	17	18	6	7
Sr	567	390	333	414	1137	370	425	390	368	386
Zr	131	172	121	205	207	108	267	184	104	156
Y	28	27	20	33	32	24	40	29	40	24
Nb	8.3	15.3	10.6	35.0	33.6	9.6	46.5	18.6	9.7	15.7
Ga	16	24	17	21	19	17	22	22	21	18
Cu	158	122	110	111	90	106	47	42	114	132
Zn	84	108	89	110	97	74	130	93	78	87
Pb	0	0	0	1	5	2	0	0	2	0
La	38	31	0	31	27	14	27	37	13	16
Ce	86	29	44	60	67	19	77	52	29	33
Th	1	0	4	3	2	0	4	2	2	2

Major elements are normalized on a volatile-free basis, with total Fe expressed as FeO.
"R" denotes a duplicate bead made from the same rock powder.
"†" denotes values >120% of our highest standard.

	WEG FQ CLAST	WEG BC -1	WEG BC -4	WEG BC -5	WEG BC -8	WEG BC -10	WEG BC -13	WEG SI TE 21	WEG 97 -CC44	WEG 97 -CC-9
Date	22-Jul-00	22-Jul-00	23-Jul-00	25-Jul-00	25-Jul-00	25-Jul-00	25-Jul-00	25-Jul-00	25-Jul-00	25-Jul-00
LOI (%)										
Unnormalized Results (Weight %):										
SiO2	49.28	55.84	53.48	54.70	55.42	54.03	54.88	58.62	42.71	47.35
Al2O3	14.43	13.88	13.65	14.25	14.35	14.28	14.37	15.69	14.74	14.83
TiO2	3.029	2.066	1.989	2.025	2.080	2.052	1.773	1.681	2.992	3.812
FeO	11.71	11.37	12.84	10.54	10.33	10.83	9.93	7.94	17.49	14.08
MnO	0.172	0.189	0.218	0.186	0.190	0.229	0.199	0.158	0.069	0.152
CaO	11.54	7.29	8.26	8.45	8.52	8.79	8.71	6.21	7.95	6.54
MgO	5.77	3.59	4.12	4.36	3.82	3.78	4.58	2.74	5.81	5.56
K2O	0.61	1.74	1.19	1.36	1.36	1.26	1.40	0.72	0.15	0.65
Na2O	2.42	3.04	3.09	2.96	2.94	3.00	2.89	4.45	2.10	2.60
P2O5	0.383	0.377	0.336	0.323	0.322	0.340	0.313	0.453	0.348	0.568
Total	99.34	99.38	99.17	99.15	99.33	98.59	99.04	98.67	94.36	96.14
Normalized Results (Weight %):										
SiO2	49.61	56.19	53.93	55.17	55.80	54.80	55.41	59.41	45.26	49.25
Al2O3	14.53	13.97	13.76	14.37	14.45	14.48	14.51	15.90	15.62	15.43
TiO2	3.049	2.079	2.006	2.042	2.094	2.081	1.790	1.704	3.171	†3.97
FeO*	11.79	11.44	12.94	10.63	10.39	10.98	10.02	8.05	†18.54	14.64
MnO	0.173	0.190	0.220	0.188	0.191	0.232	0.201	0.160	0.073	0.158
CaO	11.62	7.34	8.33	8.52	8.58	8.92	8.79	6.29	8.43	6.80
MgO	5.81	3.61	4.15	4.40	3.85	3.83	4.62	2.78	6.16	5.78
K2O	0.61	1.75	1.20	1.37	1.37	1.28	1.41	0.73	0.16	0.68
Na2O	2.44	3.06	3.12	2.99	2.96	3.04	2.92	4.51	2.23	2.70
P2O5	0.386	0.379	0.339	0.326	0.324	0.345	0.316	0.459	0.369	0.591
Trace Elements (ppm):										
Ni	83	11	18	22	11	13	16	6	161	29
Cr	109	30	35	39	36	49	54	9	282	37
Sc	31	31	37	37	31	42	46	25	27	33
V	327	335	340	350	360	332	314	161	333	341
Ba	150	717	510	536	599	563	551	251	99	182
Rb	9	45	30	32	33	29	33	34	0	11
Sr	424	321	314	328	333	326	320	416	367	429
Zr	211	182	159	162	165	166	159	181	211	278
Y	31	38	37	36	38	38	36	28	30	36
Nb	33.3	13.6	12.0	12.5	13.0	13.2	12.1	18.5	30.7	45.4
Ga	23	23	21	24	22	20	20	20	23	27
Cu	111	20	29	13	30	33	29	45	161	54
Zn	116	136	121	117	126	124	115	90	129	143
Pb	0	8	4	7	8	5	5	3	5	0
La	34	18	13	21	17	15	9	22	25	44
Ce	53	45	37	42	33	36	53	44	53	83
Th	4	6	7	6	5	3	6	4	1	4

Major elements are normalized on a volatile-free basis, with total Fe expressed as FeO.
"R" denotes a duplicate bead made from the same rock powder.
"†" denotes values >120% of our highest standard.

	WEG 97 -CC63	WEG SI TE 7d	WEG SI TE7dR	WEG 97 -CC44	WEG 97 CC44R
Date	25-Jul-00	22-Jul-00	25-Jul-00	25-Jul-00	25-Jul-00
LOI (%)					
	Unnormalized Results (Weight %):				
SiO2	46.56	47.69	47.70	42.71	42.83
Al2O3	13.82	13.64	13.67	14.74	14.72
TiO2	2.982	2.751	2.746	2.992	2.990
FeO	12.91	11.99	11.52	17.49	17.57
MnO	0.188	0.141	0.140	0.069	0.068
CaO	11.44	7.41	7.43	7.95	7.94
MgO	6.32	6.41	6.45	5.81	5.75
K2O	0.30	0.99	0.99	0.15	0.15
Na2O	2.42	3.51	3.57	2.10	2.19
P2O5	0.362	0.395	0.396	0.348	0.345
Total	97.30	94.93	94.61	94.36	94.56
	Normalized Results (Weight %):				
SiO2	47.85	50.24	50.42	45.26	45.30
Al2O3	14.20	14.37	14.45	15.62	15.57
TiO2	3.065	2.898	2.902	3.171	3.162
FeO*	13.27	12.63	12.18	†18.54	†18.58
MnO	0.193	0.149	0.148	0.073	0.072
CaO	11.76	7.81	7.85	8.43	8.40
MgO	6.50	6.75	6.82	6.16	6.08
K2O	0.31	1.04	1.05	0.16	0.16
Na2O	2.49	3.70	3.77	2.23	2.32
P2O5	0.372	0.416	0.419	0.369	0.365
	Trace Elements (ppm):				
Ni	77	67	66	161	182
Cr	117	128	133	282	291
Sc	32	30	25	27	38
V	325	299	287	333	345
Ba	152	172	177	99	87
Rb	5	20	18	0	0
Sr	434	1137	1134	367	368
Zr	213	207	205	211	210
Y	29	32	31	30	29
Nb	33.2	33.6	31.9	30.7	30.6
Ga	22	19	22	23	24
Cu	108	90	94	161	160
Zn	106	97	106	129	130
Pb	0	5	0	5	0
La	26	27	29	25	4
Ce	45	67	50	53	51
Th	2	2	2	1	4

Major elements are normalized on a volatile-free basis, with total Fe expressed as FeO.
"R" denotes a duplicate bead made from the same rock powder.
"†" denotes values >120% of our highest standard.

	WEG 54	WEG 52	WEG 102A	WEG 104	WEG 103	WEG 101	WEG 102B	WEG 51
Unnormalized Major Elements (Weight %):								
SiO2	54.17	45.49	57.08	52.50	54.94	48.98	54.30	55.68
Al2O3	13.87	15.09	15.18	15.43	15.38	13.88	13.92	13.79
TiO2	1.988	4.120	2.244	2.211	1.898	3.649	2.012	2.033
FeO	11.95	13.88	8.76	11.93	9.11	13.95	11.76	11.36
MnO	0.202	0.222	0.143	0.186	0.173	0.220	0.204	0.195
CaO	8.51	8.65	6.87	8.02	8.85	9.53	8.21	7.22
MgO	4.28	4.03	3.38	3.90	4.69	4.31	4.31	3.54
K2O	1.18	0.89	1.78	0.85	1.26	0.90	1.19	1.74
Na2O	2.91	3.12	3.26	3.89	2.87	3.19	3.06	3.13
P2O5	0.349	0.618	0.337	0.336	0.334	0.525	0.322	0.390
Total	99.40	96.11	99.04	99.26	99.51	99.13	99.29	99.08
Normalized Major Elements (Weight %):								
SiO2	54.49	47.33	57.64	52.89	55.21	49.41	54.69	56.20
Al2O3	13.95	15.70	15.33	15.55	15.46	14.00	14.02	13.92
TiO2	2.000	†4.29	2.266	2.228	1.907	†3.68	2.026	2.052
FeO*	12.02	14.44	8.85	12.02	9.16	14.07	11.85	11.47
MnO	0.203	0.231	0.144	0.187	0.174	0.222	0.205	0.197
CaO	8.56	9.00	6.94	8.08	8.89	9.61	8.27	7.29
MgO	4.31	4.19	3.41	3.93	4.71	4.35	4.34	3.57
K2O	1.19	0.93	1.80	0.86	1.27	0.91	1.20	1.76
Na2O	2.93	3.25	3.29	3.92	2.88	3.22	3.08	3.16
P2O5	0.351	†0.64	0.340	0.339	0.336	0.530	0.324	0.394
Unnormalized Trace Elements (ppm):								
Ni	10	12	11	5	10	7	9	6
Cr	37	22	27	17	53	15	33	28
Sc	41	36	35	39	38	27	43	33
V	330	344	345	347	317	346	332	332
Ba	484	201	863	220	566	229	509	700
Rb	30	17	51	13	29	14	30	46
Sr	316	457	356	367	333	428	311	314
Zr	159	280	198	163	167	264	160	179
Y	34	41	45	33	42	38	35	36
Nb	12.0	48.6	13.6	14.1	12.5	44.9	12.1	14.2
Ga	20	24	21	21	23	25	20	22
Cu	25	48	18	101	17	43	20	18
Zn	116	139	177	108	120	130	120	125
Pb	4	1	10	4	6	6	3	8
La	35	34	39	25	33	29	33	17
Ce	47	93	58	32	51	79	41	45
Th	3	7	8	1	6	1	2	8

Major elements are normalized on a volatile-free basis, with total Fe expressed as FeO.
"†" denotes values >120% of our highest standard.

APPENDIX IV
POINT COUNTS

	CC-7		CC-17		CC-48		CC-53b	
	# of points	%	# of points	%	# of points	%	# of points	%
monocrystalline quartz	103	25.75	114	28.5	122	30.5	130	32.5
polycrystalline quartz	59	14.75	51	12.75	60	15	39	9.75
biotite	20	5	45	11.25	34	8.5	7	1.75
muscovite	7	1.75	21	5.25	17	4.25	5	1.25
clinopyroxene	4	1	1	0.25	1	0.25	4	1
plagioclase	31	7.75	25	6.25	38	9.5	17	4.25
potassium feldspar	63	15.75	52	13	73	18.25	51	12.75
hornblende	0	0	0	0	1	0.25	4	1
carbonaceous material	3	0.75	56	14	10	2.5	4	1
schist & gneiss	20	5	15	3.75	13	3.25	7	1.75
quartzite	14	3.5	0	0	2	0.5	1	0.25
plutonic	23	5.75	12	3	15	3.75	1	0.25
pilotaxitic basalt	15	3.75	0	0	7	1.75	22	5.5
randomly oriented basalt	27	6.75	8	2	7	1.75	108	27
glass	0	0	0	0	0	0	0	0
other	11	2.75	0	0	0	0	0	0
total	400	100%	400	100%	400	100%	400	100%

APPENDIX V
CHEMISTRY OF METHANE SAMPLE

Channel A Results

Name	Time	Area	Area %	Conc ppm-v
methane	0.41	1765921	99.81	260.278
ethane and ethene	0.61	1555	0.09	0.121
propane	1.12	387	0.02	0.025
propene	1.34	0	0.00	0.000
i-butane	2.01	0	0.00	0.000
n-butane	2.44	0	0.00	0.000
neopentane	2.96	0	0.00	0.000
i-pentane	3.74	0	0.00	0.000
n-pentane	4.11	0	0.00	0.000
cyclopentane	4.55	0	0.00	0.000
2,2 dimethyl buta	4.82	0	0.00	0.000
2methylpentane	5.27	0	0.00	0.000
3methylpentane	5.35	0	0.00	0.000
n-hexane	5.59	0	0.00	0.000
	5.76	1363	0.08	0.041
methylcyclopentan	5.95	0	0.00	0.000
heptane	6.68	0	0.00	0.000
methylcyclohexane	6.90	0	0.00	0.000
Totals :		1769227	100.00	260.465

File : C:\EZCHROM\CHROM\NORCAL\jonesfl\MC-1
Method : C:\EZCHROM\METHODS\JFL.MET
Sample ID : MC-1 SW Oregon Cowliz fm
Acquired : Jan 07, 1998 16:01:59
Printed : Jan 07, 1998 16:42:37

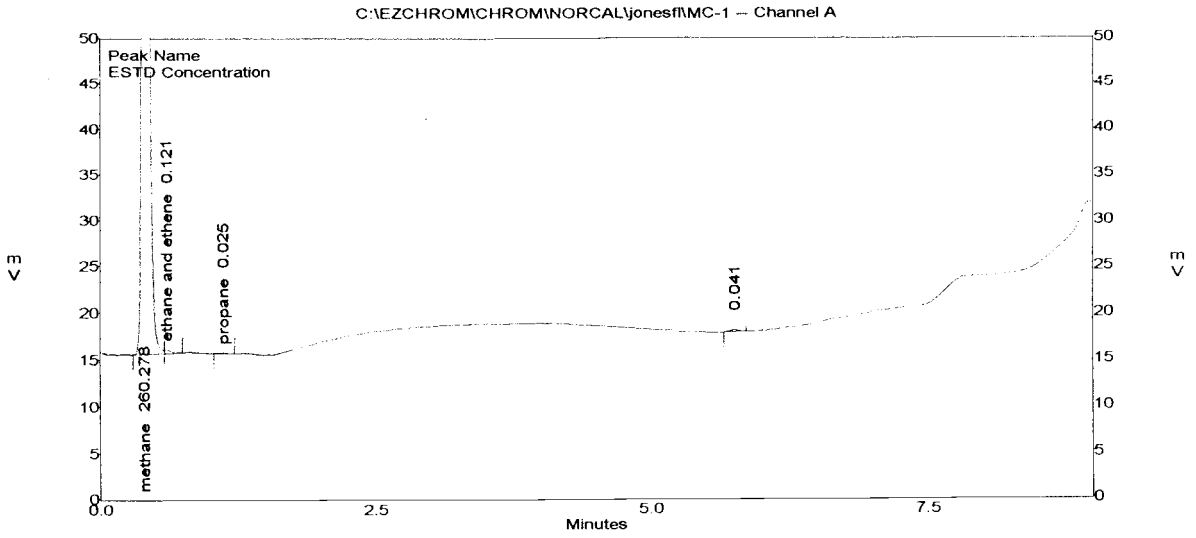

APPENDIX VI
MT. SOLO AR^{40}/AR^{39} RADIOMETRIC DATE
Noble Gas Mass Spectrometry
COAS Oregon State University, Corvallis, Oregon USA

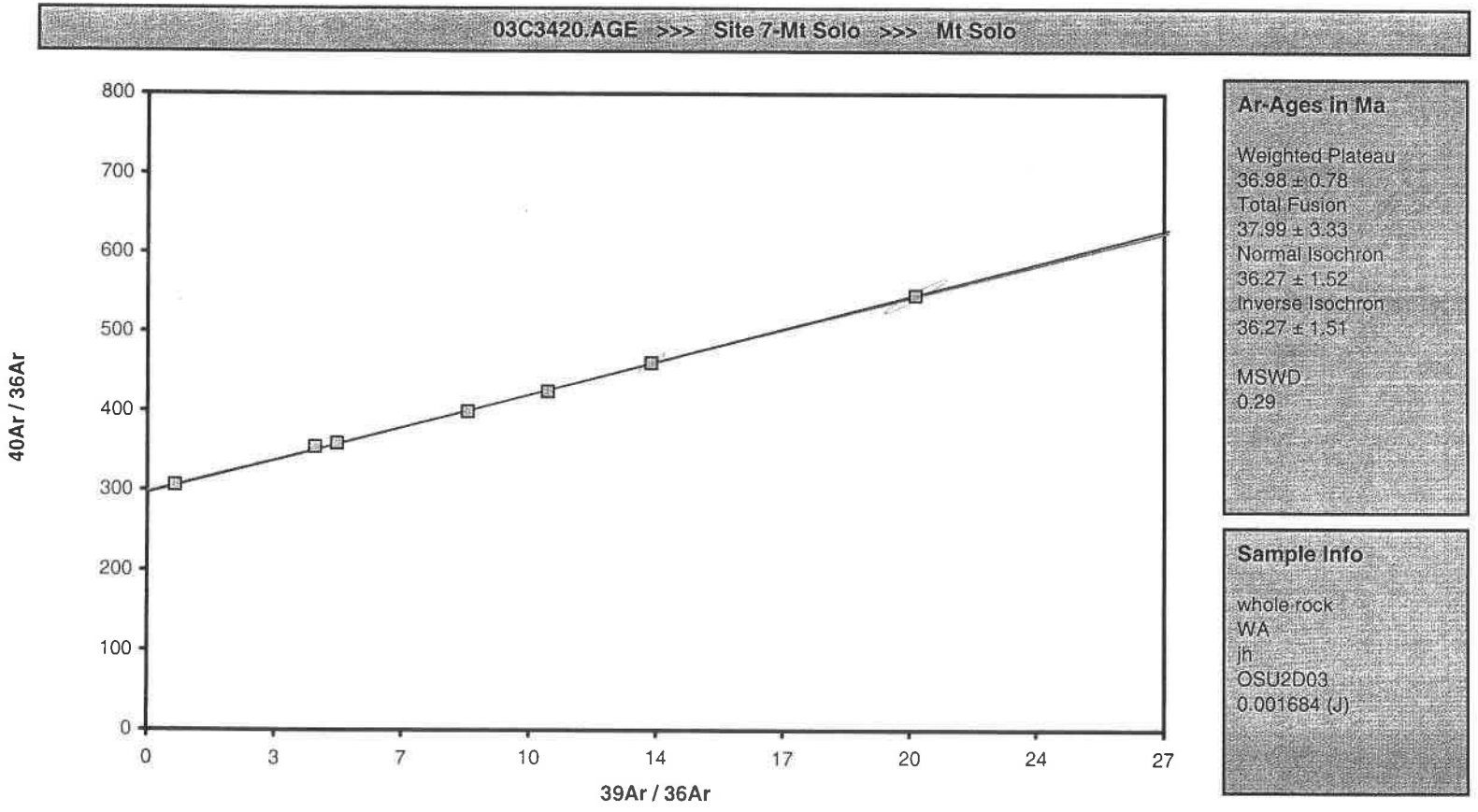

03c3420.age printed at 10/17/2003 (4:49 PM)
ArArCALC v22.1

Noble Gas Mass Spectrometry
COAS Oregon State University, Corvallis, Oregon USA

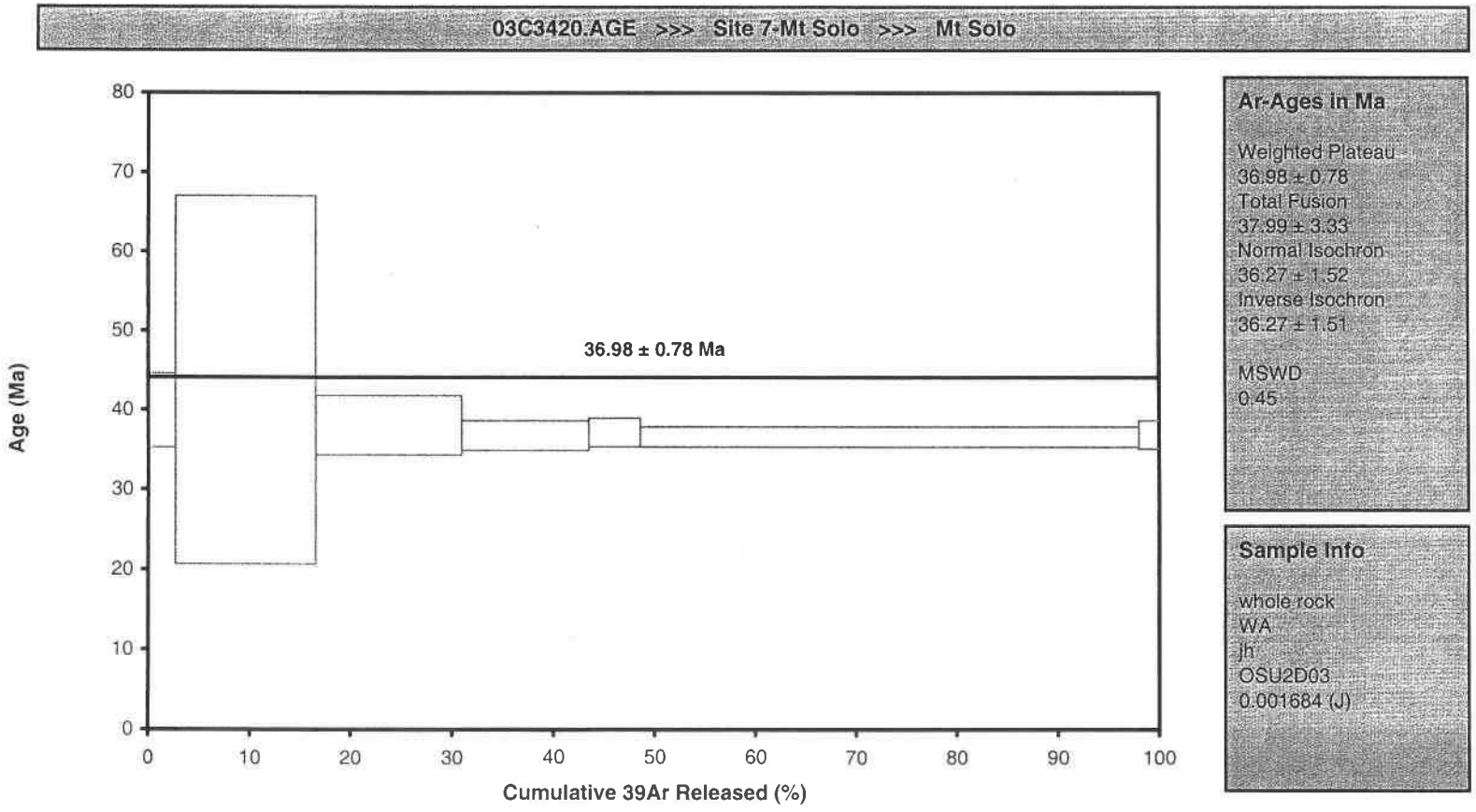

03c3420.age printed at 10/17/2003 (4:49 PM)
ArArCALC v22.1